Immune-mediated control of *Toxoplasma gondii* by a GBP1-TRIM21 complex

Clémence Caroline Foltz

The Francis Crick Institute at Mill Hill Laboratory,

formerly National Institute for Medical Research

Division of Infection and Immunity

University College London

Submitted to University College London

for the degree of Doctor of Philosophy

December 2015

Declaration

I, Clémence Caroline Foltz confirm that the work presented in this thesis is my own. Where information has been derived from other sources, I confirm that this has been indicated in the thesis.

Clémence Caroline Foltz

December 2015

À Mamie Joséphine

(1921-2013)

Acknowledgments

I would like to thank all the people who contributed to this work and made this thesis possible.

First of all, I would like to express my deep and sincere gratitude to my supervisor, Eva Frickel. Thank you for giving me the opportunity to work in your lab, for your confidence in my abilities to help you develop a new lab and a new project, for your constant support and supervision during my PhD and for critically reading this thesis. These four years have been a real challenge, but I enjoyed every sciencey and human parts of the adventure. Vielen Dank!

Other people within the Institute have given useful advice, critique and analysis during my PhD. I thank the members of my thesis committee: Maximiliano Gutierrez, Jean Langhorne and Katrin Rittinger for taking the time to critically examine my project and give me advice. I am also thankful to the members of the Parasitology division and of the Infection and Immunity division.

I am grateful to all the members of the Frickel lab, past and present, for the friendly and collaborative atmosphere that I was lucky to evolve in. It has been a real pleasure to spend four years among such friendly colleagues. Ania, Anna, Ashleigh, Barbara, Joe and Nagisa, we had great times inside and outside the lab. Thank you for the amazing bakes, the fun spirit, the good laughs, but also the support in times when I was down and the help and advice on my experiments. Oh, and also for bearing with my singing…

I am grateful to Alana Sargent and Rachel Chung for their help in making everything run smoothly in the lab.

The Francis Crick Institute and formerly the National Institute for Medical Research provide unparalleled research facilities. I would like to express my gratitude to everyone who contributed to the success of my experiments: all the staff within the biological services, the members of the flow cytometry facility, the members of the high-throughput screening facility, Kate Bishop from the confocal facility, Liz Hirst from the electron microscopy facility, and Radma Mahmood and Richard Stone from the experimental histopathology facility.

I would like to thank our collaborators at Clare Hall Laboratory, Vesela Encheva and Bram Snijders, for their help with the performance and analysis of the SILAC experiment. I am also grateful to Helena Ahlfors at the Babraham Institute for her help in analysing our RNA sequencing data. I am also thankful to Prof. Cheryl Scudamore from MRC Harwell, as well as Prof. Gordon Stamp from Imperial College London, for their help in analysing our histology data.

I would like to thank the Medical Research Council for their financial support. I am very grateful to the Boehringer Ingelheim Funds and their amazing staff, for both the financial support and all the good times spent talking science and hiking in Austria and America.

I am immensely thankful to all my friends who helped me go through the last four years. I am thankful to all my friends around the world who kept in touch with me despite the distance and sometimes even came to visit me in London. Dear “fly people” Ben, Clara, Holger, Vanessa and Rami, I am so happy I got to know you and to enjoy

great times in your company. To my dear and amazing “cottagers friends” Alex, Andy, Charlie, Jimena, Manuela and Martin, I cannot say thank you enough for supporting me and cheering me up in the bad times, but also for sharing so many happy times! The memories we built together in the cottages and in “Laurel Church Side” will stay with me forever, and I wish you good luck for your future!

Enfin et surtout, j’aimerais remercier ma famille pour son soutien sans faille durant toutes mes études et dans tous mes choix. Maman, Papa, Carole et Claire, je n’en serai pas arrivée là sans vos encouragements, votre aide et votre confiance inconditionnels. Merci!

Abstract

Infection with the parasite *Toxoplasma gondii* causes foetal abnormalities during pregnancy and encephalitis in immunocompromised individuals in both developed and developing countries. Inside the host cell, *Toxoplasma* resides in a protective parasitophorous vacuole (PV), allowing it to survive and replicate. Following infection, the cytokine interferon gamma (IFNγ) upregulates the p47 immunity-related GTPases (IRGs) and the p65 guanylate-binding proteins (GBPs). Both IRGs and GBPs are highly expressed in IFNγ-induced cells *in vitro* and accumulate at the PV of avirulent type II and III, but not virulent type I strains of *Toxoplasma*, mediating the disruption of the avirulent PV. Autophagy, the process targeting intracellular cargo for degradation by the lysosome, has been shown to be a key player in cell-autonomous resistance to *Toxoplasma*. Inflammasomes, the signalling platforms of the innate immunity detecting pathogenic and danger molecules, have been reported to regulate non-cell-autonomous restriction of *Toxoplasma*. However, the mechanisms involved in these two defence responses and what happens once the vacuole is disrupted remain unclear.

In this work, I investigate the role of ubiquitin in IFNγ-dependent resistance against *Toxoplasma* infection. I identified the E3 ubiquitin ligase TRIM21 as a novel interaction partner of GBP1. TRIM21 and GBP1 were co-recruited to the PV of avirulent but not virulent *Toxoplasma*. I show that avirulent, but not virulent *Toxoplasma*, is ubiquitinated in an IFNγ- and TRIM21-dependent manner, with TRIM21 partly mediating Lys63 ubiquitin linkages. TRIM21 differentially regulated the transcriptional and protein levels of GBP1 and GBP2, which were identified as substrates of the E3 ligase. TRIM21 also substantially upregulated the biosynthesis of

cholesterol, for which *Toxoplasma* is auxotroph. TRIM21$^{-/-}$ mice were highly susceptible to *Toxoplasma* infection and exhibited decreased levels of pro-inflammatory cytokines in their serum associated with higher parasite burden in the periphery and later in the brain. These findings suggest TRIM21 is a crucial, novel restriction factor during acute *Toxoplasma* infection.

Table of Contents

Table of Figures

Chapter 1

Chapter 2

Chapter 3

Chapter 4

Appendix

Table of Tables

Chapter 1

Chapter 2

Chapter 3

List of Abbreviations

Ab:	antibody
ADCP:	antibody-dependent cellular phagocytosis
ADCC:	antibody-dependent cellular cytotoxicity
ADIN:	antibody-dependent intracellular neutralisation
AIDS:	acquired immune-deficiency syndrome
AIF:	aluminium trifluoride
AIM2:	absent in melanoma 2
ALR:	AIM2-like receptor
ANOVA:	analysis of variance
AP-1:	activating protein-1
ASC:	apoptosis-associated speck-like protein containing a CARD
ATG:	autophagy-related
ATP:	adenosine tri-phosphate
BMDM:	bone marrow derived macrophage
BCA:	bicinchoninic acid
BSA:	bovin serum albumin
°C:	Celsius degree
CARD:	caspase activation and recruitment domain
CD:	cluster of differentiation
cDNA:	complementary DNA
C_H:	constant region heavy chain
C_L:	constant region light chain
CO_2:	carbon dioxide
DAG:	diacylglycerol
DAMP:	danger-associated molecular pattern
DC:	dendritic cell
DENV:	dengue virus
diGLY:	Glycine-Glycine
dLN:	draining lymph node
DMEM:	Dulbecco's modified Eagle medium
DNA:	deoxyribonucleic acid

dNTP:	deoxynucleoside triphosphate
dpi:	day post-infection
dsDNA:	double-stranded DNA
DTT:	dithiothreitol
E1:	ubiquitin-activating enzyme
E2:	ubiquitin-conjugating enzyme
E3:	ubiquitin ligase
E. coli:	*Escherichia coli*
EDTA:	ethylene diamine tetra-acetic acid
ELISA:	enzyme-linked immunosorbent assay
EM:	electron microscopy
EMCV:	encephalomyocarditis virus
ER:	endoplasmic reticulum
Fab:	fragment antigen binding
FACS:	fluorescence-activated cell sorting
Fc:	fragment crystallisable
FCS:	fetal calf serum
GAP:	GTPase activating protein
GBP:	guanylate binding protein
GDP:	guanosine di-phosphate
GEF:	guanine nucleotide exchange factors
GFP:	green fluorescent protein
GKS:	glycine-lysine-serine
GM-CSF:	granulocyte-macrophage colony stimulating factor
GMP:	guanosine mono-phosphate
GMS:	glycine-methionine-serine
GPI:	glycophosphatidylinositol
GTP:	guanosine tri-phosphate
GTPase:	GTP hydrolase
h:	hour
H_2O:	dihydrogen monoxide (water)
HCl:	hydrochloric acid
HCV:	hepatitis C virus

HECT:	homology to E6-AP C-terminus
HEK 293T:	human embryonic kidney 293T
HeLa:	Henrietta Lacks
HFF:	human foreskin fibroblast
HIV:	human immunodeficience virus
HRP:	horseradish peroxidase
IAP:	immunoaffinity purification
IB:	immunoblot
IC100:	inhibitory concentration 100%
IF:	immunofluorescence
IFA:	indirect fluorescence antibody assay
IFN:	interferon
Ig:	immunoglobulin
IgM-ISAGA:	Immunoglobulin M-immunosorbent agglutination assay
IL:	interleukin
IMDM:	Iscove's modified Dulbecco's media
IP:	immunoprecipitation
i.p.:	intraperitoneal
IRF:	interferon regulatory factor
IRG:	immunity-related GTPase
IVIS:	*in vivo* imaging system
K:	lysine
KO:	knockout
LAMP2:	lysosomal membrane-associated protein 2
LC:	liquid chromatography
LC3:	microtubule-associated protein 1 light chain 3
LIR:	LC3-interacting region
LPS:	lipopolysaccharide
LRR:	leucine-rich repeat
M:	molar
Mb:	megabase
M-CSF:	macrophage colony-stimulating factor
MEF:	mouse embryonic fibroblast

μg:	microgram
mg:	milligram
$MgCl_2$:	magnesium chloride
MHC:	major histocompatibility complex
min:	minute
μL:	microlitre
□L:	millilitre
mLN:	mesenteric lymph node
□m:	micrometre
mM:	millimolar
MOI:	multiplicity of infection
MS:	mass spectrometry
Mx:	myxovirus resistance
NaCl:	sodium chloride
NADPH:	nicotinamide adenine dinucleotide phosphate
NaN_3:	sodium azide
NBR1:	neighbour of BRCA1 gene 1 protein
NDP52:	nuclear dot protein 52 kDa
NF-κB:	nuclear factor κB
NH_4Cl:	ammonium chloride
NK:	natural killer
NLR:	NOD-like receptor
NLRC:	NLR family, CARD-containing
NLRP:	NLR family, pyrin domain-containing
NO:	nitric oxide
NOD:	nucleotide-binding oligomerisation domain
NP-40:	nonyl phenoxypolyethoxylethanol 40
O/N:	overnight
PAMP:	pathogen-associated molecular pattern
PBA:	PBS + 1% BSA
PBS:	phosphate buffered saline
PCR:	polymerase chain reaction
PE:	phosphatidylethanolamine

PEC: peritoneal exudate cell
PI3K: phosphatidylinositol 3-kinase
PLA: proximity ligation assay
PP: Peyer's patches
PRR: pattern recognition receptor
Pru: Prugniaud
PTM: post-translational modification
PV: parasitophorous vacuole
PVM: parasitophorous vacuole membrane
PYD: pyrin domain
qPCR: quantitative polymerase chain reaction
RabGDI: Rab dissociation inhibitor
RBCC: RING, B-box, coiled-coil domain
RIG-I: retinoic acid-inducible gene-I
RIN: RNA integrity number
RING: really interesting new gene
RNA: ribonucleic acid
RNase: ribonuclease
ROP: rhoptry protein
RPMI: Roswell Park Memorial Institute medium
RT: room temperature
SCB: sodium cacodylate buffer
SCV: *Salmonella*-containing vacuole
SCX: strong cationic exchange
SDS-PAGE: sodium dedocyl sulfate polyacrylamide gel electrophoresis
sec: second
SeV: Sendai virus
SILAC: stable isotope labelling with amino acid in cell culture
SNARE: soluble N-ethylmaleimide-sensitive factor attachment protein receptor
STAT: signal transducer and activator of transcription
T3SS: type III secretion system
TAE: Tris-Acetate-EDTA
TFA: trifluoroacetic acid

TLR: Toll-like receptor

TNF: tumor necrosis factor

Tom: tomato

Toxoplasma: *Toxoplasma gondii*

TRAF: TNF receptor-associated factor

TRIM: tripartite motif-containing protein

U: unit Ub: ubiquitin

UV: ultraviolet

V_H: variable region heavy chain

V_L: variable region light chain

VLIG: very large inducible GTPase

Vps: vacuolar protein sorting

VSV: vesicular stomatitis virus

WIPI1: WD-repeat protein interacting with phosphoinositides 1

WT: wild-type

Chapter 1

Introduction

1.1 Toxoplasmosis in the 21st century

1.1.1 Toxoplasmosis: a global health problem

Toxoplasmosis refers to an infectious disease that is caused by an opportunistic parasite called *Toxoplasma gondii* (*Toxoplasma*) and is considered one of the most common parasitic zoonoses in the world. It is estimated that up to a third of the human population is infected with *Toxoplasma*, arguably rendering it the most successful parasite. However, the seroprevalence varies greatly between countries, with incidence rates ranging between almost 0% and 90% (Figure 1.1).

In European countries such as Austria, Belgium, France, Germany, Poland, Spain and the United Kingdom, seroprevalence has been estimated to range between 9.1% and 63.2% in pregnant women. Seroprevalence is higher in Latin American countries such as Argentina, Brazil, Columbia and Venezuela (6.1-77.5%) or African countries such as Ethiopia, Ghana and Democratic Republic of Congo (25.3-92.5%). Seroprevalence is lower in Asian countries such as China, India, Japan, Korea and Thailand (0.88-45%) (Table 1.1). However, the true magnitude of the disease is most likely unknown as toxoplasmosis remains asymptomatic in most cases and pregnant women and immune-compromised patients mainly constitute the cohorts of seroprevalence studies. The differences in toxoplasmosis incidence in various countries can be attributed to a preference for eating raw or undercooked meat, but also to a geographical localisation in a warm and low altitude climate favouring the survival of *Toxoplasma* oocysts. Indeed, epidemiologic studies have identified several risk factors for *Toxoplasma* infection: being in proximity to seropositive cats in farming areas (Weigel et al., 1999); cleaning an infected cat litter box (Kapperud et al., 1996); eating raw or undercooked meat including pork, mutton, lamb, beef or mincemeat products

(Kapperud et al., 1996; Baril et al., 1999; Weigel et al., 1999; Cook et al., 2000); gardening or being in contact with soil (Weigel et al., 1999; Cook et al., 2000); eating raw or unwashed vegetables and fruits and having poor hand hygiene (Baril et al., 1999).

Toxoplasmosis is responsible for high morbidity. In the United States (US), where *Toxoplasma* infects a predicted 1.1 million persons every year (Jones and Holland, 2010), studies investigating foodborne illness have estimated toxoplasmosis to be the major foodborne disease leading to hospitalisation (Mead et al., 1999; Vaillant et al., 2005; Scallan et al., 2011; Batz et al., 2012), the second cause of death among foodborne infections (Scallan et al., 2011; Batz et al., 2012) and a leading contributor to the loss of quality-adjusted life years (Havelaar et al., 2007; Scallan et al., 2011; Batz et al., 2012). Toxoplasmosis is a zoonotic disease that has impact from both a medical and a veterinary point of view. Economically, *Toxoplasma* infection is considered to be one of the most important diseases in animals and causes a variety of clinical manifestations in humans requiring different levels of health care. The annual economic impact of toxoplasmosis in the US, determined by medical costs, income losses and costs incurred by special education or residential care required as a result of a handicap caused by congenital toxoplasmosis, is estimated to be $7.7 billion (Roberts et al., 1994; Buzby and Roberts, 1996).

1.1.2 Toxoplasmosis: clinical manifestations

In immune-competent individuals, most *Toxoplasma* infections are asymptomatic. It is estimated that 10% to 20% of *Toxoplasma*-infected immune-competent adults and children will develop symptoms of toxoplasmosis (Remington, 1974). Since the description of the lymphadenopathic form of toxoplasmosis (Gard and Magnusson,

1951), it has been recognised as the most common clinical manifestation of the disease in humans. Fever, malaise, night sweats, myalgia, sore throat and abdominal pain might accompany lymphadenopathy. Thus, the signs of infection mimic the symptoms of very common infectious diseases. If present, the symptoms usually resolve within a few months and they rarely continue over a year. In less frequent cases, immune-competent individuals will develop encephalitis (Hemsath and Pinkerton, 1956), pneumonitis (Ludlam and Beattie, 1963), pericarditis (Jones et al., 1965), hepatitis (Vischer et al., 1967), myocarditis (Theologides and Kennedy, 1969; Cunningham, 1982; Montoya et al., 1997) or myositis (Greenlee et al., 1975; Montoya et al., 1997). Infection with *Toxoplasma* has been identified as a major cause of uveitis (Montoya and Remington, 1996; Holland et al., 1999), and it is responsible for more than 85% of chorioretinitis cases in Brazil (Silveira et al., 1988). Symptoms of acute toxoplasmic chorioretinitis include blurred vision, pain, and photophobia, and can result in partial or complete loss of vision. More recently, serological surveys have suggested chronic toxoplasmosis may be a risk factor for the development of schizophrenia or other human behavioural disorders (Yolken et al., 2001; Hinze-Selch et al., 2010; Okusaga et al., 2011; Gale et al., 2014; Markovitz et al., 2015; Celik et al., 2015; Monroe et al., 2015).

Congenital infection occurs when seronegative women acquire toxoplasmosis during pregnancy and transmit the infection to the foetus. Clinical manifestations of congenital toxoplasmosis depend on the time the infection was acquired *in utero*: they are most severe if transmission of infection occurs before 24 weeks of gestation, whereas transmission after week 26 results in subclinical disease that will develop later in life (Desmonts et al., 1985; Daffos et al., 1988). Clinical manifestations of congenital toxoplasmosis often affect the retina and the central nervous system with

symptoms including chorioretinitis, strabismus, blindness, epilepsy, psychomotor or mental retardation, encephalitis, microcephaly, hydrocephalus and pneumonitis (Remington et al., 2011).

Immune-deficient individuals are at high risk of severe *Toxoplasma* infection. This specific group of hosts includes patients receiving immunosuppressive therapy with corticosteroids or cytotoxic drugs, and individuals with organ transplant or acquired immune deficiency syndrome (AIDS). Severe clinical manifestations are usually the consequence of a reactivation of a latent infection and are usually fatal if not recognised and treated (Gallino et al., 1996). After the appearance of the AIDS epidemic, the frequency of *Toxoplasma* encephalitis increased (Horowitz et al., 1983; Roué et al., 1984; Velimirovic, 1984; Enzensberger et al., 1985; Suzuki et al., 1988; Israelski and Remington, 1988). *Toxoplasma* encephalitis was a major cause of death in HIV patients before the introduction of anti-retroviral therapy (Luft et al., 1983; 1984; 1993). In the setting of AIDS, patients with reactivated toxoplasmosis most often present symptoms of encephalitis (Luft and Remington, 1992) but also less frequently symptoms of pulmonary disease (Oksenhendler et al., 1990; Derouin et al., 1990; Rabaud et al., 1996) and eye disease (Holland et al., 1988). Recipients of heart, kidney and liver transplantation have also been diagnosed with reactivated toxoplasmosis (Aubert et al., 1996; Renoult et al., 1997; Giordano et al., 2002). Infection usually develops within three months after transplantation, and clinical symptoms may arise in the central nervous system, retina or lung as observed in AIDS patients (Fernàndez-Sabé et al., 2012).

1.1.3 Toxoplasmosis: diagnosis, treatment and prevention

Possible reactivation of latent toxoplasmosis and the discovery of *Toxoplasma* cysts in asymptomatic carriers enforced the need to develop accurate methods to diagnose toxoplasmosis, especially in expecting mothers and immune-compromised individuals. As clinical signs of human toxoplasmosis are often absent or non-specific, definite diagnosis of the disease is performed by serological, histological or molecular methods. Sabin and Feldman developed the first significant serological toxoplasmosis diagnosis, the dye test, in 1948. This test relies on antibody-mediated killing of live *Toxoplasma* in the presence of complement-activated antibodies. Intact, live *Toxoplasma* parasites retain a vital dye and appear blue under the microscope when incubated with methylene blue in the presence of normal serum. However, if incubated in the presence of serum containing anti-*Toxoplasma* antibodies from an infected patient, the parasite membrane is lysed by the complement-activated neutralising antibodies and does not retain the vital blue dye (Sabin and Feldman, 1948). Although highly sensitive and specific, the dye test requires *Toxoplasma* parasites to be constantly maintained in the analysis laboratory. The development of new methods to allow for detection of *Toxoplasma*-specific antibodies enabled circumvention of this issue. The first *Toxoplasma*-specific IgM assay was developed in 1968 by Remington *et al.* and proved to be a useful tool to diagnose congenital toxoplasmosis because IgM antibodies do not cross the placental barrier whereas IgG antibodies do (Remington et al., 1968). Other serological tests allowing detection of *Toxoplasma*-specific IgM antibodies include the indirect fluorescent antibody assay (IFA) (Miller et al., 1969), the enzyme-linked immunosorbent assay (ELISA) (Naot and Remington, 1980), the IgM-immunosorbent agglutination assay (IgM-ISAGA) (Desmonts et al., 1981) and by 1989, serological tests were successfully adapted to automated systems (Schaefer

et al., 1989). In immune-competent individuals, serological tests are the method of choice. However, serological diagnosis has been complemented with histological or molecular tests in immune-deficient individuals who might not reliably produce antibodies. Developed in 1989 by Burg *et al*. (Burg et al., 1989), the detection of *Toxoplasma* DNA by polymerase chain reaction (PCR) amplification in body fluids such as blood or amniotic and cerebrospinal fluids as well as in tissues has shown to be effective and more sensitive than any other technique (Romand et al., 2001).

There is no effective treatment available to date that can eradicate chronic toxoplasmosis. As a result, immune-competent individuals latently infected with *Toxoplasma* are usually not treated. However, in rare cases when symptoms arise, after organ transplantation or in immune-compromised individuals, prophylaxis must be undertaken. The standard treatment in these cases consists in a combined therapy with sulphonamides and pyrimethamine. Although individual efficacy of sulphonamides (Sabin and Warren, 1942) has been established, its effectiveness is eight-fold higher when synergised with pyrimethamine (Eyles and Coleman, 1953). Because it does not cross the placenta, spiramycin can be used prophylactically during pregnancy in order to reduce transmission of the parasite from the mother to the foetus (Garin and Eyles, 1958; Desmonts and Couvreur, 1974).

To date, drug treatment can only control the active proliferation of the parasite but does not eradicate infection. Thus, *Toxoplasma* vaccines -ideally for the various life cycle stages- would be extremely valuable in order to limit acute parasitemia and protect against congenital toxoplasmosis, to reduce tissue cysts in livestock and to reduce oocysts secretion in felids. The live but cystless *Toxoplasma* strain S48 has been used to develop an ovine vaccine. It has been shown to reduce the rate of abortion

in sheep to a limited extend (O'Connell et al., 1988; Wilkins et al., 1988). The protection conferred by this vaccine has been evaluated up to 18 months after the initial vaccination (Buxton et al., 1993). The resulting commercially available ovine vaccine, Toxovax™, is administered as a single shot prior to mating but needs to be repeated after 2 years (Buxton and Innes, 1995). This vaccine is only licenced for veterinary purposes, as it consists of a live *Toxoplasma*, which could potentially regain virulence. There is currently no vaccine available to prevent *Toxoplasma* infection in humans. However, several measures can be adopted to prevent or minimise the risks of contamination. These include hygienic methods such as avoiding contact with or washing hands after contact with cats and their litters, wearing gloves while gardening and washing raw fruits and vegetables thoroughly before consumption. Studies revealed *Toxoplasma* tissue cysts in meat can be killed by cooking at 67°C (Dubey et al., 1990), freezing at -13°C (Kotula et al., 1991) or exposing to 0.5 krad of gamma irradiation (Dubey and Thayer, 1994). Domestic cats should also be fed thoroughly cooked meat as an alternative to dry or canned food. The easiest and most economical method to reduce contamination through meat remains freezing fresh meat overnight before human or animal consumption. Recommendations for prevention of toxoplasmosis among pregnant women and HIV patients have been published (Centers for Disease Control and Prevention, 2000; USPHSIDSA, 1999).

1.2 Biology of *Toxoplasma gondii*

1.2.1 *Toxoplasma*: a brief history of its discovery

It has been more than a century since the discovery of *Toxoplasma* at the Pasteur Institute in Tunis. In 1908, while performing research on leishmaniasis using a hamster-like rodent called *Ctenodactylus gundi*, Nicolle and Manceaux discovered a

new protozoan in the tissues of two dead animals (Nicolle and Manceaux, 1908). At the same time, Splendore reported the existence of a similar organism in the tissues of a rabbit in Brazil (Nicolle and Manceaux, 1909; Splendore, 1908). As reported during a meeting at the 'Académie des Sciences' in Paris on the 26th of October that year, Nicolle and Manceaux first thought they had identified a new species of *Leishmania* and initially called the protozoan *Leishmania gondii* (Nicolle and Manceaux, 1908). They soon realised their mistake and created a new genus of protozoan in 1909 called *Toxoplasma gondii* based on the morphology of the parasite –*toxo* meaning arc or bow in Greek- and its initial host (Nicolle and Manceaux, 1909). As early as 1937 Sabin and Olitsky, two virologists working with guinea pig brains, noticed that *Toxoplasma* multiplication was only possible inside a living cell, describing it as an obligate intracellular parasite for the first time. They were also able to successfully passage *Toxoplasma* from animal to animal via intracranial, intraperitoneal or subcutaneous infections of brain inoculum. At a time when the possibility of an insect vector was still being investigated, Sabin and Olitsky reported the possibility that 'one method of natural dissemination may be by means of the eating of toxoplasma-contaminated tissues' after mice fed on *Toxoplasma*-infected mice also became infected. Interestingly, they noted the serum of recovering *rhesus* monkeys contained "neutralising" or "protective" antibodies (Sabin and Olitsky, 1937). The first reference of toxoplasmosis in humans came several decades after the parasite's discovery, when Janku described the case of a blind, deceased 11-month old baby who suffered from hydrocephalus and chorioretinitis and harboured parasitic cysts in his right eye (Janku, 1923). In 1939, three pathologists -Wolf, Cohen and Paige- firmly identified free and intracellular *Toxoplasma* parasites in tissues from a deceased congenitally infected newborn girl. Brain parasites isolates were successfully used to infect rabbits and mice

that developed encephalitis (Wolf et al., 1939a; b; 1940). These two cases were the first reports of human congenital toxoplasmosis. In 1941, Sabin described the case of a six year-old boy with the initials R.H. who was admitted to hospital several days after being hit with a baseball bat. Following his death, brain homogenate was injected into mice who died 21 days post-infection, and *Toxoplasma gondii* strain RH isolated from this child is still being used in the laboratory (Sabin, 1941). The same year, Pinkerton and Weinman isolated *Toxoplasma* from the tissues of two adults and were able to passage them in animals (Pinkerton and Henderson, 1941). These two cases were the first reports of acquired acute toxoplasmosis in young and adult humans. As the parasites were mainly found during post-mortem histopathology in patients suffering from encephalitis and/or chorioretinitis, toxoplasmosis was thought to only lead to acute infection. Kean and Plaut were the first to note the presence of *Toxoplasma* cysts in the heart and brain of deceased asymptomatic patients, suggesting for the first time the possibility of a chronic asymptomatic *Toxoplasma* infection (Kean and Grocott, 1945; Plaut, 1946; Kean and Grocott, 1947). These combined studies confirmed *Toxoplasma* as an obligate intracellular parasite, capable of congenital as well as acquired infections in humans (Table 1.2).

1.2.2 Life cycle of the parasite

Toxoplasma has a complex life cycle that consists of two discrete phases. The sexual part of the life cycle occurs in members of the feline family, which are the only known definitive hosts of *Toxoplasma* and therefore the main reservoirs of infection (Figure 1.2). The asexual part of the life cycle takes place in the intermediate host that can be any warm-blooded animal, including humans (Figure 1.3). Both stages are essential to the life cycle of the parasite.

The feline host becomes infected with tissue cysts of *Toxoplasma* through predation of infected animals. After ingestion, the tissue cyst wall is dissolved by proteolytic enzymes in the stomach and small intestine. As the cyst breaks, the discharged parasites actively invade the epithelial cells of the small intestine. In the feline intestine, *Toxoplasma* first undergoes an asexual development of five different stages before gametogony begins. Thus, the sexual cycle starts in the cat 2 days after inoculation, and gamonts can be found in the small intestine and ileum from 3 to 15 days after ingestion of the tissue cyst. An oocyst wall is formed around the parasite after fertilisation, the infected epithelial cells rupture and the oocysts are released into the intestinal lumen. Millions of unsporulated oocysts are finally shed 3 to 10 days after initial ingestion of tissue cysts (Frenkel et al., 1970; Dubey et al., 1970; Dubey and Frenkel, 1972). Although infected cats only shed oocysts for a limited period of time, the oocysts already sporulate and become infectious 1-5 days after shedding. Under laboratory conditions, these sporulated oocysts survived storage at 4°C for up to 54 months and freezing at −10°C for 106 days, while they survived at least 32 days at 35°C and 9 days at 40°C (Dubey, 1998). *Toxoplasma* sporulated oocysts released in the environment can thus survive for up to several years under the right climate conditions.

Intermediate hosts like livestock and humans can subsequently become ‘accidentally’ infected with *Toxoplasma* in several ways: ingestion of contaminated uncooked meat or unwashed vegetables (Kapperud et al., 1996; Baril et al., 1999; Weigel et al., 1999; Cook et al., 2000), faecal contamination of drinking water or hands by soil contact (Baril et al., 1999), transmission between humans through organ transplant (Aubert et al., 1996; Renoult et al., 1997; Giordano et al., 2002), and transmission from the infected mother to the unborn child (Wolf et al., 1939a; b; 1940). There are three

possible infectious stages of *Toxoplasma* in the intermediate host: the tachyzoites, the bradyzoites and the sporozoites. The latter refer to the parasites contained within the oocysts. The tachyzoites (*tachos* meaning speed in Greek) refer to the rapidly multiplying parasites in any nucleated cell of the intermediate host. The bradyzoites (*brady* meaning slow in Greek) describe the slowly replicating parasite within a tissue cyst. After ingestion of parasites by an intermediate host, the sporozoites or bradyzoites break the oocyst or tissue cyst wall, respectively. *Toxoplasma* parasites released in the small intestine must spread into the organism. They do so either by a transmigration route across the intestinal epithelium (Barragan and Sibley, 2002), or by parasitising neutrophils within the lumen that are capable of migrating through the intestinal epithelium to the lamina propria (Coombes et al., 2013), where they encounter more neutrophils, inflammatory monocytes and dendritic cells (DCs) (Gregg et al., 2013). They then use these leucocytes, especially hypermotile DCs, as "Trojan horses" to migrate via the intestinal lymphatic system to the secondary lymphoid organs, including the spleen and the lymph nodes (Zenner et al., 1998; Da Gama et al., 2004; Lambert et al., 2006; Bierly et al., 2008; Fuks et al., 2012; Weidner et al., 2013). *Toxoplasma* parasites continue their dissemination in the blood stream in order to reach other secondary organs (Unno et al., 2008; Silveira et al., 2011). In the blood, *Toxoplasma* parasites are preferentially found in monocytes if not free (Channon et al., 2000; Courret et al., 2006; Unno et al., 2008; Silveira et al., 2011). This defines the acute phase of the infection. Finally, *Toxoplasma* tachyzoites predominantly migrate to the brain and eye by a mechanism that still remains to be described. Studies have shown *Toxoplasma*-infected monocytes can cross an *in vitro* model of blood-brain barrier (Lachenmaier et al., 2011) and can also deliver the parasites to the mouse brain (Courret et al., 2006). Parasitised DCs are able to

transmigrate across the retinal endothelium (Furtado et al., 2012). Free tachyzoites can directly infect brain microvascular endothelial cells (Lachenmaier et al., 2011) and cross multiple layers of *ex vivo* retinal cultures (Furtado et al., 2013). Once in the brain, *Toxoplasma* may infect microglia, the resident macrophages in the brain, in order to potentiate their spread (Dellacasa-Lindberg et al., 2011). Finally, *Toxoplasma* tachyzoites convert into the slow-replicating and long-lasting bradyzoites organised in tissue cysts, distributed homogenously in the brain (Berenreiterová et al., 2011). This defines the chronic phase of the infection.

1.2.3 Ultrastructure of the parasite

The three infectious stages of *Toxoplasma* –namely the tachyzoite, the bradyzoite and the sporozoite– present the same basic morphological features with only minor variations. However, due to its ease to cultivate both *in vitro* and *in vivo*, the tachyzoite has been the most widely used and described. The *Toxoplasma* tachyzoite is a 2x7 μm crescent shaped cell that presents a pointed anterior end and a rounded posterior end. The anterior end is defined by the direction of motility and is also called apical or conoidal end. The ultrastructure of *Toxoplasma* tachyzoites was extensively investigated thanks to the advancement of electron microscopy (EM). In 1954-1956, Gustafson *et al.* and then Meyer and De Mendonça carried out the first EM studies of *Toxoplasma* tachyzoites (Gustafson et al., 1954; Meyer and De Mendonça, 2007; Meyer and Porter, 2008). Their work revealed that the parasite displays the same features as any eukaryotic organism, namely a nucleus, endoplasmic reticulum, Golgi apparatus and ribosomes (Figure 1.4). *Toxoplasma* also harbours two endosymbiosis-derived organelles, a mitochondrion and an apicoplast. The whole cell is enclosed

within a pellicle, a complex membrane comprising an outer plasmalemma and an inner layer formed by two closely applied membranes.

Electron microscopy also allowed the identification of three specialised organelles – rhoptries (Garnham et al., 1962), micronemes (Garnham et al., 1961; 1962) and dense granules (Ogino and Yoneda, 1966)– that are characteristic features of Apicomplexan parasites. Rhoptries are excretory structures situated between the anterior tip and the nucleus. There are 8 to 10 of these long club-shaped organelles, each consisting of an anterior narrow neck up to 2.5 μm long and a saclike posterior end up to 0.25x1 μm long. Micronemes are short rod-shaped structures (250x50 nm) mainly located at the most anterior end of the parasite. Dense granules (0.3 μm diameter) are found throughout the cell but mostly at the posterior end of the parasite. These three specific Apicomplexan organelles play a major and sequential role during invasion of the host cell.

Toxoplasma contains a nuclear genome of about 87 Mb organised on 11 chromosomes (Wilson and Williamson, 1997; Sibley et al., 1992). Phylogenetic analyses have shown that *Toxoplasma* comprises three major genotypic lineages referred to as types I, II and III, the majority of human isolates belonging to type II (Sibley and Boothroyd, 1992; Howe and Sibley, 1995; Johnson, 1997). Although these three strains vary in their virulence in mice, there are no appreciable structural differences among the three different isolates of *Toxoplasma*.

1.2.4 Host cell invasion

Toxoplasma is able to infect any nucleated host cell in any warm-blooded animal, including humans. *Toxoplasma* tachyzoites can enter the host cell by either active

penetration through the plasmalemma, or by phagocytosis. In the first instance, the process is entirely driven by the parasite, whose successful entry into the host cell will enable it to avoid host cellular defences such as acidification or endolysosomal hydrolases. *Toxoplasma* first glides on the potential host cell using an intricate linear motor system, and probes the host cell with its conoidal tip. Once it has targeted a cell to invade, adhesion molecules stored in the vesicular micronemes are the first proteins discharged in a calcium-dependent fashion in order to tighten attachment areas with the cell to be invaded (Carruthers and Sibley, 1997; Carruthers et al., 1999; Huynh et al., 2003; Cérède et al., 2005). The second wave of secretion involves the rhoptry neck proteins (RON), interacting with the microneme-derived AMA1 protein and forming a so-called moving junction that constitute an intimate binding interface of less than 6 nm (Mital et al., 2005; Alexander et al., 2005; Lebrun et al., 2005). Another secretion of rhoptry proteins (ROP) into the host cytoplasm triggers the invagination of the host cell plasma membrane and is instrumental in the formation of a parasitophorous vacuole (PV), where *Toxoplasma* tachyzoites reside and replicate inside the host cell (Suss-Toby et al., 1996; Carruthers and Sibley, 1997). Some ROP proteins including ROP2, ROP3, ROP4 and ROP7 remain associated with the PV membrane (PVM), while other ROP proteins remain soluble and may target to other sites in the host cell (Saffer et al., 1992; Carruthers and Sibley, 1997). Finally, as the PVM pinches off and separates from the host cell membrane, the dense granule proteins GRA1, GRA2, GRA3, GRA4, GRA5 and GRA6 are released into the PV as soon as its formation is complete (Ossorio et al., 1994; Carruthers and Sibley, 1997; Mercier et al., 1998a; b).

De novo formation of the rather large 30-33 μm^2 PVM occurs in an estimated 10-20 seconds interval. It has thus been postulated and demonstrated that the majority of lipids composing the PVM are host cell derived (Suss-Toby et al., 1996). On the other

hand, other host cell proteins are completely excluded from the *Toxoplasma* PVM. Indeed, the parasite regulates the contents of the PVM by preventing host proteins like SNAREs accumulating on the PVM (Suss-Toby et al., 1996). Thus, the PV never fuses with endolysosomes (Jones et al., 1972; Mordue and Sibley, 1997) and is resistant to acidification (Sibley et al., 1985), enabling the PV to provide a safe and protective place for the parasite to survive in the host cell, allowing it to persist despite a vigorous immune response.

The *Toxoplasma* route of entry into the host cell is critical to the fate of the vacuole. Apart from the active, parasite-driven invasion, *Toxoplasma* can also be phagocytosed by host cells. *Toxoplasma* tachyzoites can be opsonised with neutralising antibodies, leading to the acidification of the PV (Sibley et al., 1985) and its fusion with the lysosome in macrophages (Jones et al., 1972; Mordue and Sibley, 1997) or CHO cells expressing Fc receptors (Joiner et al., 1990). In this instance, the absence of a protective PV leads to neutralisation of the parasite, highlighting the importance of the PV in the immune escape mechanism inside the host cell. Nevertheless, *Toxoplasma* replication *in vivo* is restricted. The molecular mechanisms underlying the host-pathogen interactions by which the parasite maintains the delicate and intricate balance between induction and suppression of host immune responses to guarantee survival and host defence are not fully understood.

1.2.5 Division inside the host cell

Once the parasite has invaded the host cell and established the protective PV, it can start replicating by a specific event called endodyogeny. This highly complex process is unique as it enables indefinite proliferation. In this form of reproduction, the parasite grows and divides to form two progenies. Briefly, the Golgi apparatus is the first

organelle to divide, forming two complexes at the anterior end of the nucleus. The *Toxoplasma* nucleus then takes the shape of a horseshoe, and each end of the nucleus moves into the apical end of the developing progeny. The inner membrane complex continues to grow and encircle one half of the nucleus, eventually pinching it in two. The newly obtained daughters formed by endodyogeny are in turn able to undergo repeated cycles of asexual reproduction, giving rise to rosette-like structures within the PV. The host cell ruptures and releases the tachyzoites when it can no longer accommodate the replication of *Toxoplasma* parasites (Goldman et al., 1958; Garnham et al., 1962; Gavin et al., 1962; Sheffield and Melton, 1968).

1.3 Host defence mechanisms against intracellular pathogens

1.3.1 The immune system

Vertebrates are possible targets of infection by numerous pathogens, including viruses, bacteria and parasites. These pathogens vary greatly in their mode of pathogenesis, but also in their size, structure and complexity. To combat them, vertebrates have evolved a dynamic and intricate immune system able to distinguish between self and non-self that comprises two different sets of mechanisms: the early, unspecific innate immunity, and the slower, long-term adaptive immunity. The successful immune response will result in the control or clearance of the pathogen, whilst limiting off-target impact and damage to the host. The constituents of the innate immunity are for the most part constitutively present and thus provide an immediate and maximal response to infection. In contrast, the adaptive immune system is pathogen-specific and hence requires time to develop an effective response. However, it involves the capacity for immunological memory, allowing a more rapid and specific response in the case of a future re-infection (Janeway, 2001).

Innate immunity is the first line of defence against infective pathogens. It is orchestrated by several cell types including macrophages, dendritic cells (DCs), natural killer (NK) cells and neutrophils. These cells carry receptors called pattern recognition receptors (PRRs) that can be triggered by different sensing mechanisms. PRRs are able to recognise and bind distinct molecular signatures associated with infections. These signatures can be pathogen-associated molecular patterns (PAMPs) or danger-associated molecular patterns (DAMPs). PAMPs are immunostimulatory invariant structures shared by large groups of microorganisms. They represent essential components for the function and survival of pathogens, are absent from the host organism and hence direct the targeted host cell to discriminate self from non-self. Classical PAMPs recognised by the PRRs are microbial nucleic acids (including DNA (Hemmi et al., 2000; Hornung et al., 2009; Fernandes-Alnemri et al., 2009), double- or single-stranded RNA (Kanneganti et al., 2006; Sabbah et al., 2009; Sander et al., 2011)), but also microbial lipoproteins (Aliprantis et al., 1999; Hirschfeld et al., 1999), surface glycoproteins (Opitz et al., 2001) or membrane components such as peptidoglycans (Yoshimura et al., 1999; Schwandner et al., 1999) or lipopolysaccharide (Poltorak et al., 1998; Hoshino et al., 1999). On the contrary, DAMPs are host components that are presented in an abnormal cellular context, such as host molecules released from stressed or damaged cells (uric acid (Shi et al., 2003), chromatin protein HMGB1 (Scaffidi et al., 2002), cytoplasmic DNA (Hornung et al., 2009; Fernandes-Alnemri et al., 2009; Sun et al., 2013a; Wu et al., 2013)) or components from damaged pathogen-containing vacuoles (extracellular hyaluronan fragments (Scheibner et al., 2006) or luminal glycans (Dupont et al., 2009; Paz et al., 2010; Thurston et al., 2012)). Various PRRs are targeted to specific subcellular compartments. Toll-like receptors (TLRs) are membrane-bound sensors and can bind

to ligands that are present on the cell surface or in endosomal vesicles (Yang et al., 1998; Kirschning et al., 1998; Qureshi et al., 1999; Schwandner et al., 1999; Underhill et al., 1999; Yoshimura et al., 1999; Campos et al., 2001; Opitz et al., 2001; Debierre-Grockiego et al., 2007; Alexopoulou et al., 2001; Poltorak et al., 1998; Hoshino et al., 1999; Hayashi et al., 2001; Takeuchi et al., 2001; Hemmi et al., 2000; Foureau et al., 2010). By contrast, NOD-like receptors (NLRs) (Chamaillard et al., 2003; Girardin et al., 2003b; a), DExD/H box (Asp–Glu–x–Asp/His box) helicases (Kang et al., 2002; Kato et al., 2005; Yoneyama et al., 2004; Rothenfusser et al., 2005; Saito et al., 2007; Satoh et al., 2010), and PYHIN (pyrin and HIN200 domain-containing) proteins (Hornung et al., 2009; Fernandes-Alnemri et al., 2009; Jones et al., 2010) are cytosolic sensors and can bind to ligands present in the cytosol. Ligand binding and subsequent activation of most PRRs leads to an inflammatory state that is characterised by the secretion of inflammatory cytokines and chemokines. These proteins work as mediators of the immune and inflammatory reactions by alerting the neighbouring cells of the infection (Janeway, 2001).

Adaptive immunity is triggered at a later stage of the infection and is orchestrated by two classes of effector cells called B lymphocytes and T lymphocytes. Both cell types recognise specific pathogen-derived antigens. B cells are central to humoral adaptive immunity and produce antibodies specific to the antigen they bind. T cells are only able to recognise antigen peptides that are presented by antigen presenting cells via the major histocompatibility complex (MHC). There are two subtypes of T cells: CD4+ helper T cells detect peptides presented by MHC II molecules and then activate macrophages and promote B cell antibody production, while CD8+ cytotoxic T cells recognise peptides displayed on MHC I molecules and once activated, kill infected cells (Janeway, 2001).

1.3.2 Compartmentalisation as a mean to escape the host immune system

Many intracellular microorganisms, including bacteria and protozoan parasites, have evolved specialised mechanisms to reside and replicate inside the host cell within plasma membrane-derived compartments called vacuoles. These vacuoles are formed during the uptake of the pathogen and separate it from the host cytosol. The uptake process can either be active if the pathogen itself drives invasion into the host cell, or it can occur by passive internalisation if the mechanism is host-driven in the case of phagocytosis. Regardless of the uptake mechanism, vacuolar pathogens will reside in a compartment that provides them with a secure niche. It is likely that vacuole-bound pathogens have developed a sequestered lifestyle in the vacuolar niche over residing in the nutrient rich cytoplasm to avoid host immune surveillance pathways (Randow et al., 2013). Several potential mechanisms can be deployed in order to establish the protective pathogenic vacuole. Shortly after invasion, many intracellular vacuolar pathogens hijack the host endomembrane system, thereby preventing or delaying the fusion with lysosomes. Originally, the vacuole is composed of host-derived membranes and shares molecular components of early endosomes. However, to resist acidification and avoid endolysosomal fusion, these compartments are gradually modified by pathogen-derived proteins and lipids translocated via secretion systems, leading to a decreased fusogenicity with host vesicules and organelles. The specificity of membrane fusion events is dictated by the presence of Rab proteins, SNAREs and tethering factors. Many vacuolar pathogens alter their recruitment to the vacuole to establish the replicative niche (Alix et al., 2011). For example, *Mycobacterium*-containing vacuoles present features of early endosomes and arrest the phagosome maturation process via the action of secreted bacterial factors such as SapM, ManLAM and PtpA that inhibit the recruitment and activity of phosphatidyl inositol 3-phosphate

effectors and Rab7 at the vacuole (Vergne et al., 2005; Bach et al., 2008). *Legionella* intercepts early secretory vesicles exiting the endoplasmic reticulum (ER) to modulate the features of its vacuole, hence avoiding lysosomal compartments. Arf1, which is implicated in vesicle budding and recycling at the Golgi apparatus, is recruited to the *Legionella*-containing vacuole by the bacterial protein RalF (Kagan and Roy, 2002). Sar1, which is involved in the formation of vesicles that exit from the ER and Sec22b, which is involved in the docking of ER-derived vesicles at the Golgi apparatus, are also recruited to the *Legionella*-containing vacuole, although the mechanism of recruitment remains unclear (Kagan and Roy, 2002; Kagan et al., 2004). Finally, as described previously, *Toxoplasma*-containing vacuoles are completely devoid of any host membrane feature and are thus disconnected from the classical host vesicular trafficking pathways (Jones et al., 1972; Jones and Hirsch, 1972).

Other potential mechanisms may also be employed for the critical maintenance of the integrity and stability of pathogenic vacuoles. Several microorganisms modulate their hosts' cytoskeletal functions to maintain and stabilise the intracellular vacuole. For example, *Salmonella* and *Chlamydia* species inject bacterial effectors into the host cytosol via secretion systems, inducing local polymerisation of actin and intermediate filaments to consolidate their vacuole. The *Salmonella* secreted effector SteC is required for the remodelling of the F-actin filament network around the *Salmonella*-containing vacuole (Poh et al., 2008). The *Chlamydia* secreted effectors RhoA and CPAF contribute to the formation of a dynamic scaffold of host cytoskeletal structures consisting of F-actin and intermediate filaments of vimentin and cytokeratin surrounding the *Chlamydia*-containing vacuole (Kumar and Valdivia, 2008).

Pathogenic secretion systems and virulence factors help to maintain vacuolar integrity and stability essential for its protective property. However, they can also constitute an opportunity for the host to detect the presence of an invading organism. Mammalian hosts have evolved multiple strategies to unmask the pathogen hiding in its vacuole, thereby leading to the engagement of powerful antimicrobial responses and the onset of robust inflammatory responses.

1.3.3 Cytosolic recognition of pathogens: the autophagy pathway

Autophagy is a fundamental cell survival mechanism that consists of capturing cytosolic organelles and proteins into double-membrane vesicles called autophagosomes in order to deliver them by fusion to lysosomes for degradation or elimination. Meaning 'self-eating' in Greek, autophagy enables the cell to generate an autonomous source of amino acids and energy when facing nutritional deprivation (Takeshige et al., 1992; Kuma et al., 2004), but also to prevent cell death in the presence of protein aggregates or faulty organelles (Elmore et al., 2001; Ravikumar et al., 2002; Fortun et al., 2003; Narendra et al., 2008). The process of autophagy can be deconstructed into four steps (nucleation, expansion, fusion and degradation) and involves 35 autophagy-related (ATG) proteins and other autophagy interaction network components (Figure 1.5). First, the initiation stage is characterised by the formation of a crescent-shaped isolation membrane called phagophore (Mizushima et al., 2001). The phagophore can be formed from rough endoplasmic reticulum (Hayashi-Nishino et al., 2009; Ylä-Anttila et al., 2009), Golgi apparatus (Yen et al., 2010), mitochondria (Hailey et al., 2010) and plasma cell membrane (Ravikumar et al., 2010). The vacuolar protein sorting 34 (Vps34), a class III phosphatidylinositol 3-kinase (PI3K), complexes with Beclin 1, ATG14 and p150 and phosphorylates lipids

on the targeted membranes destined to become the phagosome (Volinia et al., 1995; Panaretou et al., 1997; Mizushima et al., 2003b; Blommaart et al., 1997; Liang et al., 1999; Petiot et al., 2000; Kihara et al., 2001a; b; Itakura et al., 2008). Second, the small nascent phagophore elongates by recruiting effector proteins such as WD-repeat protein interacting with phosphoinositides 1 (WIPI1) that triggers the expansion of the developing membrane (Proikas-Cezanne et al., 2004). This expansion step is also promoted by the action of two ubiquitin-like conjugation systems. The first is an ATG12-ATG5-ATG16 complex (Suzuki et al., 2001; Mizushima et al., 2001; 2003b; a), that is formed by conjugation of ATG12 with ATG5 mediated by the E1-like enzyme ATG7 and the E2-like enzyme ATG10. ATG12-ATG5 subsequently complexes with ATG16. This forms an E3-like system that mediates the conjugation of the second complex between the microtubule-associated protein 1 light chain 3 (LC3) and phosphatidylethanolamine (PE), complex also termed LC3II (Kabeya et al., 2000). At this stage, most of the proteins involved in the genesis of the autophagosome (unconjugated LC3I and ATG12-ATG5-ATG16 complex) are recycled back into the cytosol, and LC3II remains the major protein located at the inner membrane of the phagophore (Kabeya et al., 2000; Fujita et al., 2008). LC3II has the ability to bind autophagy receptors such as p62 (Komatsu et al., 2007) and NDP52 (Thurston et al., 2009), allowing selection of the cargo to be engulfed in the forming autophagosome. Third, the autophagosome fuses with a lysosome in the presence of lysosomal membrane-associated protein 2 (LAMP2) and become an autolysosome (Huynh et al., 2007). Finally, as lysosomes are vesicles containing a wide range of hydrolases maintained at an acidic pH, the autolysosome allows the degradation of the luminal content through acidification and hydrolysis. The degradation products are

translocated out of the autolysosome by lysosomal transporters such as ATG22 to allow reuse in metabolic processes, and the membrane is recycled (Yang et al., 2006).

Mammalian cells have evolved the fundamental biological process of autophagy to apply it to the clearance of invading microorganisms, including vacuolar pathogens. This autophagy-mediated breakdown of pathogens has been called "xenophagy", from the Greek "to eat foreign matter" (Levine, 2005). In the context of an intracellular infection, the process of selective xenophagy is triggered by the detection of PAMPs or DAMPs by PRRs, leading to the recruitment of autophagy receptors or adapters that deliver the cytoplasmic or vacuolar microorganisms to the lysosome for clearance. For example, recognition of viral RNA or bacterial lipopolysaccharide by TLRs activates autophagy (Xu et al., 2007; Sanjuan et al., 2007; Delgado et al., 2008). Similarly, detection of bacterial peptidoglycan by NLRs also triggers autophagy activation (Travassos et al., 2010b; Cooney et al., 2010; Travassos et al., 2010a). The selectivity of xenophagy is conferred by the help of cytosolic autophagy sensors called sequestasome-like receptors (SLRs) or LC3-interacting regions (LIR) proteins. These autophagy receptors, including the proteins p62 (Pankiv et al., 2007), NBR1 (Thurston et al., 2009), NDP52 (Thurston et al., 2009), and optineurin (Wild et al., 2011) recognise and capture ubiquitinated targets via their ubiquitin-binding domain (UBD) for delivery to the LC3-positive nascent autophagosome via their LIR (Thurston et al., 2009; Dupont et al., 2009; Zheng et al., 2009; Orvedahl et al., 2010). Intracellular vacuolar pathogens known to be targeted by xenophagy include *Mycobacterium* (Gutierrez et al., 2004; Alonso et al., 2007), *Legionella* (Amer and Swanson, 2005; Khweek et al., 2013) and *Chlamydia* (Al-Zeer et al., 2009; 2013). The best-characterised xenophagy system so far remains for the targeting and clearance of *Salmonella* and will be discussed in more details.

Salmonella typhimurium is a facultative intracellular bacterium that resides and replicates within a containing vacuole called SCV. However, following type III secretion system (T3SS)-mediated damage of the SCV, a small proportion of *Salmonella* resides in damaged vacuoles or escapes in the cytosol of the host cell (Beuzón et al., 2000; Brumell et al., 2002; Perrin et al., 2004). Autophagy has been shown to restrict the cytosolic replication of *Salmonella in vitro* (Birmingham et al., 2006), and this can be achieved by not less than 6 different host mechanisms (Figure 1.6). One possible autophagy activation signal is the production of diacylglycerol (DAG) in response to the secretion of bacterial proteins into the host cytosol via the T3SS. DAG acts as a specific lipid second messenger to initiate the recruitment of LC3 to the SCV (Shahnazari et al., 2010). The E3 ubiquitin ligase LRSAM1 has been shown to directly recognise *Salmonella* via its LRR domain, leading to ubiquitination associated with the bacterium. LRSAM1 also participates in the recruitment of LC3-positive autophagosome by binding to the autophagy receptor NDP52 via its LRR domain (Huett et al., 2012). Both cytosolic and damaged SCV can be targeted by ubiquitination (Perrin et al., 2004; Fujita et al., 2013), providing the recognition signal for the autophagy receptors p62, NDP52 and optineurin which link the ubiquitinated target to LC3-positive autophagosome for clearance through LIR (Thurston et al., 2009; Zheng et al., 2009; Wild et al., 2011). In all three studies, RNA silencing demonstrated restriction of *Salmonella* by autophagy is dependent on p62, NDP52 or optineurin. Finally, galectin-8 has recently been identified as a danger receptor that can detect damaged SCV. Galectin-8 is a lectin that binds to β-galactoside sugars that are usually localised inside endosomal or lysosomal vesicles. The disruption of the β-galactosides-containing SCV provides access to the newly exposed host glycans. Galectin-8 binds to these sugars and subsequently recruits the autophagy receptor

NDP52 to the site of *Salmonella* infection, thereby directing autophagy that translates into the recruitment of LC3-positive autophagosome (Thurston et al., 2012).

Autophagy has also been linked to resistance during *Toxoplasma* infection. Interestingly, electron microscopy showed ultrastructral evidence of the autophagic elimination of *Toxoplasma* in IFNγ-stimulated macrophages. Following vacuolar disruption, released *Toxoplasma* are engulfed in autophagosome-like vesicles that subsequently fuse with lysosomes (Ling et al., 2006). ATG5 is required for IFNγ-dependent disruption of the PV, and ATG5 mediates the control of *Toxoplasma* replication both *in vitro* and *in vivo* (Zhao et al., 2008; Selleck et al., 2013). More recently, the autophagy proteins ATG3, ATG7 as well as the ATG12-ATG5-ATG16 complex were reported to mediate the disruption of avirulent *Toxoplasma* PV by LC3 and IFNγ effector proteins (Choi et al., 2014).

1.3.4 Cytosolic recognition of pathogens: the inflammasome pathway

Following invasion by a pathogen, cytosolic NLRs detect the presence of the intruder or a disruption of the cellular compartment integrity and mediate the activation of a specific innate immune response called the inflammasome. Inflammasomes are multimeric complexes that comprise a sensor protein, an adaptor protein and the inactive zymogen procaspase-1. The sensor protein can be an NLR receptor or an AIM2-like receptor (ALR). The adaptor protein is an apoptosis-associated speck-like protein containing a C-terminal CARD (caspase activation and recruitment domain) termed ASC. After activation by microbial products, the NLRs or ALRs oligomerise via their NACHT or HIN200 domain, respectively, and recruit ASC via an interaction involving the pyrin domain (PYD) of the adaptor protein and the PYD of the receptor (Vajjhala et al., 2012). Finally, ASC recruits the zymogen procaspase-1 in the complex

through its CARD domain (Cai et al., 2014; Lu et al., 2014) (Figure 1.7). This assembled molecular platform promotes the cleavage of inactive procaspase-1 into the active enzyme caspase-1, which further cleaves and activates the inactive inflammatory cytokines pro-IL-1β and proIL-18 into their active counterparts: IL-1β and IL-18 (Kostura et al., 1989; Black et al., 1989; Thornberry et al., 1992; Walker et al., 1994; Ayala et al., 1994; Li et al., 1995; Alnemri et al., 1996; Gu et al., 1997). Activation of the inflammasome also leads to a programmed cell death called pyroptosis, resulting in the release of the produced inflammatory cytokines. After pyroptosis, the inflammatory response can be amplified and prolonged by the accumulation of released ASC oligomers into the extracellular environment, where they will continue to activate caspase-1 for subsequent processing of extracellular IL-1β (Franklin et al., 2014; Fink et al., 2008; Baroja-Mazo et al., 2014).

Although NLRs and ALRs are able to detect the presence of microbial products, a direct interaction with their pathogenic stimuli has not been shown so far. Inflammasomes can be activated by extracellular, vacuolar or intracellular bacteria, viruses and protozoans. The nature of the microbial stimuli determines the specific sensor that will be activated to induce the inflammasome cascade and to translate it into a successful inflammatory response leading to clearance of the microorganism. In the case of vacuolar pathogens (Figure 1.8), *Legionella* and *Salmonella* have been shown to induce the activation of the NLRC4 inflammasome via the bacterial flagellin or protein components of the bacterial secretion systems (Amer et al., 2006; Lightfield et al., 2008; Molofsky et al., 2006; Franchi et al., 2006; Miao et al., 2006). Until recently, the NLRP1 inflammasome was thought to only be activated by a single signal, the anthrax lethal toxin secreted by *Bacillus anthracis* (Boyden and Dietrich, 2006; Fink et al., 2008). This NLRP1 activation does not require the adaptor protein

ASC, but necessitates ubiquitination of caspase-1 (Van Opdenbosch et al., 2014; Broz et al., 2010). However, *Toxoplasma* has now also been shown to activate the NLRP1 inflammasome in both human and rodent cell lines, leading to the restriction and killing of the parasite as well as the upregulation of the protective pro-inflammatory cytokine IL-1β (Lees et al., 2010; Witola et al., 2011; Ewald et al., 2013). More recently, both the NLRP1 and the NLRP3 inflammasomes have been reported to confer resistance to *Toxoplasma* infection *in vivo*, mediating the protective production of the pro-inflammatory cytokine IL-18 in the serum of mice (Gorfu et al., 2013).

1.3.5 Cytosolic recognition of pathogens: the antibody-dependent intracellular neutralisation (ADIN) pathway

Immunoglobulins (Ig), or antibodies (Ab), are a critical player in the defence against invading pathogens. Their importance is highlighted by the fact that an inability to mount an effective humoral response often leads to a persistent, or even fatal, infection. Immunoglobulins are glycoproteins produced by plasma B cells that can either be membrane-associated on B cells, or secreted as soluble circulating antibodies. Their function consists in recognising and binding to specific antigens, thereby helping eliminating the antigen or the microorganism harbouring this antigen (Male et al., 2006).

Immunoglobulins are constructed in a uniform manner, characterised by the combination of four polypeptide chains: two identical heavy chains and two identical light chains (Figure 1.9). The immunoglobulin molecule presents a variable region encompassing the N-terminal domains of each heavy and light chain (V_H and V_L, respectively) that is involved in antigen binding and is called Fab (fragment antigen binding). The C-terminal domains of the heavy and light chains form the constant

region (C_H and C_L, respectively) that distinguishes the five classes of immunoglobulin and is termed Fc (fragment crystallisable) (Porter, 1959; Inbar et al., 1972). The Fab fragment of the immunoglobulin provides the specificity for the recognition of the three-dimensional conformation of the antigen, called epitope. The Fc fragment of the immunoglobulin is recognised by Fc receptors expressed on the surface of innate immune cells such as monocytes, macrophages, neutrophils and NK cells (Jondal and Pross, 1975; West et al., 1977; Anderson, 1982; Fleit et al., 1982; Cohen et al., 1983). There are five classes of immunoglobulins in mammals: IgG (70% of total serum Igs), IgA (15% of total serum Igs), IgM (10% of total serum Igs), IgD and IgE. Their interaction with an Fc receptor triggers the immune response such as phagocytosis – termed antibody-dependent cellular phagocytosis (ADCP) (Leslie, 1980; Mellman, 1982; Mellman et al., 1983)–, or cell killing –called antibody-dependent cellular cytotoxicity (ADCC) (Rosenberg et al., 1972; Oldham and Herberman, 1973; Rakebrandt et al., 2014; Herberman et al., 1975a; b; Kiessling et al., 1975a; b)–.

Since their discovery in 1890 (Behring and Kitasato, 1890; Behring, 1890) and until recently, immunoglobulins were believed to provide protection exclusively in the extracellular environment. Pathogens were considered safe from immunoglobulins once inside the host cell. Recently, antibodies have been shown to mediate antiviral and antibacterial protection inside the host cell (McEwan et al., 2013; Mallery et al., 2010; Rakebrandt et al., 2014). This newly identified mechanism has disputed the dogma that antibodies do not have an intracellular function and has been termed antibody-dependent intracellular neutralisation or “ADIN” (Figure 1.10). Mallery *et al.* showed that adenovirus, a non-enveloped virus, is coated with immunoglobulins in the extracellular medium and carries them into the host cell after invasion. Following release from the endosomal compartment, antibody-coated viruses are sensed by a

newly discovered and ubiquitously expressed cytoplasmic antibody receptor called tripartite motif-containing protein 21 (TRIM21) (Mallery et al., 2010). McEwan *et al*. as well as Rakebrandt *et al*. demonstrated that TRIM21 also binds to antibodies surrounding intracellular, IgG-opsonised *Salmonella* (McEwan et al., 2013; Rakebrandt et al., 2014). Structural and biochemical studies have revealed that TRIM21 is characterised by a C-terminal B30.2/PRYSPRY domain that is able to strongly bind to the Fc part of immunoglobulins (Rhodes and Trowsdale, 2007; Keeble et al., 2008; Mallery et al., 2010). TRIM21 binds symmetrically to the immunoglobulin, allowing TRIM21 dimers to bind both heavy chains of the antibody at the same time. The formation of this TRIM21-immunoglobulin complex leads to an exceptionally high binding affinity, as TRIM21 is the strongest IgG receptor so far described in humans with an affinity of about 0.2-0.5 nanomolar (nM) (Keeble et al., 2008; Mallery et al., 2010). Additionally, TRIM21 has been shown to be able to bind to other classes of immunoglobulins such as IgM (17 nM) (Mallery et al., 2010) and IgA (50 nM) (Bidgood et al., 2014). The IgG receptor binding property was shown to be conserved and functionally interchangeable through murine, canine, primate and human species, suggesting an important biological role for TRIM21 (Keeble et al., 2008). In all the above investigations, restriction of the pathogen was dependent on the presence of both TRIM21 and antibodies. The TRIM21- and antibody-dependent mediation of adenoviral infection is also important *in vivo*, as TRIM21 KO mice injected with protective antisera still succumb viral infection (Vaysburd et al., 2013).

These studies position TRIM21 as a potential new DAMP receptor, alerting the cell of the presence of misplaced antibodies in the cytosol. However, in both viral and bacterial infections that were investigated, TRIM21 function did not solely consist of the recognition of antibody-bound pathogens. TRIM21 also possesses a really

interesting new gene (RING) domain exhibiting an E3 ubiquitin ligase activity (Meroni and Diez-Roux, 2005), and uses it to label the adenovirus and *Salmonellae* for degradation by the proteasome or possibly autophagy, respectively (Mallery et al., 2010; Rakebrandt et al., 2014). TRIM21 has also been shown to trigger a non pathogen-specific immune signalling that involves the activation of nuclear factor κB (NF-κB), activating protein-1 (AP-1) and interferon regulatory factors IRF3, IRF5 and IRF7 (McEwan et al., 2013). As antibody-coated latex beads can be detected by TRIM21, be subsequently labelled with ubiquitin (Mallery et al., 2010) and prompt the activation of TRIM21 immune signalling (McEwan et al., 2013), TRIM21 could be an important intracellular receptor mediating resistance against pathogens yet to be identified.

1.4 Early immune responses to *Toxoplasma* infection

1.4.1 Innate immunity against *Toxoplasma* infection

Mice are natural intermediate hosts of *Toxoplasma* and are widely used as laboratory animal models to study the mechanisms of host resistance to the parasite. Moreover, human clinical presentation of *Toxoplasma* is diverse, but can be mimicked in animal models by choosing the appropriate genetic background of mice combined with varying strains of *Toxoplasma* (Munoz et al., 2011). In the mouse model, the acute phase of infection lasts approximately 10 days. After invasion of the host cell, *Toxoplasma* activates the two surface PRRs Toll-like receptors TLR2 and TLR4 on monocytes and macrophages through its glycophosphatidylinositol (GPI) anchors (Debierre-Grockiego et al., 2007), as well as the endosomal PRRs termed TLR11 and TLR12 in dendritic cells through a protein called profilin (Yarovinsky, 2005; Raetz et al., 2013) (Figure 1.11). These activated cells are then triggered to produce cytokines

such as IL-12 and tumor necrosis factor alpha (TNFα). Production of IL-12 promotes differentiation and proliferation of both $CD4^+$ and $CD8^+$ T cells as well as natural killer cells, leading to an enhanced secretion of interferon gamma (IFNγ) (Khan et al., 1994; Gazzinelli et al., 1993; Hunter et al., 1994). This type II interferon, the major mediator of resistance against *Toxoplasma*, in turn activates the host's non-haematopoietic cells as well as haematopoietic cells, amongst them macrophages, to elicit antimicrobial activities. In order to hinder the replication of the parasite, the production of nitric oxide (NO) is triggered (Murray et al., 1985; Adams et al., 1990). This has been shown to be important during the chronic phase of the infection only (Scharton-Kersten et al., 1997). Moreover, type II interferon mediates the transcriptional upregulation of two classes of large GTPases called p47 immunity related GTPases or IRGs (Taylor et al., 2004; Taylor, 2007) and p65 guanylate binding proteins or GBPs (Virreira Winter et al., 2011; Yamamoto et al., 2012; Degrandi et al., 2007) that will be discussed in more details.

1.4.2 The family of IFNγ-inducible large GTPases

In mammals, interferon γ was identified as a major pro-inflammatory cytokine that mediates resistance against many intracellular pathogens, including *Toxoplasma*. Among the hundreds of genes that are upregulated by interferons after infection (de Veer et al., 2001), four families of large GTPases are of particular interest: myxovirus resistance (Mx) proteins (Nakayama et al., 1991), very large inducible GTPases called VLIGs (Klamp et al., 2003), p47 immunity-related GTPases termed IRGs (Gilly and Wall, 1992; Carlow et al., 1995; Lafuse et al., 1995; Sorace et al., 1995) and p65 guanylate-binding proteins called GBPs (Cheng et al., 1983; Staeheli and Sutcliffe,

1988). These IFNγ-inducible GTPases play important roles during pathogen infections.

The family of Mx proteins comprises two human proteins (MxA and MxB) encoded by genes mapped to chromosome 21 (Horisberger et al., 1988; Petersen et al., 1991), and their murine orthologs (MX1 and MX2) encoded by genes localised on chromosome 16 (Staeheli et al., 1986a; Staeheli and Sutcliffe, 1988; Reeves et al., 1988). The Mx proteins are mainly upregulated by type I interferons IFNα/β and type III interferon λ. The Mx proteins were discovered in an inbred mouse strain that exhibited a natural resistance to infection with influenza A viruses (Lindenmann, 1964; Horisberger et al., 1983). Expression of the MX1 protein was shown to confer selective resistance to viral infection by intrinsic antiviral activity, both *in vitro* and *in vivo* (Staeheli et al., 1986b; Arnheiter et al., 1990). Mice naturally susceptible to influenza infection have been reported to carry a defective *Mx1* gene (Staeheli et al., 1988), and IFNαR−deficient mice constitutively expressing human MxA were shown to survive lethal viral infections (Hefti et al., 1999). Since these first discoveries, human and mouse Mx proteins have been shown to be involved in resistance to a wide range of viruses, including *orthomyxoviridae* (influenza virus (Lindenmann, 1964; Krug et al., 1985; Staeheli et al., 1986b; Pavlovic et al., 1995; Hefti et al., 1999), Thogoto virus (Haller et al., 1995; Pavlovic et al., 1995; Frese et al., 1995; Kochs and Haller, 1999; Hefti et al., 1999), Dhori virus (Thimme et al., 1995), Batken virus (Collazo et al., 2001; Leroy et al., 2006; Klamp et al., 2003; Frese et al., 1997; Li et al., 2009a)}), *rhabdoviridae* (vesicular stomatitis virus (Pavlovic et al., 1995; 1990), rabies virus (Leroy et al., 2006)), *bunyaviridae* (Hantaan River virus (Jin et al., 2001), La Crosse virus (Frese et al., 1996; Hefti et al., 1999; Kochs et al., 2002; Reichelt et

al., 2004)), *paramyxoviridae* (measles virus (Schnorr et al., 1993; Schneider-Schaulies et al., 1994)), *hepadnaviridae* (hepatitis B virus (Gordien et al., 2001; Yu et al., 2008)) and more recently, *retroviridae* (HIV-1 (Goujon et al., 2013; Kane et al., 2013; Liu et al., 2013)). The broad range of antiviral action the Mx proteins exhibit implies that intricate and various mechanisms are involved. Several studies on the mode of action against a few viruses have demonstrated the Mx proteins may inhibit viral replication through direct interaction with essential viral components (Staeheli et al., 1986c; Haller et al., 2015).

The family of VLIGs comprises 4 putative active members and 7 pseudogenes mapped on murine chromosome 7. The two human orthologous genes, localised on chromosome 11, are deemed pseudogenes (Klamp et al., 2003; Li et al., 2009a). The murine protein VLIG1 is the only family member characterised so far, and its expression has been shown to be upregulated in the liver following infection with *Listeria monocytogenes*. As IFNγR$^{-/-}$-infected mice did not exhibit an increased expression of VLIG1 in the liver, its regulation is dependent on IFNγ (Klamp et al., 2003). No further studies on its role during infection, or on the other putative VLIGs, have been undertaken so far.

The family of p47 IRGs has been more widely studied in mouse during diverse pathogen infections. Indeed, murine IRGs have been shown to possess essential antimicrobial activity during infection involving intracellular pathogens such as *Listeria* (Collazo et al., 2001), *Mycobacterium* (MacMicking et al., 2003), *Chlamydia* (Bernstein-Hanley et al., 2006), *Salmonella* (Henry et al., 2007), *Trypanozoma* (Santiago et al., 2005) and *Toxoplasma* (Taylor et al., 2000; Collazo et al., 2001; Halonen et al., 2001). Collazo *et al*. showed Irgm1$^{-/-}$ mice fail to control *Listeria*

monocytogenes infection, exhibiting a high bacterial burden 3 days post-infection in the spleen and the liver, as well as an increased level of the cytokine IL-12 in the serum (Collazo et al., 2001). Similarly, MacMicking *et al*. reported Irgm1$^{-/-}$ mice to be highly susceptible to *Mycobacterium tuberculosis* infection. They showed Irgm1$^{-/-}$ macrophages exhibit a decreased bacterial killing compared to WT controls, which was attributed to an impaired lysosomal fusion and subsequent acidification of the *Mycobacterium*-containing phagosome (MacMicking et al., 2003). Bernstein-Hanley *et al*. demonstrated that both Irgb10 and Irgm3 are required to restrict *Chlamydia trachomatis* growth *in vitro* (Bernstein-Hanley et al., 2006). Henry *et al*. showed Irgm1$^{-/-}$ mice fail to control infection with *Salmonella typhimurium* due to an impaired bacterial killing and cell mobility in Irgm1$^{-/-}$ macrophages (Henry et al., 2007). Santiago *et al*. reported Irgm1$^{-/-}$ mice also exhibit high susceptibility to infection with *Trypanosoma cruzi*, accompanied with unchecked parasite replication, defective hematopoiesis and reduced parasite killing in macrophages (Santiago et al., 2005). Three independent studies demonstrated the role of several IRGs in resistance against *Toxoplasma*. Irgm3$^{-/-}$ mice exhibit an increased susceptibility to the parasitic infection, characterised by an uncontrolled parasite burden and increased production of the inflammatory cytokines IFNγ and IL-12 (Taylor et al., 2000). Irgm3 has also been shown to control *Toxoplasma* replication in astrocytes (Halonen et al., 2001). Irgm1$^{-/-}$ mice were also reported to exhibit an enhanced susceptibility to *Toxoplasma*, characterised by an increased parasitemia (Collazo et al., 2001).

The family of p47 IRGs can be divided in two categories, based on the sequence in the first nucleotide-binding site (G1). The three IRGM proteins bear the non-canonical glycine-methionine-serine sequence (GMS) and the remaining IRG proteins harbour the conserved canonical glycine-lysine-serine sequence (GKS) (Intemann et al., 2009;

Ling et al., 2006; Bekpen et al., 2005; Boehm et al., 1998; Che et al., 2010; Zhao et al., 2009a; Khaminets et al., 2010). In IFNγ-induced cells *in vitro*, many GKS IRGs assemble together at the PV of *Toxoplasma* and mediate killing of the parasite by vesiculation and ultimately disruption of the vacuolar compartment (Butcher et al., 2005; Martens et al., 2005; Zhao et al., 2009b). IRG proteins Irgb6, Irgb10 and Irga6 sequentially localise to PVs containing avirulent type II and III strains of *Toxoplasma* but not virulent type I strain (Ling et al., 2006; Zhao et al., 2009a; Khaminets et al., 2010). These observations suggest virulent type I parasites escape from disruption of the PV and death by preventing the substantial accumulation of IRGs on the PV. Recently, the *Toxoplasma* virulence factor ROP18 from virulent type I *Toxoplasma* has been shown to phosphorylate two members of the IRG family, Irga6 and Irgb6, thereby preventing their recognition of the vacuole (Steinfeldt et al., 2010; Fentress et al., 2012). The pseudokinase ROP5 mediates ROP18 action by blocking the target IRG proteins in their inactive GDP-bound form, allowing the active kinase ROP18 to access the threonine phosphorylation sites (Fleckenstein et al., 2012). ROP18 forms a complex with the pseudokinases ROP2 and ROP8 as well as with the dense granule GRA7. The latter also binds to Irga6 and increases its turnover, probably preventing it from recruiting to the PV (Alaganan et al., 2014). This summer, GRA7 has been localised to avirulent *Toxoplasma* PV in complex with ROP5, hence allowing the specific phosphorylation and inactivation of Irga6 by ROP18 (Hermanns et al., 2015). Recently, the subfamily of GMS proteins has been reported to regulate the recruitment of their GKS counterparts to the PV. Localisation studies of the two groups have shown GMS proteins are present on endomembranes and largely absent from foreign membranes such as the PVM, while GKS proteins mainly recognise and recruit to GMS-free endomembrane components (Haldar et al., 2013). How exactly murine

IRGs accumulate at the PV, as well as which cellular functions and molecular mechanisms this class of GTPases regulate in *Toxoplasma* infection remains unknown.

So far, 23 genes corresponding to IRGs have been identified in the mouse genome, localised on chromosomes 7, 11 and 18 (Bekpen et al., 2005) (Figure 1.12). Despite their presence in several mammals, IRG genes appear to be degenerated in humans with only two members localised on chromosomes 5 and 19 (Bekpen et al., 2005). As both human *IRGC* and *IRGM* genes do not entail any interferon responsive elements and do not respond to stimulation by interferons *in vitro*, their role in infection was considered non-existent. However, IRGM has been reported to be required for induction of autophagy in human macrophages in both normal conditions by mediating the conversion of LC3I into LC3II, and during infection with *Mycobacterium tuberculosis* by regulating the maturation of the phagosome (Singh et al., 2006). Human population genetic studies revealed that two single nucleotide polymorphisms (-261TT and -1208AA) of the human gene encoding IRGM provide protection against *Mycobacterium tuberculosis* infection (Intemann et al., 2009; Che et al., 2010).

In contrast to the p47 IRGs, the homologous IFNγ-induced GTPases, the p65 GBPs, are highly conserved throughout the vertebrate lineage with 13 copies in the mouse genome clustered on chromosomes 3 and 5, and 7 copies in the human genome on chromosome 1 (Kresse et al., 2008; Shenoy et al., 2008). Both the mouse and human p65 GBPs are inducible by interferons, rendering them interesting from a medical point of view.

1.4.3 The p65 guanylate binding proteins

The p65 guanylate binding proteins are 67-73kDa proteins that were identified for the first time in 1979 by Gupta *et al*. in IFNγ-stimulated human fibroblasts (Gupta et al., 1979). In 1983, Cheng *et al.* discovered their murine orthologs in IFNγ-stimulated mouse fibroblasts (Cheng et al., 1983). Although IFNγ is the major inducer of GBP expression, their upregulation has also been reported by type I interferons (IFNα/β), interleukin-1β (IL-1β) and TNFα in rodents and humans (Lubeseder-Martellato et al., 2002; Tripal et al., 2007). Multiple sequence alignments of either human or murine GBPs highlighted regions of conservations within their amino acid sequences (Olszewsky et al., 2006). The N-terminal region of the GBPs is the most conserved and contains the GTP (guanosine triphosphate)-binding domain, comprising the four consensus sequences: the G1 or P-loop (GxxxxGKS, where "x" is any amino acid) coordinating the phosphates, the G2 or Switch1 (a single T residue) and the G3 or Switch2 (DxxG) involved in catalysis and moving during nucleotide hydrolysis, and the G4 motif (TLRD). In contrast, the C-terminal region is the most diverse and interestingly, some human and mouse GBPs (hGBP1, hGBP3, hGBP5, mGBP1, mGBP2 and mGBP5) share an amino acid motif called "CaaX" sequence with members of the Ras superfamily of GTPases. This "CaaX" motif ("C" represents cysteine, "a" is an aliphatic residue and "X" is any residue) encodes a potential site for prenylation, a posttranslational modification consisting of the addition of an isoprenyl lipid, allowing the protein to anchor to cellular membranes (Maltese, 1990) (Figure 1.13).

In the last 30 years, several studies have been carried out in order to characterise the structural and biochemical properties of the GBPs. Crystal structures have been

obtained for full-length hGBP1 in either the free state (Prakash et al., 2000a), bound to a non-hydrolysable analog of GTP (GppNHp) (Prakash et al., 2000b), in complex with GDP/AIF3 or GMP/AIF4 (Ghosh et al., 2006). The N-terminal catalytic domain is globular and is linked to an elongated C-terminal series of α-helices via a short middle region consisting of a two-stranded beta-sheet and a helix (Figure 1.14).

GTPases are enzymes catalysing the hydrolysis of GTP to GDP (guanosine di-phosphate). GTPases are referred to as inactive when in a GDP-bound state while active when GTP is bound. hGBP1 has been observed to oligomerise in a nucleotide-dependent manner (Figure 1.15), so that active GTP-bound hGBP1 dimerises whereas inactive GDP-bound does not (Prakash et al., 2000a; Voepel et al., 2014). hGBP1 has been of great interest from a biochemical point of view due to its unique ability to bind GTP, GDP and GMP (guanosine mono-phosphate) with an equivalent low affinity (Cheng et al., 1983; Praefcke et al., 1999). hGBP1 has also been shown to catalyse the hydrolysis of GTP to GDP as well as to GMP in a two-step fashion, GMP being the major end product of the reaction (Schwemmle and Staeheli, 1994). As the affinity for GMP is low, these reactions are performed at a high nucleotide dissociation rate or turn-over and at a fast hydrolysis rate of up to 80-100 min^{-1}, suggesting that the GBPs are not regulated by GTPase activating proteins (GAPs) or guanine nucleotide exchange factors (GEFs) like small GTPases are. However, the structures of the N-terminal GTPase domain of hGBP1 in complex with GTP, GDP and GMP obtained by X-ray crystallography implied GBPs are self-activating upon dimerisation (Ghosh et al., 2006; Kunzelmann et al., 2006). Moreover, the intermediate helical domain of hGBP1 has been shown to play a key role in the structural stabilisation by allosteric interaction of residues during dimerisation and in the regulation of the GTPase activity

of the protein, and has as such been referred to as an internal GAP (Abdullah et al., 2009; 2010).

1.4.4 Implication of the p65 GBPs in infections

Although the GBPs have been known for more than 30 years, little is known about their biological relevance after infection. Research with mice lacking either type I interferon receptor or type II interferon receptor demonstrated type I interferons are involved in antiviral responses, whereas type II interferon is important for resistance against intracellular bacteria and parasites (van den Broek et al., 1995). As the p65 GBPs can be induced by both types of interferons, their role is likely to encompass antiviral, antibacterial and antiparasitic host defence. Most of the studies on the implication of the GBPs have been carried out in the mouse, mainly due to technical challenges involved with working with human cells and generating knockout systems. However, recent investigations have allowed for more insights into the contribution of the GBPs during infection.

1.4.4.1 Implication of human GBPs in infection

Members of the family of human p65 GBPs have been shown to be involved in mediating resistance against intracellular viral and bacterial infections. Overexpression of hGBP1 in human Henrietta Lacks (HeLa) cells confers modest resistance against vesicular stomatitis virus (VSV) and encephalomyocarditis virus (EMCV) as seen by a reduction in morphological changes induced by the viral infections and a decreased viral replication. The combination of hGBP1-silencing and induction with type I IFNα or type II IFNγ in HeLa cells showed hGBP1 is involved in the IFNα-mediated response against EMCV and in the IFNγ-mediated response against both VSV and EMCV (Anderson et al., 1999). Another overexpression study

of hGBP1 in human hepatoma Huh7 cells showed a decrease in hepatitis C virus (HCV) replicon replication by almost 40%, while knock down of hGBP1 increased it by more than 45% (Itsui et al., 2006). This antiviral effect against HCV has later been attributed to the GTPase activity of hGBP1, as in normal conditions the viral NS5B protein interacts with hGBP1 to inhibit the GTPase activity and repress the inhibition of viral replication (Itsui et al., 2009). hGBP1 has also been reported to participate in the host defence against dengue virus (DENV), as silencing of hGBP1 lead to a higher viral load accompanied with an impaired NF-κB signalling and a downregulation of inflammatory cytokines (Pan et al., 2012). Overexpression of hGBP1, hGBP3 and of a new hGBP3ΔC splice variant were shown to reduce influenza viral titers in human A549 cells. The most potent anti-influenza GTPase, hGBP3ΔC, inhibits the activity of the viral polymerase complex upon binding to, but not hydrolysis of, guanosine triphosphate (Nordmann et al., 2012).

As far as bacterial infections are concerned, both hGBP1 and hGBP2 participate in the defence against *Chlamydia trachomatis*. Tietzel *et al*. demonstrated that hGBP1 and hGBP2 localise at the *Chlamydia* inclusion membranes and restrict the growth of the bacteria in HeLa cells when harbouring a functional GTPase domain (Tietzel et al., 2009). Interestingly, hGBP5 has been shown to promote the activation of the NLRP3 inflammasome following infection with live *Salmonella* and *Listeria* in IFNγ-stimulated human THP-1 macrophages. Tetramerised hGBP5 binds to the PYD domain of the sensor protein NLRP3, which subsequently assembles with the adaptor protein ASC to activate procaspase-1, thereby triggering its autoproteolysis into caspase-1 and production of the inflammatory cytokines IL-1β and IL-18 (Shenoy et

al., 2012). The involvement of human GBPs in defence against other bacterial models has not been investigated so far.

Human p65 GBPs have recently been studied during the course of infection with *Toxoplasma*. Using an antibody recognising hGBP1-5 (commercially available from Santa Cruz), Niedelmann *et al*. showed hGBPs do not recruit to the *Toxoplasma* PVs (<1%) in IFNγ-stimulated HFFs, and individual knock down of either hGBP1 or hGBP2 in HFFs does not increase the susceptibility to the parasite (Niedelman et al., 2013). Using the same antibody for their immunofluorescence studies, Ohshima *et al*. reported the recruitment of endogenous hGBPs to the parasitophorous vacuole of avirulent *Toxoplasma* in human HAP1 cells in an IFNγ-dependent manner at 6h post-infection. However, this accumulation of the hGBPs was observed for only about 6% of the parasite PVs, and the knock down of the clusters of hGBPs in the cell line did not lead to any enhanced susceptibility to *Toxoplasma* infection (Ohshima et al., 2014). The low accumulation of hGBPs to the PV could be explained by the absence of p47 IRGs found to be recruited in the mouse system. The function of all the hGBPs, either at the *Toxoplasma* PV or acting elsewhere in the cell without localisation to the PV, remains to be assessed in different hematopoietic and non-hematopoietic cell types.

1.4.4.2 Implication of mouse GBPs in infections

More extensive research on the family members of the murine p65 GBPs has highlighted their importance in host defence against viruses, bacteria and protozoa. The putative murine ortholog of hGBP1, mGBP2, has also been shown to have antiviral activities during infection with the viruses VSV and EMCV, as seen by a 50% and 60% reduction in viral load, respectively, following overexpression of mGBP2 in mouse NIH3T3 cells. However, the GTP-binding domain was required for the

inhibition of EMCV replication, but not VSV (Anderson et al., 1999; Carter et al., 2005). mGBP4 has been reported as a novel regulator of antiviral response during Sendai virus (SeV) infection by dampening the production of IFNα. Indeed, mGBP4 interacts with the inhibitory domain of interferon regulatory factor 7 (IRF7), a transcription factor that mediates the production of IFNα. This interaction inhibits IRF7 SeV-induced phosphorylation and TRAF6-induced ubiquitination, hence negatively regulating IRF7-mediated antiviral response (Hu et al., 2011).

Various mouse GBPs have been implicated in host recognition and/or defence against bacteria such as *Chlamydia trachomatis*, *Salmonella enterica*, *Listeria monocytogenes* and *Mycobacterium tuberculosis* (Haldar et al., 2013; Rupper and Cardelli, 2008; Kim et al., 2011). mGBP1 and mGBP2 were found to accumulate at *Chlamydia* inclusion membranes, characterised by the absence of GMS p47 IRGs, in IFNγ-stimulated mouse embryonic fibroblasts (MEFs) (Haldar et al., 2013). Although the accumulation of mGBPs at the *Chlamydia* inclusions is known to be regulated by the autophagy proteins ATG3 and ATG5 (Haldar et al., 2014), the role they exert at the inclusions has not been elucidated yet. Following *Salmonella* infection, mGBP5 is recruited to bacteria-containing phagosomes. Moreover, overexpression of mGBP5 in IFNγ-stimulated RAW264.7 macrophages leads to an increased pyroptosis following *Salmonella* infection, while knock down of mGBP5 results in a higher susceptibility to the *Salmonella*-induced programmed cell death (Rupper and Cardelli, 2008). The mechanisms by which mGBP5 potentiates *Salmonella*-induced pyroptosis still require elucidation. Four members of the mGBPs have been found to mediate immunity against listerial and mycobacterial infections, some of them acting both *in vitro* and *in vivo*. Using a family-wide shotgun strategy combining three loss-of-function

approaches, mGBP1, mGBP6, mGBP7 and mGBP10 were reported to mediate cell-autonomous defence against *Listeria* and *Mycobacterium* in IFNγ-stimulated macrophages, translated by an increased bacterial load following gene silencing. In addition, mGBP1/3/7/10 were recruited to *Listeria*- and *Mycobacterium*-containing vacuoles. Protein interaction studies revealed mGBP1 and mGBP7 to complex with proteins involved in oxidative killing and autophagy. mGBP1 was found to assemble with the ubiquitin-binding protein p62, thereby promoting delivery of ubiquitinated bacteria to autolysosomes. mGBP7 interacted with the nicotinamide adenine dinucleotide phosphate (NADPH) oxidase that generates superoxide, possibly helping its assembly on bacterial phagosomes. mGBP7 also interacted with the autophagy protein ATG4B, thus prompting the extension of the phagophore around damaged bacteria-containing vacuoles. At the organismal level, the study showed $GBP1^{-/-}$ mice failed to control *Listeria* or *Mycobacterium* replication and succumbed to the infection (Kim et al., 2011). Finally, mGBP5 was demonstrated to participate in the defence against *Listeria* infection *in vitro* and *in vivo*. Similarly to hGBP5, mGBP5 activates the NLRP3 inflammasome and promotes its assembly following live bacteria infection. $mGBP5^{-/-}$ bone marrow-derived macrophages exhibit impaired association between NLRP3, ASC and procaspase-1, leading to an absence of caspase-1 production and IL-1β and IL-18 secretion. mGBP5-deficient mice present a higher bacterial burden accompanied with a 50 to 80% decrease in active caspase-1-expressing macrophages in the mesenteric lymph nodes (Shenoy et al., 2012). Earlier this year, several mGBPs were shown to regulate the activation of the AIM2 inflammasome during infection with the cytosolic bacterium *Francisella novisida*. Infection of BMDMs lacking the mGBPs clustered on chromosome 3 (comprising mGBP1, 2, 3, 5 and 7, called hereafter GBP^{ch3}) led to a decreased cell death

accompanied with lower levels of active caspase-1, IL-1β and IL-18. Individual gene silencing narrowed the involved mGBPs to be mGBP2 and mGBP5. Both mGBP2 and mGBP5 were recruited to *Francisella* bacteria that were subsequently lysed, releasing the bacterial DNA into the cytosol for recognition and activation of the AIM2 inflammasome (Meunier et al., 2015; Man et al., 2015). mGBP2$^{-/-}$ as well as mGBP5$^{-/-}$ macrophages failed to control bacterial replication *in vitro* (Man et al., 2015), and mice lacking GBP2 or GBP^{ch3} were highly susceptible to *Francisella* infection and exhibited a high bacterial burden (Meunier et al., 2015).

Apart from regulating the canonical NLRP3 and AIM2 inflammasomes, mGBPs have been implicated in the activation of the non-canonical caspase-11 inflammasome pathway during *Legionella* and *Salmonella* infection. The non-canonical caspase-11 inflammasome leads to the activation of caspase-11 that triggers rapid cell death, independently of caspase-1 activation (Kayagaki et al., 2011; Casson et al., 2013; Kayagaki et al., 2013). GBP^{chr3} BMDMs showed lower levels of caspase-11 activation, decreased *Legionella*-induced pyroptosis and failed to control bacterial load. Induction of the caspase-11 inflammasome was reported to be triggered by the presence of cytosolic *Legionella* LPS (Pilla et al., 2014). Similarly, GBP^{chr3} were reported to regulate caspase-11 inflammasome activation during *Salmonella* infection by localising to the SCV and promote its lysis, thereby releasing the bacteria into the cytosol and rendering the LPS visible to inflammasome sensor. However in this study, cytosolic *Salmonella* LPS or *Escherichia coli* LPS did not trigger the activation of the caspase-11 inflammasome (Meunier et al., 2014). In both infection systems, the caspase-11 sensor still remains to be identified.

As far as *Toxoplasma* is concerned, several mGBPs are highly expressed in IFNγ-induced cells *in vitro* upon infection with the parasite (Degrandi et al., 2007). Following IFNγ stimulation, mGBP1, 2, 3, 5, 6, 7 and 9 actively accumulate at the PV of avirulent type II and III, but not virulent type I strains of *Toxoplasma* (Degrandi et al., 2007; Virreira Winter et al., 2011). Moreover, some mGBPs (namely mGBP1, mGBP2 and mGBP5) have been reported to interact at the PV in an IFNγ-dependent manner, suggesting they act jointly with each other and effector proteins in order to combat *Toxoplasma* (Virreira Winter et al., 2011). In an elegant *in vivo* study involving the GBP^{chr3} knockout mouse, Yamamoto *et al.* demonstrated GBP^{chr3} are required for IFNγ-mediated control of *Toxoplasma* spread and proliferation *in vivo*, as well as for clearance and inhibition of *Toxoplasma* burden *ex vivo* by affecting the recruitment of p47 IRGs to the PV and its subsequent disruption (Yamamoto et al., 2012). Another study revealed that a $GBP2^{-/-}$ mouse is susceptible to *Toxoplasma* infection as a result of a defect in controlling parasite replication (Degrandi et al., 2013). However, reintroduction of GBP2 in GBP^{chr3} cells did not rescue resistance to *Toxoplasma* (Yamamoto et al., 2012), suggesting that mGBP2 alone does not suffice to control *Toxoplasma* infection.

Invasion of *Toxoplasma* into the host cell triggers the secretion of proteins from three different parasitic organelles, micronemes, rhoptries, and dense granules, a process essential to intracellular survival and replication of the parasite (Carruthers, 1999). As mentioned in section 1.3.2, some of these secreted proteins have been shown to mediate the recruitment of IRGs to the PV of *Toxoplasma.* The rhoptry protein ROP18, a kinase from virulent type I *Toxoplasma,* is able to selectively phosphorylate conserved threonine residues within the switch loop 1 of certain IRGs, preventing them from being recruited to the PV of the parasite (Steinfeldt et al., 2010). In previous work

by Eva Frickel, ROP18 from virulent type I *Toxoplasma* can mediate the evasion of mGBP1 recruitment to vacuoles of avirulent type III parasites. In the same study, expression of the virulent type I *Toxoplasma* rhoptry protein ROP16, a tyrosine kinase, in an avirulent type II strain of *Toxoplasma* also significantly reduces the recruitment of mGBP1 to the PV of the parasite. Deletion of the avirulent type II dense granule protein GRA15 leads to a decreased recognition of the PV by mGBP1 (Virreira Winter et al., 2011). A few host proteins have also been reported to mediate the recruitment of mGBPs to avirulent *Toxoplasma*. Last year, Ohshima *et al*. showed that deletion of the autophagy proteins ATG7 and ATG16L leads to a reduction in the accumulation of mGBPs to avirulent PV following IFNγ-stimulation, as well as an inability to control parasite replication (Ohshima et al., 2014). Choi *et al.* reported the autophagy proteins ATG3, ATG7 and the ATG12-ATG5-ATG16 complex mediate the disruption of *Toxoplasma* PV by LC3 and IFNγ effector proteins (Choi et al., 2014). This summer, Ohshima *et al*. showed that the Rab dissociation inhibitor alpha (RabGDIα) is a negative regulator of mGBP recruitment to avirulent *Toxoplasma*. RabGDIα interacts with mGBP2, and deletion of RabGDIα leads to an increased resistance to *Toxoplasma* infection both *in vitro* and *in vivo*. This was associated with an increased accumulation of mGBP2 and mIrga6 at the vacuole (Ohshima et al., 2015). The precise mechanism of negative regulation of mGBP2 and mIrga6 by RabGDIα is still unclear. Despite all these findings, which place the mGBPs at the avirulent PV of *Toxoplasma* to participate in its clearance, the comprehensive cellular functions of the p65 mGBPs during infection with *Toxoplasma* remain unknown.

1.5 Aim of this work

Parasitic infections are characterised by a constant race between the host and the pathogen to evolve and adapt in order to survive. The vacuolar parasite *Toxoplasma* actively invades any nucleated host cell, where it safely resides and replicates by avoiding fusion with lysosomes and subsequent acidification. Its conversion from the fast replicative form called tachyzoite, to the slowly replicative form termed bradyzoite, allows the establishment of a chronic, life-long infection within the host. The murine host has developed immune strategies to counteract *Toxoplasma*, which have to be deployed timely and orchestrated effectively in order to successfully contain the parasite without causing lethal inflammation (Figure 1.16).

IFNγ is the major mediator of the host defence against *Toxoplasma*, activating a wide range of antimicrobial processes in both immune and non-immune cells. In monocytes and macrophages, the production of nitric oxide can lead to parasite damage, but this is only effective during chronic infection. In contrast, members of the autophagy proteins as well as the two families of large GTPases named p47 IRGs and p65 GBPs, contribute to the clearance of the parasite in hematopoietic and non-hematopoietic cells during the acute phase of the infection. Both IRGs and GBPs have been shown to mediate destruction of *Toxoplasma*. Both have also been shown to interact with autophagy and inflammasome proteins, which also contribute to resistance against *Toxoplasma*. Interestingly, *Toxoplasma* has been shown to carry monoclonal antibodies inside the host cell, which could possibly be detected after vacuolar disruption (Zapata et al., 2005; Karunajeewa et al., 2001; Rosso et al., 2008; Dubremetz et al., 1985). Thus, the three cytosolic recognition pathways described in sections 1.3.3 to 1.3.5 could act jointly to combat *Toxoplasma* infection.

The molecular mechanisms occurring at the interface of host-pathogen interaction – namely the PV– involving both the IFNγ-induced host response by GBPs and evading tactics mediated by secreted parasitic proteins, remain unknown. How are mGBPs recruited to the PV of *Toxoplasma*? What happens after PV disruption, leading to *Toxoplasma* being exposed in the host cytosol? What detection mechanisms are triggered? What sensor molecules are involved? How do parasitic secretory proteins allow virulent type I *Toxoplasma* to evade recognition by GBPs at its PV? What are the molecular and organismal consequences of vacuolar recognition by GBPs and other effectors? Answering these questions will advance our understanding of the molecular function of the GBPs in the resistance to *Toxoplasma* infection. The work described in this thesis aimed at identifying what host factors play a role at the PV and in mediating resistance against *Toxoplasma* (Figure 1.17). As the study has been performed in the mouse model, mGBP proteins will be referred to as GBPs hereafter.

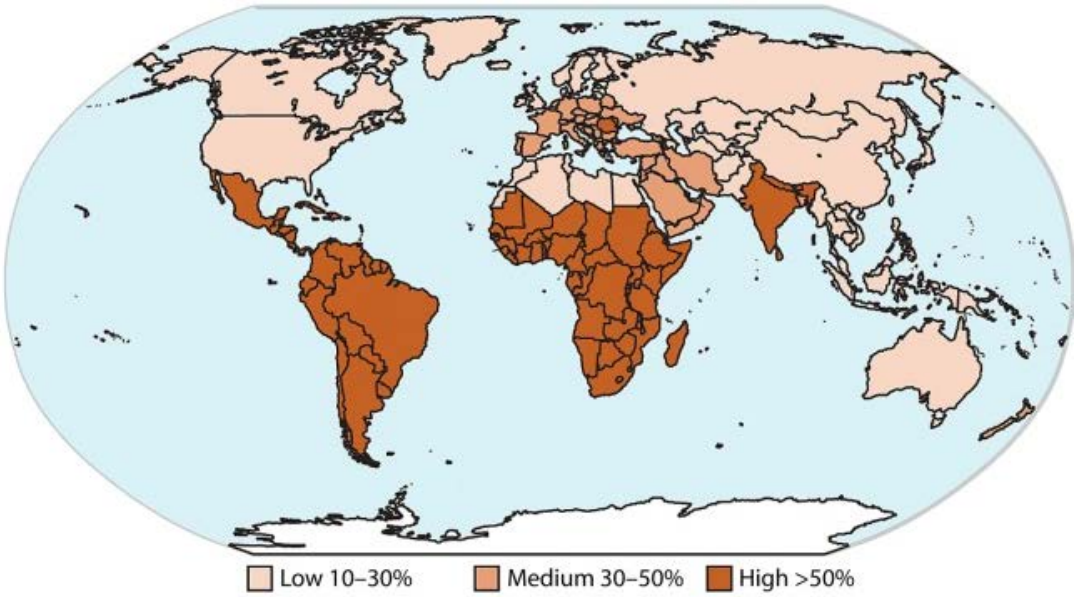

Figure 1.1: Global human seroprevalence of *Toxoplasma*.
Low seroprevalence (<30%) is shown in light orange, medium seroprevalence (30-50%) is shown in orange and high prevalence (>50%) is shown in dark orange. Adapted and reprinted with permission from (Esch and Petersen, 2013).

Country	Year	Prevalence (%)
Australia	2001	23 (Karunajeewa et al., 2001)
Austria	2011	31 (Sagel et al., 2011)
Belgium	2004	48.7 (Breugelmans et al., 2004)
Brazil	2012-2008	49.5 (Fonseca et al., 2012)-77.5 (Porto et al., 2008)
Burkina Faso	2006	25.3 (Simpore et al., 2006)
China	2013	11.8 (Sun et al., 2013b)
Columbia	2008	45.8 (Rosso et al., 2008)-63.5 (Castro et al., 2008)
Costa Rica	2005	55 (Zapata et al., 2005)
Cuba	2003	61.8 (Sanchez-Gutierrez et al., 2003)
Czech Republic	2007	19.8 (Kanková and Flegr, 2007)
Denmark	1999	27.8 (Lebech et al., 1999)
Ethiopia	2013-2015	81.4 (Gebremedhin et al., 2013)-65.8 (Tilahun et al., 2015)
Finland	1992	20.3 (Lappalainen et al., 1992)
France	1996	54.3 (Ancelle et al., 1996)
Germany	1999	63.2 (Fiedler et al., 1999)
Ghana	2009	92.5 (Ayi et al., 2009)
Greece	2004	29.4 (Antoniou et al., 2004)
India	2007-2004	41.6 (Borkakoty et al., 2007)-45 (Singh and Pandit, 2004)
Iran	2008-2007	33.5 (Fallah et al., 2008)-48.3 (Saeedi et al., 2007)
Italy	2008-2013	22.7 (De Paschale et al., 2008)-30.2 (Mosti et al., 2013)
Japan	2012	10.3 (Sakikawa et al., 2012)
Jordan	2005	47.1 (Jumaian, 2005)
Mexico	2006	6.1 (Alvarado-Esquivel et al., 2006)
Morocco	2007	50.6 (Mansouri et al., 2007)

New Zealand	2004	35.4 (Morris and Croxson, 2004)
Norway	1998	10.9 (Jenum et al., 1998)
Poland	2002-2006	35.8 (Niemiec et al., 2002)-41.3 (Nowakowska et al., 2006)
RDC	2014	80.3 (Doudou et al., 2014)
Singapore	2000	17.2 (Wong et al., 2000)
slovakia	2008	22.1 (Studenicová et al., 2008)
Slovenia	2002	34 (Logar et al., 2002)
South Korea	2005	0.8 (Song et al., 2005)-3.7 (Han et al., 2008)
Spain	2004-2015	18.8 (Gutiérrez-Zufiaurre et al., 2004)-35.2 (Asencio et al., 2015)
Sudan	2003	34.1 (Elnahas et al., 2003)
Sweden	2001	18 (Evengård et al., 2001)
Switzerland	2006	35 (Signorell et al., 2006)
Taiwan	2008	31 (Lin et al., 2008)
Thailand	2013-2001	2.6 (Sakae et al., 2013)-21.5 (Tantivanich et al., 2001)
Turkey	2004	60.4 (Harma et al., 2004)
UK	2005	9.1 (Nash et al., 2005)
US	2014	9.1 (Jones et al., 2014)
Venezuela	2006	38 (Triolo-Mieses and Traviezo-Valles, 2006)

Table 1.1: Seroprevalence of *Toxoplasma*-specific immunoglobulin G in pregnant women.

Date	Finding
1908	New protozoa discovered in the rodent *Ctenodactylus gundi* in North Africa and in a rabbit in Brazil
1909	Name *Toxoplasma gondii* proposed for the first time
1937	*Toxoplasma* isolated from and passaged in animals for the first time
1937	*Toxoplasma* described as an obligate intracellular parasite
1939	*Toxoplasma* isolated from human for the first time
1939-1940	Congenital transmission demonstrated in human
1941	Acquired acute infection demonstrated in human child
1941	Acquired acute infection demonstrated in human adults
1945-1947	Chronic asymptomatic infection demonstrated in human adults

Table 1.2: Summary of landmarks in the history of *Toxoplasma.*

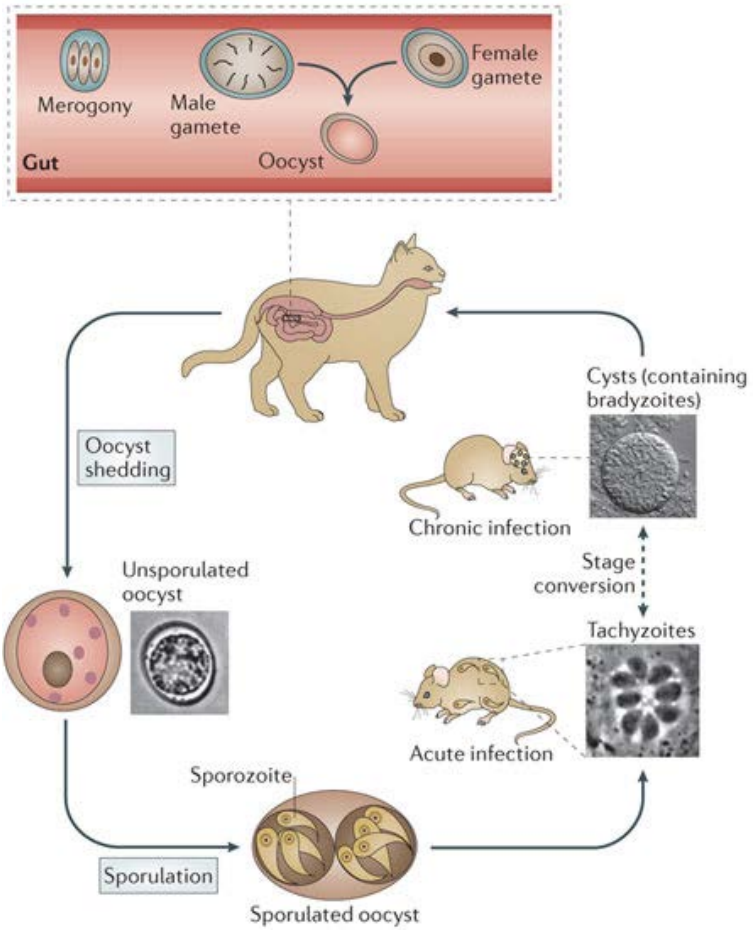

Figure 1.2: Sexual life cycle of *Toxoplasma*.
Felines (shown here as a cat) are *Toxoplasma*'s definitive host, where the parasite can sexually replicate in the gut. Oocysts are shed in the cat's feces and undergo sporulation to become infectious. Asexual replication occurs in the intermediate host (shown here as a rodent). Acute infection is characterised by the fast replication of *Toxoplasma* tachyzoites disseminated throughout the body. Chronic infection is characterised by the presence of slow-replicating *Toxoplasma* bradyzoites within tissue cysts. Ingestion of tissue cysts leads to infection of a new intermediate or definitive host, reinitiating the asexual or sexual life cycle of the parasite, respectively. Reprinted with permission from (Hunter and Sibley, 2012).

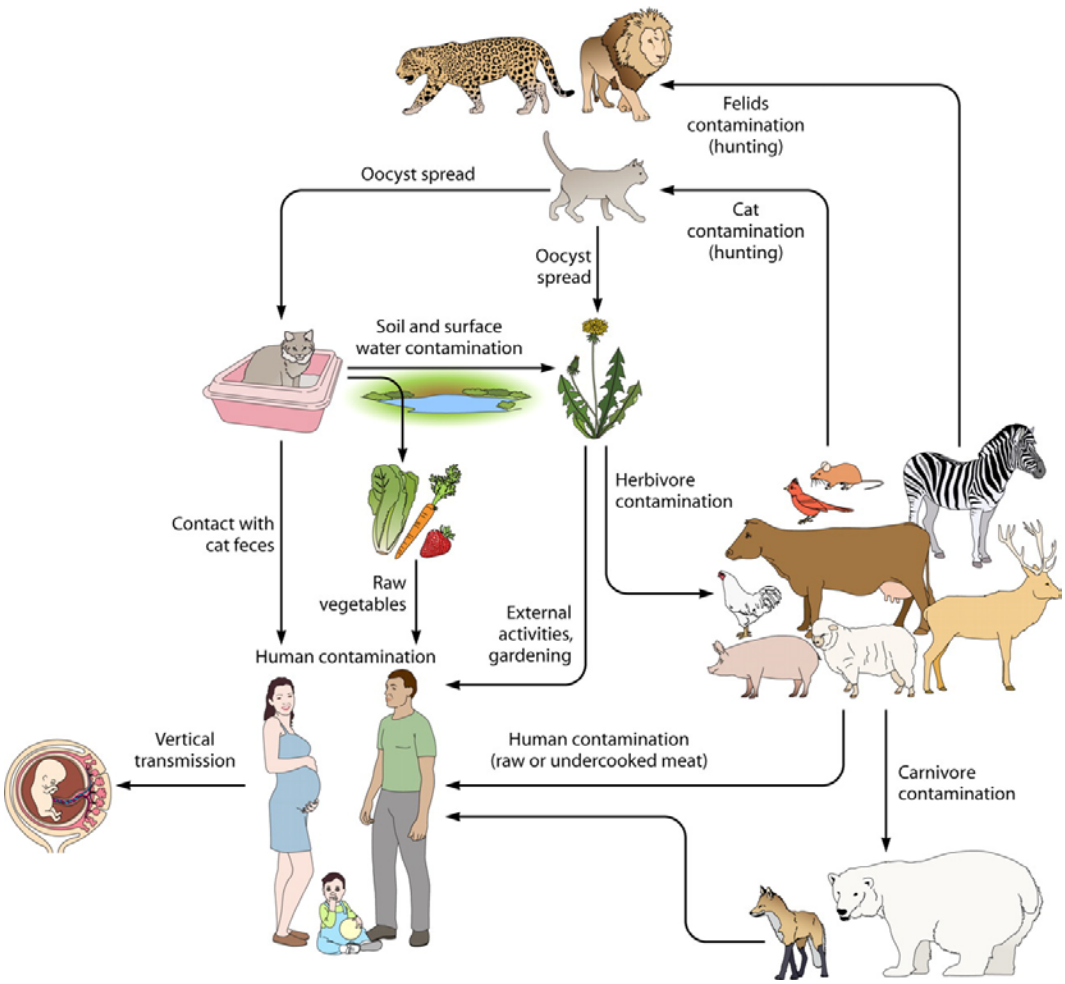

Figure 1.3: Asexual life cycle of *Toxoplasma*.
All warm-blooded animals may serve as intermediate hosts, wherever the *Toxoplasma* asexual life cycle occurs. Intermediate hosts, including humans and livestock, are infected by ingestion of food (meat, fruits and vegetables), soil or water contaminated by oocysts. The intermediate phase of the *Toxoplasma* life cycle also occurs by transmission from the acutely infected mother to the unborn foetus or by an organ transplant, as well as by carnivorism between intermediate hosts. Reprinted with permission from (Robert-Gangneux and Dardé, 2012).

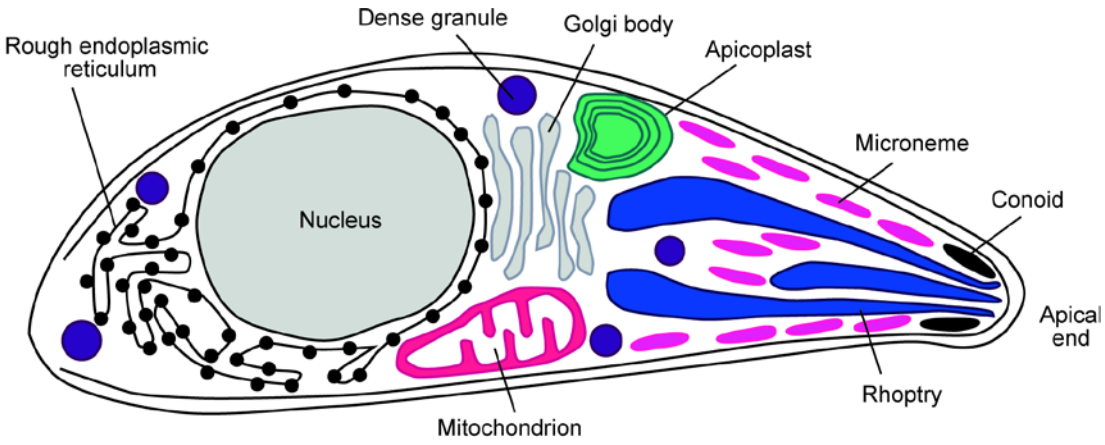

Figure 1.4: Schematic representation of the ultrastructure of a *Toxoplasma* tachyzoite.
Toxoplasma tachyzoites are comprised of eukaryotic universal organelles (nucleus, Golgi apparatus, endoplasmic reticulum and ribosomes), Apicomplexan secretory organelles (rhoptries, micronemes and dense granules) and endosymbiosis-derived organelles (mitochondrion and apicoplast) enclosed in a pellicule. Reprinted with permission from (Ajioka et al., 2001).

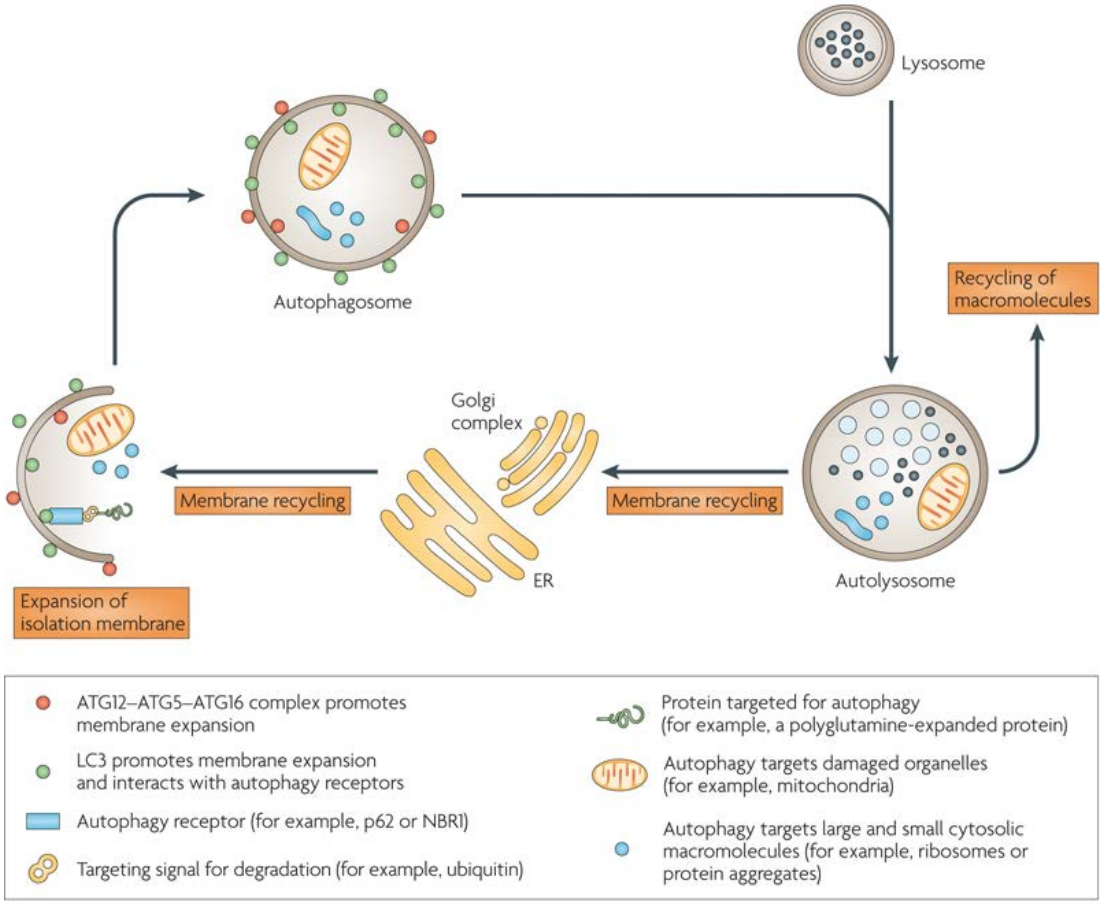

Figure 1.5: The autophagy pathway in mammalian cells.
The first step of the autophagy process involves the nucleation of a crescent-shaped isolation membrane called phagophore, arising from the endoplasmic reticulum (ER), the Golgi apparatus or the plasma cell membrane. The nucleation step is mainly driven by the complexation of Vps34, Beclin-1, ATG14 and p150 leading to the phosphorylation of lipids on the nascent membrane. Second, two ubiquitination-like systems mediate the expansion of the isolation membrane that will eventually fuse to form a new double-membraned vesicle termed the autophagosome. The large multimeric complex ATG12–ATG5–ATG16 is thought to act as a structural support for membrane expansion, and the microtubule-associated protein light chain 3 (LC3) is conjugated with phosphotidylethanolamine (PE). LC3 also has the ability to bind autophagy receptors, such as p62, NDP52 or NBR1, which permits selective autophagy. Third, LAMP2 mediates the fusion of the autophagosome with the acidic and hydrolase-containing lysosome, forming a so-called autolysosome. Finally, the luminal content is degraded, and the obtained products are translocated to the cytoplasm for reuse in metabolic processes and the membrane is recycled. Adapted and reprinted with permission from (La Spada and Taylor, 2010).

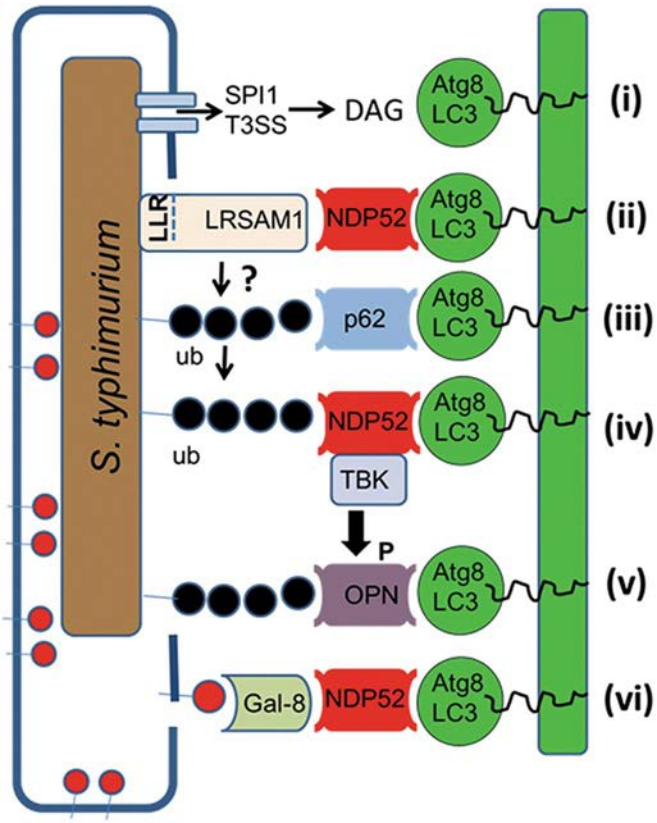

Figure 1.6: Autophagy receptors and adapters in the context of *Salmonella typhimurium* infection. Inside the host cell, *Salmonella* resides in a specialised compartment called *Salmonella*-containing vacuole (SCV). However, the SCV can be damaged and break, releasing free bacteria in the cytosol and exposing the content of the intraluminal membrane. (**i**): Autophagy can be activated by the secretion of bacterial effectors into the cytosol via the type III secretion system (T3SS). This induces the formation of diacylglycerol (DAG) that recruits LC3 to the SCV. (**ii**): LRSAM1 is an E3 ubiquitin ligase that binds to free cytosolic *Salmonella* via its LRR domain and to the autophagy receptor NDP52, recruiting LC3 to the site of infection. LRSAM1 might also target the free bacterium by ubiquitination (ub: ubiquitin, black circles). (**iii-v**): Ubiquitination at the surface of *Salmonella* can recruit the autophagy receptors p62, NDP52 and optineurin, which in turn bind to LC3-positive autophagosomes. (**vi**): Disruption of the SCV exposes luminal host glycans for recognition by galectin-8, which recruits NDP52 and thereby recruits LC3-positive autophagosomes. Reprinted with permission from (Wileman, 2013).

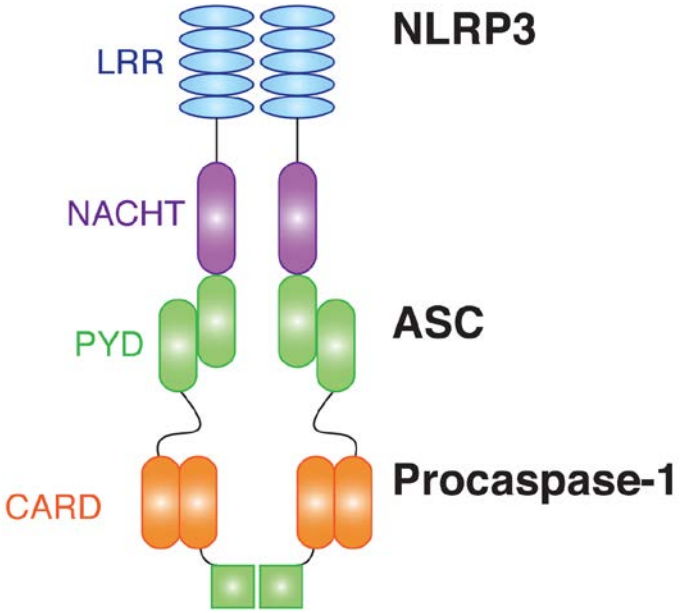

Figure 1.7: Schematic representation of the structure of the NLRP3 inflammasome.
Following activation, the sensor NLRP3 oligomerises via its NACHT domains and recruits the adaptor protein ASC through their respective pyrin domains (PYD). ASC finally recruits the inactive procaspase-1 via a CARD-CARD (caspase activation and recruitment domain) interaction.

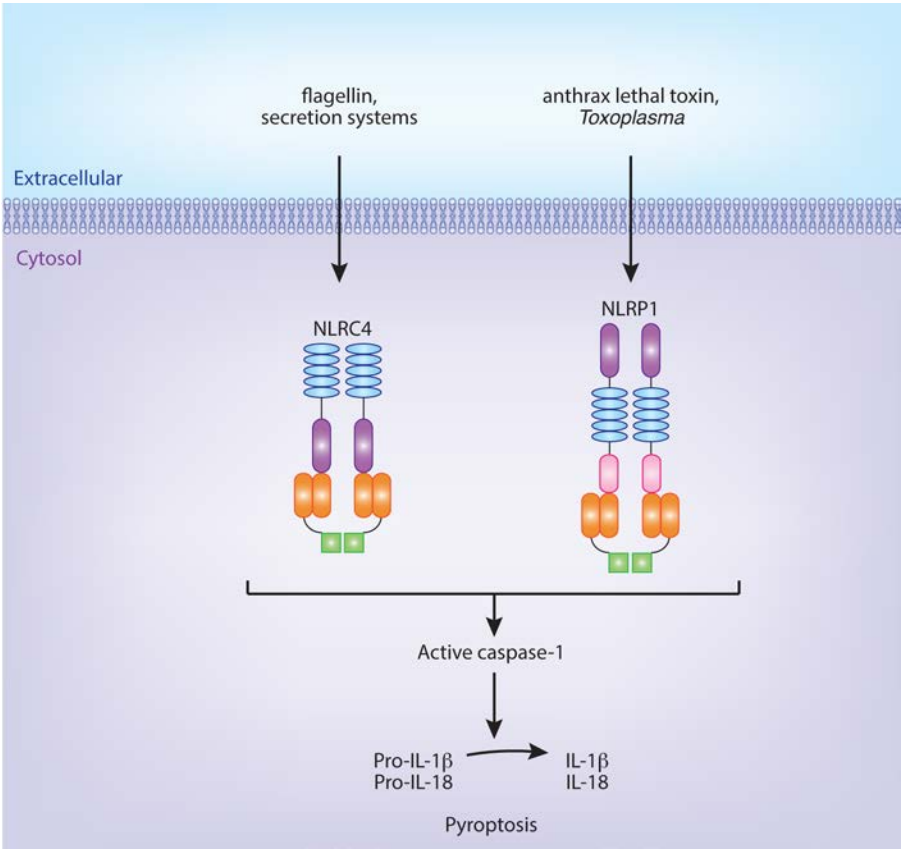

Figure 1.8: Inflammasomes implicated in the recognition of vacuolar pathogens.
NLRC4 detects *Salmonella* or *Legionella* flagellin as well as proteins from their respective secretion systems. NLRP1 is a known sensor for *Bacillus anthracis* lethal toxin, and *Toxoplasma* has recently been shown to trigger its activation as well. Once activated, these sensors can complex with the adaptor protein ASC and recruit procaspase-1, which is autoprocessed into active caspase-1. Caspase-1 cleaves the inflammatory precursors pro-IL-1β and pro-IL-18 into their active forms IL-1β and IL-18 and thus prompts programmed cell death termed pyroptosis.

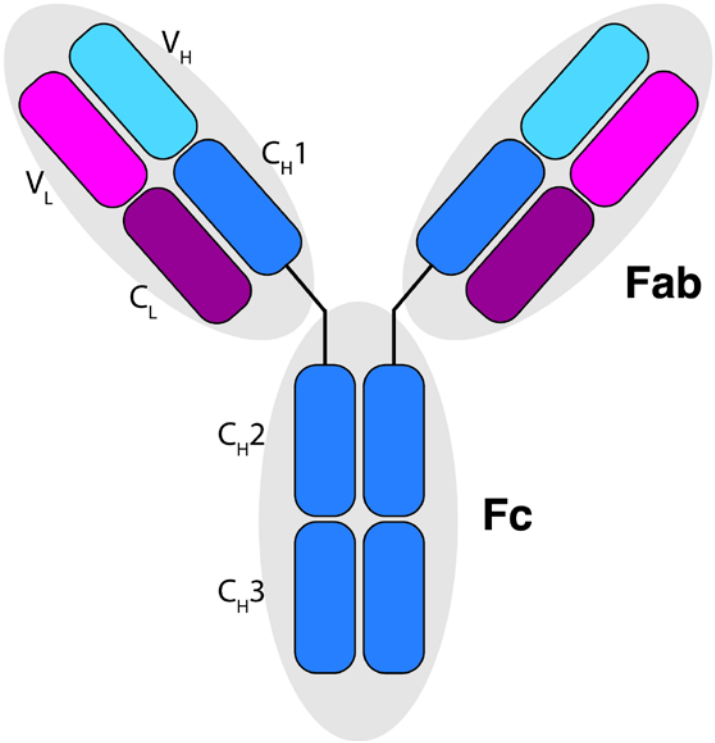

Figure 1.9: Stylised structure of an IgG.
Colouring shows heavy chains (H) in blue and light chains (L) in pink. Constant regions (C) are in dark colour and variable regions (V) are in light colour. The antibody-binding fragment (Fab) is made of the light chain, C_H1 and V_H. The crystallisable fragment (Fc) is made of the C_H2 and C_H3 regions.

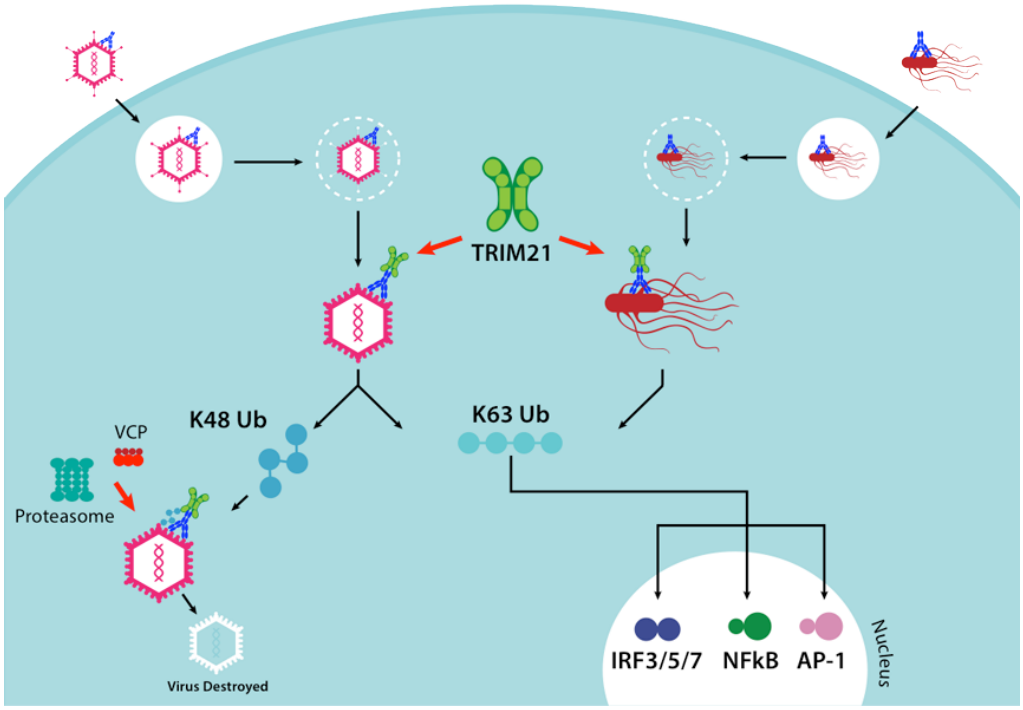

Figure 1.10: Schematic representation of the antibody-dependent intracellular neutralisation of pathogens.
In the extracellular environment, viruses and bacteria are coated with antibodies. Following invasion, the pathogens retain the immunoglobulins on their surface, which can be detected by the cytosolic Fc receptor TRIM21. Using the E3 ubiquitin ligase activity conferred by its RING domain, TRIM21 labels the pathogens for degradation and triggers innate immune signalling. Figure by Leo Hillier reprinted with permission from Leo James' personal group webpage: http://www2.mrc-lmb.cam.ac.uk/groups/lcj/research2.php.

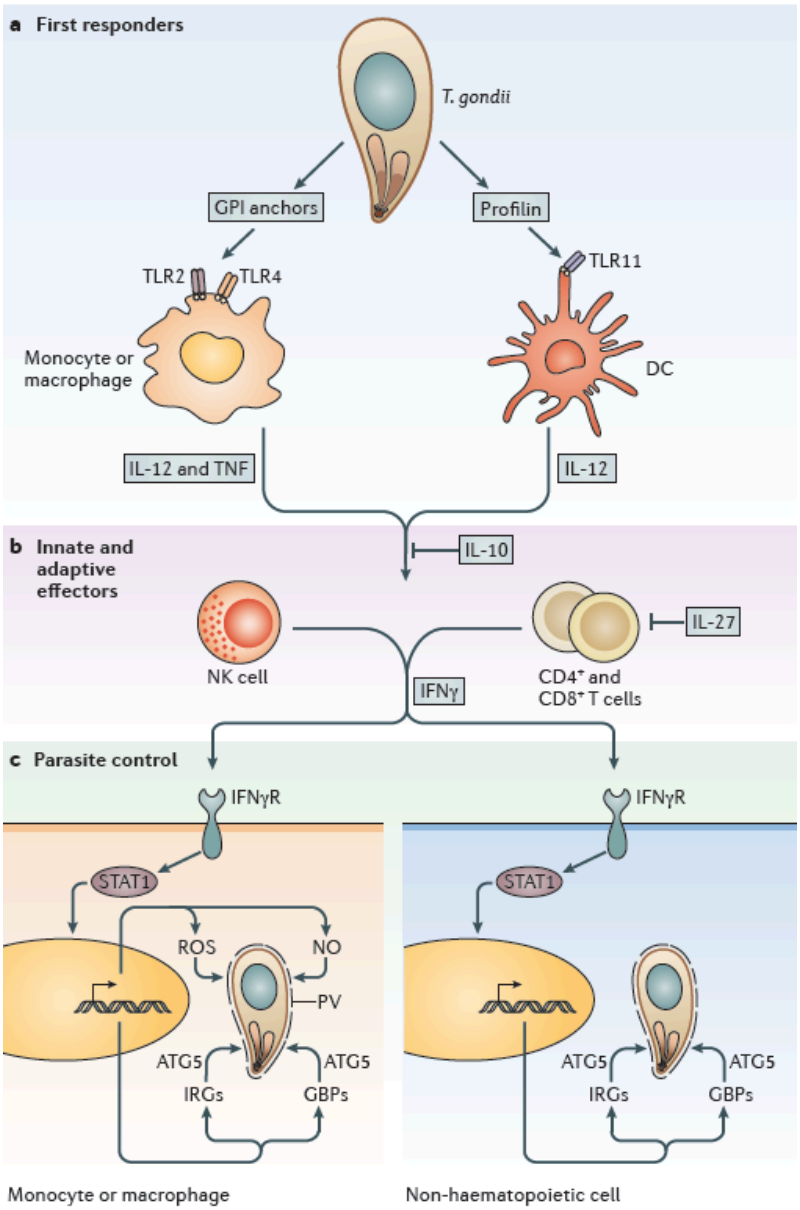

Figure 1.11: Early immune responses to *Toxoplasma gondii* infection.
Following invasion, *Toxoplasma* is recognised by monocytes, macrophages and dendritic cells (DCs) via their Toll-like receptors (TLRs). These activated cells secrete IL-12 as well as tumor necrosis factor (TNF), which stimulate the production of the cytokine interferon gamma (IFNγ) by natural killer (NK) cells and T cells. IFNγ, the main mediator of the anti-*Toxoplasma* immune response, triggers a wide range of antimicrobial processes in both hematopoietic and non-hematopoietic cells. These responses include the production of nitric oxide (NO) and the transcriptional upregulation of the immunity-related GTPases (IRGs) and guanylate-binding proteins (GBPs), leading to the destruction of the parasite. Reprinted with permission from (Hunter and Sibley, 2012).

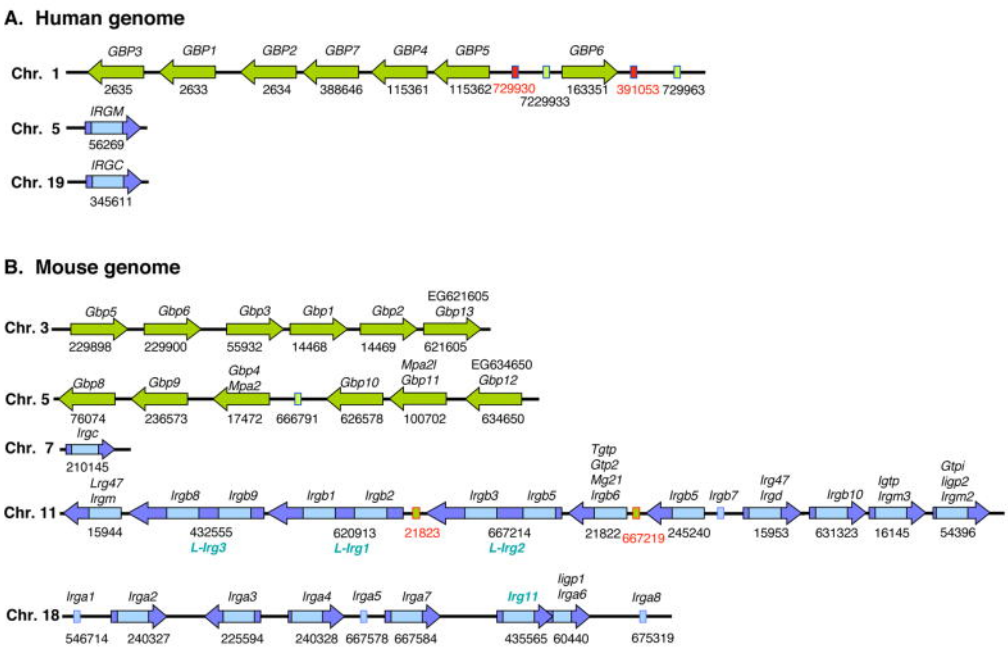

Figure 1.12: Genomic organisation of human and mouse p47 IRGs and p65 GBPs.
(**A**) Schematic representation of the human p47 *IRG* (blue) and p65 *GBP* (green) genes on chromosomes 1, 5 and 19. (**B**) Schematic representation of the mouse p47 *IRG* (blue) and p65 *GBP* (green) genes on chromosomes 3, 5, 7, 11 and 18. Blue and green boxes represent putative pseudogenes. Red boxes indicate genes unrelated to the GTPases. Gene orientation is given by the direction of the arrow. The gene nomenclature is shown above the arrows, and the NCBI gene identification numbers are shown below. Reprinted with permission from (Shenoy et al., 2008).

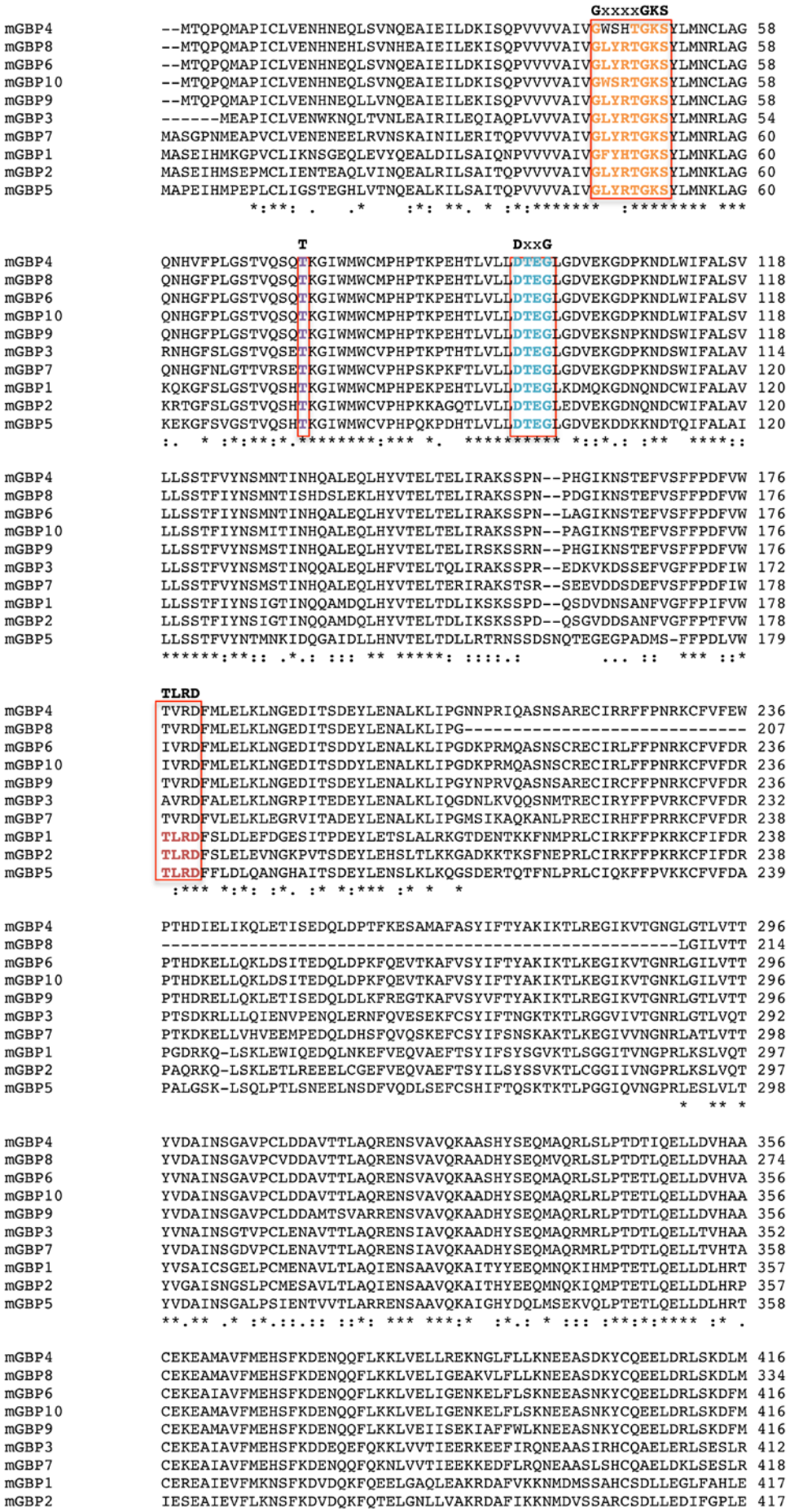
GxxxxGKS
T
DxxG
TLRD

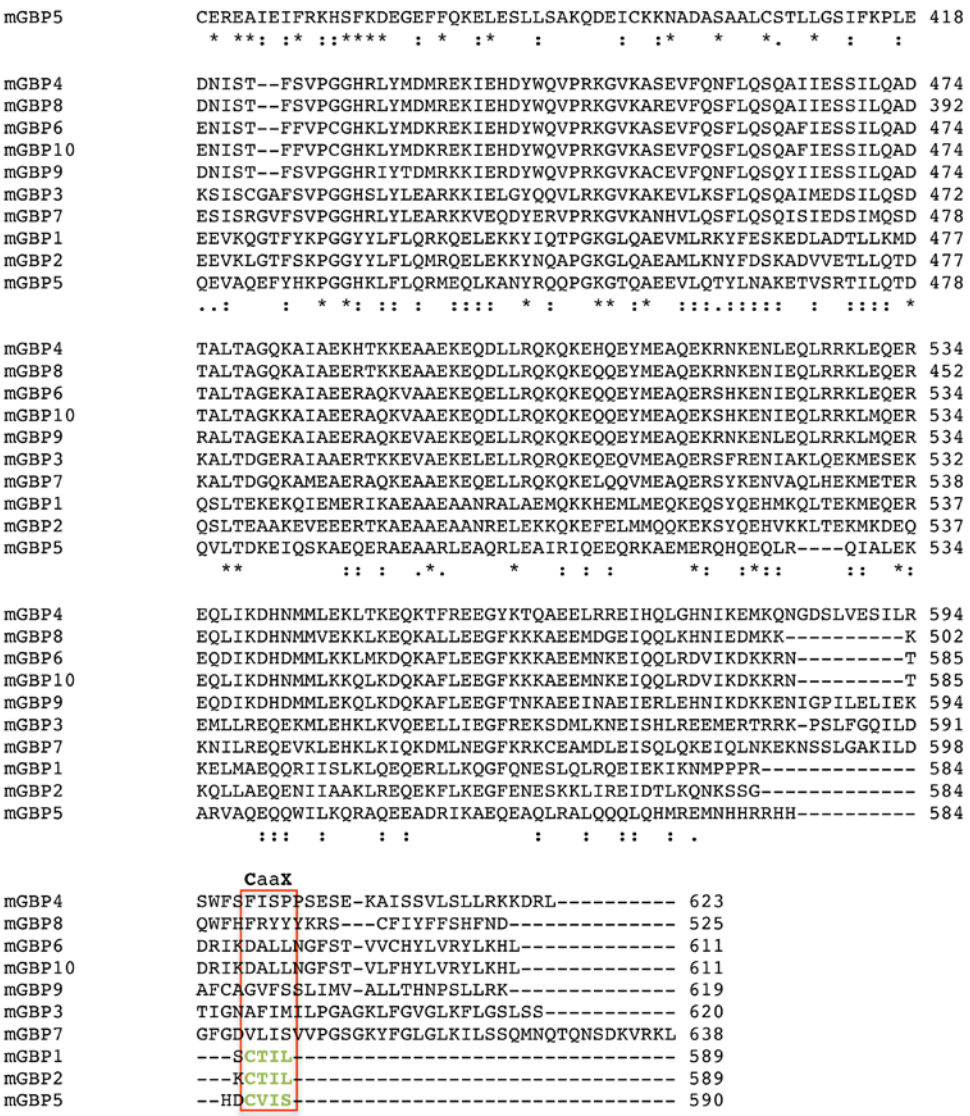

Figure 1.13: Multiple sequence alignment of the mouse p65 GBPs.
Red boxes highlight the four N-terminal consensus sequences within the GTP-binding domain and the C-terminal CaaX motif. The consensus sequences are shown above the aligned areas. Residues marked with an asterisk (*) are invariant, fully conserved amino acids. Residues marked with a colon (:) indicate amino acids with strongly similar properties. Residues marked with a period (.) indicate amino acids with weakly similar properties. Dashes indicate gaps in the aligned sequences. Multiple sequence alignment was generated with ClustalW2.

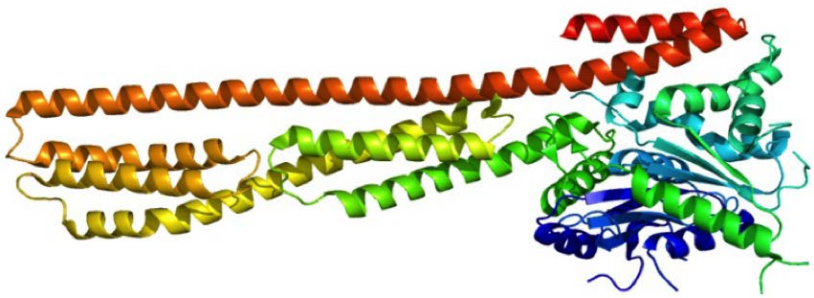

Figure 1.14: Ribbon representation of the overall structure of human GBP1:GppNHp.
The structure was determined by X-ray crystallography at a resolution of 1.7Å (PDB entry 1F5N). The N-terminal domain containing the GTP-binding site is globular, the C-terminal domain is elongated. Reprinted with permission from (Prakash et al., 2000b)**.**

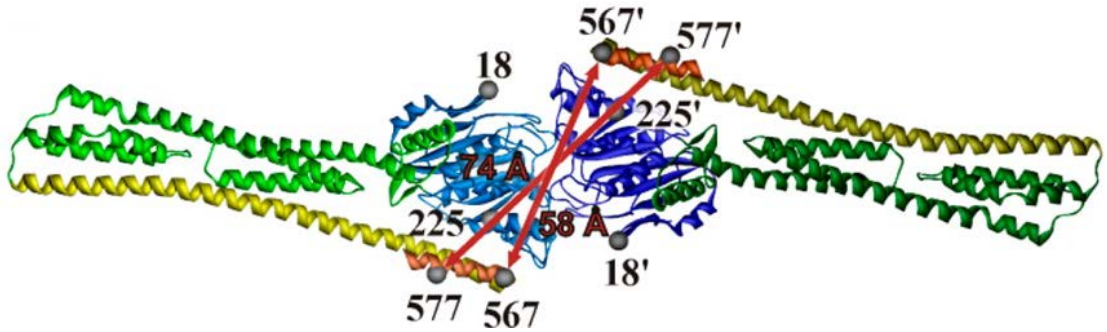

Figure 1.15: Model representation of human GBP1 dimerisation.
The presumed head-to-head dimer in presence of the GTP analog GppNHp. The expected distance between the respective K567 and Q577 residues is indicated in red arrows and numbers. Reprinted (adapted) with permission from Vöpel *et al*., Biochem (2014). Copyright (2015) American Chemical Society.

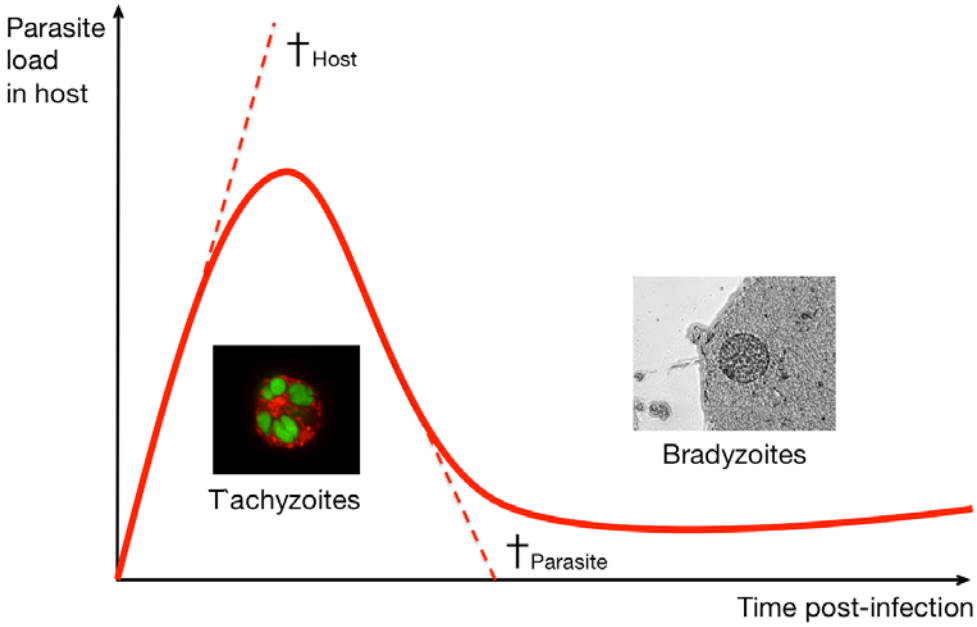

Figure 1.16: Battle between the host immune defence and *Toxoplasma* survival strategy.
Toxoplasma actively invades the host cell and resides in a parasitophorous vacuole as the fast replicative form called the tachyzoite. Its conversion to the slowly replicative form termed bradyzoite allows the establishment of a chronic, life-long infection within the host. The infected host must develop immune strategies to counteract *Toxoplasma*, which have to successfully contain the parasite without causing lethal inflammation.

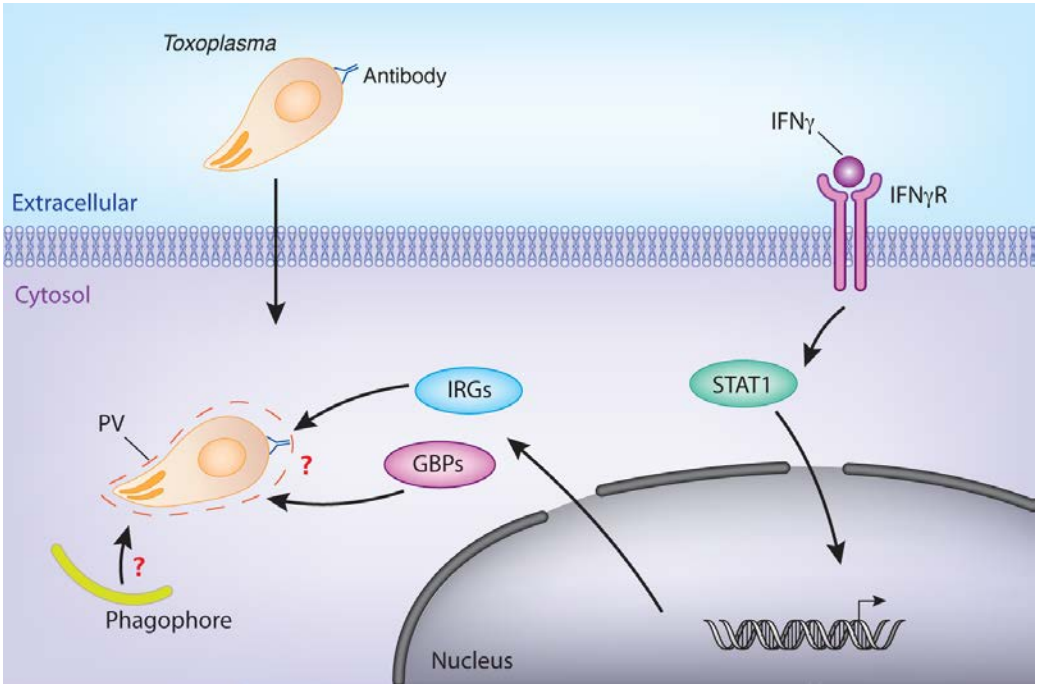

Figure 1.17: Known key players involved in the resistance against *Toxoplasma gondii* and outstanding questions to be answered.
Following infection with *Toxoplasma*, interferon gamma (IFNγ) is the main cytokine produced. Signalling through its receptor (IFNγR), IFNγ activates the signal transducer and activator of transcription 1 (STAT1). This nuclear transcription factor in turn upregulates the expression of two defence proteins called immunity-related GTPases (IRGs) and guanylate-binding proteins (GBPs), which recruit to the *Toxoplasma* parasitophorous vacuole (PV) and mediate its disruption and the killing of the parasite. Autophagy has also been linked to the clearance of *Toxoplasma*. As *Toxoplasma* can be coated with antibodies and retains them once it has invaded the cell, the breakage of the PV could release the immunoglobulins in the host cytosol where they could serve as danger-associated molecular pattern (DAMP). How the GBPs exert their function at the PV remains unknow, as well as what signals trigger the activation of the autophagy pathway. The aim of this thesis is to identify what other factors play a role at the PV and in mediating the resistance against *Toxoplasma*.

Chapter 2

Experimental Procedure

2.1 Tissue culture: cells and parasites

2.1.1 Culture of mammalian cells

All cell lines were grown in an incubator maintained at 37°C with 5% CO_2. Human foreskin fibroblasts (HFFs, ATCC, Manassas, VA, USA), Raw 264.7 macrophages (ATCC), human embryonic kidney 293T cells (HEK 293T, ATCC) and primary mouse embryonic fibroblasts (MEFs, home-made) were cultivated in Dulbecco's Modified Eagle Medium (DMEM, Gibco, Life Technologies, Carlsbad, CA, USA) supplemented with 10% fetal calf serum (FCS, Gibco).

Raw 264.7 cells were split every 3-4 days when confluency was about 90%. Cells were washed once with PBS and scraped in 1mL PBS. After resuspension in culture medium, cells were passaged at a 1:20 ratio into new 10 cm dishes (Corning, Corning, NY, USA).

HFFs, MEFs and HEK 293T were split about every week when confluency was 90%. Cells were washed once with PBS and treated with 0.05% trypsin-EDTA (Gibco) for 3 min at 37°C. Cells were resuspended in culture medium and centrifuged at 900 g for 5 min. The pellet was then resuspended in culture medium and cells were split into new flasks (for HFFs) or new 10 cm dishes (for MEFs and HEK 293T).

2.1.2 Culture of *Toxoplasma gondii* parasites

2.1.2.1 *Toxoplasma gondii* cell lines

Unless stated otherwise, the virulent type I strain RH and the nonvirulent type II strain Prugniaud (Pru) were used. Both strains were either WT or genetically modified to express a fluorescent protein in their cytoplasm. Virulent type I RH parasites express

tomato while avirulent type II Prugniaud (Pru) parasites express GFP and firefly luciferase (kind gifts from Marc-Jan Gubbels and Jeroen Saeij) (Yoshimi et al., 2009; Wang et al., 2006; Roos et al., 1994; Kim et al., 2007).

2.1.2.2 *Toxoplasma gondii* passage

All strains of *Toxoplasma* were maintained by serial passage on monolayers of HFFs as described previously (Garnham et al., 1962). Briefly, HFFs with *Toxoplasma* vacuoles were scraped off the flask and were passed through a 25 or 27 gauge needle (Terumo, Somerset, NJ, USA) to disrupt cells. A few drops of medium containing the parasites were transferred to a new, confluent flask of HFFs to passage the parasites.

2.1.3 Induction with interferon gamma

Cells were induced with interferon gamma (IFN-γ) by supplementing the culture medium with 100 U/mL murine IFNγ (R&D Systems, Minneapolis, MN, USA) for 16 h.

2.1.4 Infection of mammalian cells with *Toxoplasma gondii* parasites

To infect cells, parasites were isolated from HFF cultures as described above. After needle lysis, the collected parasites were centrifuged at 1230 g for 7 min and the pellets containing *Toxoplasma* were resuspended in a small volume of DMEM. Concentrations of parasites were determined by counting them in a disposable FastRead102 counting chamber. For infections, cells were incubated with *Toxoplasma* at a multiplicity of infection (MOI) ranging from 0.5-10 and dishes were centrifuged at 900 g for 2 min and incubated for 1 h at 37°C with 5% CO_2 before cells were lysed or fixed.

2.2 Primers

All primers used for the generation of constructs described or used in this work, as well as for the sequencing of plasmids or the genotyping of animals, are listed in the below. The nucleotide sequence is indicated from 5' to 3' direction.

Cloning into pMSCVNneo

CF1: myc-TRIM21 fwd	ATCCGGCTCGAGATGGAGCAGAAGCTGATCTCCGAGGAGCT GGACCTGATGTCACCCTCTACAACCTCAAAAATGTCTCTGG
CF2: TRIM21 rev	ATCCGGACCGGTCTACATCTTTAGTGGACAGAGCTTTAGAGG

Site-directed mutagenesis

CF75: myc-TRIM21 EcoRI Fwd	ATCCGGGAATTCATGGAGCAGAAGCTGATCTCCGAGGAGGA CCTGATGTCACCCTCTACAACCTCAAAAATGTCTCTGG
CF76: myc-TRIM21 EcoRI dRING Fwd	ATCCGGGAATTCATGGAGCAGAAGCTGATCTCCGAGGAGGA CCTGATGCAACAGTTTCTGCTCCGAAACCTCAGG98C
CF77: myc-TRIM21 EcoRI dBbox Fwd	ATCCGGGAATTCATGGAGCAGAAGCTGATCTCCGAGGAGGA CCTGATGGCTGCTAAGGTATACCAGGAGAAGATCCAC
CF78: TRIM21 AgeI dPRYSPRY Rev	ATCCGGACCGGTCTACCAACACGTCCTCAGCATCTTCTTCCG

Sequencing

CF25: pMSCVn fwd	CCCTTGAACCTCCTCGTTCGACC
CF26: pMSCVn rev	ACTTCCTGACTAGGGGAGGAGTA

Genotyping of TRIM21 KO mice

CF27: FW Trim21-geno	CCTTGGCATTATTTGGGGGA
CF28: RV Trim21-geno	CTCCATGCTTCATGCAGTGC
CF29: RV Trim21-mut	GCGGATCTTGAAGTTCACCT

Table 2.1: List of primers used for any application described in this thesis.

2.3 Molecular cloning

2.3.1 Origin of DNA templates for polymerase chain reaction

The DNA templates for the polymerase chain reaction (PCR) were either full-length constructs already available in the lab or full-length cDNA clones commercially available.

Gene name	IMAGE ID	Sequence accession nb	cDNA type
Trim21	3584654	BC010580	Mouse verified Full-Length cDNA

Table 2.2: List of the cDNA clone. Information available from the I.M.A.G.E Consortium online at http://www.imageconsortium.org/.

2.3.2 DNA amplification by polymerase chain reaction

Coding sequences of mGBP1, mGBP2, mGBP5, mTRIM21, mSEC23A, mSEC23B, mSEC24A, mSEC24B and mIRF8 were amplified by PCR. Primers were purchased from Sigma-Aldrich (St. Louis, MO, USA) and were used to introduce FLAG or HA epitope tags as well as recognition sites for restriction endonucleases. The two restriction sites are not complementary to prevent the vector from re-annealing to form transformable circular DNA and to allow control of the correct orientation of the inserted PCR product. Short overhangs were placed 5' to the recognition sites to allow more efficient cutting of linear DNA by restriction enzymes. The content of the PCR reaction mix is listed in Table 2.3 and the PCR program is shown in Figure 2.1.

DNA template	100 ng
Forward primer (10µM)	2.5 µL
Reverse primer (10µM)	2.5 µL
dNTPs mix (10mM)	1 µL
5x buffer HF	10 µL
Phusion DNA polymerase	0.5 µL
H_2O	to 50 µL
Total	**50 µL**

Table 2.3: PCR reaction mix.

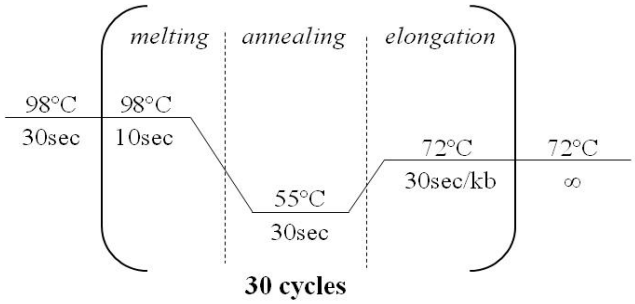

Figure 2.1: PCR cycling conditions.

Amplification of the genes of interest was verified on a 1% agarose gel (Bio-Rad Laboratories, Hercules, CA, USA) containing the fluorescent dye ethidium bromide by electrophoresis in 1X Tris-Acetate-EDTA (TAE) buffer (TAE Buffer 50X, National Diagnostics, Atlanta, GA, USA) at 100V until the migration was completed. DNA samples were visualized under UV light.

2.3.3 Preparation of the inserts and vectors

2.3.3.1 Cloning into the pMSCVneo vector

Both the PCR amplicons and the pMSCVneo vector were double digested for 1 h at 37°C as indicated in Table 2.4. The restriction enzymes (Fermentas, Thermo Scientific

Molecular Biology, Waltham, MA, USA) were inactivated for 5 min at 80°C and the digested products were run on a 0.8% agarose gel as described above. The linearised vector and digested inserts were purified in 20 µL final using the Nucleospin PCR & Gel Clean-Up kit (Macherey-Nagel, Düren, Germany) according to the manufacturer's instructions.

Enzyme 1	2 µL
Enzyme 2	2 µL
PCR amplicon	20 µL
10x FastDigest buffer	3 µL
H_2O	1 µL
Total	**30 µL**

Enzyme 1	1 µL
Enzyme 2	1 µL
Vector	1 µg
Alcaline phosphatase	1 µL
10x Fast Digest buffer	2 µL
H_2O	to 20 µL
Total	**20 µL**

Table 2.4: Restriction digest reaction mixes for the inserts and vectors.

The inserts and plasmids were ligated using T4 DNA ligase (Thermo Scientific) for 1 h at RT as listed in Table 2.5. Finally, 5 µl of the ligation mix was used for transformation as described below (see section 2.3.5).

Linearised pMSCVneo	variable
Cut purified insert	variable
10x buffer	1 µL
T4 DNA ligase	0.5 µL
H_2O	to 10 µL
Total	**10 µL**

Table 2.5: Ligation into pMSCVneo reaction mix.

2.3.3.2 Cloning into the pGEM-T vector

pGEM-T vector (Promega, Madison, WI, USA) is an open vector exhibiting a T-overhang, enabling for ligation with A-overhang inserts. As the PCR amplicons

produced by a high fidelity DNA polymerase are blunt-ended, a normal Taq polymerase was used to add an additional A at the end of the PCR fragments for 30 min at 72°C as indicated in Table 2.6.

Purified PCR amplicon	6.2 µL
10x buffer	1 µL
$MgCl_2$ (25mM)	0.8 µL
dATP (2mM)	1 µL
Taq polymerase (5U/µL)	1µL
Total	**10 µL**

Table 2.6: A-tailing reaction mix.

The inserts and plasmids were ligated using T4 DNA ligase (Thermo Scientific) overnight (O/N) at 4°C as listed in Table 2.7. Finally, 2 µl of the ligation mix was used for transformation as described below (see section 2.3.5).

pGEM-T 50ng/µL	1 µL
A-tailed insert	3 µL
2x buffer	5 µL
T4 DNA ligase	1 µL
Total	**10 µL**

Table 2.7: Ligation into pGEM-T reaction mix.

2.3.4 Site-directed mutagenesis

Site-directed mutagenesis was used to introduce the R48A and K51A mutations into mGBP2 and mGBP5. The retroviral vectors pMSCVhygro-HA-mGBP2 and pMSCVhygro-HA-mGBP5 were used as templates for the PCR reactions. Primers were designed to encompass the sequence surrounding the mutation to be introduced, according to the instructions of the QuikChange II Site-Directed Mutagenesis Kit

(Agilent Technologies Inc., Santa Clara, CA, USA) and are described in Appendix 9.2. The polymerase, buffers and deoxynucleotides (dNTPs) were all purchased from New England Biolabs (Ipswich, MA, USA).

DNA template	100 ng
Forward primer (10µM)	1.5 µL
Reverse primer (10µM)	1.5 µL
5x Q5 buffer	10 µL
5x GC enhancer buffer	10 µL
dNTPs (10mM)	1 µL
Q5 polymerase	1 µL
H_2O	to 50 µL
Total	**50 µL**

Table 2.8: Site-directed mutagenesis PCR reaction mix.

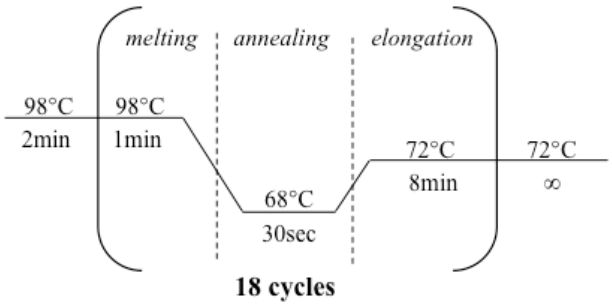

Figure 2.2: Site-directed mutagenesis PCR cycling conditions.

The generated PCR products were then directly digested with 1 µL DpnI endonuclease that recognises methylated parental vector. Finally, 2 µL of the remaining mutated retroviral vectors generated by PCR were used for transformation as described below.

2.3.5 Transformation into *E. coli* and plasmid preparation

For each transformation, 2-5 µL DNA of the ligation reaction was added to 50 µL chemically competent DH5α library-efficient cells (Invitrogen Life Technologies, Paisley, UK). After incubation on ice for 30 min, chemical transformation was performed by heat shock for 45 sec at 42°C followed by 2 min incubation on ice. Cells were recovered in 950 mL SOC medium and shaken at 225 rpm for 1 h at 37°C. After spreading onto selective plates, cells were incubated at 37°C overnight.

The constructs were first screened by restriction digestion analysed on a 1% agarose gel. Briefly, an overnight culture of a single positive colony was grown at 37°C to extract plasmid DNA using the NucleoSpin Plasmid Kit (Macherey-Nagel) according to the manufacturer's instructions. Concentration of DNA was measured by UV spectrometry with a NanoDrop (ThermoScientific) and 1 µg DNA was digested with the appropriate restriction enzyme as described previously. Presence of an insert of the right size was assessed by gel electrophoresis. DNA of positive bacterial clones was sequenced by GATC Biotech (Konstanz, Germany). Sequences were analysed with the SeqMan Pro program (DNAStar Lasergene, Madison, WI, USA).

2.4 Production of retroviruses

HEK 293T cells are a human cell line that can be transfected with plasmid DNA at high efficiency. The cell line was derived from the HEK293 cell line by the addition of the SV40 large T-antigen, leading to an increased production of some viral vectors, including retroviruses. For optimal efficiency, 293T cells were freshly thawed and kept in a low passage number. 24 h before transfection, HEK 293T were seeded in 10 cm dishes to achieve 80% confluency the next day. Cells were then transfected with the appropriate plasmid using TransIT®-293 Transfection Reagent (Mirus, Madison, WI,

USA) as follow. DNA and transfection reagents were separately mixed with Opti-MEM® (Invitrogen), briefly vortexed and incubated 10 min at RT.

Retroviral vector	4 µg
VSV-G	3 µg
gag-pol	3 µg
Opti-MEM®	10 µL
Total	**20 µL**

Opti-MEM®	200 µL
TransIT®293	30 µL
Total	**230 µL**

Table 2.9: Transfection mixes for the production of retroviruses.

DNA and transfection reagents were then mixed, vortexed, and incubated for 15 min at RT before transfection mixes were added uniformly drop by drop to the HEK 293T cells. Dishes were swirled and incubated at 37°C and 5% CO_2 for 8 h before medium was changed to DMEM + 10% FCS. Supernatants containing viruses were collected 48 h and 72 h post-transfection and pooled together. After centrifugation at 900 g for 5 min at 4°C, 1 mL aliquots of the supernatants were frozen at -80°C for long-term storage or used for viral transduction immediately.

2.5 Determination of the IC100 for specific antibiotics

Transduced cells having incorporated the gene of interest can be segregated from non-transduced cells by selection with an antibiotic whose resistance gene is encoded on the introduced plasmid, thus generating stable cell lines for the gene of interest. To determine the right concentration of the antibiotic to use for the selection of transduced cells, the inhibitory concentration 100% (IC100) was assessed for hygromycin B (Invitrogen), puromycin (Sigma-Aldrich) and geneticin (G-418, Gibco). Raw 264.7 were seeded at 50% confluency in 6-wells plates and incubated with rising concentrations of each antibiotic. The IC100 corresponds to the minimum

concentration of antibiotic leading to the death of all Raw 264.7 cells. Table 2.10 shows the IC100 concentrations for Raw 264.7 cells found for the three antibiotics.

Antibiotics	Concentration
Hygromycin B	150 µg/mL
Geneticin	850 µg/mL
Puromycin	2.5 µg/mL

Table 2.10: Concentration of antibiotics for selection of Raw 264.7.

2.6 Generation of stable cell lines

24 h before transduction, Raw 264.7 cells were seeded in a 6-wells plate to achieve 50% confluency the next day. For each viral construct, 2 ml of virus-containing supernatants were added to a well. 8 µg/ml Polybrene (Santa-Cruz Biotechnology, Dallas, TX, USA) was added to each well to improve attachment of viral particles to the cells. Plates were then centrifuged at 600g for 90min and incubated at 37°C and 5% CO_2 for 16 h before the medium was replaced with DMEM + 10% FCS. After 24h, the medium was supplemented with the appropriate antibiotics. After successful selection of cells that stably expressed the transduced constructs, aliquots of cells were frozen at -80°C and subsequently moved to liquid nitrogen storage or cells were used for experiments.

2.7 Generation of primary cell lines

2.7.1 Generation of mouse embryonic fibroblasts

The uterus was taken out of a female 13.5 or 14.5 days post-coïtum and put in iodine solution (poly(vinylpyrrolidone)-iodine complex at 100 mg/mL in PBS; Sigma-

Aldrich). The uterus was incubated sequentially for 1min twice in iodine solution, twice in 70% ethanol and twice in PBS. The embryos were taken out of the uterus one by one by carefully removing the amnion and the placenta. Each embryo was transferred into 150 mm dish (Corning) and placed looking to the right to see the liver. The liver, the intestine and the heart were carefully removed, as well as the head, but the neck and the arms were kept. The embryo was placed in a new 150 mm dish and 100 µL of 0.15% trypsin were added. The embryo was finely chopped with two scalpels and placed in the incubator at 37°C, 5% CO_2 for 5-10 min. The homogenate was loosened from the plate in 5 mL DMEM supplemented with 15% FCS, 50 µM beta-mercaptoethanol (Sigma-Aldrich), 1X non-essential amino-acids (PAA Laboratories, Pasching, Austria) and penicillin/streptomycin. Cells were then resuspended in an additional 20 mL of medium and were incubated for 3 days at 37°C, 5% CO_2 without touching or moving the dishes. At day 3, 15 mL medium was taken off each plate and replaced with fresh media. Cells were grown until confluent and frozen in liquid nitrogen.

2.7.2 Generation of mouse bone marrow-derived macrophages

Both mouse leg bones were isolated and kept on ice in sterile PBS (Sigma Aldrich). Cells were extracted from bones by crushing in a mortar in sterile PBS. After filtering through a 70 µm filter (Sartorius, Göttingen, Germany) and spinning at 900 g for 5 min at RT, cells were resuspended in 20 mL DMEM supplemented with Penicillin/Streptomycin, 10% FCS and 100 U/mL M-CSF (=macrophage complete medium). Total bone marrow progenitor cells count was determined using a haemocytometer and the cell concentration was adjusted to a final concentration of $4x10^6$ in macrophage complete medium. Cells were seeded at a density of $4x10^6$ in 10

cm sterile culture dishes and incubated for at 37°C, 5% CO_2. After 3 days, 5 mL of complete macrophage medium was added to each dish. After another 4 days, culture supernatants were discarded and cells were washed with 5 mL pre-warmed PBS. Cells were then incubated for 10-15 min in ice-cold PBS at 4°C and cells were detached by pipetting up and down. Cells were pooled together, spun at 900 g for 5 min at RT and resuspended in 3-5 mL DMEM supplemented with Penicillin/Streptomycin and 10% FCS (=DMEM/F12-10). Cells were then either frozen at $4x10^6$ per vial or seeded for experiments at $2x10^5$ cells per well in 24-well plates or $1x10^6$ cells per well in 6-well plates.

2.8 Immortalisation of primary BMDMs

Both mouse leg bones were isolated and kept on ice in sterile PBS. Cells were extracted from bones by crushing in a mortar in IMDM supplemented with 15% FCS. After filtering through a 70 μm filter and spinning at 900 g for 5 min at RT, cells were resuspended in 5 mL red blood cell lysis solution (Sigma Aldrich)at RT for no longer than 5 min. The solutions was neutralised with 10 mL PBS, cells were span at 900 g for 5 min, resuspended in 20 mL PBS and filtered through a 40 μm filter. Total bone marrow progenitor cells count was determined using a haemocytometer. 100 μL of separation buffer (PBS, 0.5% BSA, 2mM EDTA) and 10 μL of anti-CD117-biotin antibody (Miltenyi Biotec, Bergisch Gladbach, Germany) were added per 1.10^7 cells. After incubation at 4°C for a minimum of 10 min, cells were resuspended in 10 mL PBS and span at 900 g for 5 min. 100 μL of separation buffer and 10 μL of anti-biotin beads (Miltenyi Biotec) were added per 1.10^7 cells. After incubation at 4°C for 15 min, cells were resuspended in 10 mL PBS and span at 900 g for 5 min. The pellet was

resuspended in 500 mL separation buffer and CD117-positive macrophage progenitors were separated on a MACS purification column.

The cells were loaded on a MACS purification column previously equilibrated with 3x3 mL of separation buffer. Unbound material was washed with 3x3 mL of separation buffer. BMDMs were eluted with 2 mL separation buffer in a new collection tube by flushing out the magnetic beads vigorously with the plunger. PBS was added to obtain a final volume of 10 mL. Successful purification was assessed by determining the cell concentration, which should yield 1/3 of the initial cell load. Cells were span at 900 g for 5 min, washed once in 10 mL IMDM + 15% FCS, span at 900 g for 5 min before final resuspension in 8 mL IMDM + 15% FCS supplemented with IL-3 (10 ng/mL), IL-6 (20 ng/mL) and SCF (25 ng/mL). The cells were split in two wells of a 6-well pate and incubated for 48h at 37°C, 5% CO_2.

Homeobox protein 8 (HOXB8) has been shown to block differentiation of myeloid progenitors {(Schroeder et al., 2006; Yoshimi et al., 2009; Wang et al., 2006). Infection of bone marrow cells with retroviruses encoding oestrogen-dependent HOXB8 enables generation of myeloid progenitors, which can be cultured in presence of granulocyte-macrophage colony stimulating factor (GM-CSF) and oestrogen. After incubation for 2 days, non-adherent cells were span at 900 g for 5 min and resuspended in 1 mL of IMDM + 15% FCS supplemented with IL-3, IL-6 and SCF. Cells were transduced with 2 mL of HOXB8 retroviruses in presence of 8 μg/mL polybrene and span at 600 g for 90 min. Cells were washed once to remove any trace of remaining polybrene and extracellular retroviruses, resuspended in 4 mL IMDM + 15% FCS supplemented with IL-3, IL-6 and SCF and incubated 48h at 37°C, 5% CO_2. Transduced non-adherent progenitor cells were selected by replacing the medium with

IMDM + 15% FCS supplemented with 1 μM fresh estradiol, 10 ng/mL GM-CSF and 1.5 μg/mL puromycin. Cells were selected and expanded for a minimum of 15-19 days before induction of differentiation.

Selected positively-transduced myeloid progenitors can be differentiated into immortalised macrophages by removing oestrogen from the culture medium. Cells were washed three times in RPMI 1640 + 10% FCS to remove the estradiol. Cells were finally transferred in RPMI1640 + 10% FCS supplemented with 10 ng/mL GM-CSF for 3-4 days until they differentiated into macrophages and became adherent.

2.9 Protein biochemistry

2.9.1 Antibodies

Primary antibodies used for immunoprecipitation, immunoblot or immunofluorescence were: rabbit polyclonal anti-GBP1 (Virreira Winter et al., 2011), goat polyclonal anti-TRIM21 (#sc-21365, Santa-Cruz Biotechnology), mouse monoclonal anti-myc (#2276, Cell Signalling, Danvers, MA USA), mouse monoclonal anti-ubiquitin FK2 (#PW8810, Enzo Life Sciences, Farmingdale,NY, USA), rabbit monoclonal anti-ubiquitin Lys48 (#05-1307, Merck Millipore, Billerica, MA, USA), rabbit monoclonal anti-ubiquitin Lys63 (#05-1308, Merck Millipore) and mouse monoclonal anti-p62 (#56416, Abcam, Cambridge, UK). Secondary antibodies for immunoblotting were from KPL (Gaithersburg, MD, USA): goat anti-mouse HRP (#474-1806), goat anti-rabbit HRP (#474-1506) and rabbit anti-goat (#14-13-06). Secondary antibodies for immunofluorescence were from Molecular Probes: AlexaFluor®488 chicken anti-rabbit (#A21441), AlexaFluor®488 chicken anti-goat (#A21467), AlexaFluor®568 goat anti-rabbit (#A11011), AlexaFluor®568 donkey

anti-goat (#A11057) and AlexaFluor®568 goat anti-mouse (#A11004). The dilution or concentration of the different antibodies according to their use is are listed in Table 2.11.

Antibody	**Application**		
	Immunoblot	**Immunoprecipitation**	**Immunofluorescence**
anti-GBP1	1:10000	1:1000	1:500
anti-TRIM21	1:200	2 μg/mL	1:200
anti-myc tag	1:1000	1:1000	/
anti-Flag tag	1:500	3 μg/mL	/
anti-ubiquitin FK2	/	/	1:500
anti-ubiquitin Lys48	/	/	1:500
anti-ubiquitin Lys63	/	/	1:500
anti-p62	/	/	1:250
anti-mouse HRP	1:5000	/	/
anti-goat HRP	1:5000	/	/
anti-rabbit HRP	1:5000	/	/
AlexaFluor®488 anti-rabbit	/	/	1:5000
AlexaFluor®488 anti-goat	/	/	1:5000
AlexaFluor®568 anti-rabbit	/	/	1:5000
AlexaFluor®568 anti-goat	/	/	1:5000
AlexaFluor®568 anti-mouse	/	/	1:5000

Table 2.11: Concentration or dilution of antibodies for biochemistry and cell biology use.

2.9.2 Cell lysis

Cells were washed twice in ice cold PBS and lysed in 600 □L perwell ice cold lysis buffer (25 mM TrisHCl pH 7.4; 5 mM $MgCl_2$; 150 mM NaCl; 0.5% NP-40; 1 tablet protease inhibitor cocktail (Roche, Basel, Switzerland) per 10 mL). After rocking for 1 h minimum at 4°C, lysates were centrifuged for 20 minutes at 16200 g to separate soluble from insoluble fractions. The supernatants containing the soluble proteins were kept for protein quantification and further experiments.

2.9.3 Protein quantification

Protein concentration of the cell lysates were determined using Pierce® BCA Protein Assay Kit (Thermo Scientific) according to the manufacturer's instructions. For each sample, an undiluted sample as well as a 1:5 dilution sample were used to guarantee a fit within the standard curve.

2.9.4 Immunoprecipitation

All steps were performed at 4°C or on ice. Cells were washed twice in PBS and lysesd in ice cold lysis buffer (25 mM TrisHCl pH 7.4; 5 mM $MgCl_2$; 150 mM NaCl; 0.5% NP-40; cOmplete EDTA-free protease inhibitor cocktail (Roche)). After rocking for 1 h minimum, lysates were centrifuged for 20 min at 11 000 g. Total protein was quantified by the Bradford Dye assay (Pierce® BCA Protein Assay Kit, Thermo Scientific). Following pre-clearing for 3 h with protein G sepharose (Sigma Aldrich), supernatants containing 0.5-1 mg proteins were incubated overnight with anti-myc or anti-TRIM21 antibody and protein G beads. Immunoprecipitated proteins were eluted from the beads at 92°C for 10 min in 1X NuPAGE protein loading buffer (NuPAGE 4X, Invitrogen) supplemented with 1mM dithiothreitol (DTT, Sigma Aldrich).

2.9.5 SDS-PAGE gel electrophoresis

Proteins were separated according to their size by sodium dodecyl sulfate polyacrylamide gel electrophoresis (SDS-PAGE). SDS-PAGE gels consisting of Tris-glycine separating and stacking gels were prepared (Protogel 30%; 4X ProtoGel Resolving Buffer; Protogel Stacking Buffer; National Diagnostics) on the day of use in a Bio-Rad casting system. After polymerization, gels were placed in the appropriate Bio-Rad electrophoresis system, and Tris-glycine running buffer (National Diagnostics) was added. 5-10 µg of protein lysate samples or 7.5 µL of the 40 µL of immunoprecipitated samples were added into each lane. Each marker lane was filled with 10 µl of Precision Protein Plus Dual Color Standards (Bio-Rad Laboratories, Hercules, CA, USA). Proteins were separated by running the gel at 125V until the dye front reached the end of the gel. Gels were then used for immunoblot.

2.9.6 Immunoblot

Immunoblot was used to quantitatively detect specific protein bands after separation of proteins on 12% NuPAGE Bis-Tris SDS-PAGE gels (Life Technologies). Proteins were transferred onto nitrocellulose membrane by dry-blotting (iBlot®, Life Technologies). Blots were blocked at RT 1 h in a 5% non-fat dried milk/PBS solution (Blotto). The membrane was then incubated with primary antibody in Blotto + 0.1% Tween 20 for a minimum of 1 h at RT or overnight at 4°C. On the next day, blots were washed three times for 10 min in Blotto + 0.1% Tween 20 (except α-GBP1 required 3x1 h washes). Blots were incubated for 1 h with HRP-conjugated secondary antibodies in Blotto + 0.1% Tween 20. Blots were washed three times for 15 min in Blotto + 0.1% Tween 20 (except α-GBP1 required 3x1 h washes). Finally, blots were developed with Pierce ECL Western Blotting Substrate (Thermo Scientific) or

Immobilon Western Chemiluminescent HRP Substrate (Merck Millipore). After incubation at RT for 1 min or 5 min respectively, blots were exposed to CL-XPosure film (Thermo Scientific) and films developed.

2.10 Immunofluorescence

Immunofluorescence was performed on 12 mm, 1.5 mm coverslips (Thermo Fisher) in 24-well plates (Nunc). Cells were stimulated with 100 U/mL recombinant murine IFNγ (R&D) overnight and infected with *Toxoplasma* at an MOI of 5-10. After the indicated infection time, cells were washed three times with PBS and fixed in 3% paraformaldehyde (Sigma Aldrich) at RT for 20 min. Cells were permeabilised for 15 min at RT with 50 mM NH_4Cl/0.2% saponin/PBS and kept at 4°C for up to a week in 0.2% fish skin gelatin/0.02% saponin/0.02% NaN_3/PBS (PGAS) until antibody staining. Briefly, coverslips were incubated with appropriate primary antibody in a humid chamber at RT for 1 h. Coverslips were then washes three times in PGAS and subsequently incubated with appropriate secondary antibody in a humid chamber at RT for 1 h in the dark and washed three times in PGAS solution followed by three washes in PBS. Nuclei were stained with 1 µg/mL Hoechst 33442 solution (Sigma-Aldrich). Coverslips were mounted on Superfrost® Plus glass slides (Thermo Scientific) with 50 µL Mowiol® 4-88 solution (Sigma-Aldrich) and kept in the dark at 4°C. The frequency of *Toxoplasma*-positive vacuoles was determined by counting 100 PVs per technical replicate using an AxioPlan II fluorescent microscope (Carl Zeiss) equipped with DAPI, GFP and rhodamine filters. Images were captured with a Leica TCS-SP5 inverted confocal microscope (Leica Microsystems, Wetzlar, Germany) fitted with conventional photomultiplier tubes and hybrid detectors and using a 100x Leica HCX PL APO CS (numerical aperture 1.4) oil immersion objective.

Images were processed in Fiji/ImageJ software (National Institute of Health, Bethesda, MD, USA).

2.11 Proximity ligation assay

The DuoLink *In situ* proximity ligation assay (Olink Bioscience, Uppsala, Sweden) was used according to the manufacturer's instructions. Briefly, MEFs were seeded, infected, washed, fixed and permeabilised as described in Immunofluorescence. Coverslips were incubated with primary antibodies (rabbit anti-GBP1 1:500 and goat anti-TRIM21 1:200) for 1 h at 37°C and washed three times in PGAS. Coverslips were then incubated with PLA probes anti-rabbit PLUS/MINUS and anti-goat PLUS/MINUS diluted 1:5 in PGAS for 1 h at RT and washed 2x5min in 1x wash buffer A. Ligation solution at a 1:5 dilution supplemented with ligase at a 1:40 dilution was then added onto the coverslips and incubated for 30 min at 37°C. After 2x2 min washes in 1x wash buffer A, amplification solution at a 1:5 dilution supplemented with polymerase at a 1:80 dilution was added onto the coverslips for 100 min at 37°C. Coverslips were washed 2x10 min in 1x wash buffer B and 1x1 min in 0.01x wash buffer B. After drying for 15 min at RT in the dark, coverslips were mounted in DuoLink *In situ* mounting medium with DAPI and stored at -20°C until analysis on a Leica TCS-SP5 inverted confocal microscope fitted with conventional photomultiplier tubes and hybrid detectors and using a 100x Leica HCX PL APO CS (numerical aperture 1.4) oil immersion objective. Images were processed in Fiji/ImageJ software.

2.12 *In vitro* plaque assay

MEFs were passaged 24 h before infection in 24-well plates at a seeding density of $2x10^5$ and induced with 100 U/mL IFNγ 16h before infection. The next morning, cells were infected with 100 GFP-expressing Pru tachyzoites per well. The plates were left

untouched for 3 days and the number of fluorescent plaques was subsequently counted using an Olympus CKX41 (Olympus, Center Valley, PA, USA) epifluorescent microscope.

2.13 Transmission electron microscopy

WT and TRIM21 KO MEFs were induced with IFNγ for 16h and infected with avirulent Pru *Toxoplasma* as described previously (see 2.1.4). Preparation of the samples and ultrastructural analysis of *Toxoplasma*-infected WT or TRIM21 KO MEFs was subsequently performed by Liz Hirst in the dedicated service provided within the Crick at Mill Hill Laboratory. Cells were washed three times in PBS before 0.05% tryspin-EDTA treatment. After centrifugation at 900 g for 5 min, cells were immersion fixed in 2% glutaraldehyde/2% paraformaldehyde in 0.1M sodium cacodylate buffer, pH7.2, embedded in 2% agarose and spun for 3 min at 13000 rpm before being returned to 2% glutaraldehyde/2% paraformaldehyde in 0.1 M sodium cacodylate buffer, pH7.2 O/N. Samples were washed in sodium cacodylate buffer 0.1 M pH7.2 (SCB) for 10 min, post-fixed in 1% osmium tetroxide/SCB for 1.5 hour, washed in SCB for 10 min and stained on bloc in 1% aqueous uranylacetate for 1.5 hour. Samples were dehydrated in 50% ethanol, 75% ethanol and 90% ethanol for 10 min each, 3x10 min in 100% ethanol and 2x30 min in propylene oxide. Samples were embedded in epon resin (Agar Scientific, Stansted, UK) for 5 changes over 8 h and polymerised at 70°C O/N. 50 nm sections were mounted on pioloform-coated slot grids and stained with uranyl acetate for 30 min and with Reynold's lead citrate for 7 min. Samples were observed with a JEOL 1200 EX transmission electron microscope (JEOL, Tokyo, Japan) equipped with an Orius 1000 CCD camera (Gatan, Pleasanton, CA, USA).

2.14 Fluorescence Activated Cell Sorting of cultured cells

After IFNγ induction for 16h, WT and TRIM21-deficient MEFs were infected for 1 h 15 min with type II avirulent tomato-expressing Prugniaud at an MOI of 5. Cells were washed three times in PBS and treated with 0.05% tryspin-EDTA for 1 min at 37°C. Cells were resuspended in culture medium and centrifuged at 900 g for 5 min at 4°C. The pellet was then resuspended in PBS to eliminate any phenol red remaining from the culture medium and centrifuged at 900 g for 5 min at 4°C.

Unstained samples were resuspended in 200 µL phenol red-free RPMI supplemented with 2% FCS and filtered twice through 40 µm FACS strainers to a final volume of 500 µL RPMI 2% FCS supplemented with 2.5 mM EDTA.

All other samples were resuspended in 100 µL PBS and stained with LIVE/DEAD® fixable near IR dead cell stain kit (Life Technologies) on ice for 20 min. After washing once in 100 µL PBS, cells were spun at 900 g for 5 min at 4°C and the pellet was resuspended in 200 µL phenol-free RPMI supplemented with 2% FCS. Cells were finally filtered twice through 40 µm FACS strainers to a final volume of 500 µL RPMI 2% FCS supplemented with 2.5 mM EDTA.

Cells were kept on ice until sorting on a cat.2 Influx cell sorter. Live uninfected control samples were gated on APC-Cy7$^-$/PE TexasRed$^-$ cells and live *Toxoplasma*-infected samples were gated on APC-Cy7$^-$/PE TexasRed$^+$ cells. For each sample, 110000 cells were collected and a purity check was performed to check for any contamination. Cells were then span at 900 g for 5 min at 4°C and the pellet was resuspended in 500 µL Trizol before storage at -80°C.

Sample	Number of cells sorted	Purity of the sort
WT uninfected triplicate 1	110000	92.24%
WT uninfected triplicate 2	110000	93.68%
WT uninfected triplicate 3	110000	96.37%
WT infected triplicate 1	36396	93.95%
WT infected triplicate 2	38752	91.60%
WT infected triplicate 3	36491	90.85%
TRIM21 KO uninfected triplicate 1	110000	70.77%
TRIM21 KO uninfected triplicate 2	110000	97.53%
TRIM21 KO uninfected triplicate 3	110000	96.65%
TRIM21 KO infected triplicate 1	110000	92.14%
TRIM21 KO infected triplicate 2	109667	93.73%
TRIM21 KO infected triplicate 3	103394	98.89%

Table 2.12: Number of cells and purity obtained for each FACS-sorted sample.

2.15 RNA extraction of FACS-sorted cells

All steps were performed with RNAse-free tubes and using lab equipment previously cleaned with RNaseZap (Ambion, Life Technologies). Pellets were thawed on ice and 200 µL chloroform was added per tube. After vigorous vortexing for 5 sec and incubation at RT for 10 min, the mix was spun at 13 000 rpm for 15 min at 4°C. The upper aqueous phase containing the extracted RNA was transferred to a new tube containing 500 µL ethanol. The mix was then purified using the miRNeasy kit (Qiagen, Venlo, The Netherlands), according to the manufacturer's instructions. Briefly, the mix was transferred to a mini spin column and span at 13 000 rpm for 1 min at 4°C. Membranes were washed once with 500 µL RW1 buffer and twice with RPE buffer

before dry-spinning at 13 000 rpm for 1 min at 4°C. The RNA was eluted with 14 µL RNA-free water into a new tube and samples were stored at -80°C.

2.16 RNA sequencing

The following steps were performed by the High-Throughput Screening facility service provided within the Crick at Mill Hill Laboratory.

2.16.1 Verification of RNA quality

The quality of RNA was assessed using an Agilent 2100 Bioanalyser (Agilent Technologies, Santa Clara, CA, USA). All RNA samples present an RNA integrity number (RIN) higher than 7 (Figure 2.3), meaning the RNA was not degraded and of high quality (Schroeder et al., 2006).

2.16.2 Preparation of samples for RNA sequencing

The RNA samples isolated from 3 technical replicates were poly-A purified and converted into cDNA libraries using the Illumina TruSeq Library Preparation kit v2. Samples were sequenced using the Illumina HiSeq 2500 platform with paired-end read lengths of 100 nucleotides.

2.16.3 RNA sequencing analysis

The following steps were performed by Helena Alhfors (Babraham Institute, Babraham, UK). The quality of the sequencing data was assessed using the FastQC tool version 0.11.2 (http://www.bioinformatics.babraham.ac.uk/projects/fastqc/). Reads were aligned using Tophat version 2.0.12, allowing a maximum of 2 mismatches (Kim et al., 2013). The aligned data was sorted and indexed using SAMtools version 0.1.18 (Li et al., 2009b). HTSeq-count version 0.5.4 (Anders et al.,

2015) was used to count the reads mapping to genes using gtf file version 78. The quality of the count data was analysed using SeqMonk version 0.30.0 (http://www.bioinformatics.babraham.ac.uk/projects/seqmonk/) and DESeq2 (R package). The differentially expressed genes were identified from the count data using DESeq2. Data visualisation was performed with R/bioconductor.

2.17 Stable Isotope Labelling by Amino acids in Cell culture

In order to incorporate the heavy-labelled isotopes into WT and TRIM21 KO MEFs, cells were cultivated for a minimum of 5 doublings (equivalent to 4-5 passages) with DMEM supplemented with 84 mg/L heavy ^{13}C-arginine and 146 mg/L heavy ^{13}C-lysine in presence of 10% FCS (SILAC dialysed, 1000 Da cut-off, Dundee Cell Products, Dundee, UK) and 40 mg/L unlabelled proline to avoid arginine-to-proline conversion. Unlabelled cells were cultivated in parallel in DMEM supplemented with 84 mg/L light ^{12}C-Arg and146 mg/L light ^{12}C-Lys in presence of 10% FCS (SILAC dialysed, 1000 Da cut-off) and 40 mg/L unlabelled proline. Labelled and unlabelled cells were induced with IFNγ for 16h and infected with avirulent Pru *Toxoplasma* as described previously (see 2.1.4). Cells were trypsinised and washed three times in PBS. Pellets were mixed at a 1:1 ratio as a forward sample (WT heavy/TRIM21 KO light) and as a reverse sample (WT light/TRIM21 KO heavy). Both sample pellets were flash-frozen in liquid nitrogen and kept at -80°C. Preparation of the samples was then performed by Dr. Vesela Encheva in the dedicated service provided within the Crick in Clare Hall Laboratory. Analysis of the raw data was performed with the help of Dr. Vesela Encheva using the Perseus software.

2.17.1 Quantitative diGly Proteomics

Cells were lysed in 9 M urea, 20 mM HEPES, pH=7.8, supplemented with 100 units/ml of benzonase and sonicated to reduce viscosity (3 mm probe, 50% amplitude, 3 x 15 sec bursts, on ice). Between 30-40 mg of protein per sample were used as estimated by Bradford protein assay. Lysates were reduced with 10 mM DTT for 30 min at room temperature, followed by alkylation with 20 mM chloroacetamide (Sigma Aldrich) for 30 min at room temperature in the dark. Lysates were digested initially with LysC for 2 hours at 37°C. The lysates were then diluted with 100 mM ammonium bicarbonate, 5% acetonitrile to a final urea concentration of less than 2 M. The samples were digested 1:100 enzyme to protein ratio (w/w) with trypsin (Promega) overnight at 37°C. The next day, two additional aliquots of trypsin were added and incubated at 37°C for four hours each. After the digestion the samples were acidified with trifluoroacetic acid (TFA, Thermo Fisher Scientific) to a final concentration of 1% (v/v). All insoluble material was removed by centrifugation and the supernatant was desalted with Sep-Pak C_{18} cartridges (Waters, Milford, MA, USA) and lyophilised for 2 days.

Peptides containing the diGly remnant were enriched using K-ϵ-GG affinity resin (Cell Signalling Technology) according to the manufacturer's instructions. Briefly, digests were reconstituted in 1.4 mL of immunoaffinity purification (IAP) buffer as supplied by the manufacturer. One aliquot (~40 µL packed bead volume) was washed four times with PBS and mixed with the peptide sample. Incubation of sample and beads was performed with gentle rotation at 4°C for 2 hours followed by a 30 sec 2000 × *g* spin to pellet the beads. The antibody beads were washed twice with ice-cold IAP buffer followed by three washes with ice-cold water. DiGly peptides were eluted from the

beads with the addition of 50 µL of 0.15% TFA and allowed to stand at room temperature for 5 min. After a 30 sec 2000 × *g* spin, the supernatant was carefully removed and retained for further analysis. A second 55-µL aliquot of 0.15% TFA was added to the beads followed by a 30 sec 2000 × *g* spin, and the supernatant was added to the first elution. The eluted peptides were lyophilised for 2 days and used for strong cationic exchange (SCX) fractionation.

2.17.2 Strong cationic exchange fractionation of diGly peptides

For SCX fractionation, peptides eluted from the K-ϵ-GG affinity resin were dissolved in 35 µL of 10 mM ammonium formate pH=2.9, 25% acetonitrile. The samples were sonicated and insoluble material was removed by centrifugation. Peptide separation and fraction collection was performed using the micro pump on an RSLCnano U3000 (Thermo Fisher Scientific) at a flow rate of 50 µL/min. The peptides were loaded on 15-cm Polysulfoethyl-Asp SCX column (1 mm inner diameter, 5 µm particle size, PolyLC). Solvent A was 10 mM ammonium formate pH=2.9, 25% acetonitrile, and solvent B was 500 mM ammonium formate pH=6.8, 25% acetonitrile. The samples were run on a linear gradient of 0-80% solvent B in 45 min, total run time was 75 min including column conditioning. A total of 30 fractions were collected every minute between 15-45 min after injection (1 fraction= 50 µL). The collected fractions were vacuum dried and used for liquid chromatography-mass spectrometry/mass spectrometry (LC-MS/MS) analysis.

2.17.3 Liquid chromatography-mass spectrometry/mass spectrometry

For MS analysis, peptides were resuspended in 0.1% TFA and loaded on 50-cm Easy Spray PepMap column (75 µm inner diameter, 2 µm particle size, Thermo Fisher Scientific) equipped with an integrated electrospray emitter. Reverse phase

chromatography was performed using the RSLCnano U3000 (Thermo Fisher Scientific) with a binary buffer system at a flow rate of 250 nL/min. Solvent A was 0.1% formic acid, 5% DMSO, and solvent B was 80 % acetonitrile, 0.1% formic acid, 5% DMSO. The diGly enriched samples were run on a linear gradient of solvent B (2-40%) in 90 min, total run time of 120 min including column conditioning. The nanoLC was coupled to a Q Exactive mass spectrometer using an EasySpray nano source (Thermo Fisher Scientific).

The Q Exactive was operated in data-dependent mode acquiring HCD MS/MS scans (R=17,500) after an MS1 scan (R=70, 000) on the 10 most abundant ions using MS1 target of $1x10^6$ ions, and MS2 target of $5x10^4$ ions. The maximum ion injection time used for MS2 scans was 120 ms, the HCD normalised collision energy was set at 28, the dynamic exclusion was set at 10 s, and the peptide match and isotope exclusion functions were enabled.

2.17.4 Data processing and analysis

Raw data files were analysed with MaxQuant software (version 1.3.0.5) as described previously (Cox et al., 2009). Parent ion and tandem mass spectra were searched against UniprotKB *Mus musculus* database (August 2012). A list of 247 common laboratory contaminants provided by MaxQuant was also added to the database. For the search the enzyme specificity was set to trypsin with maximum of three missed cleavages for the diGly datasets. The precursor mass tolerance was set to 20 ppm for the first search (used for mass re-calibration) and to 6 ppm for the main search. Carbamidomethylation of cysteines was specified as fixed modification, oxidised methionines and N-terminal protein acetylation were searched as variable modifications. Di-glycine-lysine was added to the list of variable modifications when

samples enriched for ubiquitinated were searched. The datasets were filtered on posterior error probability to achieve 1% false discovery rate on protein, peptide and site level.

2.18 Mice

2.18.1 Ethics statement

All procedures involving mice were approved by the local ethical committee of the Crick at Mill Hill Laboratory and are part of a project license approved by the Home Office, UK, under the Animals (Scientific Procedures) Act 1986.

2.18.2 Genotyping of TRIM21$^{-/-}$ mice

A TRIM21$^{-/-}$ mouse (Yoshimi et al., 2009) available from the Jackson Laboratory was acquired and rederived into the NIMR. This mouse is on the Jackson lab C57BL/6 background, which was maintained throughout rederivation. The pups were genotyped by PCR of genomic DNA from earpieces. Briefly, the earpieces were lysed in 500 µL lysis buffer (100 mM Tris-HCl pH 8.5, 200 mM NaCl, 5 mM EDTA, 0.2% SDS, 0.1 mg/mL proteinase K) for 3 h at 56°C under agitation at 800 rpm. Lysates were then centrifuged at 16200 g for 5 min and the supernatant was thoroughly mixed with 500 µL isopropanol. After centrifugation at 16200 g for 5 min, the pellet was dried at RT and resuspended in 500 µL H_2O. PCR was performed as described in the literature (Yoshimi et al., 2009).

2.18.3 Infection of mice

Wild-type (WT) and TRIM21 deficient (Yoshimi et al., 2009) mice on the C57BL/6 background were bred and intercrossed at the Mill Hill Laboratory under specific pathogen-free conditions. Experiments were performed on 6 to 8-week-old females.

For oral infections, cysts of *Toxoplasma* avirulent type III strain ME49 (generous gift from Michael Grigg, NIH, USA) were isolated from the brain of an infected Parkes mouse by syringe lysis of the brain. Mice were infected with 5-40 cyst resuspended in 200 μL PBS by oral gavage.

For intraperitoneal (i.p.) infections, *Toxoplasma* avirulent type II strain Pru expressing GFP and firefly luciferase were harvested from the peritoneum of a 4-day infected C57BL/6 mouse and passaged through a 26 gauge needle (Terumo). Parasites were washed twice with PBS and mice were injected i.p. with $5x10^4$ parasites resuspended in 200 μL PBS.

For *in vivo* imaging, mice were injected i.p. with 3 mg firefly D-luciferin (Perkin Elmer, Waltham, MA, USA), left for 10 min and imaged with an IVIS Spectrum-bioluminescent and fluorescent imaging system (Xenogen Corporation, Caliper Life Sciences, Hopkinton, MA, USA) under isoflurane anaesthesia (Abbott, Chicago, IL, USA).

2.19 Blood sampling and tissue harvesting

Blood was withdrawn at 4 and 7 days post-infection (dpi) from the saphenous vein after shaving the right leg and puncturing the superficial vein with a 27 gauge needle (Terumo). Blood was collected in microvette CB 300 (Sarstedt, Nümbrecht, Germany)

tubes, incubated for 1 hour at 4°C and spun 2x10 min at 5 000 rpm at 4°C before storage at -20°C until further use. Alternatively, blood was collected by terminal cardiac puncture at 7 dpi. Animals were anesthetised with 75 mg/kg ketamine (Vetalar®, Zoetis, Florham Park, NJ, USA) and 1 mg/kg medetomidine (Medetor®, Chanelle, Loughrea, Ireland) and blood was withdrawn directly from the heart with a 25 gauge gauge needle (Terumo) and collected in 1.1 mL Z-gel microtubes (Sarstedt), incubated for 10 min at RT and span 10 min at 5 000 rpm before storage at -20°C until further use.

Single cell suspensions were prepared from peritoneal exudate cells (PECs) obtained by peritoneal wash with 6 mL of PBS. Single cell suspensions were prepared from spleen, draining lymph nodes, mesenteric lymph nodes and Peyer's patches by grinding the organs through a 40 μm filter (BD) and resuspending them in PBS + 1% bovine serum albumin (PBA). Red blood cells were then lysed at RT for 3 min with 1 mL 0.86% ammonium chloride (Sigma Aldrich) and resuspended in PBA.

2.20 Isolation of brain mononuclear cells

Brain mononuclear cells were isolated on a Percoll gradient following the procedure described by Pino & Cardona (Pino and Cardona, 2011). Briefly, WT and TRIM21 KO mice were culled at 7 dpi by overdose of pentobarbital (Virbac, Carros, France). 10 mL of ice-cold PBS were perfused in the heart using an 18 gauge gavage needle, and the brain was carefully extracted and kept in 1 mL of ice-cold PBS. Brain tissues were disrupted through a 1 mL syringe (Terumo) and subsequently through a 19 gauge needle (Terumo). The cell suspension was fractionated on a 30-70% Percoll gradient (Sigma-Aldrich) for 30 min at 500 g without break. The mononuclear cells in the

interphase were washed once with PBS before resuspension in 1% PBA and immediately used for further experiments.

2.21 Fluorescence Activated Cell Sorting of *ex vivo* cells and parasites

2.21.1 FACS antibodies

All antibodies used for FACS staining were purchased from BioLegend. Innate cells were stained with CD11c, CD11b, Ly6C, Ly6G, F4/80 and CD45. Lymphocytes were stained with CD3, CD4, CD8, CD19, NK1.1, TCRγδ and IFNγ. Brain- or peritoneum-derived parasites were stained with IgG and IgM.

Specificity	Label	Clone	Dilution
CD11c	BV785	N418	1:200
CD11c	APC	N418	1:200
CD11b	PerCP-Cy5.5	M1/70	1:200
CD11b	PE	M1/70	1:200
Ly6C	PB	HK1.4	1:200
Ly6G	APC-Cy7	1A8	1:200
F4/80	APC	BM8	1:200
F4/80	PerCP-Cy5.5	BM8	1:200
CD45	PE	30-F11	1:400
CD3	APC-C7	17A2	1:200
CD4	BV605	RM4-5	1:200
CD8	PerCP-Cy5.5	53-6.7	1:100
CD19	BV786	6D5	1:200
NK1.1	APC	PK136	1:200
TCRγδ	PE	GL3	1:300

IFNγ	PE-Cy7	XMG1.2	1:200
IgG	APC	Poly4053	1:200
IgM	PerCP-Cy5.5	RMM-1	1:200
Live/dead Zombie Aqua™	PO	/	1:200

Table 2.13: List of antibodies used for FACS staining.

2.21.2 FACS staining and analysis

Innate cells for staining were blocked in FcγII/III block solution (Biolegend) at 4°C for 15 min. Innate cells and lymphocytes were then stained in 50 μL on ice for 20 min in presence of Zombie Aqua™ fixable viability kit (BioLegend), washed with PBA and fixed in 4% formaldehyde at RT for 20 min. For intracellular staining, lymphocytes were permeabilised with Perm/Wash (BD) for 15 min at room temperature and stained with anti-cytokine for 30 min at 4°C. Lymphocytes were then washed and resuspended in 200 mL PBA. Finally, 25 μL of CountBright absolute counting beads (Life Technologies) were added to both innate cells samples and lymphocytes samples. Samples were run and analysed immediately or kept at 4°C O/N before acquisition on an LSR Fortessa (BD), following the gating strategy explained in Figure 2.4. Data analysis was performed with the FlowJo software (Treestar, Ashland, OR, USA). Compensation controls were single colour stained cells from splenocytes.

Parasites were isolated as described previously from either tissue culture (see 2.1.2), from the peritoneum and brain of a 4- or 7-day infected C57BL/6 mice (see 2.18.3). Parasites were stained in 100 μL for 20 min on ice, washed with PBA and fixed in 4% paraformaldehyde at RT for 20 min. After washing in PBA, parasites were analysed

immediately on an LSR Fortessa. Data analysis was performed with the FlowJo software (Treestar). Compensation controls were single colour stained cells from peritoneal exudate cells.

2.22 Parasite counting in the brain

The brain was removed at 7 dpi from infected animals and placed in 1 mL PBS. The organ was mashed with a 1 mL syringe, 10 μL of the suspension was placed on a coverslip and GFP-expressing parasites were counted blindly using an AxioPlan II fluorescent microscope (Carl Zeiss) equipped with a GFP filter. At least 4 mice per group were assessed for each independent experiment.

2.23 RNA extraction from infected brains

All steps were performed with RNAse-free tubes and using lab equipment previously cleaned with RNaseZap (Ambion). The brain of a 7 dpi mouse was mashed as described in 2.22 and spun for 5 min at 900 g. The pellet was resuspended in 1 mL Trizol and kept at -80°C until use. Pellets were thawed on ice and resuspended at RT for 5 min on a shaker before centrifugation at 8000 g for 5 min to get rid of the lipids, present in abundance in the brain. 200 μL chloroform was added to the supernatant and after gentle mixing for 15 sec and incubation at RT for 5 min, the mix was spun at 9000 rpm for 15 min at 4°C. The upper aqueous phase containing the extracted RNA was transferred to a new tube and mixed with 1:2 (v:v) Trizol and 200 μL chloroform, gently mixed for 15 sec, incubated at RT for 5 min before centrifugation at 9000 rpm for 15 min at 4°C. The upper aqueous phase containing the extracted, lipid-free RNA was transferred to a new tube containing 1:1 (v:v) 70% ethanol. The mix was then purified using the RNeasy® Mini kit (Qiagen), according to the manufacturer's instructions. Briefly, the mix was transferred to a mini spin column and spun at 13000

rpm for 15 sec at 4°C. Membranes were washed once with 500 µL RW1 buffer and twice with 500 µL RPE buffer before dry-spinning at 13 000 rpm for 1 min at 4°C. The RNA was eluted with 30 µL RNA-free water into a new tube and samples were stored at -80°C.

2.24 Real-time quantitative PCR

cDNA was synthesised from isolated brain RNA using the RT^2 First Strand kit (Qiagen) according to the manufacturer's instructions. Briefly, genomic DNA was eliminated by mixing 1 µg RNA with 2 µL of Buffer GE (final volume of 10 mL) and incubating for 5 min at 42°C, then cooling immediately on ice. Reverse transcription of RNA to cDNA was performed at 42°C for 15 min and stopped by incubating at 95°C for 5 min. The retrotranscription mix is detailed in Table 2.14. Finally, 91 µL RNase-free water was added to each reaction.

5x Buffer BC3	4 µL
Control P2	1 µL
RE3 Reverse Transcriptase Mix	2 µL
Nuclease-free water	3 µL
Total	**10 µL**

Table 2.14: Retrotranscription mix.

Gene expression was determined in 384 plates by real-time quantitative PCR using the RT^2 Profiler PCR array (Qiagen) for mouse cytokines and chemokines (PAMM-150ZA) as well as mouse pain: neuropathic and inflammatory (PAMM-162ZA) according to the manufacturer's instructions. Briefly, qPCR components were mixed as detailed in Table 2.15, and 10 µL of reaction was added per well. Each plate included 3 retrotranscription controls and 3 positive PCR controls.

2x RT^2 SYBR Green Mastermix	650 μL
cDNA synthesis reaction	102 μL
RNase-free water	548 μL
Total	**1300 μL**

Table 2.15: RT^2 qPCR reaction mix.

Data were analysed by calculating the relative gene expression to the housekeeping gene *Gapdh* using the standard ΔCt method.

2.25 Cytokines and chemokines expression in infected mice

2.25.1 Quantification of cytokines and chemokines by multiplex

Blood was collected at day 3 and 7 post-infection from the saphenous vein or by terminal cardiac puncture, respectively. Serum was obtained after coagulation at RT for 30 min and centrifugation at 4°C for 10 min at 1000 g. Serum cytokines and chemokines analysis was performed by mouse 32-plex Discovery Assay® (Eve Technologies, Calgary, Alberta, Canada).

2.25.2 Quantification of cytokines by ELISA

Blood and peritoneal lavage were collected at 7 days post-infection as described previously. Wild-type or TRIM21 KO bone marrow-derived macrophages were left uninduced or stimulated with 100 U/mL IFNγ overnight and infected with avirulent *Toxoplasma* for 24h. Supernatants were collected and analysed by enzyme-linked immunosorbent assay (ELISA). Commercially available kits were used according to the manufacturer's instructions to quantify the concentration of IFNα (eBioscience,

San Diego, CA, USA), IFNβ (PBL Assay Science, Piscataway, NJ, USA), IFNγ (R&D Sciences), IL-1β (BD), IL-12p40 (R&D Sciences) and TNFα (R&D Sciences). Standard curves and cytokine concentrations were determined using Excel (Microsoft, Redmond, WA, USA).

2.25.3 Quantification of cytokines by qPCR

Wild-type or TRIM21 KO bone marrow-derived macrophages were left uninduced or stimulated with 100 U/mL IFNγ overnight and infected with avirulent *Toxoplasma* for 24h. Cells were washed three times in PBS and resuspended in 500 µL Trizol. RNA was extracted following the procedure described in 2.15 and reverse transcribed into cDNA using the SuperScript® VILO™ cDNA Synthesis kit (Thermo Fischer Scientific) according to the manufacturer's instructions. Briefly, 50 ng RNA were used per assay and mixed with the reaction components as indicated in . The reverse transcription was performed for 10 min at 25°C, followed by an incubation for 60 min at 42°C and a final deactivation for 5 min at 85°C.

5x VILO™ Reaction Mix	4 µL
10X SuperScript® Enzyme mix	2 µL
RNA	50 ng per reaction
RNAse-free water	to 20 µL
Total	**20 µL**

Table 2.16: SuperScript® VILO™ reverse transcription mix.

The quantitative PCR was then performed using the TaqMan® Real-Time PCR Assay system (Applied Biosystems) according to the manufacturer's instructions. Reaction mixes were made-up in 96-well plates (optical reaction plates, Applied Biosystems) as described in Table 2.17.

2x TaqMan® Master Mix	5 μL
cDNA	2 μL
Probe	1 μL
RNase-free water	2 μL
Total	**10 μL**

Table 2.17: TaqMan® qPCR reaction mix.

The primer-probes used are summarised in Table 2.18. The qPCR was carried out on an Applied Biosystem 7900HT real-time PCR machine.

Target gene	Applied Biosystems code
Hprt	Mm03024075_m1
Il1b	Mm00434228_m1
Il10	Mm01288386_m1
Il12b	Mm01288989_m1
Nfkbia	Mm00477798_m1

Table 2.18: TaqMan® primer-probes used for qPCR.

2.26 Blood biochemistry in infected mice

Blood was collected at day 7 post-infection by cardiac puncture. Serum was obtained as described above (see 2.25) and diluted 1:10 in PBS. Analysis of biomarkers for organ malfunction and damage was performed on a Cobas C111 analyser (Roche).

2.27 Histology

Following terminal cardiac puncture, animals were sacrificed at 7 dpi by an overdose of ketamine and medetomidine. Animals were sprayed with ethanol and the brain was

isolated first. Briefly, an incision was done along the neck and the skin was cut between the eyes and completely removed from the skull. The skull was then opened and the brain was carefully removed, washed once in PBS, cut in half so that the left hemisphere was fixed in 4% formalin and the right hemisphere was kept in 1 mL PBS on ice for parasites count or FACS analysis. Then, the abdomen of the mice was opened and entrails including guts, stomach, pancreas, spleen and kidneys were removed at once and fixed in 4% formalin. The rib cage was opened and the lungs were inflated through the trachea with 1 mL 4% formalin (Leica Microsystems). Trachea, lungs and heart were subsequently removed at once and fixed in 4% formalin. After a minimum of 48 h fixation, organs were washed in 70% ethanol and placed into cassette for paraffin embedding. Preparation of the samples for H&E staining was done in the dedicated services by Dr. Radma Mahmoud within the Crick at Mill Hill Laboratory, or by Richard Stone within the Crick at Lincoln Inn Fields Laboratory. Analyses of the slides were performed by Prof. Cheryl Scudamore at MRC Harwell or by Prof. Gordon Stamp at Imperial College London.

2.28 Statistical analysis

All statistical significance analyses were performed using Prism software (GraphPad Software). Comparisons of data were performed with unpaired Student's *t*-test or using two-way ANOVA with Sidak multiple comparison correction. Survival rates were compared by log-rank survival analysis of Kaplan-Meier curves.

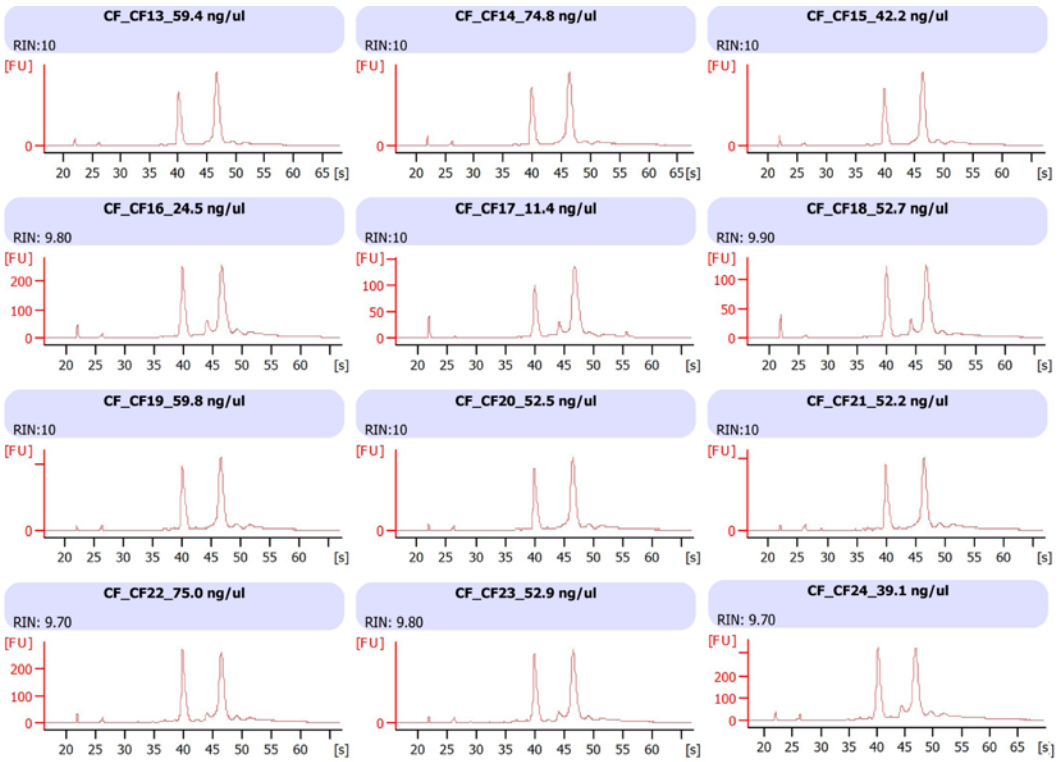

Figure 2.3: Verification of the RNA quality for RNA sequencing.
The quality of RNA extracted from wild-type or TRIM21-deficient mouse embryonic fibroblasts infected with avirulent *Toxoplasma* for 1h was assessed using an Agilent 2100 Bioanalyser. All RNA samples present an RNA integrity number (RIN) higher than 7, meaning the RNA is not degraded and is of high quality (Schroeder et al., 2006).

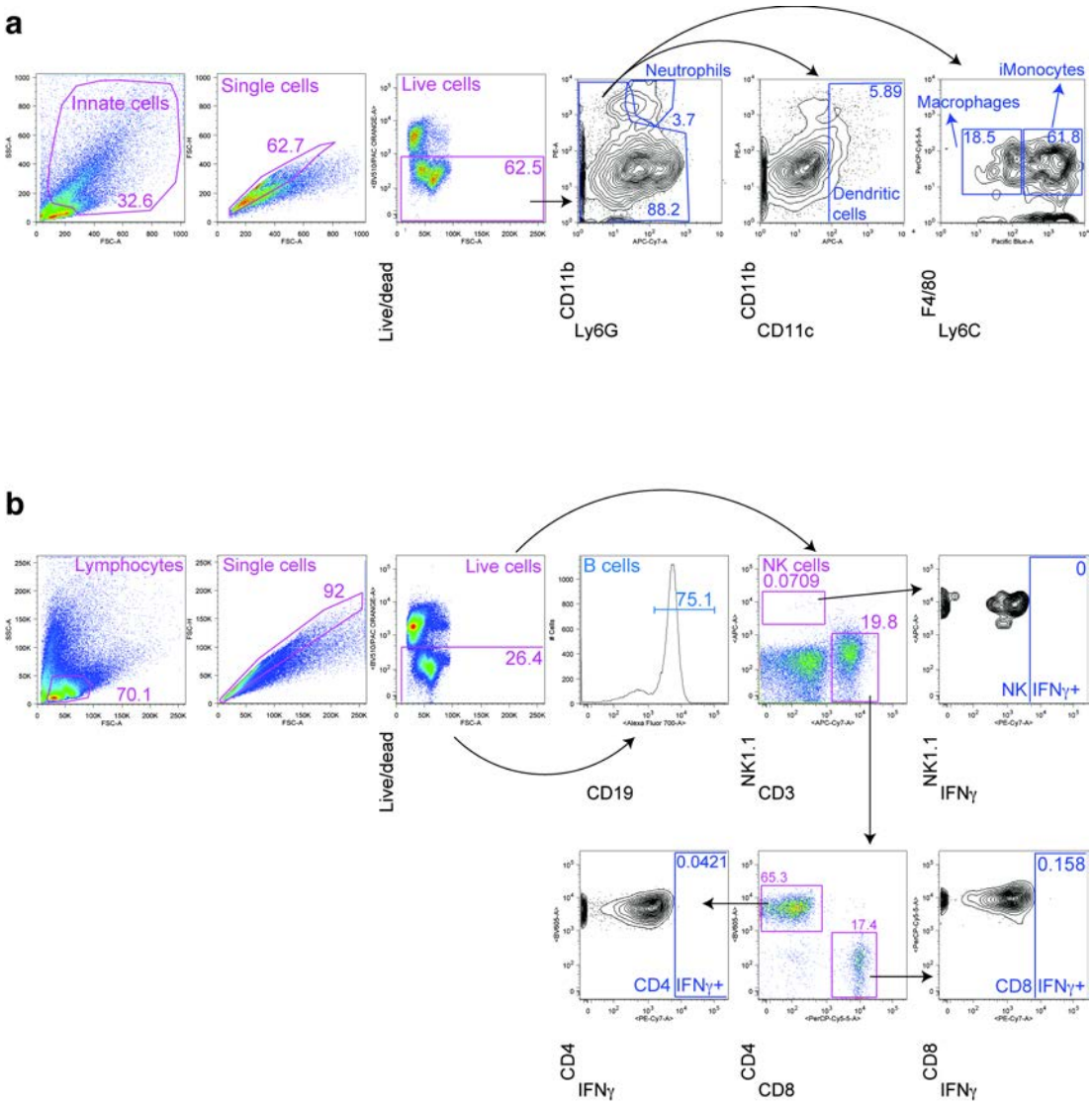

Figure 2.4: Gating strategies used for the analysis of innate cells and lymphocytes.
The graphs show FACS plots illustrating the gating strategies used to analyse innate cells (**a**) and lymphocytes (**b**). Innate cells were gated on side-scatter low/high and forward-scatter low/high. Lymphocytes were gated on side-scatter low and forward-scatter low. Flow cytometry data was excluded for doublets and dead cells. All future FACS plot data will have been performed following this gating strategy, and will thus not show the scatter plot, doublets exclusion plot and dead cell exclusion plot.

Chapter 3

TRIM21 mediates Lys63-linked ubiquitination around GBP1-positive *Toxoplasma* vacuoles and impacts the cholesterol biosynthesis

3.1 Introduction

3.1.1 The ubiquitin system

3.1.1.1 Overview

Ubiquitination is a post-translational modification (PTM) event that involves the covalent attachment of a protein called ubiquitin (Ub) onto a protein substrate. This modification of the target proteins regulates their activity and function in several critical cellular pathways such as cell cycle (Vaysburd et al., 2013; Ciechanover et al., 1984; Finley et al., 1994), DNA repair (Jentsch et al., 1987; Xu et al., 2009; Hofmann and Pickart, 1999), immune response (Deng et al., 2000) or proteasomal degradation (Chau et al., 1989). The importance of the ubiquitin system is also highlighted by the fact that ubiquitin is one of the most conserved eukaryotic proteins, with only three amino acids out of the seventy six residues differing between yeast and human ubiquitin (Graham et al., 1989). The process of ubiquitination requires the sequential collaboration of three groups of enzymes including a ubiquitin-activating enzyme E1, the ubiquitin-conjugating enzymes E2 and the ubiquitin ligases E3. These enzymes catalyse the covalent conjugation of ubiquitin onto the protein substrate first, then onto one of the internal lysine residues within the ubiquitin itself until a chain of conjugated ubiquitin is synthesised, resulting in the downstream possible effect on the targeted protein (Pickart, 2001).

3.1.1.2 Ubiquitination

In 2004, the Nobel Prize in Chemistry was awarded to Aaron Ciechanover, Avram Hershko and Irwin Rose for their discovery of the ubiquitin system (Ciechanover et al., 1980; Hershko et al., 1980). The ubiquitination process is performed in a well-

orchestrated three-step enzymatic cascade (Figure 3.1). The first step is ATP-dependent and consists in the activation of ubiquitin by the E1 ubiquitin-activating enzyme that forms a thiol-ester linkage between its active cysteine residue and the C-terminal glycine present in ubiquitin. Secondly, the activated ubiquitin is transferred onto an active cysteine harboured by the E2 ubiquitin-conjugating enzyme. Finally, the substrate-specific E3 ubiquitin ligase acts as an adaptor protein between the E2 and the target protein and facilitates the formation of a covalent isopeptide bond between ubiquitin and a lysine residue of the substrate. Some protein substrates are mono-ubiquitinated on a single lysine residue (mono-ubiquitination), while others are mono-ubiquitinated on several lysines (multi-mono-ubiquitination) or present a chain of ubiquitins on one or multiple lysines (poly-ubiquitination). Indeed, once a first ubiquitin is covalently linked on its substrate, the process can be repeated so that additional ubiquitin molecules are charged via their C-terminal glycine residue to specific lysine residues within the previous ubiquitin. In fact, ubiquitin itself exhibits seven lysine residues (K6, K11, K27, K29, K33, K48 and K63), which can accept another ubiquitin molecule to form ubiquitin chains. Additionally, the C-terminal glycine of a ubiquitin molecule can also be connected to the amino-terminal methionine (M1) of another ubiquitin. Thus, as ubiquitination can come in different flavours, different ubiquitin chain types are involved in distinct cellular processes and signalling events so that the nature of the ubiquitin chain will dictate the fate of the protein substrate.

3.1.1.3 Functions of protein ubiquitination

Lys48- and Lys63-linked chains have been the most extensively studied. Lys48-linked ubiquitin chains were for a long time believed to be the main chain type. Proteins harbouring a polymer of ubiquitins linked via their Lys48 side chain are targeted for

degradation by the proteasome (Chau et al., 1989). During substrate degradation by the proteasome, the ubiquitin molecules are removed and recycled by enzymes called deubiquitinating enzymes (DUBs) associated with the 20S core of the proteasome. In contrast to Lys48 side chains, Lys63-linked chains are involved in promoting non-degradative cellular events such as endocytosis (Geetha et al., 2005; Kamsteeg et al., 2006; Duncan et al., 2006), DNA repair (Hofmann and Pickart, 1999) and immune signalling (Deng et al., 2000). Although Lys63 chains have been considered to participate in non-proteasomal functions, recent studies suggested they could possibly target proteins for proteasomal degradation as well (Hofmann and Pickart, 2001; Saeki et al., 2009). How Lys63-linked chains would only target some proteins and not all for degradation remains unknown, and it is still debated whether Lys63-linked chains serve as proteasomal signals. The remaining lysine residues (K6, K11, K27, K29 and K33) have all been reported to possibly target substrates for proteasomal degradation (Baboshina and Haas, 1996; Xu et al., 2009). Moreover, Lys6-linked chains are involved in DNA repair (Sobhian et al., 2007), Lys11-linked chains regulate the cell cycle (Jin et al., 2008), Lys29-linked chains mediate lysosomal degradation (Chastagner et al., 2006), and Met1-linked linear chains participate in immune signalling (Tokunaga et al., 2009; Rahighi et al., 2009).

3.1.1.4 E3 ubiquitin ligases

The human genome encodes two ubiquitin-specific E1 ubiquitin-activating enzymes (Kudo et al., 1991; Zhu et al., 2004), thirty-seven E2 ubiquitin-conjugating enzymes (Markson et al., 2009) and more than 600 E3 ubiquitin ligases (Li et al., 2008). The latter carry out the last step of the ubiquitination cascade and are responsible for the specificity of the substrate to be ubiquitinated. The E3 ubiquitin ligases can be divided into three main domain families: the Really Interesting New Gene (RING) finger

domain family, the Homology to E6-AP C-Terminus (HECT) domain family and the ligases resembling neither the RING nor the HECT domain families.

RING ubiquitin ligases are the most abundant type of E3 ligases in the cell. The canonical E3 RING domain is a cysteine-rich globular domain that contains eight conserved cysteine or histidine residues, which coordinate two zinc ions in a cross-brace structure (Freemont et al., 1991; Barlow et al., 1994; Borden et al., 1995). The RING domain is responsible for both binding to the N-terminal helix of the ubiquitin-conjugating enzyme E2 and promoting the transfer of ubiquitin to the substrate at the same time. RING ubiquitin ligases perform the catalytic attack of the substrate lysine on the E2-ubiquitin thioester in one single step, resulting in direct transfer of ubiquitin from the E2 enzyme to the substrate (Lorick et al., 1999; Joazeiro et al., 1999; Seol et al., 1999; Zheng et al., 2000). The structural and conformational mechanisms underlying the positioning of the reactive E2-ubiquitin thioester and the acceptor lysine for the efficient transfer of ubiquitin still remain to be deciphered.

In contrast to RING ubiquitin ligases, HECT ubiquitin ligases perform two distinct ubiquitination steps. First, ubiquitin is transferred from the active cysteine on the ubiquitin-conjugating E2 enzyme to a cysteine on the HECT domain. Secondly, the substrate lysine attacks the HECT-ubiquitin thioester to result in the ubiquitinated substrate (Huibregtse et al., 1995). Structural studies showed the HECT domain comprises two subdomains connected by a flexible linker: the N-terminal lobe that binds to the E2 and the C-terminal lobe that contains the catalytically active cysteine. The flexible linker allows conformational rearrangements between the two distal lobes, thereby bringing the E2-ubiquitin thioester in close proximity to the active cysteine (Huang et al., 1999; Verdecia et al., 2003). Once the E3-ubiquitin thioester is

formed, the C lobe rotates to bring the donor ubiquitin to the acceptor lysine on the substrate, interacting with the N lobe (Kamadurai et al., 2009; 2013; Maspero et al., 2013).

TRIM21, the focus of this study, is a RING ubiquitin ligase. The following section will present an overview of the protein, including its ubiquitin ligase properties, its known substrates as well as other important information necessary to understand this chapter.

3.1.2 The RING ubiquitin ligase TRIM21

3.1.2.1 The TRIM family of proteins

The family of tripartite motif-containing (TRIM) proteins is the second largest subgroup of RING E3 ubiquitin ligases, with 64 members in the mouse genome and ~100 members in the human genome (Sardiello et al., 2008; Han et al., 2011). The TRIM proteins, also called RBCC proteins, are characterised by a conserved N-terminal structure comprising three protein domains: a RING (R) domain followed by one or two B-box (B) domains and a helical coiled-coil (CC) domain (Ozato et al., 2008).

The RING domain is composed of 40-60 amino acids and has a cysteine-rich consensus sequence reading Cys-X_2-Cys-X_{11-16}-Cys-X-His-X_2-Cys-X_2-Cys-X_{7-74}-Cys-X_2-Cys, where x can be any amino acid (Borden et al., 1995). The RING domain has been the most widely studied, and is now known to mediate protein-protein interactions and exhibit E3 ligase activity. For example, the TRIM25 ubiquitin ligase activity is essential for the robust Lys63-linked ubiquitination and subsequent activation of the retinoic acid-inducible gene-I (RIG-I), leading to the production of

IFNβ following RNA virus infection (Gack et al., 2007). Moreover, RING-dependent TRIM5α auto-ubiquitination is required for proteasomal degradation of the TRIM5α-virus complex during HIV-I infection (Diaz-Griffero et al., 2006; Rold and Aiken, 2008; Lukic et al., 2011).

The B-box domain exists in two different forms, B1 and B2, which consist of zinc-binding motifs of ~40 residues. The B-boxes are exclusively found in TRIM proteins. Structural studies have shown B-box 1 to share some conserved ternary structures with the RING domain, and B-box 2 to exhibit a RING-like structure, suggesting that all three domains are similar and may have evolved from a common ancestral domain (Massiah et al., 2006; 2007). Although the B-box domains have not been widely studied, they have been implicated in antiviral resistance. For example, mutational studies have shown that B-box 2 forms high order oligomers, thereby promoting binding to retrovirus capsids and hence triggering HIV-1 restriction (Li and Sodroski, 2008; Diaz-Griffero et al., 2009).

The coiled-coil domain is formed by multiple α-helices and has been shown to be necessary and sufficient for the formation of homomeric and heteromeric interactions between TRIM proteins (Reymond et al., 2001; Cao et al., 1997; Cainarca et al., 1999). This allows TRIM members to form large oligomers via antiparallel helical hairpins that allows them to exert their functions (Sanchez et al., 2014). For example, dimerisation of TRIM5α is mediated by its coiled-coil domain and promotes binding of the TRIM protein to the viral capsid and subsequently to restrict HIV-1 (Ganser-Pornillos et al., 2011; Sanchez et al., 2014).

The N-terminal RBCC domains are followed by one or several C-terminal domains that divide the TRIM proteins into 11 categories (Short and Cox, 2006; Ozato et al., 2008) (Figure 3.2). As the N-terminal domain is very conserved among TRIM proteins, it is likely that the C-terminal domain dictates their functional diversity by recruiting interacting partners. The most common C-terminal feature found in TRIM proteins is the B30.2 motif or PRYSPRY motif. It comprises the PRY domain made of 61 residues followed by the SPRY domain including 120 amino acids (Grütter et al., 2006; Woo et al., 2006). The B30.2 motif has been shown to participate in protein-protein interactions as well as RNA binding and is involved in the antiviral activity of several TRIM proteins (Nisole et al., 2005). For example, it has been shown that the B30.2 domain of TRIM5α binds to HIV-1 viral capsids, and one single amino acid substitution (R332P) in the B30.2 domain abolishes the ability of human TRIM5a to restrict HIV-1 (Yap et al., 2005; Stremlau et al., 2005; Nakayama et al., 2005; Perez-Caballero et al., 2005).

3.1.2.2 Functions of TRIM21

Ro52 has been identified in 1988 as one of the major autoantigens in the autoimmune disease called Sjögren's syndrome (Ben-Chetrit et al., 1988). The *Ro52* gene has been mapped on human chromosome 11 (Frank et al., 1993) and mouse chromosome 7 (Rajsbaum et al., 2008). Cloning and expression of human Ro52 allowed the discovery of the presence of zinc finger domains and a leucine zipper motif at the N-termini of the protein (Itoh et al., 1991; Chan et al., 1991). Later, structural studies revealed Ro52 comprises an N-terminal RBCC domain and a B30.2 C-terminal domain. As such, the protein presents the features of a tripartite motif-containing protein and was named TRIM21 (Reymond et al., 2001; Ottosson et al., 2006).

As discussed previously in section 1.2.5, the TRIM21 B30.2 domain was shown to strongly bind to the Fc part of IgG, IgM and IgA (Rhodes et al., 2002; Keeble et al., 2008; Bidgood et al., 2014). Due to this antibody-binding property, TRIM21 has been reported to bind to invading antibody-coated adenoviruses as well as *Salmonellae* in the cytosol, and target them for degradation by the proteasome by virtue of its RING-dependent E3 ligase activity (Mallery et al., 2010; McEwan et al., 2013; Rakebrandt et al., 2014).

TRIM21 has also been shown to mediate immune signal transduction pathways via its E3 ubiquitin ligase activity. TRIM21 was proposed to trigger the production of IL-12p40 in macrophages stimulated with IFNγ and bacterial unmethylated CpG via a mechanism that involves the non-proteolytic ubiquitination and upregulation of the interferon regulatory factor IRF8 (Kong et al., 2007). Moreover, TRIM21 was proposed to negatively regulate NF-κB signalling in mouse embryonic fibroblasts following stimulation with LPS or poly(I:C), thereby downregulating the production of IL-1β, TNFα and IL-6 (Yoshimi et al., 2009). TRIM21 has also been reported to act as a negative regulator of IFNβ production by promoting the ubiquitination and proteasomal degradation of IRF3 upon stimulation with LPS, polyI:C, infection with Sendai virus (Higgs et al., 2008) or with Japanese encephalitis virus (Manocha et al., 2014). However, another study suggested TRIM21 inhibits the degradation of IRF3 by binding to the protein and hence abolishing the degradation-inducing interaction between IRF3 and a protein called Pin1 (Yang et al., 2009). TRIM21 has been reported to promote the ubiquitination and subsequent proteasomal degradation of IRF7 (Higgs et al., 2010). Following adenovirus and *Salmonella* infection in mouse embryonic fibroblasts, TRIM21 was suggested to mediate the formation of Lys63-linked chains

and upregulate IRF3, IRF5, IRF7, NF-κB and AP-1, thereby inducing the production of proinflammatory cytokines (McEwan et al., 2013). These four studies suggest TRIM21 can mediate both positive and negative regulatory pathways depending on the stimulatory conditions and the cell lines used. Moreover, this also indicates TRIM21 is involved in signal pathways triggered by both degradation and non-degradation signals. Finally, TRIM21 has been demonstrated to regulate a type I interferon response to cytosolic dsDNA via the ubiquitination and proteasomal degradation of the dsDNA-sensor DDX41 (Zhang et al., 2013). All these data indicate TRIM21 is involved in the regulation of immune signalling following stimulation with several pathogens.

3.1.3 Aims

During the course of *Toxoplasma* infection in mouse, the formation of the autophagophore around denuded parasites and subsequent fusion with lysosomes have been observed by electron microscopy (Ling et al., 2006). Moreover, some autophagy proteins along with IRGs and GBPs have been shown to mediate clearance of *Toxoplasma* in IFNγ-stimulated cells (Zhao et al., 2008; Selleck et al., 2013; Choi et al., 2014; Ohshima et al., 2014). However, the sensor proteins as well as the signals triggering the formation of the autophagosome still remain unknown.

Autophagy is known to participate in the clearance of other vacuolar pathogens such as *Salmonella*. In this case, the bacteria released in the host cytosol are recognised and targeted by ubiquitination for destruction by autophagy (Huett et al., 2012; Perrin et al., 2004; Fujita et al., 2013; Thurston et al., 2009; Zheng et al., 2009; Wild et al., 2011). The *Salmonella* infection model hence gives some clues about which

recognition and targeting pathways can be involved in vacuolar pathogen recognition and clearance.

The aim of this project was thus to identify new host factors involved in the restriction of *Toxoplasma* in IFNγ-induced murine cells. Ultimately, the goal was to decipher the molecular and organismal consequences of *Toxoplasma* vacuolar recognition by GBPs and other effector proteins.

3.2 Results

3.2.1 Ubiquitin accumulates in the vicinity of avirulent *Toxoplasma*

Ubiquitin is involved in the clearance of intracellular pathogens. However, ubiquitination around the *Toxoplasma* vacuole has not been demonstrated yet. To study the possible role of ubiquitin during the course of *Toxoplasma* infection, I first assessed whether *Toxoplasma* or its parasitophorous vacuole could be ubiquitinated. Immunofluorescence for total ubiquitin in IFNγ-treated mouse embryonic fibroblasts reveals that ubiquitin accumulates around the PV of avirulent *Toxoplasma* expressing GFP, but does not decorate virulent *Toxoplasma* expressing tomato (Figure 3.3a). Quantitative analysis of the number of vacuoles positive for ubiquitin shows that the molecule accumulates at the vicinity of up to 52% of avirulent *Toxoplasma*, whereas it could not be found around any (0%) virulent parasites (Figure 3.3b).

3.2.2 IFNγ mediates ubiquitin decoration around avirulent *Toxoplasma*

Interferon gamma is the main mediator of the immune response during *Toxoplasma* infection, upregulating the expression of hundreds of genes. To determine whether the parasite recognition by ubiquitin is dependent on the cytokine, I next performed

immunofluorescent staining for total ubiquitin in IFNγ-stimulated or non-treated cells. I observed accumulation of ubiquitin around avirulent vacuoles only when the cells were induced with IFNγ (Figure 3.4a). Indeed, this accumulation of ubiquitin in the vicinity of avirulent *Toxoplasma* was dependent on stimulation with IFNγ, as the quantitative analysis demonstrates that less than 1% of avirulent *Toxoplasma* is decorated with ubiquitin in unstimulated cells (Figure 3.4b). In contrast, up to 52% of avirulent *Toxoplasma* were decorated with ubiquitin in IFNγ-treated cells. These observations suggest that the mechanism involved in the ubiquitination around *Toxoplasma* requires the presence of a cofactor whose expression and/or localisation to the vacuole is induced by IFNγ.

3.2.3 GBP1 and ubiquitin colocalise to avirulent *Toxoplasma*

Given the accumulation pattern of ubiquitin around avirulent *Toxoplasma* exclusively and in IFNγ-stimulated conditions only, this was reminiscent of the recruitment pattern of GBP1 (Virreira Winter et al., 2011). To assess the putative role of GBP1 in the presence of ubiquitin around the parasite, I performed colocalisation studies for endogenous GBP1 and total ubiquitin by immunofluorescence. As can be seen in Figure 3.5a, GBP1 and ubiquitin corecruit to the parasitophorous vacuole of avirulent *Toxoplasma* in IFNγ-stimulated cells. Analytical tools of the distinctive fluorescence signals such as the plot profile analysis (Figure 3.5b) and the 3D surface plot analysis (Figure 3.5c) reveal both proteins exhibit the same localisation, completely surrounding the avirulent parasite.

3.2.4 *Toxoplasma* virulence factors interfere with GBP1 and ubiquitin localisation around the vacuole

The recruitment of GBP1 to avirulent *Toxoplasma* vacuoles has been reported to be counteracted by parasitic virulence factors secreted in the host cell cytoplasm. Two threonine kinases expressed by the virulent type I *Toxoplasma* strain, called Rop16 and Rop18, alter the recruitment of GBP1 to avirulent PVs (Virreira Winter et al., 2011). Rop18 has been reported to phosphorylate and hence inactivate the GTPase (Fentress et al., 2010; Steinfeldt et al., 2010). In order to determine whether these virulence factors also influence the accumulation of ubiquitin in the vicinity of avirulent *Toxoplasma*, we used the transgenic type II Pru *Toxoplasma* strain expressing the type I version of Rop16 (Pru Rop16I), as well as the transgenic type III CEP *Toxoplasma* strain expressing the type I version of Rop18 (CEP Rop18I). Immunofluorescence for GBP1 and ubiquitin in IFNγ-stimulated mouse embryonic fibroblasts first shows that GBP1 is present at avirulent ubiquitin-positive vacuoles only (Figure 3.6). Indeed, 47.5% of avirulent type II Pru *Toxoplasma* and 54% of avirulent type III CEP *Toxoplasma* are decorated with both GBP1 and ubiquitin, while none of them are positive for GBP1 alone. Moreover, the transgenic strains Pru Rop16I and CEP Rop18I show significantly reduced accumulation of GBP1 and ubiquitin compared to their respective parental strains, dropping to 17% and 15%, respectively (Figure 3.6). This suggests that *Toxoplasma* virulence factors interfere with the recruitment of both GBP1 and ubiquitin to the parasitophorous vacuoles.

3.2.5 TRIM21 interacts with GBP1 in an IFNγ–dependent manner

My results imply that an IFNγ-inducible factor and/or a GBP1-interacting partner is recruited in the vicinity of avirulent *Toxoplasma*, which could be an already

ubiquitinated protein or an E3 ubiquitin ligase. To identify an E3 ubiquitin ligase that could be recruited to avirulent *Toxoplasma* vacuoles, we searched for potential GBP1 interactors using a mass spectrometry approach. Eva Frickel had already performed an immunoprecipitation of Flag-GBP1 in IFNγ-stimulated Raw 264.7 macrophages infected with the avirulent type II Pru *Toxoplasma* strain, and the putative immunoprecipitated proteins had been identified by mass spectrometry analysis done by Eric Spooner at the Whitehead Institute in Boston. The close examination of the generated list of putative GBP1 interaction partners lead to the identification of an E3 ubiquitin ligase called tripartite-motif protein 21 (TRIM21), which presents a peptide coverage of 39% (Figure 3.7a). I then confirmed this interaction using an immunoprecipitation/immunoblot approach. The E3 ubiquitin ligase TRIM21 has been described to strongly bind to the Fc part of IgG, IgM and IgA antibodies (see section 1.3.5). I consequently verified the interaction in IFNγ-stimulated Raw 264.7 cells infected with either virulent type I RH *Toxoplasma* or avirulent type II Pru *Toxoplasma* by immunoprecipitating for TRIM21 in order to avoid unspecific binding of TRIM21 to the anti-GBP1 antibody during the immunoprecipitation process. In order to avoid unspecific binding of proteins to the beads, the protein samples were precleared by incubation with the agarose beads for 3h. The remaining protein lysates, free of proteins unspecifically bound to the beads, were then used to perform the immunoprecipitation. Endogenous TRIM21 interacts with endogenous GBP1 in IFNγ-stimulated cells independently of the presence of *Toxoplasma* and regardless of the virulence strain (Figure 3.7b). Additionally, overexpressed myc-TRIM21 interacts with overexpressed Flag-GBP1 (upper band) and endogenous GBP1 (lower band) in IFNγ-induced samples only, and independently of the virulence strain of *Toxoplasma* (Figure 3.7c). These results demonstrate the E3 ubiquitin ligase TRIM21 interacts with

GBP1 in a strain-independent but IFNγ-dependent manner. However, as GBP1 is expressed at a high level following induction with IFNγ, one cannot exclude that even after pre-clearing, GBP1 could unspecificaly bind to the beads rather than to TRIM21. One control to test for this possibility would be to perform an immunoprecipitation in TRIM21 KO cells. Should GBP1 only bind to TRIM21, no GBP1 should be recovered following preclearing, anti-TRIM21 immunoprecipitation and anti-GBP1 immunoblot. Another approach to circumvent this issue could be to perform an immunoprecipitation and immunoblot for the overexpressed, tagged proteins in cells only expressing endogenous proteins.

3.2.6 TRIM21 follows GBP1 recruitment to avirulent *Toxoplasma*

Localisation studies were performed in mouse embryonic fibroblasts in an effort to gain some knowledge about the possible function of GBP1 and its TRIM21 interaction partner. As both proteins of interest are induced by IFNγ, the specificity of the primary rabbit anti-GBP1 and goat anti-TRIM21 antibodies was determined by immunostaining fixed cells uninduced or induced with 100U/mL IFNγ. To demonstrate the specificity of the secondary antibody, experiments were performed without the addition of the primary antibody. Briefly, cells induced with 100 U/mL IFNγ were fixed and immunostained with a secondary goat anti-rabbit antibody or donkey anti-goat antibody to ensure they do not bind non-specifically to endogenous mouse proteins (data not shown).

Although our homemade GBP1 antibody has already been characterized for immunofluorescence microscopy (Virreira Winter et al., 2011), normal subcellular localisation of GBP1 was first assessed in uninfected unstimulated or IFNγ–stimulated

mouse embryonic fibroblasts. GBP1 was expressed uniformly in the cytoplasm of IFNγ-stimulated MEFs only (data not shown). Subcellular localisation of GBP1 was then assessed in IFNγ-stimulated cells infected with the avirulent *Toxoplasma* expressing GFP. As can be observed in Figure 3.8a (top panel), GBP1 is recruited at the parasitophorous vacuole of the avirulent parasite.

Next, normal subcellular localisation of TRIM21 was assessed in uninfected unstimulated or IFNγ–stimulated mouse embryonic fibroblasts. TRIM21 was expressed uniformly in the cytoplasm of IFNγ-stimulated MEFs only (data not shown). Thus, I presume the commercial TRIM21 antibody is suitable for immunofluorescence to recognise native endogenous TRIM21 in paraformaldehyde (PFA)-fixed samples. Subcellular localisation of TRIM21 was then assessed in IFNγ-stimulated cells infected with the avirulent strain of *Toxoplasma* expressing GFP. As can be observed in Figure 3.8a (lower panel), TRIM21 is also recruited to the parasitophorous vacuole of the avirulent parasite.

By quantitative analysis of the number of vacuoles positive for GBP1, I could reproduce published results and confirm the targeting of GBP1 to the vacuole of 55% of avirulent *Toxoplasma* in IFNγ-stimulated mouse embryonic fibroblasts, while only 3% of virulent *Toxoplasma* were decorated (Figure 3.8b, top panel). Similarly, TRIM21 was preferentially recruited to the vacuole of avirulent *Toxoplasma* (26%) rather than of virulent *Toxoplasma* (1%, Figure 3.8b, lower panel). These results suggest TRIM21 follows the recruitment pattern of GBP1 to avirulent *Toxoplasma* vacuoles.

3.2.7 TRIM21 and GBP1 colocalise at avirulent *Toxoplasma* vacuoles

As TRIM21 mimics the recruitment of GBP1 to avirulent vacuoles, I next studied whether TRIM21 was co-recruited to GBP1-positive avirulent *Toxoplasma* vacuoles. Immunofluorescence shows GBP1 and TRIM21 colocalise to the parasitophorous vacuole of avirulent *Toxoplasma* in IFNγ-stimulated cells (Figure 3.9a). Analytical tools of the distinctive fluorescence signals such as the plot profile analysis (Figure 3.9b) and the 3D surface plot analysis (Figure 3.9c) reveal both proteins exhibit the same localisation around the avirulent parasite. Quantitative analysis of the protein recruitment reveals TRIM21 is mainly recruited to the parasitophorous vacuole of the ~30% GBP1-positive *Toxoplasma* rather than to the 1.5% remaining GBP1-negative avirulent *Toxoplasma* (Figure 3.9d). Thus, about half of the GBP1-positive avirulent *Toxoplasma* are also decorated with TRIM21. These results suggest TRIM21 is preferentially recruited to GBP1-positive avirulent *Toxoplasma* parasitophorous vacuoles.

3.2.8 TRIM21 and GBP1 form a complex in the cytoplasm and recruit to avirulent *Toxoplasma*

Both GBP1 and TRIM21 are highly inducible by IFNγ (Degrandi et al., 2007). Moreover, the immunoprecipitation/immunoblot data as well as the immunofluorescence localisation studies strongly suggest TRIM21 and GBP1 could already interact in the cytoplasm upon stimulation with IFNγ, rather than forming a complex upon invasion of *Toxoplasma* in the cell. To test this hypothesis, I used the proximity-ligation (PL) assay, allowing to detect proteins that are in very close physical proximity (limiting detection distance just above 10 nm) (Söderberg et al., 2006; Jarvius et al., 2007). I detected very limited PL signal between endogenous

GBP1 and TRIM21 in unstimulated cells infected with avirulent *Toxoplasma* (Figure 3.10a). In contrast, I observed strong PL signals in the cytoplasm (Figure 3.10b) or around avirulent *Toxoplasma* vacuoles (Figure 3.10c) in IFNγ-stimulated mouse embryonic fibroblasts. These results show GBP1 and TRIM21 form a complex in the cytoplasm of uninfected cells upon IFNγ stimulation and relocalise together to the vacuole of avirulent *Toxoplasma* upon invasion. As discussed previously, TRIM21 has been described to strongly bind to the Fc part of IgG, IgM and IgA antibodies (see section 1.3.5). Thus, one cannot exclude that the positive signal observed is due to TRIM21 unspecifically binding to the anti-GBP1 antibody. An additional control to address this issue would be to perform the experiment in GBP^{chr3} cells lacking GBP1. Should TRIM21 only bind to GBP1 and not to the Fc part of the anti-GBP1 antibody, no PL signal should be observed in the absence of the GBP1 protein.

3.2.9 TRIM21 influences GBP1 localisation to avirulent *Toxoplasma*

Although both TRIM21 and GBP1 colocalise to avirulent *Toxoplasma*, the sequence and possible co-dependence of their recruitment is unknown. I next investigated the requirement of one of the interacting partners for the recruitment of the other to the avirulent vacuoles. TRIM21 recruitment was not altered in IFNγ-stimulated GBP DKO cells lacking all GBP1-GBP10 (Figure 3.11a). However, GBP1 recruitment to avirulent *Toxoplasma* vacuoles was partly but significantly decreased from 51% to 36.5% in IFNγ-stimulated cells not expressing TRIM21 (Figure 3.11b). These results suggest that TRIM21 positively regulates the localisation of GBP1 to avirulent *Toxoplasma* vacuoles. Thus, it is likely that TRIM21 plays the role of the primary sensor and recruits its effector GBP1 to the avirulent *Toxoplasma* vacuole. However,

as TRIM21 only partly influences GBP1 localisation to avirulent *Toxoplasma*, other factors yet to be determined must be involved.

3.2.10 TRIM21 and GBP1 localisation at the vacuole is altered by parasitic virulence factors

I previously demonstrated that GBP1 and ubiquitin colocalisation to avirulent *Toxoplasma* vacuoles could be impaired by the secretion of virulence factors (see section 3.2.4). I then investigated whether parasitic virulence factors could also alter the recruitment of TRIM21 and GBP1. Immunofluorescence staining for GBP1 and TRIM21 in IFNγ-stimulated mouse embryonic fibroblasts shows that both proteins also colocalise to avirulent type III CEP *Toxoplasma* strain (Figure 3.12). However, the transgenic strain CEP Rop18I exhibits significantly reduced accumulation of GBP1 and TRIM21 compared to its parental strain, decreasing from 31.5% to 7% (Figure 3.12). Interestingly, the proportion of *Toxoplasma* vacuoles decorated with both TRIM21 and GBP1 compared to the proportion of total GBP1-positive avirulent vacuoles remains the same (50%). This suggests that *Toxoplasma* virulence factors interfere with the recruitment of both GBP1 and TRIM21 to the parasitophorous vacuoles.

3.2.11 TRIM21 mediates Lys63-linked ubiquitination around avirulent *Toxoplasma*

Distinct ubiquitin linkages have been associated with specific cellular functions. Lys48-linked ubiquitinated substrates have been shown to be targeted for degradation by the proteasome (Chau et al., 1989; Finley et al., 1994), while Lys63-linked ubiquitinated substrates have been shown to be involved in DNA repair and activation of immune signalling (Hofmann and Pickart, 2001; Deng et al., 2000). I investigated

the ubiquitin linkages present at the vicinity of avirulent *Toxoplasma*. Immunofluorescence for Lys48 ubiquitin and Lys63 ubiquitin shows both linkage types can be found around *Toxoplasma* vacuoles in IFNγ-stimulated wild-type (Figure 3.13a) and TRIM21-deficient (Figure 3.13b) mouse embryonic fibroblasts.

TRIM21 has been described as a RING-type E3 ubiquitin ligase that acts as a transfer protein between ubiquitin and the substrate to be ubiquitinated. I thus investigated the ubiquitination of avirulent *Toxoplasma* vacuoles in TRIM21-deficient cells. TRIM21-deficiency led to a third decrease in avirulent *Toxoplasma* PV ubiquitination, dropping from 54% to 37% in TRIM21 knockout cells, suggesting TRIM21-mediated ubiquitination accounts at least in part for the presence of ubiquitin at the vicinity of the parasite (Figure 3.14a). Next, I examined the ubiquitin linkages involved in TRIM21-mediated avirulent *Toxoplasma* ubiquitination. TRIM21-deficiency did not affect the Lys48-linked ubiquitination of avirulent *Toxoplasma* (Figure 3.14a). However, Lys63-linked ubiquitination of avirulent *Toxoplasma* was decreased by half in TRIM21 KO cells compared to WT cells as the proportion of Lys63-linked ubiquitination dropped from 57% to 25%, mimicking the ubiquitination pattern of total ubiquitin (Figure 3.14a). This suggests the IFNγ-dependent, TRIM21-mediated ubiquitination of the avirulent parasites is specific to Lys63-linked polyubiquitin chains.

I showed previously that TRIM21 recruitment to avirulent *Toxoplasma* vacuoles is not impaired in the absence of expression of the GBPs (see section 3.2.9). I next assessed the ubiquitination of avirulent *Toxoplasma* in IFNγ-stimulated cells lacking all GBPs. Total ubiquitination, Lys48-linked ubiquitination and Lys63-linked ubiquitination were not altered in the absence of GBPs (Figure 3.14b). In accordance with my

previous findings, these observations confirm that TRIM21 can decorate avirulent *Toxoplasma* vacuoles in the absence of GBP1, leading to an accumulation of ubiquitin at the vicinity of the parasites.

3.2.12 TRIM21 does not mediate cell-autonomous resistance to *Toxoplasma*

I next investigated the downstream effects of TRIM21-mediated avirulent *Toxoplasma* ubiquitination. Mallery *et al.* showed that TRIM21 binds to invading antibody-coated adenoviruses and targets them for degradation by the proteasome due to its E3 ligase activity. More recently, TRIM21 was shown to also restrict *Salmonella* intracellular infection in an antibody-dependent manner (Rakebrandt et al., 2014). I thus assessed whether TRIM21-mediated ubiquitination of avirulent *Toxoplasma* enables restriction of intracellular parasitic infection. The IFNγ-mediated killing of *Toxoplasma* parasites was determined by an *in vitro* plaque assay, which consists in measuring the number of plaques formed on a monolayer of uninduced *vs*. IFNγ-induced cells. This assay has been used to determine whether a single protein has an effect on the IFNγ-mediated clearance of *Toxoplasma* (Niedelman et al., 2013; Haldar et al., 2015). In both wild-type and TRIM21-deficient mouse embryonic fibroblasts, the number of plaques formed following *Toxoplasma* infection was reduced in the IFNγ-induced samples compared to the uninduced samples (Figure 3.15a). Indeed, TRIM21 deficiency did not lead to a decrease in plaque loss, as IFNγ stimulation reduced the number of plaques to 66.5% in TRIM21 KO cells, whereas IFNγ-induced restriction in WT cells was translated by a reduction in plaques from 69.4% (Figure 3.15b). The plaque assay suggests TRIM21 alone does not help restrict intracellular *Toxoplasma* infection *in vitro*. However, as IFNγ upregulates hundreds of genes, and it cannot be excluded that

TRIM21 might have an effect on *Toxoplasma* restriction that is redundant and would thus be masked by the presence of another IFNγ-dependent factor.

The clearance of *Toxoplasma* in IFNγ-stimulated cells is characterised by a blebbing and disruption of the parasitophorous vacuole membrane (Martens et al., 2005; Ling et al., 2006; Yamamoto et al., 2012). I thus investigated by transmission electron microscopy the integrity of the PVM of avirulent *Toxoplasma* in IFNγ-stimulated WT or TRIM21 KO mouse embryonic fibroblasts 2h post-infection. Disruption and blebbing of the PVM of avirulent *Toxoplasma* was not markedly impaired in TRIM21-deficient cells (Figure 3.15c). Due to the size of *Toxoplasma* and to the nature of the transmission electron microscopy experiment, ultrastructural analysis of the *Toxoplasma* PV is always performed in a qualitative rather than quantitative way (Ling et al., 2006; Yamamoto et al., 2012; Selleck et al., 2013; Muniz-Feliciano et al., 2013; Dupont et al., 2014). The presence or absence of disruption of the vacuoles is considered rather than the number of intact *versus* broken vacuoles. Thus, our results suggest TRIM21 is not involved in the cell-autonomous, IFNγ-induced killing of *Toxoplasma*.

Ubiquitination of pathogens has been shown to lead to their clearance via the autophagy pathway (see section 1.3.3). *Toxoplasma* resistance is dependent on autophagy proteins, and the formation of the phagophore has been observed around the parasite. I thus tested whether the TRIM21-mediated ubiquitination of avirulent *Toxoplasma* provides the recognition signal for the autophagy receptor p62. Immunofluorescence staining for p62 was performed in IFNγ-stimulated wild-type or TRIM21-deficient mouse embryonic fibroblasts infected with avirulent *Toxoplasma*. As can be seen in Figure 3.16, the quantitative analysis of the number of vacuoles

positive for p62 reveals that the adaptor protein decorates avirulent parasites to a similar extent in both the wildtype (44.5%) and the TRIM21 KO (33%) cells. These results are in accordance with the killing assay and the ultrastructural analysis of the vacuolar integrity, indicating that TRIM21 does not regulate the cell-autonomous, IFNγ-dependent restriction of avirulent *Toxoplasma*.

3.2.13 TRIM21 does not regulate cytokine production in *Toxoplasma*-infected macrophages

As TRIM21 does not mediate cell-autonomous restriction of *Toxoplasma in vitro*, I investigated whether the E3 ubiquitin ligase plays a role in immune signalling during *Toxoplasma* infection. TRIM21 has already been shown to inhibit the activation of the NF-kB pathway and subsequent production of TNFα, IL-1β, IL-6 and IP-10 in mouse embryonic fibroblasts stimulated with poly(I:C) (Keeble et al., 2008) Moreover, TRIM21 has been reported to induce a proinflammatory state, characterised by the production of TNFα, IL-6, IP-10, CCL2 and CCL4, in mouse embryonic fibroblasts infected with adenovirus (McEwan et al., 2013). Using RT-qPCR, I compared the expression of transcripts for the NF-κB transcription factor and some selected inflammatory cytokines (TNFα, IL-12p40, IL-10 and IL-1β) in IFNγ-stimulated wild-type and TRIM21-deficient bone marrow-derived macrophages following infection with avirulent *Toxoplasma*. As can be seen in Figure 3.17, TRIM21-deficient cells show equal levels of mRNA for all the genes tested at all time points compared to the wild-type controls. I also assessed the secreted protein levels of the pro-inflammatory cytokines IFNα, IFNβ and IL-6 in wild-type and TRIM21-deficient bone marrow-derived macrophages infected with *Toxoplasma* for 24h. As can be observed in Figure 3.18, TRIM21-deficient cells exhibit similar cytokine production compared to the

wild-type cells. These results suggest that for the time points and proteins tested, TRIM21 does not regulate the production of inflammatory cytokines *in vitro* in macrophages following *Toxoplasma* infection.

3.2.14 TRIM21 mediates ubiquitination of large GTPases

Although I demonstrated TRIM21 partly mediates the Lys63-linked ubiquitination at the vicinity of avirulent *Toxoplasma* in IFNγ-stimulated cells (see section 3.2.11), it does not lead to cell-autonomous killing of the parasite (see section 3.2.12) nor does it regulate an immune response *in vitro* (see section 3.2.13). In order to decipher the consequences of the TRIM21-dependent accumulation of Lys63-linked ubiquitin to avirulent *Toxoplasma*, I investigated the potential ubiquitinated substrates of the E3 ubiquitin ligase during *Toxoplasma* infection. To that end, I used the stable isotope labelling of amino acid in cell culture (SILAC) technique in collaboration with Dr. Bram Snijders and Dr. Vesela Encheva at the Crick in Clare Hall Laboratory. Briefly, I performed the infection of SILAC-labelled MEFs and prepared the forward and reverse samples. Dr. Encheva then performed the trypsin digestion, diGLY immunoprecipitation and LC-MS/MS of the samples.

3.2.14.1 Identification of ubiquitinated proteins by SILAC

SILAC is a quantitative proteomics tool that consists of *in vivo* isotopically labelling two cellular samples (in my case wild-type and TRIM21-deficient cells) with either heavy or light lysine and arginine residues, mixing the labelled samples together, digesting the proteins with trypsin and comparing the generated peptides by liquid chromatography coupled with mass spectrometry (LC-MS/MS). At Clare Hall, the method has been adapted to specifically determine ubiquitination targets and their sites of ubiquitination. It is based on the fact that ubiquitinated proteins subjected to trypsin

digestion will leave a remnant Gly-Gly (diGLY) site that can be captured using an anti-diGLY antibody. Thus, an additional immunoprecipitation step with the anti-diGLY antibody post-trypsinisation allows enrichment of the sample with ubiquitinated peptides before LC-MS/MS analysis (Figure 3.19).

3.2.14.2 Optimisation of culture conditions for efficient SILAC labelling

A high incorporation rate of the labelled isotopes into the cells is a key factor for the success of the SILAC method. In order to ensure the highest level of incorporation, the cells have to undergo a theoretical 4 to 6 doublings, so that all newly synthesised proteins will be made up with isotopes only. The addition of labelled isotopes into the culture medium can alter the growth of the cells, rendering their expansion in the SILAC medium challenging. My primary mouse embryonic fibroblasts did not initially proliferate well in the SILAC medium. This issue was finally solved by using a SILAC-specific FCS that is dialysed at a cut-off of 1000 Da.

Once the optimum culture conditions had been determined, wild-type mouse MEFs were grown for 4 to 5 doublings in "heavy" (^{13}C-arginine, ^{13}C-lysine and unlabelled proline) or "light" (^{12}C-arginine, ^{12}C-lysine and unlabelled proline) medium. Cells were mixed at a 1:1 ratio, proteins were extracted, submitted to digestion with trypsin and analysed by liquid chromatography coupled with mass spectrometry. The incorporation efficiency was assessed by plotting the peptide intensity against the $\log_2$ ratio of the "heavy" mass-to-charge ratio over the "light" mass-to-charge ration (ratio H/L). Thus, a good incorporation is translated by a high H/L ratio. As can be seen on Figure 3.20a, both the arginine and the lysine signals are situated on the high end of the graph. Lysine residues exhibit a $\log_2(16)=4$, which is equivalent to an incorporation rate of 93.75% (as 1/16=0.0625). Similarly, arginine residues exhibit a $\log_2(64)=6$,

which is equivalent to an incorporation rate of 98.44% (1/64=0.0156). This indicates the cells divided well and incorporated the labelled isotopes enough to allow SILAC analysis.

Along with the challenging culture conditions and the necessity of a high incorporation rate, another limiting factor in the SILAC method is the possible arginine-to-proline conversion. Indeed, arginine is a metabolic precursor for proline biosynthesis, and natural conversion of arginine to proline can occur at a high rate in the cell. This can lead to an unbalanced heavy isotope labelling, with a diminution of the heavy arginine portion and the apparition of satellite heavy proline signals. To prevent and correct the arginine-to-proline conversion, unlabelled proline is added to the SILAC media. However, the efficiency of the approach and the extent of the possible conversion have to be evaluated. As can be observed in Figure 3.20b, the arginine signals are evenly and randomly distributed on the graph, while an important arginine-to-proline conversion would be translated by the appearance of a cloud of arginine signals located on the light (e.g. left) side of the graph. This indicates that the addition of unlabelled proline in the SILAC culture media is sufficient to prevent the metabolic arginine-to-proline conversion.

3.2.14.3 TRIM21 regulates the protein level of some GBPs

To identify the ubiquitination substrates of TRIM21, wild-type and TRIM21 KO mouse embryonic fibroblasts were cultivated in both “heavy” (^{13}C-arginine, ^{13}C-lysine and unlabelled proline) and “light” (^{12}C-arginine, ^{12}C-lysine and unlabelled proline) medium, induced for 16h with IFNγ and infected for 1h with avirulent *Toxoplasma*. Two samples were generated by mixing at a 1:1 ratio the “heavy” WT with the “light” TRIM21 KO cells (forward sample) and by mixing at a 1:1 ratio the “light” WT with

the “heavy” TRIM21 KO cells (reverse sample). This allows for checking of the reproducibility of the data and enables correlation studies between the forward and reverse samples.

To control for alterations in the total abundance of proteins, a small portion of each mixed cell lysates was used for gross protein quantification. This enables determination of whether any change in ubiquitination can be attributed to a change in the protein abundance. The graph pictured in Figure 3.21 shows all retrieved proteins from the quantification analysis. As the thin blue diagonal line indicates the close correlation between forward and reverse samples, the closer a dot is to this line the greater the correlation is and thus confidence in protein quantification. The dots localised close to the intersection of the *x* and *y* axes represent proteins that do not exhibit a differential protein level. Strikingly, one protein highlighted in blue appears to have a higher protein level in the WT cells, and its quantification correlated well between the forward and reverse samples. Very interestingly, this protein is GBP1, implying that TRIM21 upregulates the protein level of GBP1. Moreover, analysis of the protein levels of other GBPs reveals that GBP2 (red dot) is present at a higher protein level in TRIM21 KO cells, suggesting that TRIM21 downregulates the protein level of GBP2 (Figure 3.21).

A separate analysis of the protein quantification data was also performed in the forward sample only (Figure 3.22a) and in the reverse sample only (Figure 3.22b). On both graphs, GBP1 (blue dot) clearly shows a higher protein level in WT cells whereas GBP2 (red dot) clearly shows a higher protein level in TRIM21-deficent cells. In the forward sample (Figure 3.22a), another GBP represented by a green dot, namely GBP4, seems to exhibit a higher protein level in the WT cells, but this has not been

confirmed in the reverse sample. Some IRGs, represented by orange dots, appear to have mainly similar protein levels in both cell lines.

3.2.14.4 TRIM21 mediates the ubiquitination of members of the family of IFNγ-induced large GTPases

To identify the ubiquitinated substrates of TRIM21, forward and reverse samples were digested with trypsin, and enrichment for ubiquitinated peptides was achieved by anti-diGLY immunoprecipitation. DiGLY-containing peptides were analysed by liquid chromatography coupled with mass spectrometry. A total of 2058 diGLY sites were recovered from the forward WT "heavy" sample, while 1997 diGY sites were retrieved from the reverse WT "light" sample (Figure 3.23). 448 diGLY sites were only found in the forward WT "heavy" sample and 387 diGLY sites were only found in the reverse WT "light" sample. 221 diGLY sites were not assigned, probably due to a low signal to noise ratio. Finally, 1610 diGLY sites were common in the forward and the reverse samples and could be analysed further on the correlation plot shown in Figure 3.24. The graph shows the diGLY sites retrieved from the forward and reverse samples. The thin blue diagonal line represent the best correlation, so that the closer a dot is to this line the greater the correlation is and thus confidence in protein ubiquitination. The dots localised close to the intersection of the *x* and *y* axes represent proteins that do not exhibit a differential ubiquitination profile. The analysis of the family of IFNγ-induced large GTPases reveals that the GBPs (blue, red and green dots), the IRGs (orange dots) and VLIG1 (pink dots) all present ubiquitination sites that correlate very well between the forward and reverse samples. Interestingly, GBP2 and VLIG1 seem to be more ubiquitinated in TRIM21-deficient cells (Figure 3.24).

A separate analysis of the ubiquitination sites was performed in the forward sample only (Figure 3.25a) and in the reverse sample only (Figure 3.25b). The further away from the *y* axis a dot is, the stronger the corresponding ubiquitination signal from mass spectrometry is. On both graphs, the red dots representing GBP2 cluster on the side of TRIM21-deficient cells, indicating GBP2 is more ubiquitinated in cells lacking TRIM21. Similarly, the pink dots representing VLIG1 group on the side of TRIM21 KO cells, suggesting VLIG1 is more ubiquitinated in the absence of TRIM21. In contrast, the blue dots representing GBP1 cluster on the side of wild-type cells, implying GBP1 is more ubiquitinated in the presence of TRIM21. However, these latter ubiquitination sites could only be retrieved from the reverse sample. Finally, the ubiquitination pattern of the other GBPs and of the IRGs appear to be more consistent between the wild-type and TRIM21-deficient cells, indicating their ubiquitination status is not dependent on TRIM21. Altogether, these SILAC data identify TRIM21 as a positive regulator of the ubiquitination of GBP1, and a negative regulator of the ubiquitination of GBP2 and VLIG1.

3.2.15 TRIM21 mediates cholesterol biosynthesis

3.2.15.1 Transcriptional analysis of *Toxoplasma*-infected TRIM21-deficient cells: quality control

As TRIM21 appears to regulate resistance against *Toxoplasma* infection on a non-cell autonomous level, I decided to perform a transcriptional analysis by RNAseq in wild-type and TRIM21-deficient mouse embryonic fibroblasts following *Toxoplasma* infection. Live, *Toxoplasma*-infected cells were sorted by flow cytometry and RNA was extracted as described in section 2.15. The alignment, mapping, analysis and visualisation of the RNAseq data were performed by Dr. Helena Ahlfors (Babraham

Institute, Cambridgeshire, UK). First, the quality of the reads was assessed using the FastQC tool as described in section 2.16.3. The reads were subsequently aligned to the mouse genome and were counted using HTSeq-count. The generated data were finally analysed with DESeq2. The quality of the data produced was assessed using the dispersion parameter. This consists in estimating the correlation of the variance, or "dispersion", of the biological replicates and the mean count for each gene. First, it estimates a dispersion value for each gene. Second, it fits a curve through the estimates. Finally, it assigns to each gene a dispersion value, using a value that ranges between the gene estimate and the fitted value. As can be seen on Figure 3.26a, the empirical dispersion estimates cluster well along the fitted dispersion curve, indicating that the biological variance between each gene's triplicates is minimal, and validating the RNAseq data.

Second, the principal component analysis (PCA) can be used to visualise the distance between samples. It is a statistical ordination method that consists in determining the largest possible variance between data points to accordingly spread the samples onto the *x* axis of a 2D plane. Then, the second largest possible variance is identified in order to spread the same samples onto the *y* axis of the same 2D plane. The resulting PCA plot thus represents the optimal spread between samples and allows to determine how well samples cluster or differ. As can be observed in Figure 3.26b, four different and well-defined groups can be observed. The three replicates within each condition cluster together, while the distance between each condition is optimal. This suggests that the triplicates are of good quality and that the four conditions tested exhibit different and distinct gene expression profiles.

3.2.15.2 Differential gene expression in TRIM21-deficient mouse embryonic fibroblasts upon *Toxoplasma* infection

The comparative analysis of the gene expression profiles in the four conditions tested was first performed using the MA plot. This test generates a scatter plot that represents the fold change gene expression (log_2) between two samples versus the mean of the normalised counts. The graphs shown in Figure 3.27 represent the comparison of gene expression between two conditions at a fold change cut-off of 2 (above and below the blue dotted lines) and an adjusted p-value of 0.05. At the steady state, corresponding to the comparison between uninfected TRIM21-deficient cells and uninfected wild-type cells, 866 genes are upregulated and 915 genes are downregulated in the TRIM21 KO cells (Figure 3.27a). When considering the TRIM21-deficient cells only, 774 genes are upregulated and 167 genes are downregulated following infection with avirulent *Toxoplasma* (Figure 3.27b). Similarly, if considering wild-type cells only, 1411 genes are upregulated and 206 genes are downregulated upon infection with avirulent *Toxoplasma* (Figure 3.27c). Finally and more interestingly, 437 genes are upregulated and 787 genes are downregulated in TRIM21-deficient cells compared to wild-type cells following infection with avirulent *Toxoplasma* (Figure 3.27d). As this particular comparison corresponds to the "snapshot" that exemplifies the situation the *Toxoplasma* parasites encounter in the cell, the following gene expression analysis will be mainly performed in this *Toxoplasma*-infected TRIM21 KO *versus Toxoplasma*-infected wild-type comparison .

Finally, in order to corroborate to the proteomic data obtained by SILAC suggesting that TRIM21 deficiency influences the abundance of both GBP1 and GBP2 at the protein level, we had a closer look at their respective gene expression level. The expression level of *Gbp1* is downregulated by a fold change of 7.7 in the TRIM21-

deficient cells compared to the wild-type controls. Moreover, the expression level of *Gbp2* is upregulated at a fold change of 2.4 in cells lacking TRIM21 compared to the WT controls.

Gene name	**Gene ID**	**Fold change (TRIM21 KO *vs.* WT)**
Gbp1	ENSMUSG00000040264	-7.7
Gbp2	ENSMUSG00000028270	2.4

Table 3.1: Gene expression levels of selected GBPs in TRIM21-deficient cells compared to wild-type cells.

Thus, the differential protein levels of GBP1 and GBP2 observed in the SILAC experiment could be explained by a differential expression at the genomic level, implying that TRIM21 somehow regulates some GBPs at the RNA level. One could speculate that TRIM21 could play a role in the stability or transport of GBP1 and GBP1 mRNAs, or alternatively could mediate the degradation of the mRNAs. The exact mechanism underlying this regulation remains to be investigated.

3.2.15.3 *Toxoplasma*-infected TRIM21-deficient cells display an upregulated cholesterol biosynthesis

Differential gene expression analysis revealed that 437 genes are upregulated and 787 genes are downregulated in *Toxoplasma*-infected TRIM21-deficient mouse embryonic fibroblasts compared to infected wild-type controls. In order to identify the biological pathways and related networks these genes are involved in, we ran an Ingenuity Pathway Analysis (IPA) that analyses the functional connectivity of genes using computational algorithms from information obtained within the IPA database. Canonical biological pathways are scored by identifying the number of differentially

expressed genes that map to a specific pathway. As can be seen in Figure 3.28, IPA identified the 10 top canonical biological pathways whose genes are differentially regulated in *Toxoplasma*-infected TRIM21 KO cells compared to the infected WT cells. Strikingly, among those 10 pathways associated with differentially expressed genes, 2 are involved in the biosynthesis of cholesterol or its precursor, zymosterol. For each of these biosynthesis pathways, all genes appear to be upregulated in TRIM21-deficient cells following *Toxoplasma* infection. Interestingly, the biological pathway for hepatic stellate cell (HSC) activation is also differentially regulated in TRM21-deficient cells infected with avirulent *Toxoplasma*, with about half of the genes being upregulated and the other half of the genes being downregulated. Originally termed "fat-storing cells", HSCs are hepatic cells that are responsible for the storage of 80-90% of the retinoid stored in the liver, as well as of a significant quantity of triglycerides, phospholipids, cholesterol, and free fatty acids in cytoplasmic lipid droplets (Friedman, 2008). During liver damage, HSCs are activated and these lipid droplets are lost. Furthermore, two other biological pathways found to be differentially regulated in infected TRIM21 KO cells are liver receptor X (LXR) and retinoid receptor X (RXR) activation, as well as IL-1 mediated RXR inhibition. LXRs have been shown to act as cholesterol sensors and modulate the expression of genes involved in cholesterol and lipid metabolism in response to changes in cellular cholesterol status (Zhao and Dahlman-Wright, 2010). RXRs are nuclear receptors that modulate lipids metabolism by forming activating heterodimers with other nuclear receptors such as LXRs and the fatty acid receptors called peroxisome proliferator-activated receptor (PPAR). Finally, the other biological pathways differentially regulated in *Toxoplasma*-infected TRIM21-deficient cells compared to WT infected cells are granulocyte and agranulocyte adhesion and diapedesis, cyclic adenosine

monophosphate (cAMP)-mediated signalling, G-protein coupled receptor signalling and IL-10 signalling (Figure 3.28).

As cholesterol biosynthesis appears to be the main biological pathway differentially regulated in *Toxoplasma*-infected TRIM21-deficient mouse embryonic fibroblasts compared to infected wild-type controls, the genes involved in cholesterol biosynthesis were retrieved and analysed with the IPA software. As can be observed in Figure 3.29, wild-type cells seem to downregulate the genes involved in cholesterol biosynthesis following *Toxoplasma* infection compared to uninfected wild-type. In contrast, at the steady state, uninfected TRIM21-deficient cells have a higher expression level of the genes involved in cholesterol biosynthesis when compared to uninfected controls, and this upregulation is exacerbated upon infection with avirulent *Toxoplasma*. Thus, these results suggest that TRIM21 mediates the downregulation of cholesterol biosynthesis during *Toxoplasma* infection, and that one major organ where this regulation occurs could be the liver.

3.2.16 Discussion

The murine host has developed immune strategies, orchestrated by the major cytokine interferon γ, in order to successfully contain the *Toxoplasma* parasite without causing lethal hyper-inflammation. This IFNγ-mediated response involves the recruitment of the two families of large GTPases p47 IRGs and p65 GBPs to the avirulent parasitophorous vacuole, leading to the disruption of the parasite's replicative niche and its subsequent clearance by autophagy. Although *Toxoplasma* clearance has been shown to be dependent on proteins involved in the autophagy and inflammasome pathways, the mechanisms triggered after the disruption of the parasitophorous

vacuole remain unclear. The aim of this work was to identify host factors that play a role at the parasitophorous vacuole and mediate the restriction of *Toxoplasma*.

In this thesis, I report for the first time the presence of ubiquitin at the vicinity of avirulent type II and type III strains of *Toxoplasma* (see sections 3.2.1 and 3.2.4). I further demonstrate that this ubiquitination around avirulent parasites is strictly mediated by the major cytokine IFNγ (see section 3.2.2), and that virulence factors secreted by the parasite in the host cytosol interfere with the decoration of the vacuole with ubiquitin (see section 3.2.4). As this IFNγ-dependent ubiquitin accumulation pattern around avirulent *Toxoplasma* mimics the one of the p65 guanylate-binding protein GBP1, I performed colocalisation studies and show that all GBP1-positive vacuoles are also decorated with ubiquitin (see section 3.2.3). Two different experimental approaches, combining immunoprecipitation with either mass spectrometry or immunoblot, identified the E3 ubiquitin ligase TRIM21 as a GBP1 interaction partner (see section 3.2.5). Here, I also show that TRIM21 complexes with GBP1 in the cytoplasm and that both proteins colocalise to the parasitophorous vacuole of avirulent *Toxoplasma* in an IFNγ-dependent fashion (see sections 3.2.7 and 3.2.8). This therefore makes TRIM21 a novel and the first identified interaction partner of GBP1 -as well as of any other GBPs- at the vacuole of avirulent *Toxoplasma*. As the formation of the TRIM21-GBP1 complex is dependent on IFNγ stimulation, an IFNγ-induced cofactor yet to be determined is necessary for the newly discovered interaction. This could be resolved in the future by performing an anti-TRIM21 immunoprecipitation followed by a native gel electrophoresis and analysis of the binding partners by mass spectrometry. A confirmation of the putative new but necessary member of the TRIM21-GBP1 complex would then need to be performed.

Alternatively, the BioID technique could also be used. It would consist in fusing either TRIM21 or GBP1 with a promiscuous BirA biotin ligase, so that any interacting protein in close proximity would be biotinylated and could thus be immunoprecipitated with streptavidin and further identified by mass spectrometry.

Despite their identification in 1983, little is known about the biological relevance of IFNγ-induced mouse guanylate binding proteins after *Toxoplasma* infection. Which cellular functions this class of IFNγ-inducible GTPases mediate is currently vaguely defined at best. Considering GBP1 and TRIM21 colocalise together at the PV of avirulent *Toxoplasma*, I hypothesised that the GBPs provide the cell with a recognition system to distinguish avirulent from virulent *Toxoplasma*, and they co-recruit their effector molecules to the vacuole to position them to exert their anti-pathogenic effect. This theory was initially reinforced by the observation that GBP1 and TRIM21 corecruitment to avirulent *Toxoplasma* is impaired by the secretion of parasitic virulence factors, implying that the absence of GBP1 at the vacuole leads to an altered presence of TRIM21 as well (see section 3.2.10). However, localisation studies of the individual interaction partners in cells lacking their counterpart reveals that TRIM21 is partly mediating the recruitment of GBP1 to avirulent vacuoles, whereas GBP1 deficiency does not alter TRIM21 accumulation around the parasite (see section 3.2.9). Thus, it is likely that TRIM21 plays the role of the primary sensor and recruits its effector GBP1 to the avirulent *Toxoplasma* vacuole.

The role of TRIM21 has mainly been described during the course of viral infection in the mouse. Mallery *et al*. who demonstrated that TRIM21 mediates an intracellular antibody response have disputed the dogma that antibodies do not have an intracellular function. They showed that TRIM21 binds to invading antibody-coated adenoviruses

and targets them to degradation by the proteasome due to its E3 ligase activity (Mallery et al., 2010), thereby enabling to control viremia *in vivo* (Vaysburd et al., 2013). The *in vitro* experiments reported in this work have been performed in medium supplemented with FCS, where antibodies can hence be present. As a result, it remains to be assessed whether the recruitment of TRIM21 and GBP1 to avirulent *Toxoplasma* vacuoles is dependent on antibodies. However in this study, I demonstrate that TRIM21 mediates Lys63-linked ubiquitination in the vicinity of avirulent *Toxoplasma* (see section 3.2.11). Interestingly, as assessed by killing assay and ultrastructural analysis of the integrity of the PV membrane, the TRIM21-mediated ubiquitination around *Toxoplasma* does not lead to the degradation of the parasite (see section 3.2.12) in contrast to its role during viral infection. TRIM21 acts on a non cell-autonomous level during *Toxoplasma* infection by a mechanism that still needs elucidation. In fact, assessment of the mRNA and protein levels of several inflammatory molecules did not indicate a role for TRIM21 in mediating immune signalling *in vitro*.

Although TRIM21 is one of the GBPs partner molecules operating at the avirulent *Toxoplasma* vacuole, it is undoublty not the sole E3 ubiquitin ligase depositing ubiquitin at the vicinity of the parasite, as can be deduced from the remaining ubiquitination level around the PV in TRIM21-deficient cells (see section 3.2.11). These additional E3 ubiquitin ligases, as well as their recruitment kinetics and targets, are still to be identified and characterised. One other candidate is the E3 ubiquitin ligase TRAF6, that we recently shown to mediate IRGM-dependent ubiquitination of avirulent *Toxoplasma* vacuoles, thereby promoting the recruitment of the autophagy protein p62 and of the GBPs (Haldar et al., 2015). Thus, as p62 recruitment to avirulent vacuoles is not impaired in TRIM21-deficient cells, we propose that TRIM21 acts downstream of the E3 ligase TRAF6 and the autophagy protein p62, by complexing

with GBP1 in the cytoplasm and promoting its recruitment to TRAF6-positive and ubiquitin-positive *Toxoplasma* PVs via regulation of GBP1 ubiquitination. The question remains whether other ubiquitin adaptor proteins such as NDP52 are involved in the direction of GBPs to the vacuoles.

TRIM21 comprises three N-terminal protein domains: a RING domain involved in protein-protein interactions that endows it with an E3 ligase activity, two B-box domains that are zinc-binding motifs and a helical coiled-coil domain important for protein-protein interactions (Reymond et al., 2001; Ottosson et al., 2006). TRIM21 is also characterised by a C-terminal B30.2/PRYSPRY domain that was shown to strongly bind to the Fc part of antibodies (Rhodes and Trowsdale, 2007; Keeble et al., 2008). It is tempting to speculate that the E3 ligase activity of TRIM21 mediates the Lys63-linked ubiquitination at the vicinity of avirulent *Toxoplasma*. I have generated retroviral constructs for wild-type TRIM21 as well as for TRIM21 mutants lacking the RING domain (ΔRING), the B-box domain (ΔB-box) or the B30.2 domain (ΔPRYSPRY). I have already produced the corresponding retroviruses, which will be used in the future to reintroduce the wild-type or mutant proteins in TRIM21-deficient cells to study their effect on the ubiquitination of avirulent *Toxoplasma*, as well as the recruitment of GBP1 to the vacuoles.

Similarly, it is very appealing to define TRIM21 ubiquitination substrates around the avirulent *Toxoplasma* vacuoles, whether host or parasite proteins. Preliminary results from stable isotope labelling with amino acids in cell culture identified several members of the family of IFNγ-induced large GTPases to be differentially ubiquitinated in the absence of TRIM21 (see section 3.2.14.4). Indeed, GBP2 and VLIG1 were found to be more ubiquitinated in TRIM21-deficient mouse embryonic

fibroblasts, while GBP1 was less ubiquitinated. The increased ubiquitination of GBP2 and VLIG1 could be explained by either a downregulation of a deubiquitinase activity, or compensatory ubiquitination by other E3 ubiquitin ligases. For example, it has been shown that the expression of other TRIM proteins, some of them bearing E3 ligase activities, is upregulated in TRIM21-deficient fibroblasts (Yoshimi et al., 2009). The decreased ubiquitination of GBP1 in TRIM21-deficient cells could explain the decreased Lys63-linked ubiquitination around avirulent *Toxoplasma* observed in TRIM21 KO cells, as well as the decreased recruitment of GBP1 to avirulent vacuoles. This would imply that TRIM21 mediates the recruitment of GBP1 via the ubiquitination process, thereby altering GBP1 antiparasitic activity. However, the SILAC results and the RNAseq data also show that the protein abundance of both GBP1 and GBP2 is altered in cells lacking TRIM21 (see section 3.2.14.3). As a consequence, one cannot exclude that the differential ubiquitination profile of the GTPases is simply due to a difference in the protein level in TRIM21-deficient cells. To address this, a new SILAC experiment with a targeted quantification of the GBPs protein levels as well as with a targeted analysis of the GBPs diGLY sites would enable to assess whether the ubiquitination patterns observed are real. Moreover, the difference in ubiquitination profiles will be confirmed by immunoprecipitating ubiquitinated proteins in wild-type and TRIM21 KO cells and immunoblotting for GBP1 or GBP2.

Considering TRIM21 does not mediate cell-autonomous restriction of *Toxoplasma*, we performed RNAseq in order to discover what biological pathways are differentially regulated in *Toxoplasma* infected TRIM21-deficient mouse embryonic fibroblasts compared to infected wild-type cells. Very strikingly, multiple regulators of the cholesterol biosynthesis pathway are upregulated in infected TRIM21 KO cells.

Additionally, pathways related to the activation of hepatic stellate cells and the activation of the liver X receptor, involved in cholesterol storage and metabolism, respectively, appear to be also differentially regulated in TRIM21-deficient cells infected with avirulent *Toxoplasma*. It is thus likely that TRIM21 downregulates the biosynthesis of cholesterol, possibly mainly in the liver which is the organ where cholesterol is sequestrated. This is of particular importance, as *Toxoplasma* has been reported to be auxotroph for cholesterol (Coppens et al., 2000). As a consequence, TRIM21 could act at the transcriptional level by downregulating the level of cholesterol available, thereby impairing *Toxoplasma* replication.

Finally, the possible role of TRIM21 during *Toxoplasma* infection remains to be investigated in human cells. Earlier this year, TRIM21 has been identified as one of eight E3 ubiquitin ligases present at the *Legionella*-containing vacuoles in human macrophages (Bruckert and Abu Kwaik, 2015). Preliminary data in the Frickel laboratory suggest avirulent *Toxoplasma* is decorated with Lys63-linked ubiquitin in IFNγ-stimulated non-hematopoietic cells (personal communication, Dr. Barbara Clough, unpublished data). It would thus be interesting to assess whether TRIM21 recruits to avirulent vacuoles in human cells and mediates the IFNγ-dependent Lys63-linked ubiquitination like it does in the mouse cells. Shall TRIM21 prove to decorate *Toxoplasma* vacuoles in human cells, its precise role could be further studied by knocking out the *Trim21* gene using the recently developed CRISPR technology.

In summary, I have identified the E3 ubiquitin ligase TRIM21 as the first GBP1 interaction partner at the vacuole of avirulent *Toxoplasma*. Mediating the ubiquitination of GBP1 and its recruitment to the vacuole, TRIM21 is an important effector molecule in the IFNγ-induced non cell-autonomous resistance to *Toxoplasma*

in the *in vitro* mouse model (Figure 3.30). This complex and cooperative mechanism between TRIM21 and GBP1 highlights a new host defence mechanism against the intracellular pathogen. The consequences of the deletion of the newly discovered *Toxoplasma* resistance factor TRIM21 at the organismal level will be the focus of the next chapter.

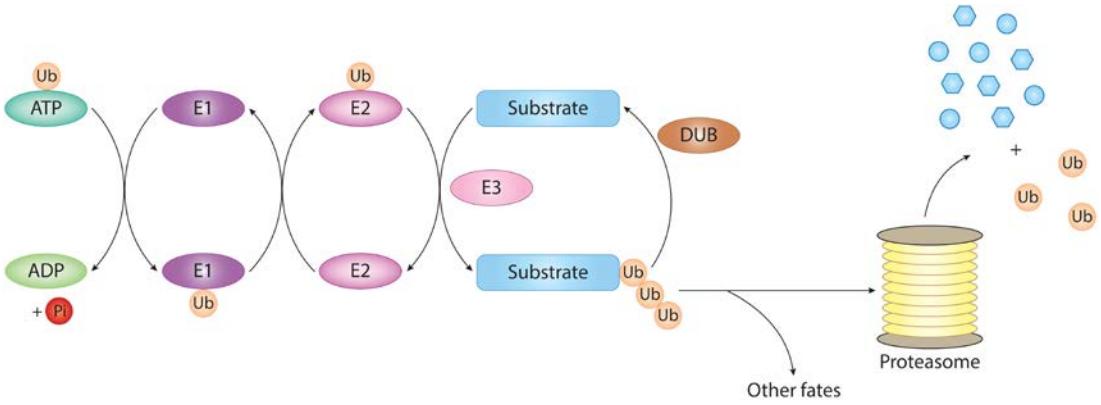

Figure 3.1: The ubiquitination process.
Ubiquitination is an ATP-dependent post-translational modification process by which a molecule of ubiquitin is attached to a substrate protein. Ubiquitin is activated by an E1 ubiquitin-activating enzyme, resulting in the formation of a thioester linkage between the C-terminus of ubiquitin and an active cysteine on the E1 enzyme. As an E2 ubiquitin-conjugating enzyme binds to both the E1 enzyme and the activated ubiquitin, the ubiquitin is then transferred to an active cysteine on an E2 enzyme. Finally, an E3 ubiquitin ligase enzyme interacts with both the E2 enzyme and the substrate. The E3 ubiquitin ligase catalyses the transfer of ubiquitin from the E2 enzyme to the target protein, resulting in an isopeptide bond between the C-terminal glycine of the ubiquitin molecule and a lysine on the substrate protein. The process is repeated until a ubiquitin chain is formed. The ubiquitin-labelled protein is then either degraded into peptides by the proteasome, releasing free ubiquitin molecules, or it can regulate cellular processes such as the cell cycle or the immune response. Enzymes called deubiquitinases (DUBs) remove ubiquitin molecules from the substrate, thereby recycling the cellular pool of ubiquitin or regulating the function of the ubiquitinated substrate.

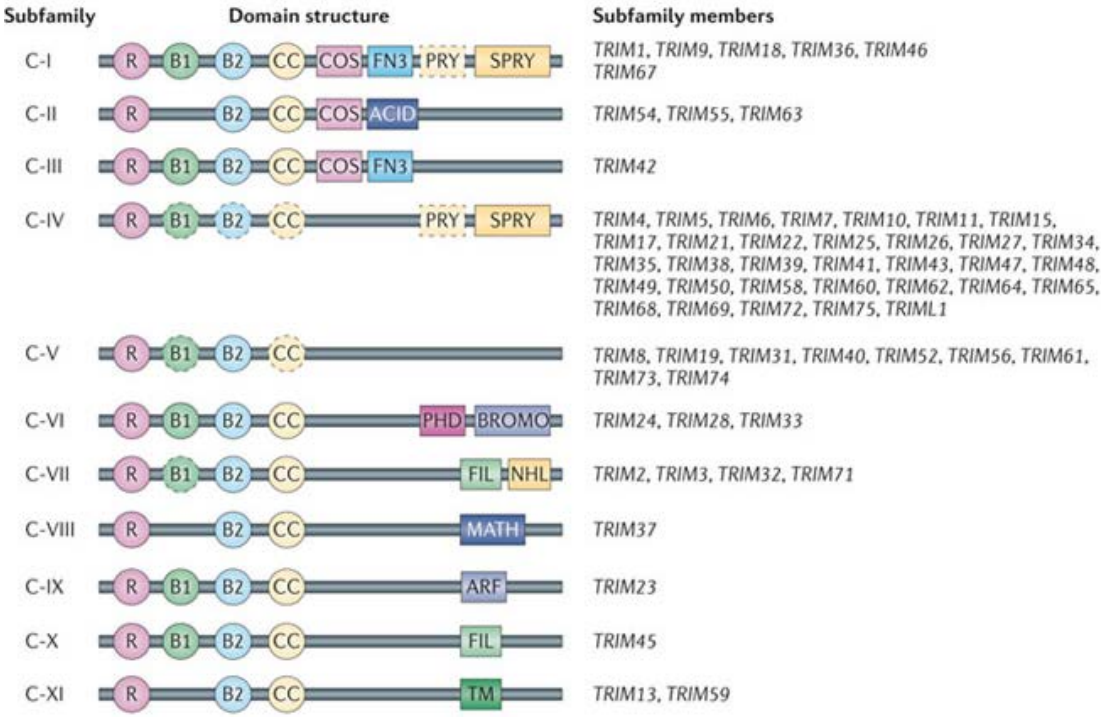

Figure 3.2: Schematic structures of the human TRIM proteins.
TRIM proteins all comprise a RING (R) domain, one or two B-box (B) domains and one coiled-coil (CC) domain. They are classified (C-I to C-XI) according to their C-terminal features. COS: cos-box; FN3: fibronectin type III repeat; ACID: acid-rich region; PHD: PHD domain; BROMO: bromodomain; FIL: filamin type I G domain; NHL: NCL1, HT2A and LIN41 domain; MATH: meprin and TRAF homology domain; ARF: ADP-ribosylation factor family domain; TM: transmembrane region. Reprinted with permission from (Hatakeyama, 2011).

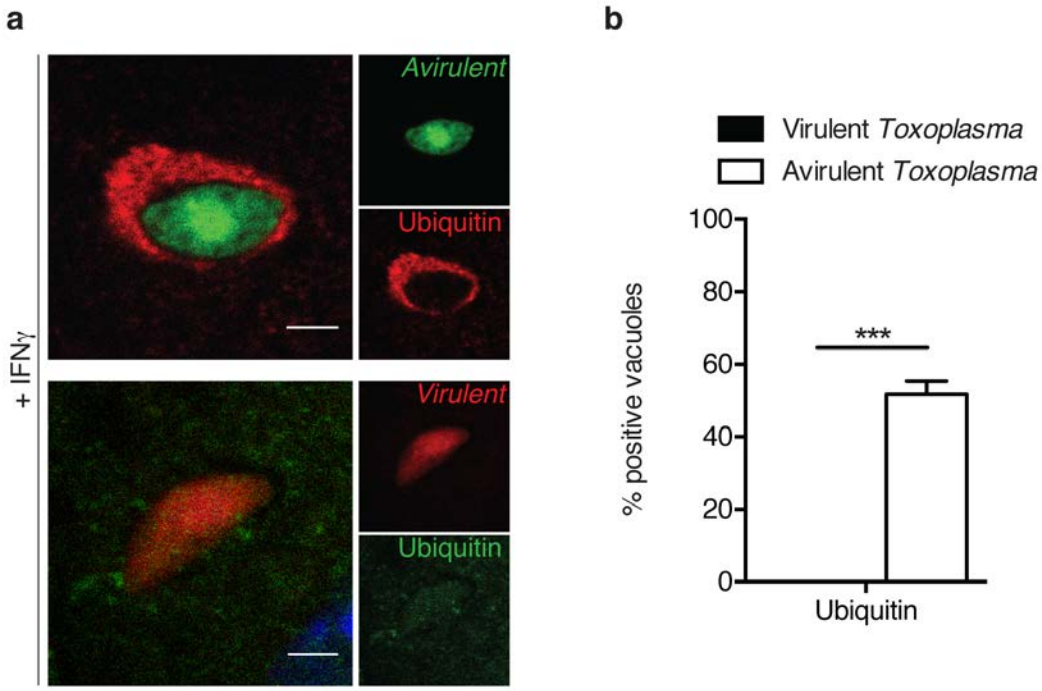

Figure 3.3: Ubiquitin accumulates at the vicinity of avirulent *Toxoplasma*.
a) Representative immunofluorescence confocal images of IFNγ-stimulated mouse embryonic fibroblasts infected with avirulent *Toxoplasma* expressing GFP (top panel) or virulent *Toxoplasma* expressing tomato (lower panel) and stained with ubiquitin (FK2, Enzo Life Sciences). Ubiquitin decorates avirulent, but not virulent *Toxoplasma* vacuoles. MEFs were induced with 100 U/mL IFNγ overnight and infected for 1h with *Toxoplasma*. Cells were fixed in 3% paraformaldehyde and stained with goat anti-mouse antibody (Molecular Probes). Nuclei were stained with Hoechst. Scale bar is 2 μm. **b)** Quantification of ubiquitin-positive parasite-containing PVs in IFNγ-stimulated MEFs infected with virulent or avirulent *Toxoplasma*. Ubiquitin decorates avirulent, but not virulent *Toxoplasma* vacuoles. For each strain, at least 100 vacuoles of invaded *Toxoplasma* were checked for ubiquitin recruitment. Data pooled from three independent experiments. Mean + SEM, *** p=0.0002, unpaired t-test.

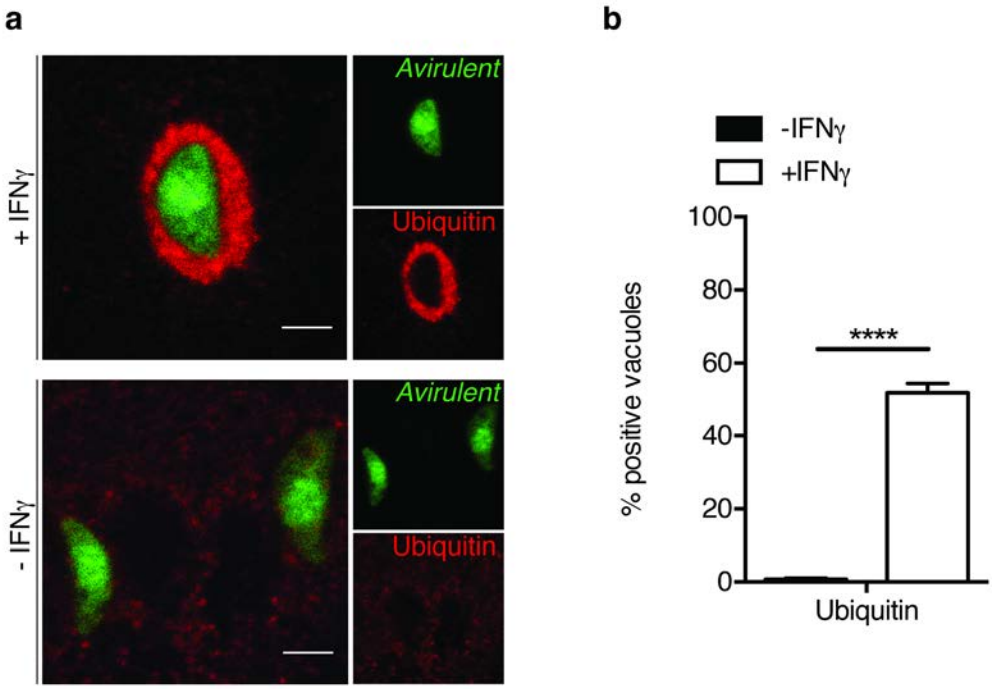

Figure 3.4: IFNγ mediates accumulation of ubiquitin at the vicinity of avirulent *Toxoplasma*.
a) Representative immunofluorescence confocal images of mouse embryonic fibroblasts infected with avirulent *Toxoplasma* expressing GFP with (top panel) or without (lower panel) IFNγ stimulation and stained with ubiquitin (FK2, Enzo Life Sciences). Ubiquitin decorates avirulent *Toxoplasma* vacuoles in IFNγ-stimulated cells only. MEFs were induced with 100 U/mL IFNγ overnight and infected for 1h with *Toxoplasma*. Cells were fixed in 3% paraformaldehyde and stained with goat anti-mouse antibody (Molecular Probes). Nuclei were stained with Hoechst. Scale bar is 2 µm. **b)** Quantification of ubiquitin-positive parasite-containing PVs in MEFs infected with avirulent *Toxoplasma* with or without IFNγ stimulation. Ubiquitin decorates avirulent *Toxoplasma* vacuoles in IFNγ-stimulated cells only. For each strain, at least 100 vacuoles of invaded *Toxoplasma* were checked for ubiquitin recruitment. Data pooled from three independent experiments. Mean + SEM, **** $p<0.0001$, unpaired t-test.

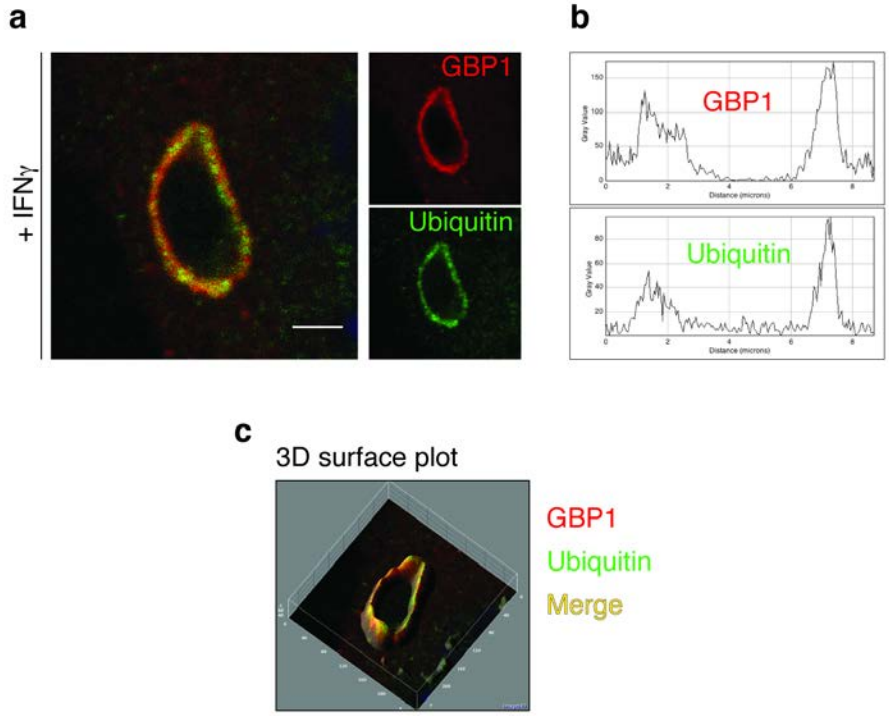

Figure 3.5: GBP1 and ubiquitin colocalise to avirulent *Toxoplasma* vacuoles.
a) Representative immunofluorescence confocal images of IFNγ-stimulated mouse embryonic fibroblasts infected with avirulent *Toxoplasma* and co-stained for GBP1 (home-made antibody) and ubiquitin (FK2, Enzo Life Sciences). GBP1 and ubiquitin colocalise to avirulent *Toxoplasma* vacuoles in IFNγ-stimulated cells. MEFs were induced with 100 U/mL IFNγ overnight and infected for 1h with avirulent *Toxoplasma*. Cells were fixed in 3% paraformaldehyde and stained with a goat anti-rabbit antibody and goat anti-mouse antibody (Molecular Probes), respectively. Nuclei were stained with Hoechst. Scale bar is 2 μm. Plot profile analysis **b)** and 3D surface plot analysis **c)** show GBP1 and ubiquitin exhibit a similar localisation pattern and colocalise around the avirulent *Toxoplasma* vacuole.

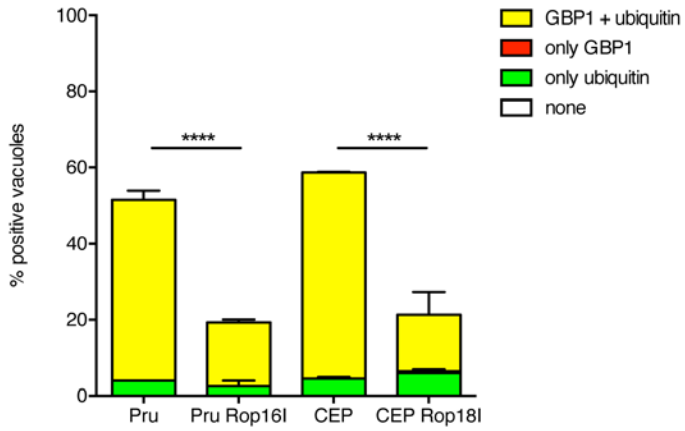

Figure 3.6: *Toxoplasma* virulence factors interfere with GBP1 and ubiquitin colocalisation to the vacuole.
Quantification of ubiquitin- and/or GBP1-positive parasite-containing vacuoles in IFNγ-stimulated mouse embryonic fibroblasts infected with the canonical avirulent *Toxoplasma* type II (Pru) and type III (CEP) strains, as well as with avirulent *Toxoplasma* type II strain transgenic for the virulent version of type I Rop16 (Pru Rop16I), and avirulent *Toxoplasma* type III strain transgenic for the type I version of Rop18 (CEP Rop18I). Transgenic avirulent strains expressing virulence factors show less GBP1 and ubiquitin colocalisation compared to their respective parental strain. For each strain, at least 100 vacuoles of invaded *Toxoplasma* were checked for ubiquitin recruitment. Data pooled from two experiments. Mean + SEM, **** $p<0.0001$, 2-way ANOVA.

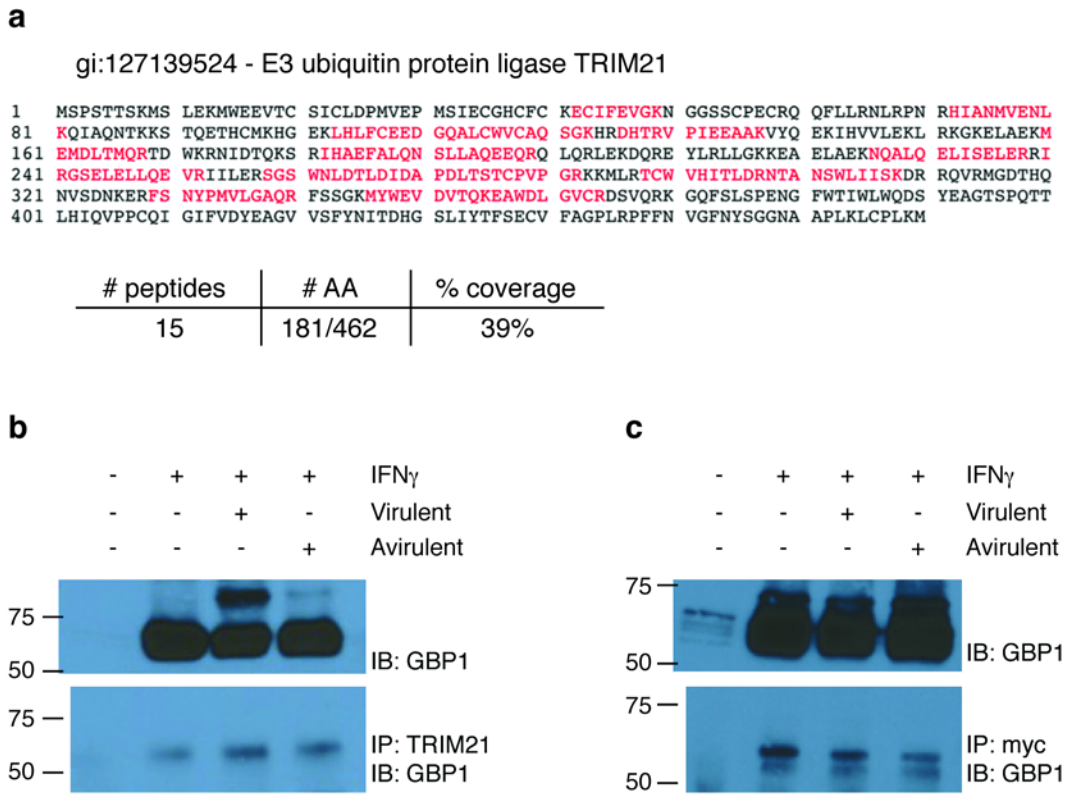

Figure 3.7: TRIM21 interacts with GBP1 in an IFNγ-dependent manner.
a) Immunoprecipitation and subsequent MS/MS analysis were performed on IFNγ-stimulatedRAW 264.7 cells overexpressing Flag-GBP1 and infected with avirulent *Toxoplasma*. Unique peptides recovered from TRIM21 are shown in red. The number of unique peptides recovered, the total number of unique amino acids (# AA), and the percentage of peptide coverage are indicated in the table. **b)** Immunoprecipitation of endogenous TRIM21 followed by immunoblot analysis of endogenous GBP1 in IFNγ-stimulated Raw 264.7 cells infected with virulent RH or avirulent Pru *Toxoplasma*. **c)** Immunoprecipitation of myc-tagged TRIM21 followed by immunoblot analysis for GBP1 was performed in IFNγ–stimulated Raw 264.7 cells overexpressing Flag-GBP1 and myc-TRIM21 and infected with virulent RH or avirulent Pru *Toxoplasma*. Cells uninduced or induced with 100 U/mL IFNγ were infected for 1h with virulent RH strain or avirulent Pru strain of *Toxoplasma* and lysed in 0.5% NP-40 lysis buffer. Proteins were then IP'ed with anti-TRIM21 (Santa-Cruz Biotechnology) or anti-myc antibody (Cell Signaling). 10 μg of input and 7.5 μL of IP were loaded on each gel. IBs representative of three independent experiments.

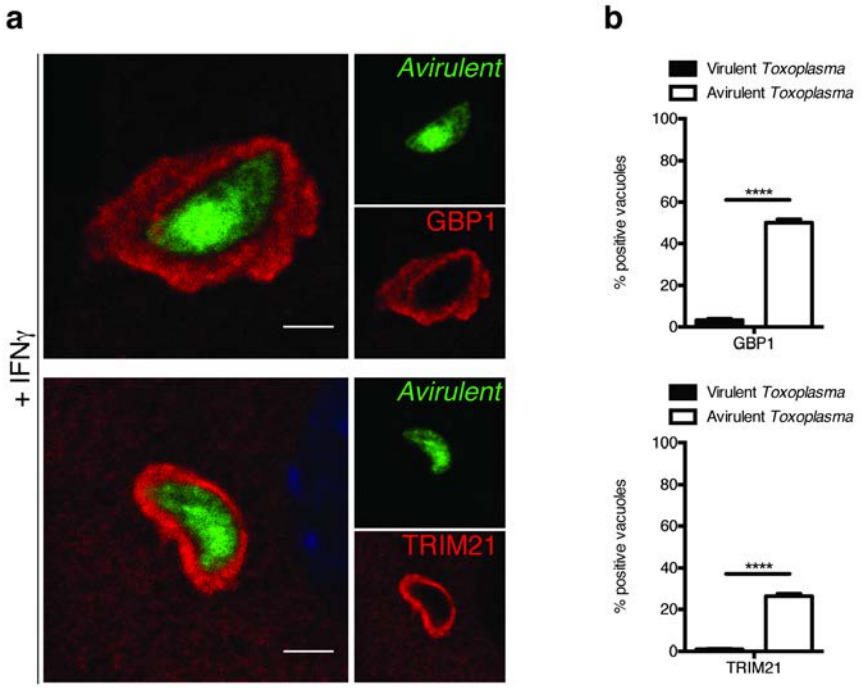

Figure 3.8: TRIM21 follows the recruitment pattern of GBP1 to avirulent *Toxoplasma* parasitophorous vacuoles.
a) Representative immunofluorescence confocal images of IFNγ-stimulated mouse embryonic fibroblasts infected with avirulent *Toxoplasma* expressing GFP and stained for endogenous GBP1 (top panel; home-made antibody) or TRIM21 (bottom panel; Santa-Cruz Biotechnology). Both GBP1 and TRIM21 individually recruit to avirulent *Toxoplasma* in IFNγ-stimulated cells. MEFs were induced with 100 U/mL IFNγ overnight and infected for 1h with avirulent *Toxoplasma*. Cells were fixed in 3% paraformaldehyde and stained with a goat anti-rabbit antibody or rabbit anti-goat antibody (Molecular Probes), respectively. Nuclei were stained with Hoechst. Scale bar is 2 μm. **b)** Quantification of GBP1 (top panel) and TRIM21 (bottom panel) localisation on the parasite-containing vacuoles. Both GBP1 and TRIM21 recruit to avirulent *Toxoplasma* in an IFNγ-dependent manner. For each staining, at least 100 vacuoles of invaded *Toxoplasma* were checked for GBP1 or TRIM21 recruitment. Data pooled from three independent experiments. Mean + SEM, **** $p<0.0001$, unpaired t-test.

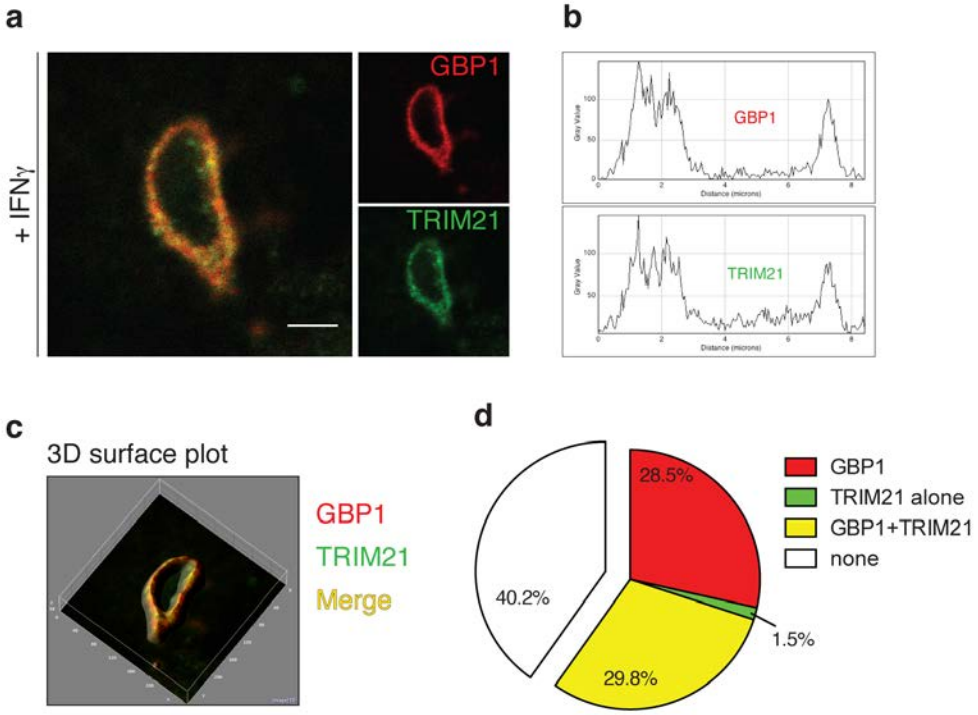

Figure 3.9: TRIM21 is preferentially recruited to GBP1-positive avirulent parasitophorous vacuoles of *Toxoplasma.*

a) Representative immunofluorescence confocal images of IFNγ-stimulated mouse embryonic fibroblasts infected with avirulent *Toxoplasma* and co-stained for GBP1 (home-made antibody) and TRIM21 (Santa-Cruz Biotechnology). GBP1 and TRIM21 colocalise to avirulent *Toxoplasma* vacuoles in IFNγ-stimulated cells. MEFs were induced with 100 U/mL IFNγ overnight and infected for 1h with avirulent *Toxoplasma*. Cells were fixed in 3% paraformaldehyde and stained with a goat anti-rabbit antibody and rabbit anti-goat antibody (Molecular Probes), respectively. Nuclei were stained with Hoechst. Scale bar is 2 µm. Plot profile analysis **b)** and 3D surface plot analysis **c)** show GBP1 and TRIM21 exhibit a similar localisation pattern and colocalise around the avirulent *Toxoplasma* vacuole. **d)** Quantification of GBP1 and TRIM21 co-recruitment to the parasite-containing vacuoles. TRIM21 mainly recruits to GBP1-positive avirulent *Toxoplasma* in an IFNγ-stimulated cells. For each staining, at least 100 vacuoles of invaded *Toxoplasma* were checked for GBP1 and/or TRIM21 recruitment. Data pooled from three independent experiments.

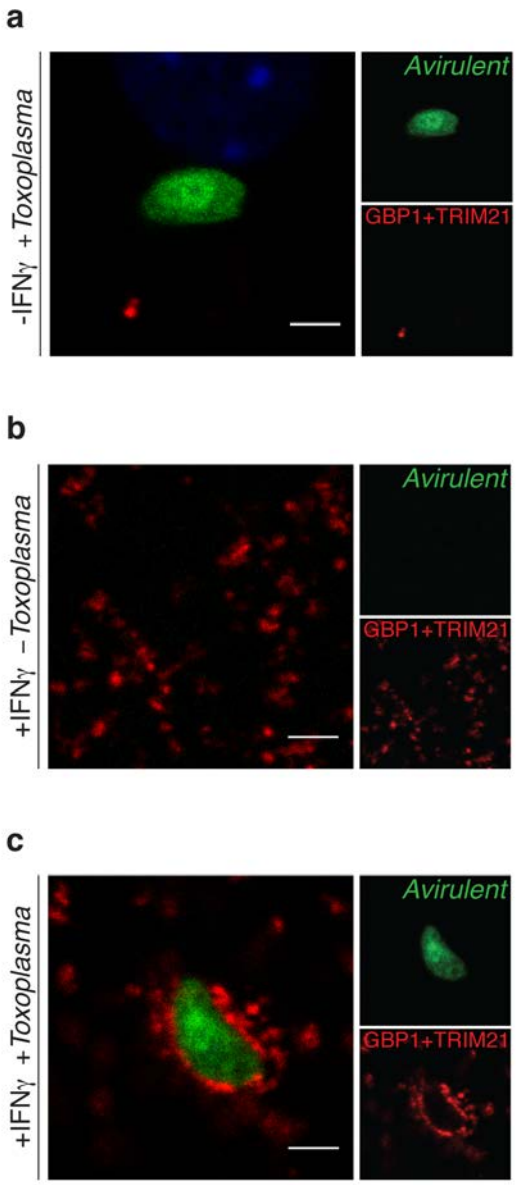

Figure 3.10: TRIM21 and GBP1 complex in the cytoplasm and recruit together to avirulent *Toxoplasma* vacuoles.
Confocal images of the IFNγ-dependent GBP1 and TRIM21 cytoplasmic (**a+b**) and vacuolar (**c**) complex. Proximity-ligation assay was performed in mouse embryonic fibroblasts with (**b, c**) or without (**a**) stimulation with 100 U/mL IFNγ. Cells were infected for 1h with avirulent *Toxoplasma* expressing GFP (**a, c**), fixed in 3% paraformaldehyde and stained with rabbit anti-GBP1 (home-made) and goat anti-TRIM21 (Santa-Cruz Biotechnology) before ligation and polymerisation of the secondary antibodies (Olink Bioscience). Red signals indicate positive proximity-ligation between GBP1 and TRIM21. Nuclei were stained with Hoechst. Scale bar is 2 μm. Representative images of two independent experiments.

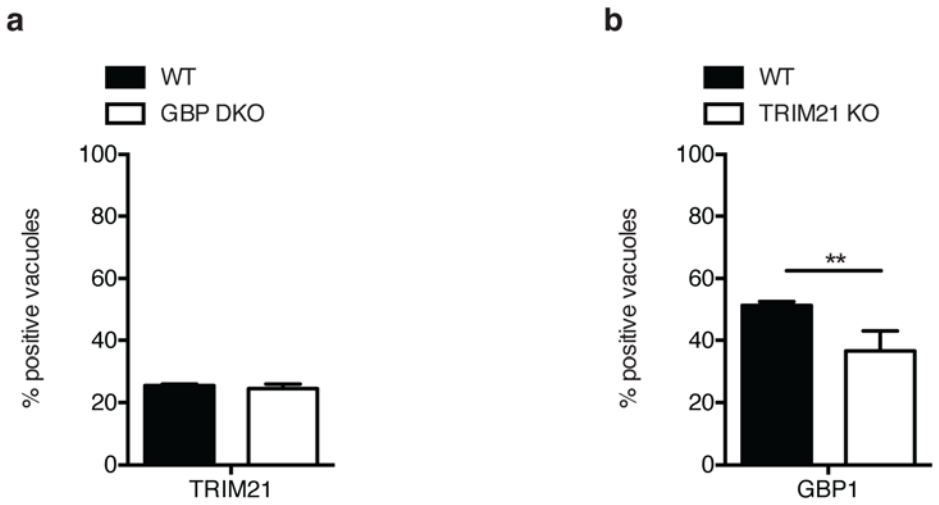

Figure 3.11: TRIM21 positively regulates GBP1 recruitment to avirulent *Toxoplasma*.
a) Quantification of TRIM21 localisation on the parasite-containing PVs in WT *vs*. GBP$^{chr3/chr5}$ (GBP DKO, lacking all GBPs) mouse embryonic fibroblasts. Cells were induced with 100 U/mL IFNγ overnight and infected for 1h with avirulent *Toxoplasma*. Data were pooled from two independent experiments. Mean + SEM, unpaired t-test. **b)** Quantification of GBP1 localisation on the parasite-containing vacuoles in WT *vs*. TRIM21 KO mouse embryonic fibroblasts. Cells were induced with 100 U/mL IFNγ overnight and infected for 1h with avirulent *Toxoplasma*. Data pooled from two independent experiments. Mean + SEM, ** p=0.0053, unpaired t-test.

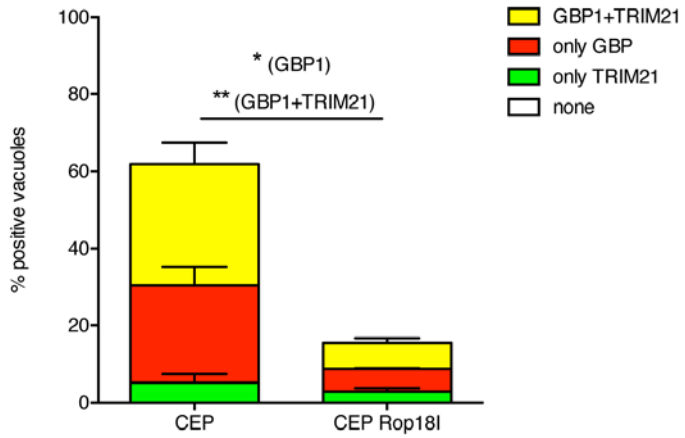

Figure 3.12: *Toxoplasma* virulence factors interfere with GBP1 and TRIM21 colocalisation at the vacuole.

Quantification of TRIM21- and/or GBP1-positive parasite-containing vacuoles in IFNγ-stimulated mouse embryonic fibroblasts infected with the canonical avirulent *Toxoplasma* type III (CEP) strain and avirulent *Toxoplasma* type III strain transgenic for the type I version of Rop18 (CEP Rop18I). The transgenic avirulent strain expressing the virulence factor Rop18I shows less GBP1 recruitment as well as less GBP1 and TRIM21 colocalisation compared to the parental strain. For each strain, at least 100 vacuoles of invaded *Toxoplasma* were checked for ubiquitin recruitment. Data pooled from two experiments. Mean + SEM, * $p<0.05$, ** $p<0.005$, 2-way ANOVA.

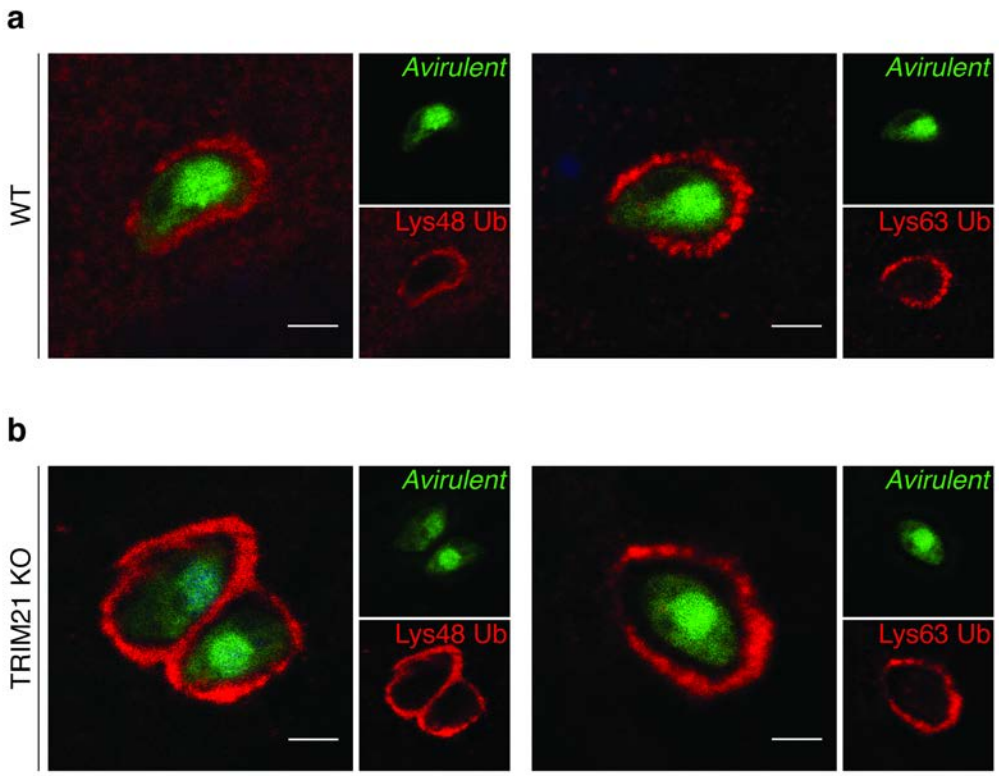

Figure 3.13: Lys48 and Lys63 ubiquitin decorate avirulent *Toxoplasma* vacuoles.
Representative immunofluorescence confocal images of IFNγ-stimulated WT (**a**) or TRIM21 KO (**b**) mouse embryonic fibroblasts infected with avirulent *Toxoplasma* expressing GFP and stained for Lys48 ubiquitin (left panel; Merck Millipore) or Lys63 ubiquitin (right panel; Merck Millipore). Lys48 ubiquitin and Lys63 ubiquitin decorate avirulent *Toxoplasma* vacuoles in IFNγ-stimulated cells. MEFs were induced with 100 U/mL IFNγ overnight and infected for 1h with avirulent *Toxoplasma*. Cells were fixed in 3% paraformaldehyde and stained with a goat anti-rabbit antibody (Molecular Probes). Nuclei were stained with Hoechst. Scale bar is 2 μm.

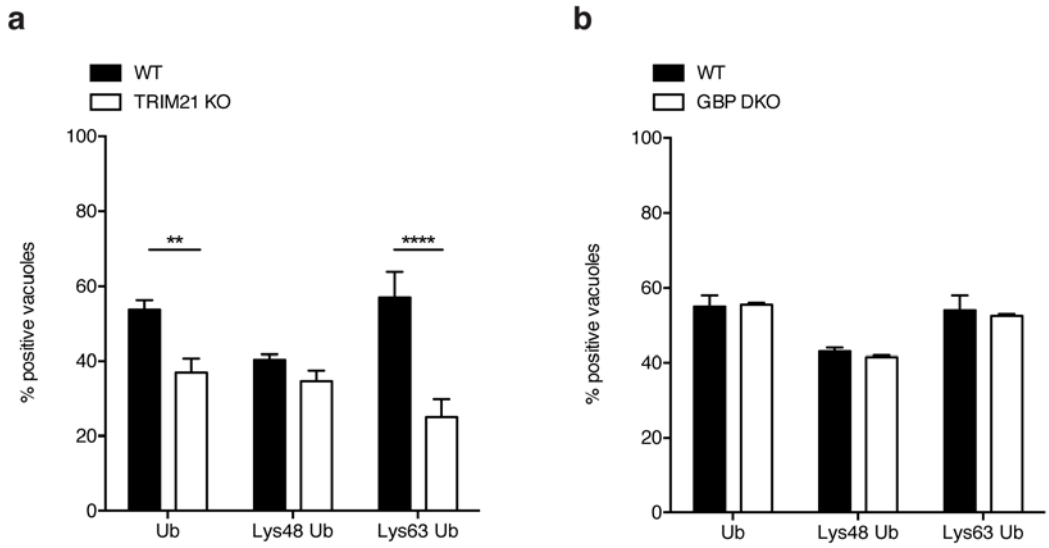

Figure 3.14: Lys63-linked ubiquitination around avirulent *Toxoplasma* vacuoles is significantly mediated by TRIM21.
a) Quantification of ubiquitin- (Ub), Lys63 ubiquitin- and Lys63 ubiquitin-positive parasite-containing vacuoles in IFNγ-stimulated WT *vs*. TRIM21 KO mouse embryonic fibroblasts infected with avirulent *Toxoplasma*. TRIM21 deficiency induces a decrease in total ubiquitin and Lys63 ubiquitin accumulation at avirulent *Toxoplasma* vacuoles in IFNγ-stimulated cells. Data were pooled from three independent experiments. Mean + SEM, ** $p<0.005$, **** $p<0.0001$, 2-way ANOVA. **b)** Quantification of ubiquitin-, Lys63 ubiquitin- and Lys63 ubiquitin-positive avirulent *Toxoplasma* vacuoles in IFNγ-stimulated WT *vs*. $GBP^{chr3/chr5}$ (GBP DKO, cells lacking all GBPs) mouse embryonic fibroblasts infected with avirulent *Toxoplasma*. Deletion of the GBPs does not influence the accumulation of ubiquitin at avirulent *Toxoplasma* vacuoles. Data pooled from two independent experiments. Mean + SEM, 2-way ANOVA.

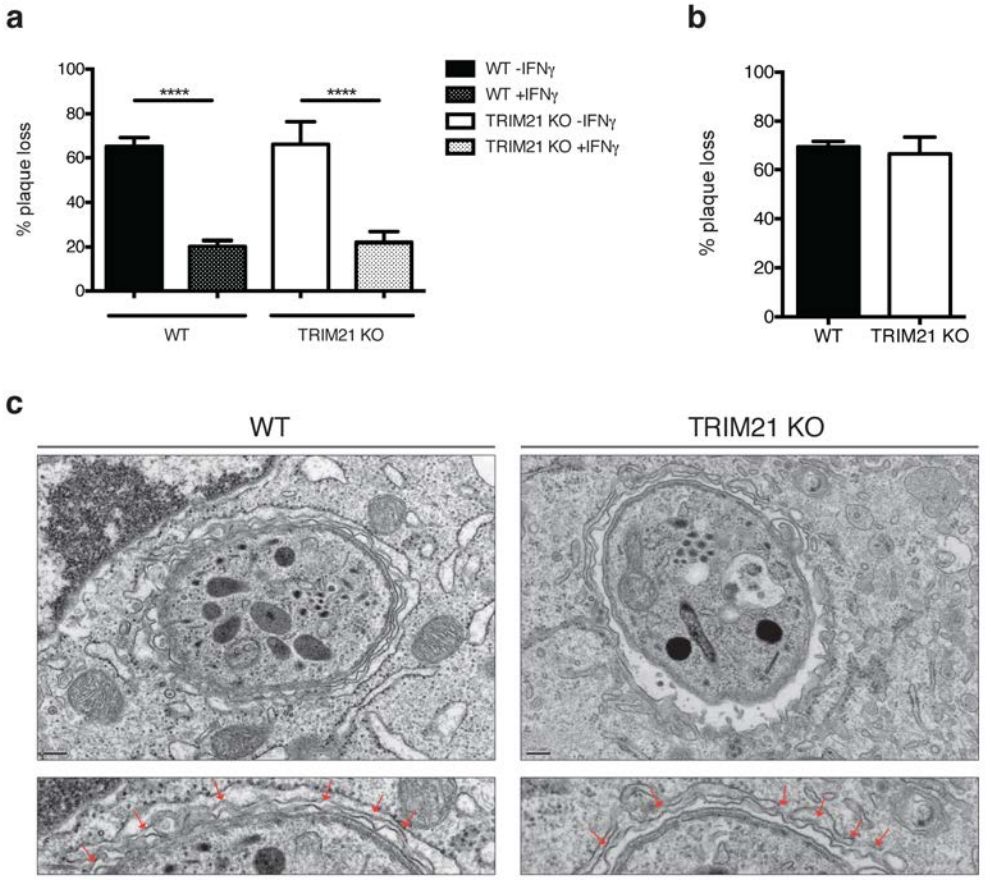

Figure 3.15: TRIM21 does not mediate cell-autonomous control of *Toxoplasma* infection *in vitro*. **a)** IFNγ-induced parasite killing was assessed by quantification of the number of avirulent *Toxoplasma*-forming plaques after 3 days on IFNγ-stimulated or unstimulated WT *vs*. TRIM21 KO mouse embryonic fibroblasts. IFNγ mediates the killing of avirulent *Toxoplasma* in both WT and TRIM21 KO cells. Data pooled from three independent experiments. Mean +SEM, **** $p<0.0001$, 2-way ANOVA. **b)** Quantification of the number of avirulent *Toxoplasma*-forming plaques after 3 days on IFNγ-stimulated WT *vs*. TRIM21 KO mouse embryonic fibroblasts compared to unstimulated cells. IFNγ mediates the killing of avirulent *Toxoplasma* in both WT and TRIM21 KO cells. Data pooled from three independent experiments. Mean +SEM, unpaired t-test. **c)** Ultrastructural analysis of avirulent *Toxoplasma* PVM in IFNγ-stimulated WT *vs*. TRIM21 KO mouse embryonic fibroblasts. Cells were induced with 100 U/mL IFNγ overnight and infected for 1h with avirulent *Toxoplasma* before analysis by electron microscopy. The lower images are enlarged views from the upper images. Red arrows indicate blebbing and disruption of the parasitophorous vacuole. Deletion of TRIM21 does not impair the disruption of *Toxoplasma* parasitophorous vacuole in IFNγ-induced cells. Scale bar is 200 nm. Representative images of two independent experiments. Images taken by Liz Hirst.

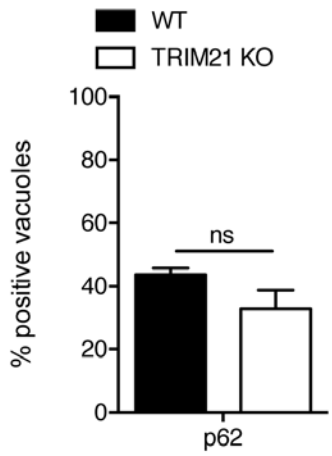

Figure 3.16: TRIM21 does not mediate the recruitment of the autophagy adaptor p62 to avirulent *Toxoplasma*.
The graph shows quantification of the localisation of p62 on the parasite-containing vacuoles in IFNγ-stimulated mouse embryonic fibroblasts. Deletion of TRIM21 does not impair p62 recruitment to avirulent *Toxoplasma* vacuoles in IFNγ-stimulated cells. MEFs were induced with 100 U/mL IFNγ overnight and infected for 1h with avirulent *Toxoplasma*. Data pooled from two independent experiments. Mean + SEM, unpaired t-test.

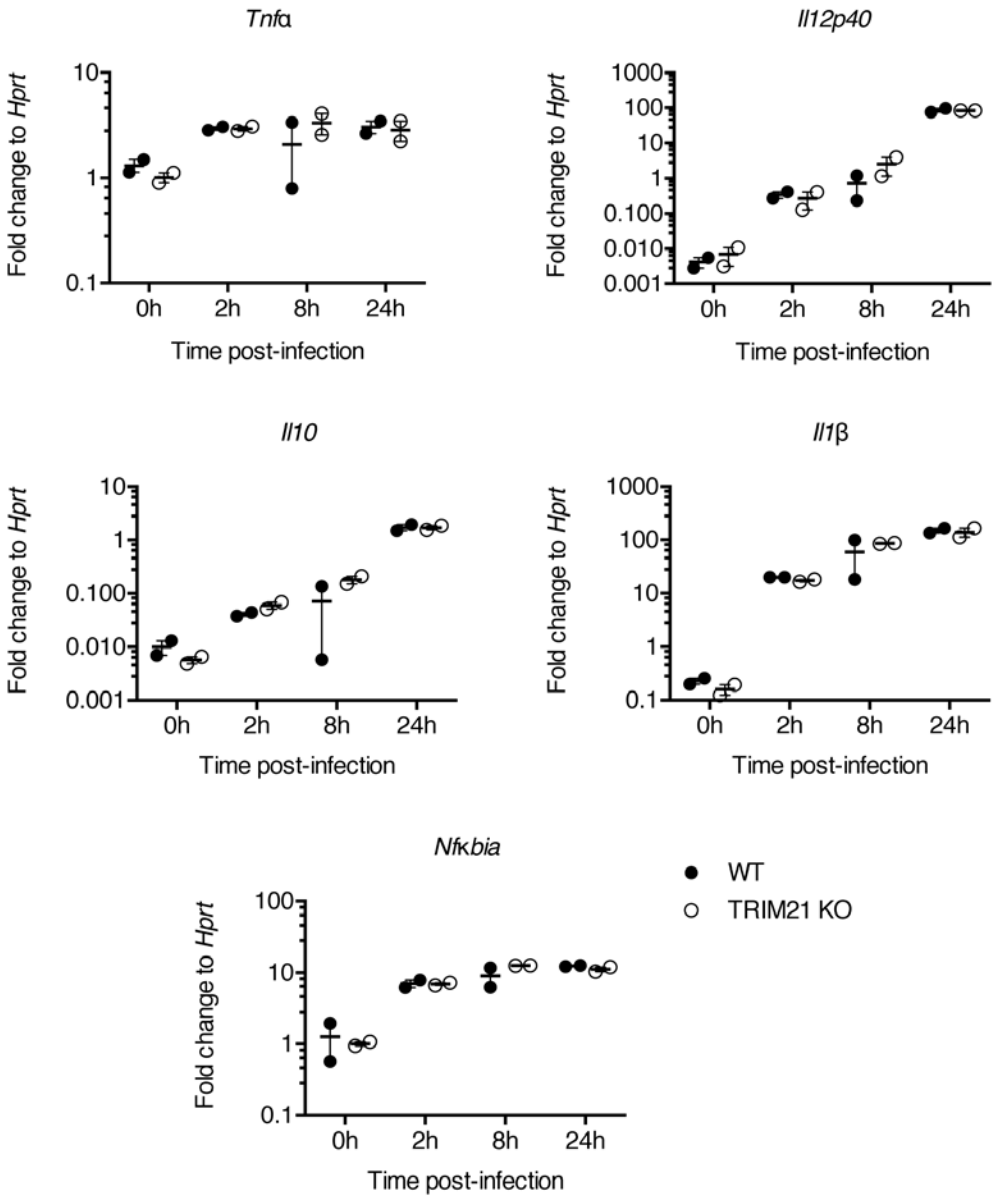

Figure 3.17: TRIM21-deficient bone marrow macrophages exhibit equal mRNA levels of selected inflammatory cytokines and transcription factor following *Toxoplasma* infection.
Wild-type (WT) or TRIM21 KO bone marrow-derived macrophages were induced with 100 U/mL IFNγ overnight and infected with avirulent *Toxoplasma* for several time points. Cells were then lysed in tri-reagent and RNA was purified and reverse-transcribed to cDNA as described in the Experimental Procedure. The level of expression of the depicted genes was determined by qRT-PCR relative to the expression of the housekeeping gene *Hprt*. At all times post-infection, TRIM21-deficient cells do not exhibit differential mRNA expression of inflammatory cytokines or transcription factor. Data shown are from one experiment. Mean + SEM.

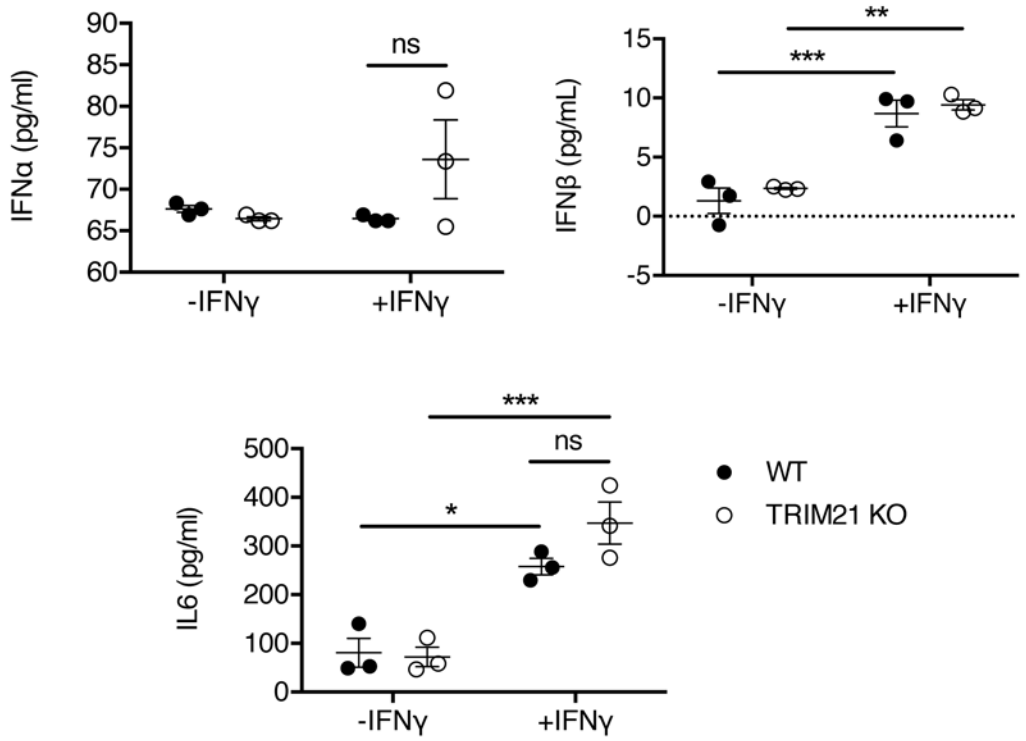

Figure 3.18: TRIM21-deficient bone marrow macrophages exhibit equal protein levels of selected inflammatory cytokines following *Toxoplasma* infection.
Wild-type (WT) or TRIM21 KO bone marrow-derived macrophages were left uninduced or stimulated with 100 U/mL IFNγ overnight and infected with avirulent *Toxoplasma* for 24h. Supernatants were collected and analysed by enzyme-linked immunosorbent assay (ELISA) as described in the Experimental Procedure. Graphs show the level of expression of the depicted proteins. TRIM21-deficient cells do not exhibit differential protein expression of inflammatory cytokines. Data representative of two independent experiments. Mean + SEM, * $p<0.05$, ** $p<0.01$, *** $p<0.005$, 2-way ANOVA.

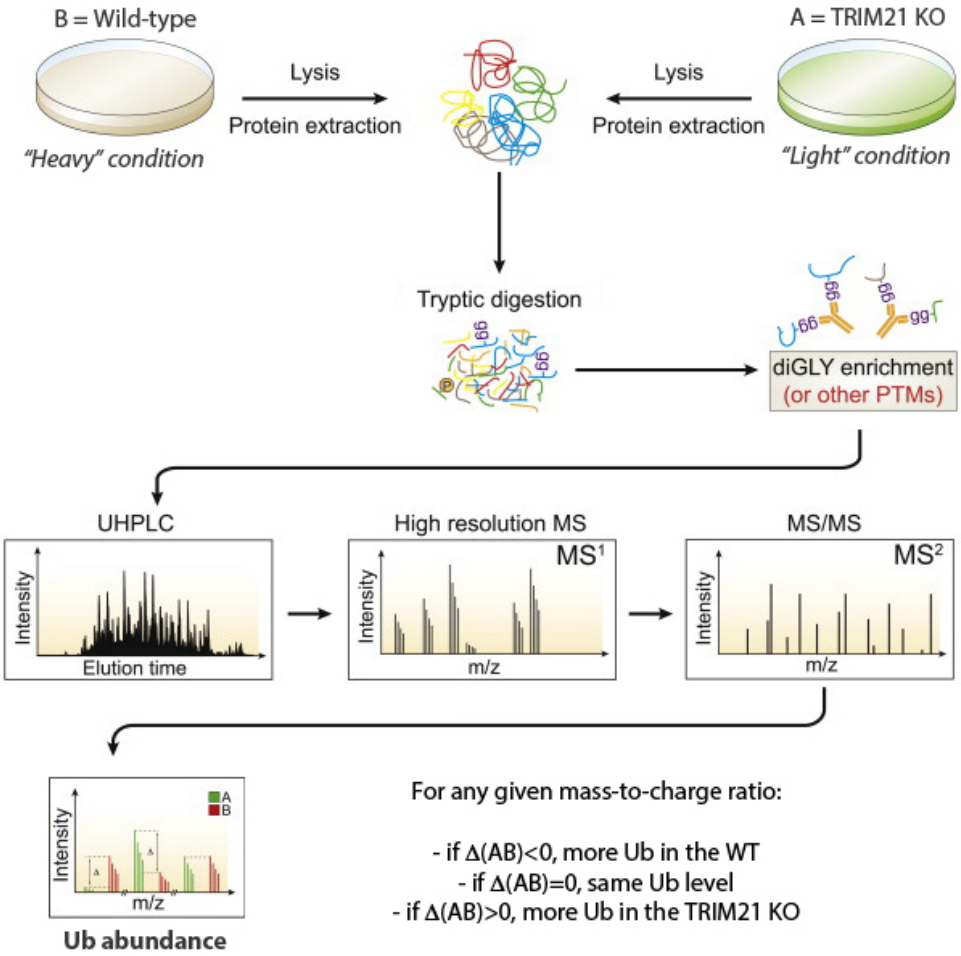

Figure 3.19: Workflow for detection and analysis of ubiquitinated proteins by SILAC.
Schematic representation of the experimental steps performed for the identification of putative TRIM21 ubiquitination substrates. Wildtype and TRIM21-deficient mouse embryonics fibroblasts were cultivated in "heavy" (^{13}C-arginine, ^{13}C-lysine and unlabelled proline) or "light" (^{12}C-arginine, ^{12}C-lysine and unlabelled proline) medium for a minimum of 4-6 doublings to allow for a good incorporation of the heavy or light isotopes. Cells were induced for 16h with 100 U/mL of IFNγ and infected with avirulent *Toxoplasma* for 1h. Cells were mixed at a 1:1 ratio, proteins were extracted and submitted to digestion with trypsin. Ubiquitinated peptides harbouring diGLY sites were immunoprecipitated with an anti-diGLY antibody, and enriched ubiquitinated peptides were analysed by liquid chromatography coupled with mass spectrometry. UHPLC: ultra-high performance liquid chromatography; MS: mass spectrometry; m/z: mass-to-charge ration; Ub: ubiquitin. Adapted and reprinted with permission from (Ordureau et al., 2015).

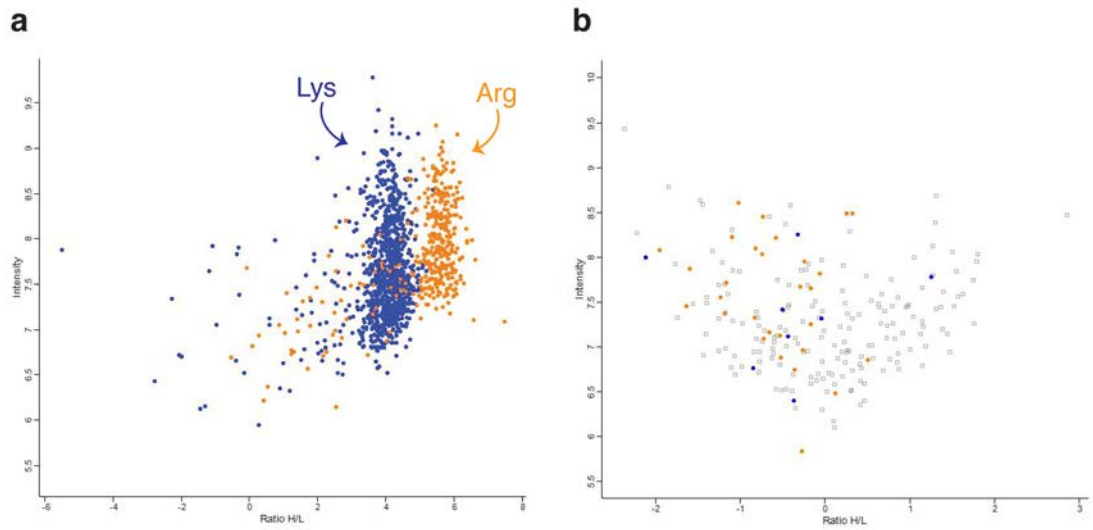

Figure 3.20: Assessment of the heavy isotope integration and arginine-to-proline conversion in cells for stable isotope labelling with amino acids in cell culture.
Wild-type mouse embryonic fibroblasts were cultivated in "heavy" (^{13}C-arginine, ^{13}C-lysine and unlabelled proline) and "light" (^{12}C-arginine, ^{12}C-lysine and unlabelled proline) for a minimum of 4-6 doublings to allow for a good incorporation of the heavy or light isotopes. **a**) Assessment of sufficient incorporation was performed using the $\log_2$ heavy/light (H/L) ratio and shows a lysine incorporation of 93.75% (as $\log_2(16)=4$ and $1/16=0.0625$) and an arginine incorporation of 98.44% (as $\log_2(64)=6$ and $1/64=0.0156$), indicating the cells had doubled enough to enable for a successful incorporation. **b**) Assessment of arginine-to-proline conversion was performed using the $\log_2$ heavy/light (H/L) ratio and shows no significant shift of the heavy-labelled arginine signal, indicating no major arginine-to-proline conversion.

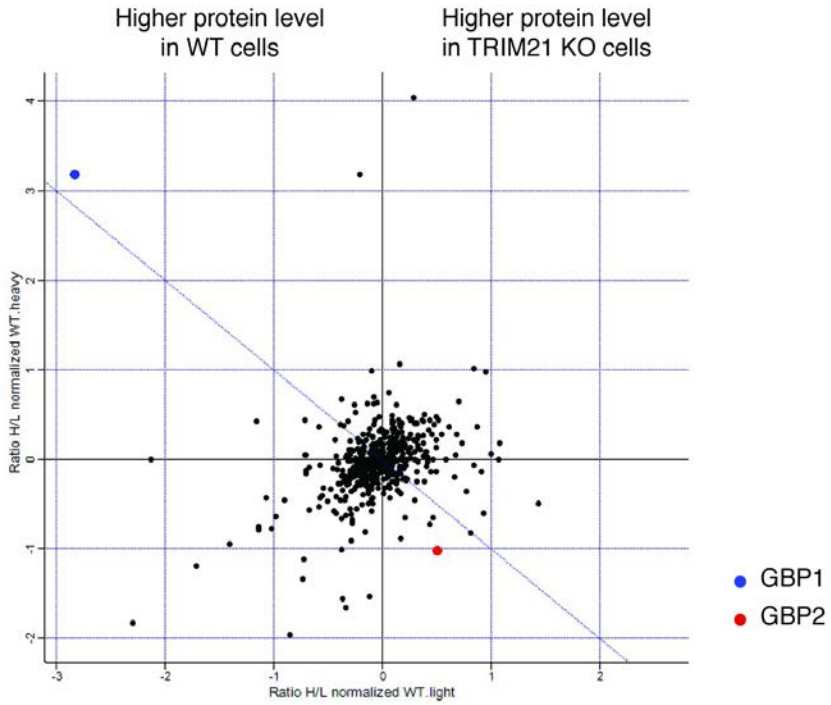

Figure 3.21: GBP1 and GBP2 exhibit differential protein levels in TRIM21-deficient mouse embryonic fibroblasts.
Wild-type and TRIM21 KO mouse embryonic fibroblasts were cultivated in "heavy" (^{13}C-arginine, ^{13}C-lysine and unlabelled proline) or "light" (^{12}C-arginine, ^{12}C-lysine and unlabelled proline) medium, induced for 16h with IFNγ and infected for 1h with avirulent *Toxoplasma*. A small portion of cell lysate was used for gross protein quantification before SILAC analysis. The graph shows all retrieved proteins from the quantification analysis. The thin blue diagonal line indicates the close correlation between forward (WT heavy/KO light) and reverse (WT light/KO heavy) samples. GBP1 (blue dot) is present at a higher protein level in WT cells, whereas GBP2 (red dot) is present at a higher protein level in TRIM21 KO cells, with a good protein quantification correlation between forward and reverse data.

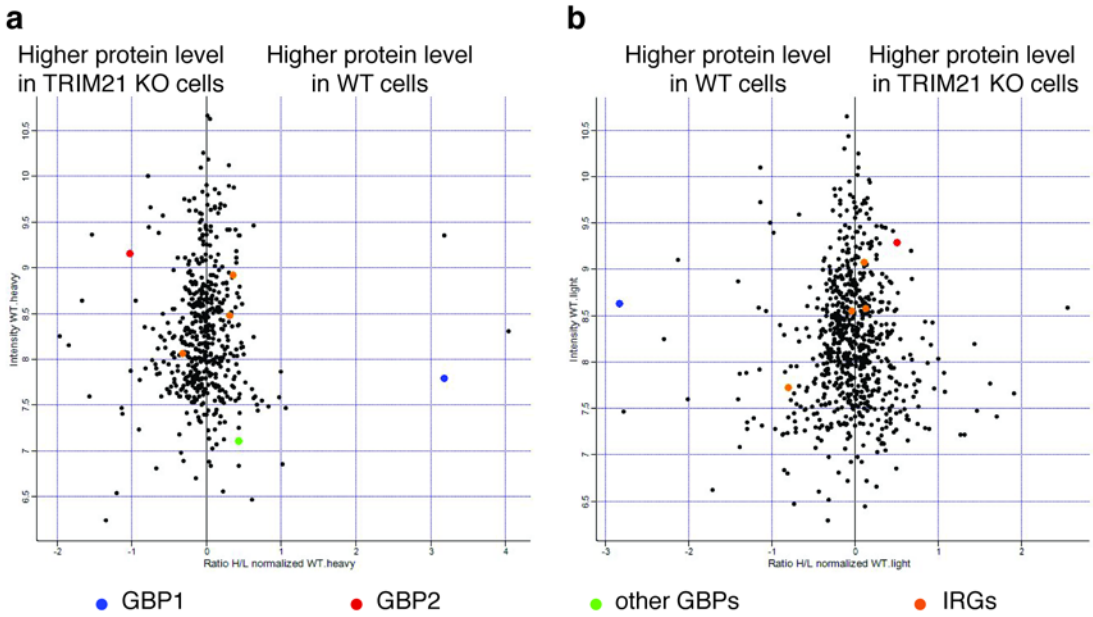

Figure 3.22: Quantification of the GBPs and IRGs protein levels in wild-type *v*ersus TRIM21-deficient mouse embryonic fibroblasts.
Wild-type and TRIM21 KO mouse embryonic fibroblasts were cultivated in "heavy" (^{13}C-arginine, ^{13}C-lysine and unlabelled proline) or "light" (^{12}C-arginine, ^{12}C-lysine and unlabelled proline) medium, induced for 16h with IFNγ and infected for 1h with avirulent *Toxoplasma*. A small portion of cell lysate was used for gross protein quantification before SILAC analysis in both the forward (**a**, WT heavy/KO light) and reverse (**b**, WT light/KO heavy) experiment. The graphs show all retrieved proteins from the quantification analysis. GBP1 (blue dot) is present at a higher protein level in WT cells in both forward (**a**) and reverse (**b**) samples, whereas GBP2 (red dot) is present at a higher protein level in TRIM21 KO cells in both forward (**a**) and reverse (**b**) samples. Some immunity-related GTPases (IRGs, orange dots) as well as one other guanylate-binding protein, GBP4 (green dot) were quantified with no major protein level differences.

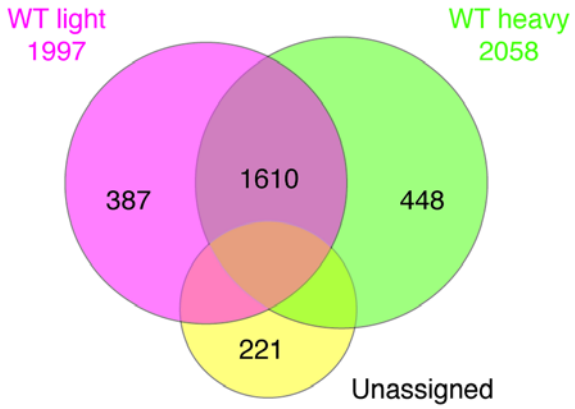

Figure 3.23: Venn diagram of the Gly-Gly-containing peptides retrieved by LC-MS/MS.
Cell lysates of wild-type and TRIM21 KO mouse embryonic fibroblasts cultivated in "heavy" (^{13}C-arginine, ^{13}C-lysine and unlabelled proline) or "light" (^{12}C-arginine, ^{12}C-lysine and unlabelled proline) medium, induced for 16h with IFNγ and infected for 1h with avirulent *Toxoplasma*, were digested with trypsin to reveal Gly-Gly (diGLY) sites remnant on digested ubiquitinated proteins. Enrichment of the diGLY sites was performed by immunoprecipitation with an anti-diGLY antibody, and diGLY-containing peptides were analysed by liquid chromatography coupled to mass spectrometry (LC-MS/MS). More diGLY sites were obtained from the WT heavy sample (2058 sites) than from the WT light sample (1997 sites), and a total of 1610 diGLY sites were found in both the forward and the reverse sample.

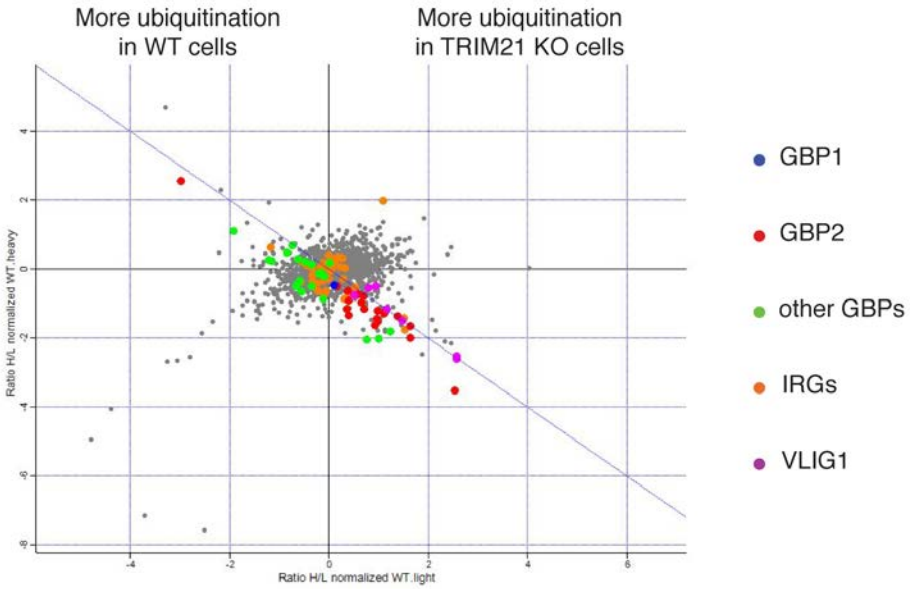

Figure 3.24: Forward and reverse SILAC experiments show consistent ubiquitination of the members of the family of IFNγ-induced large GTPases.
Cell lysates of wild-type and TRIM21 KO mouse embryonic fibroblasts cultivated in "heavy" (^{13}C-arginine, ^{13}C-lysine and unlabelled proline) or "light" (^{12}C-arginine, ^{12}C-lysine and unlabelled proline) medium, induced for 16h with IFNγ and infected for 1h with avirulent *Toxoplasma*, were digested with trypsin to reveal Gly-Gly (diGLY) sites remnant on digested ubiquitinated proteins. Enrichment of the diGLY sites was performed by immunoprecipitation with an anti-diGLY antibody, and diGLY-containing peptides were analysed by liquid chromatography coupled to mass spectrometry (LC-MS/MS). The graph shows all retrieved diGLY sites from both forward (WT heavy/KO light) and reverse (WT light/KO heavy) samples. The thin blue diagonal line indicates the close correlation between forward and reverse samples. GBP1 (blue dot), GBP2 (red dots), other GBPs (green dots), IRGs (orange dots) and VLIG1 (pink dots) all retrieved diGLY sites indicating of ubiquitinated lysines, which correlate well between the two samples. GBP2 and VLIG1 have more ubiquitinated lysines in TRIM21 KO cells, whereas other GBPs tend to have less ubiquitinated lysines in TRIM21 KO cells.

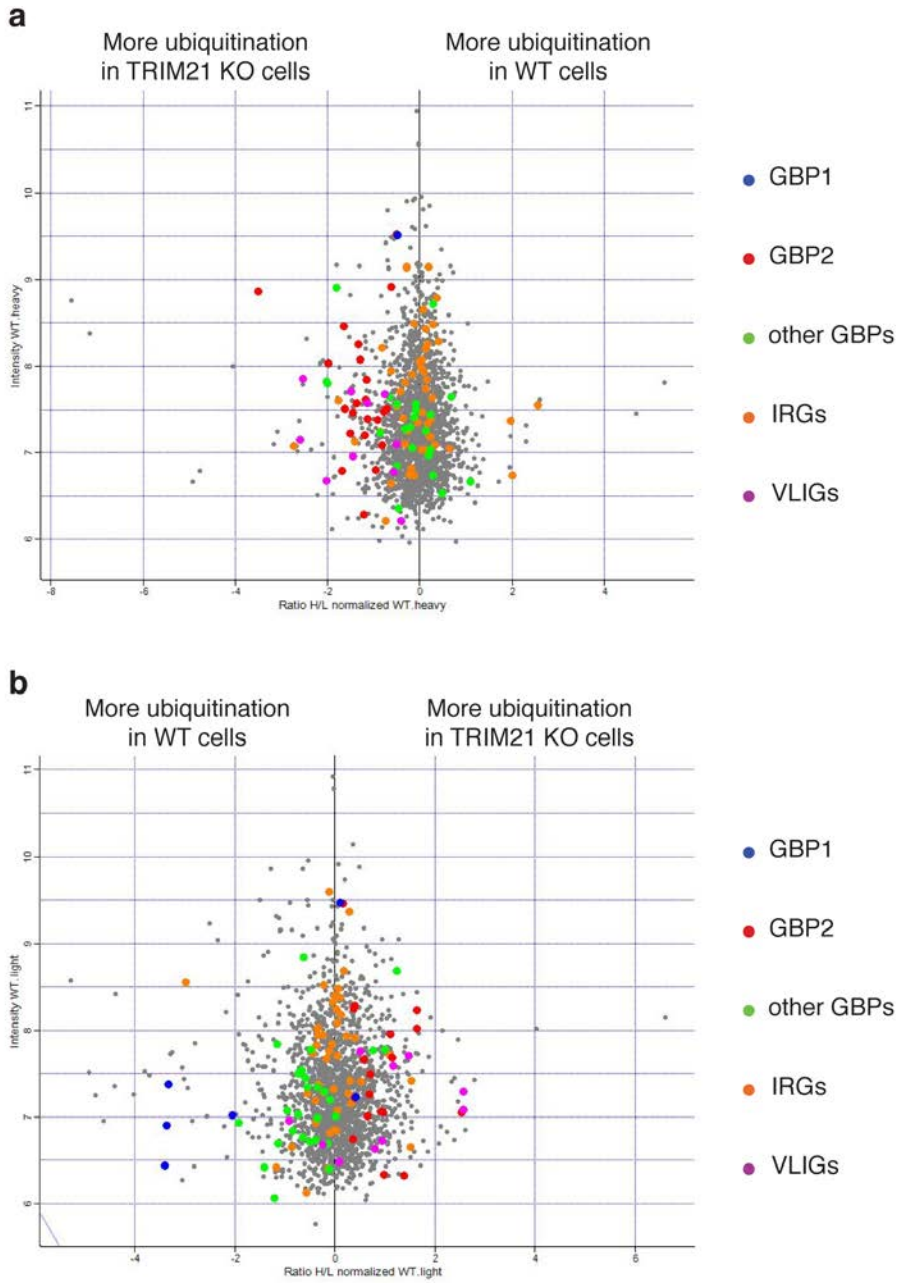

Figure 3.25: Members of the family of IFNγ-induced large GTPases exhibit differential ubiquitination status in TRIM21-deficient cells.
Cell lysates of wild-type and TRIM21 KO mouse embryonic fibroblasts cultivated in "heavy" (^{13}C-arginine, ^{13}C-lysine and unlabelled proline) or "light" (^{12}C-arginine, ^{12}C-lysine and unlabelled proline) medium, induced for 16h with IFNγ and infected for 1h with avirulent *Toxoplasma*, were digested with trypsin to reveal Gly-Gly (diGLY) sites remnant on digested ubiquitinated proteins. Enrichment of the diGLY sites was performed by immunoprecipitation with an anti-diGLY antibody, and diGLY-containing peptides were analysed by liquid chromatography coupled to mass spectrometry (LC-MS/MS). The graphs show all retrieved diGLY sites from both forward (**a**, WT heavy/KO light) and reverse (**b**, WT light/KO heavy) samples. GBP2 (red dots) and VLIG1 (pink dots) have more ubiquitinated lysines in TRIM21 KO cells, as indicated in both forward (**a**) and reverse (**b**) samples. GBP1 (blue dots) shows less ubiquitinated lysines in TRIM21 KO cells as indicated in the reverse (**b**) sample. The ubiquitinated lysines on the other GBPs (green dots) and on the IRGs (orange dots) appear more consistent between WT and TRIM21 KO cells.

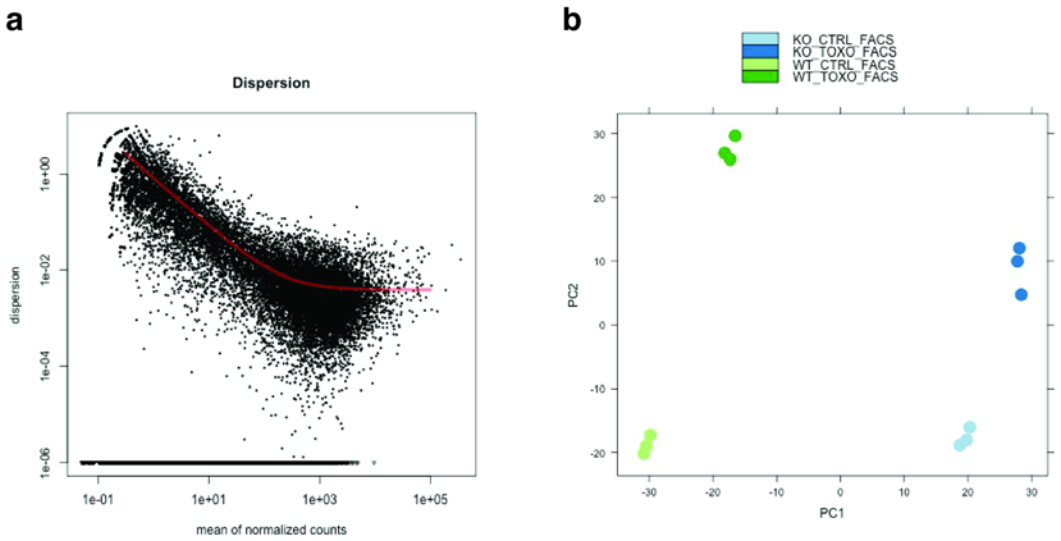

Figure 3.26: Quality control of the RNAseq raw data generated from wild-type and TRIM21-deficient mouse embryonic fibroblasts with or without infection with avirulent *Toxoplasma*.
Wild-type and TRIM21-deficient cells were stimulated for 16h with 100 U/mL IFNγ and infected or not with avirulent *Toxoplasma* for 1h. 100 000 live, uninfected or *Toxoplasma*-infected cells were sorted by flow cytometry and RNA was extracted as described in the Experimental procedure section. Each condition performed in triplicates. **a**) The graph shows the empirical (black dots) and fitted (red line) dispersion values plotted against the mean of the normalised counts. The dispersion of the nucleotide sequence counts obtained cluster around the red line and indicate a good coverage. **b**) The graph shows the principal component analysis (PCA) of the gene expression profiles in the 4 conditons tested: WT uninfected (light green), *Toxoplasma*-infected WT (dark green), TRIM21 KO uninfected (light blue) and *Toxoplasma*-infected TRIM21 KO (dark blue). PCA indicates triplicates within each condition cluster nicely together and all 4 conditions tested present different gene expression profiles. Graphs created by Dr. Helena Ahlfors.

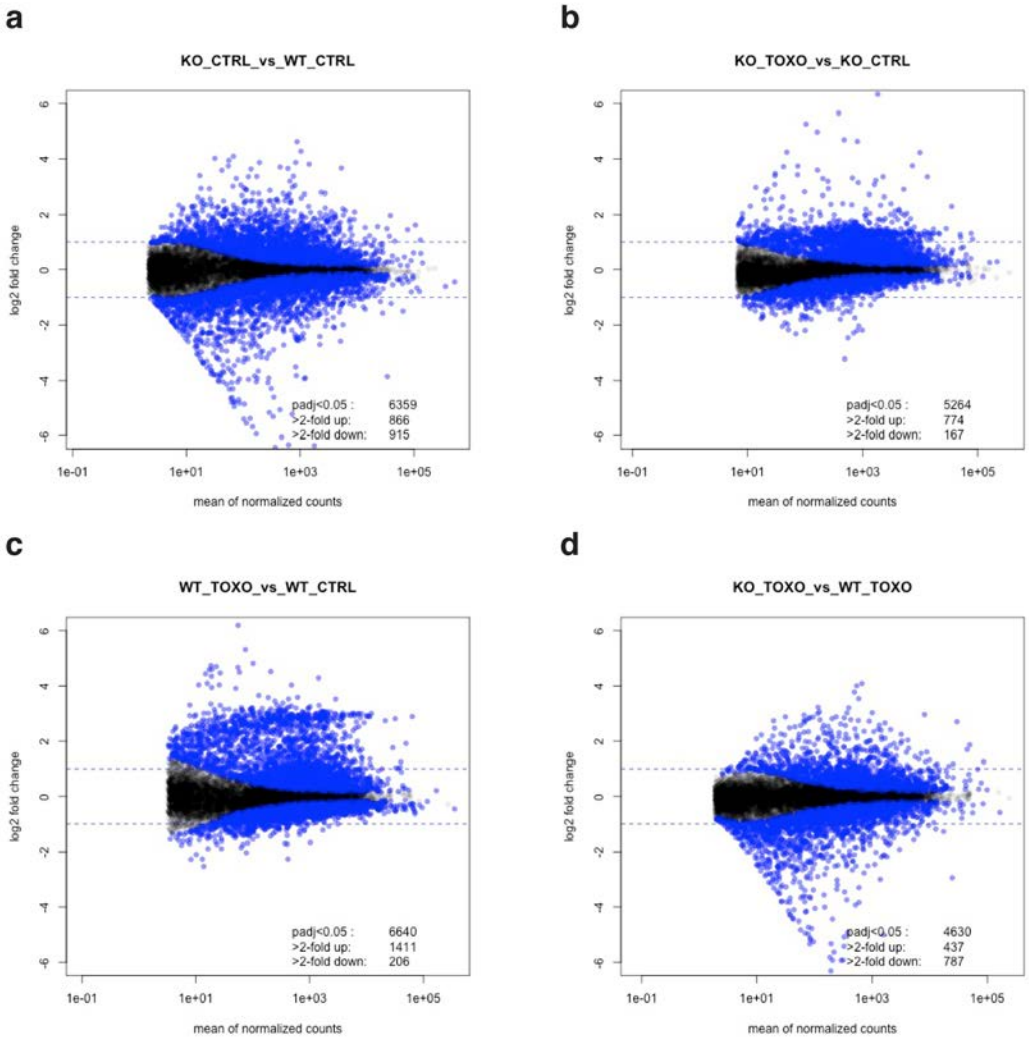

Figure 3.27: Comparison of the differential gene expression across the four RNAseq samples generated.
The graphs are MA plots that show the scatter plots of the fold change (log_2) gene expression between two conditions against the mean of the normalised counts. The blue dots represent the genes differentially expressed with an adjusted p-value of 0.05. The two dotted blue lines represent the limits to define the genes whose expression has a fold change greater than 2 between the conditions compared. The 4 comparisons are: uninfected TRIM21 KO against uninfected wild-type (**a**), *Toxoplasma*-infected TRIM21 KO against uninfected TRIM21 KO (**b**), *Toxoplasma*-infected wild-type against uninfected wild-type (**c**) and *Toxoplasma*-infected TRIM21 KO against *Toxoplasma*-infected wild-type (**d**). Graphs created by Dr. Helena Ahlfors.

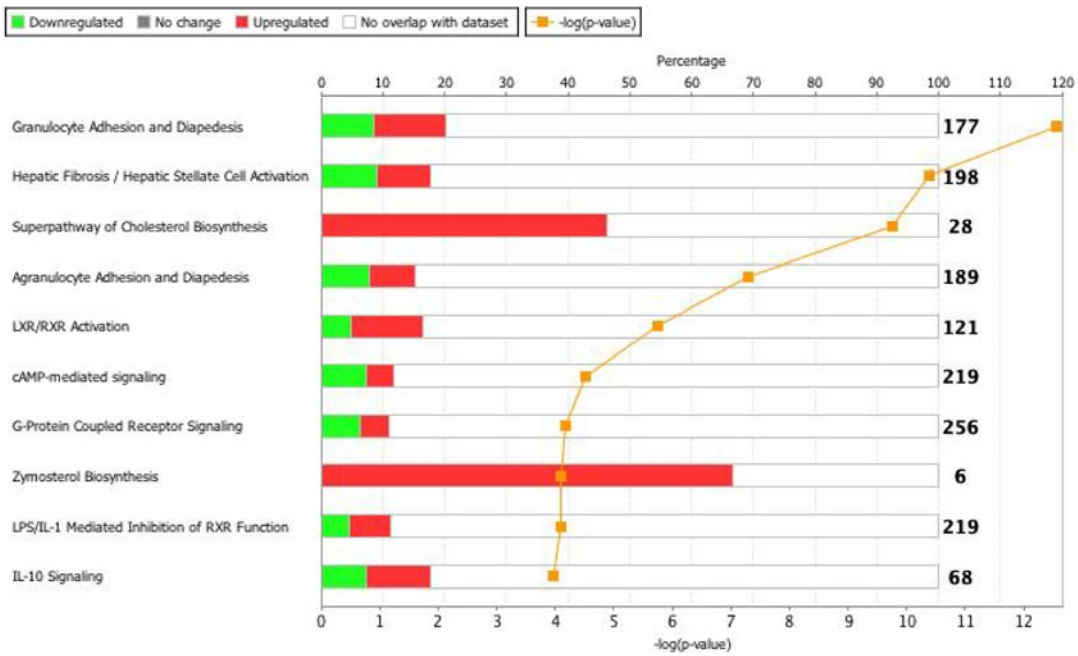

Figure 3.28: Cholesterol biosynthesis is substantially upregulated in *Toxoplasma*-infected TRIM21-deficient mouse embryonic fibroblasts.
The graph represents the Ingenuity pathway analysis of differentially expressed genes in avirulent *Toxoplasma*-infected TRIM21-deficient mouse embryonic fibroblasts compared to infected wild-type controls. The top 10 biological pathways associated with differentially expressed genes between *Toxoplasma*-infected TRIM21 KO cells and wild-type cells are shown. Top axis represents the percentage overlap between input genes and genes in the pathway. Bottom axis denotes Benjamini-Hochberg corrected –log(p-value), represented by the gold line, for pathway association. Upregulated genes are coloured in red, downregulated genes are coloured in green. Among the top 10 biological pathways associated with differentially expressed genes, 2 are involved in the biosynthesis of cholesterol or its zymosterol precursor. Graph created by Dr. Helena Ahlfors.

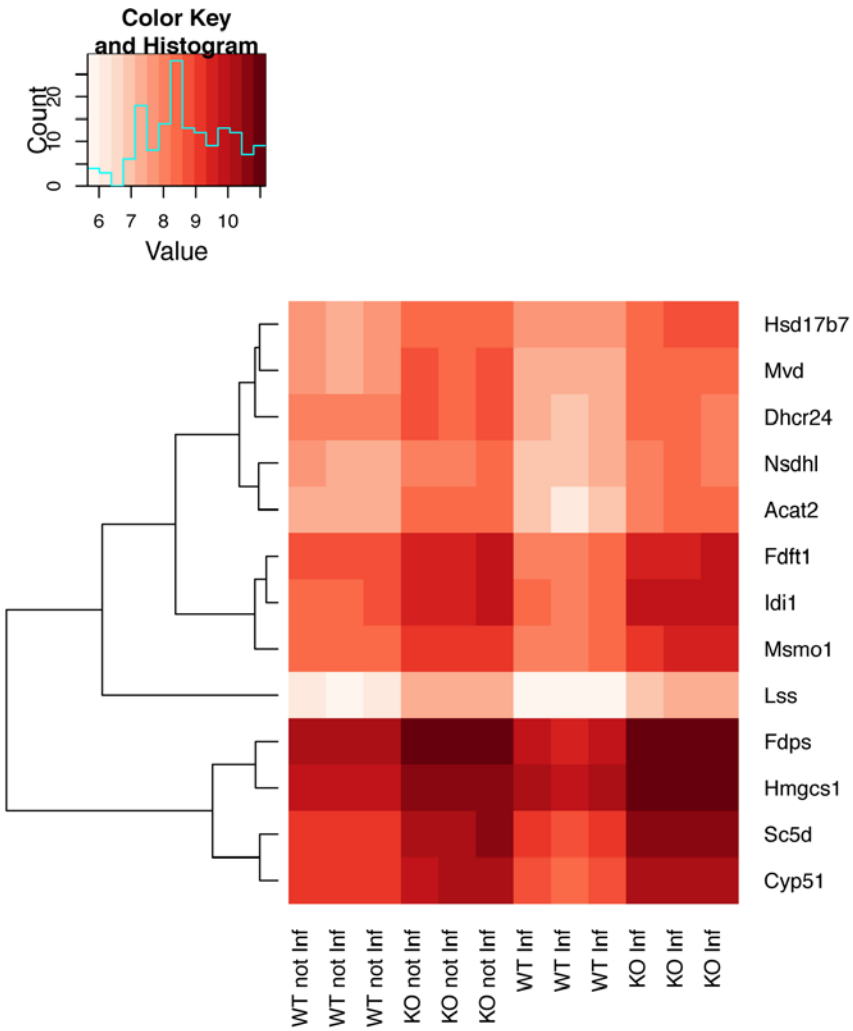

Figure 3.29: Differential expression of genes involved in cholesterol biosynthesis in *Toxoplasma*-infected TRIM21-deficient and wild-type mouse embryonic fibroblasts.
Heat map shows hierarchical clustering of the 13 genes involved in the biosynthesis of cholesterol identified as differentially expressed in TRIM21-deficient mouse embryonic fibroblasts infected with avirulent *Toxoplasma*. Data show the log2 value of each triplicate within the 4 conditions tested, from left to right: uninfected TRIM21 KO, *Toxoplasma*-infected WT and *Toxoplasma*-infected TRIM21 KO. Downregulated genes are coloured in white, upregulated genes are coloured in red. Colour range denotes intensity of expression. Genes involved in cholesterol biosynthesis are upregulated at the steady state in uninfected TRIM21-deficient cells compared to uninfected wild-type controls, and this upregulation is accentuated following infection with avirulent *Toxoplasma*. Heat map created by Dr. Helena Ahlfors.

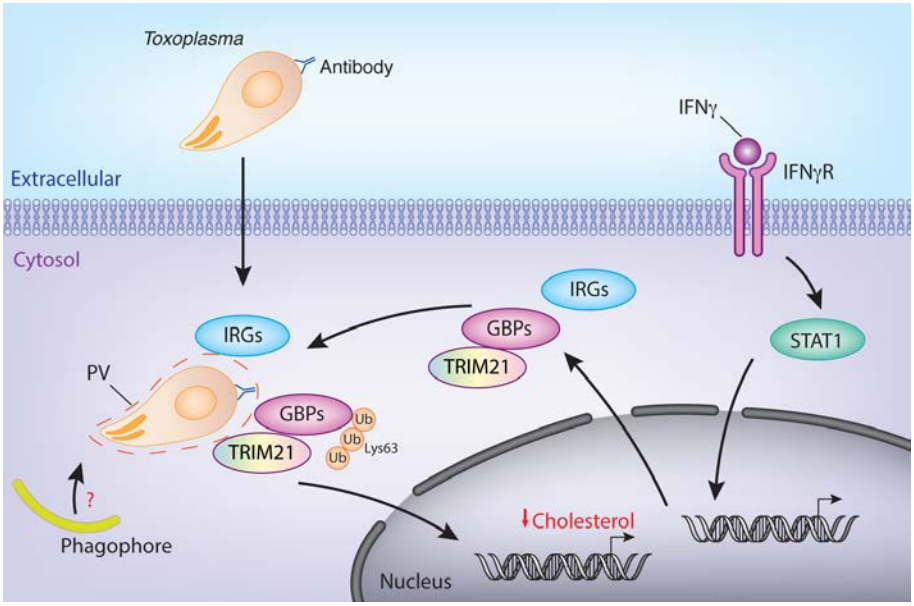

Figure 3.30: TRIM21 regulates Lys63 ubiquitination and recruitment of GBP1 to avirulent *Toxoplasma* vacuoles.

Following infection with *Toxoplasma*, interferon gamma (IFNγ) is the main cytokine produced. Signalling through its receptor (IFNγR), IFNγ activates the signal transducer and activator of transcription 1 (STAT1). This nuclear transcription factor in turn upregulates the expression of the immunity-related GTPases (IRGs), guanylate-binding proteins (GBPs) and TRIM21. The IRGs recruit to the avirulent *Toxoplasma* PV and mediate its disruption. GBP1 complexes with the E3 ubiquitin ligase TRIM21 in the cytoplasm and, following Lys63-linked ubiquitination, they recruit to the PV of avirulent *Toxoplasma*. TRIM21 also downregulates the biosynthesis of cholesterol, which is essential for the growth of the auxotroph *Toxoplasma* parasite. As *Toxoplasma* can be coated with antibodies and retain them once it has invaded the cell, the breakage of the PV could release the immunoglobulins in the host cytosol where they could serve as danger-associated molecular pattern (DAMP). Whether the Fc receptor TRIM21 binds to the unmasked antibody-coated *Toxoplasma* remains unclear. Similarly, the autophagy sensors mediating recruitment of the autophagosome are still unknown.

Chapter 4

TRIM21 mediates resistance to *Toxoplasma* infection in the mouse via parasite control in the immune privilege brain

4.1 Introduction

4.1.1 TRIM21 knockout mouse models

In order to study the function of a protein, the mouse model can be an invaluable tool. Knocking out the activity of a gene in a mouse, by disrupting or replacing it, provides precious hints or evidence about what that gene normally does. As far as TRIM21 is concerned, two knockout mouse models have been generated and published in 2009. In the first model, Espinosa *et al*. disrupted the *Trim21* gene by targeting exons 5 to 8. They reported their TRIM21 knockout mice to develop a profound lupus-like disease characterised by an aberrant cytokine response in all immune cells that involves the Th17 pathway (Espinosa et al., 2009). However, as their targeting strategy results in exons 1 to 4 to remain in the mouse genome and as the START codon is situated in exon 3, the possibility that a truncated TRIM21 protein harbouring the E3 RING ubiquitin ligase domain, the B-box domain and a part of the coiled-coil domain is still expressed could explain the observed phenotype. Moreover, the PGK-neo cassette used for embryonic stem cell selection has not been removed in this TRIM21 knockout model and could account for the inflammatory phenotype. In the second model, Yoshimi *et al*. disrupted the *Trim21* gene by replacing exons 3 to 5 with EGFP, thereby including the translation start site. The absence of TRIM21 was confirmed at the protein level, and their mouse model does not develop any abnormal developmental or physiological phenotype. It is of note that although the composition of the immune cells population and their immune response was comparable to that of wild-type mice, the production of IL-1β, TNFα, IL-6, and CXCL10 was enhanced in TRIM21-deficient fibroblasts (Yoshimi et al., 2009). The latter TRIM21 knockout mouse has now been established as the reference model to study TRIM21 *in vivo*.

4.1.2 TRIM21 in viral *in vivo* infection

Yoshimi *et al.*'s TRIM21 knockout mouse model has recently been used to study the role of the protein during infection with mouse adenovirus 1 (MAV-1). Indeed, Vaysburd *et al*. reported that TRIM21-deficient mice are more susceptible to MAV-1 infection and exhibit higher viral load in the brain but no differential serum inflammatory cytokine production compared to wild-type controls. In addition, this TRIM21-dependent mediation of adenoviral infection was shown to be linked to the intracellular Fc binding property of the protein, as TRIM21-deficient mice injected with protective antisera still succumb to fatal viral infection whereas wild-type mice can control viremia and are hence rescued by serum passive transfer (Vaysburd et al., 2013). Altogether, these results highlight the role of TRIM21 in the humoral response to mouse adenovirus infection. This study remains the sole *in vivo* investigation of the role of TRIM21 during any infection to date.

4.1.3 Aims

Initial work reported in this thesis has centered on the impact of TRIM21 during *Toxoplasma* infection *in vitro*, highlighting its role in Lys63-linked ubiquitination of avirulent *Toxoplasma* vacuoles, in the regulation of some GBPs and in mediating cholesterol biosynthesis. However, the biological relevance for TRIM21 during *Toxoplasma* infection at the organismal level remains to be elucidated. The importance of TRIM21 in eukaryotic infection models is poorly addressed in the literature. What phenotype do TRIM21-deficient mice develop upon *Toxoplasma* infection? Can they also control parasite burden *in vivo*? What correlates with the absence of TRIM21 at the avirulent *Toxoplasma* vacuole? This section investigates the consequences of the deletion of TRIM21 in the *in vivo* mouse model of *Toxoplasma* infection.

4.2 Results

4.2.1 Oral infections with *Toxoplasma* cysts

The major natural route of infection with *Toxoplasma* in humans is oral with bradyzoite cysts or oocysts, after ingesting contaminated food or water. In the rodent animal model, this is mimicked by orally infecting the mice with bradyzoites of a type II avirulent strain of *Toxoplasma* called ME49, a clone of the type II Pru strain used previously. In order to reproduce the most biologically relevant model of infection, I first infected wild-type controls and TRIM21-deficient mice *per os* with 10 or 40 cysts and followed the outcome by assessing the overall condition of the animals. TRIM21-deficient mice were generated on the C57BL/6 genetic background, which are naturally susceptible to oral infection with *Toxoplasma* and usually succumb during the acute phase (Munoz et al., 2011). Following oral infection with 10 or 40 avirulent *Toxoplasma* ME49 cysts, both the wild-type and TRIM21-deficient animal had to be sacrificed 7 days post-inoculation. This suggests that TRIM21 knock out does not confer a disadvantage during *Toxoplasma* infection. The production of 32 cytokines in the serum of wild-type and TRIM21-deficient mice was assessed at 3 and 7 days post-infection for both infectious doses tested. TRIM21-deficient mice infected with 40 *Toxoplasma* cysts exhibit a slight but significantly decreased level of the neutrophil chemoattractant LIX at 3 days post-infection, as well as a slight but significantly increased level of the monocyte chemotactic protein 1 (MCP-1) at 7 days post-infection (Figure 4.1). Moreover, TRIM21-deficient mice infected with 10 *Toxoplasma* cysts exhibit slight but significantly lower levels of IL-9 and macrophage colony-stimulator factor (M-CSF) at 3 days post-infection, as well as a slight but significantly decreased level of IL-1β at 7 days post-infection (Figure 4.2). As these

cytokine profiles differ according to the infectious dose, this suggests that the response to infection is modulated depending on the parasite dose inoculated. However, since both TRIM21-deficient and wild-type mice succumb to acute *Toxoplasma* infection, no conclusions on the immunological mechanism can be drawn from these results.

Finally, a very low infection dose of 5 avirulent *Toxoplasma* ME49 cysts was inoculated into experimental mice. As can be seen on Figure 4.3, although the animals survived the infection longer than after infection with 10 or 40 cysts, both wild-type and TRIM21-deficient mice succumb to infection at a very similar rate and presented a similar weight loss (Figure 4.3). This indicates that TRIM21 does not negatively impact the resistance to *Toxoplasma* infection in the oral infection mouse model. However, TRIM21 KO animals often appeared sicker, presenting stronger manifestations of the typical signs of *Toxoplasma* infection such as ruffled fur, hunched position and even immobility. However, as it is difficult to assess whether TRIM21 enhances susceptibility during *Toxoplasma* infection in the mouse model where the wild-type controls are already susceptible, the oral infection was abandoned and the intraperitoneal route of infection was favoured for the rest of the study.

4.2.2 Intraperitoneal infections with *Toxoplasma* tachyzoites

4.2.2.1 TRIM21-deficient mice infected intraperitoneally are susceptible to *Toxoplasma* infection

As opposed to oral infection, mice on the C57BL/6 background are resistant to peritoneal infection with *Toxoplasma* during the acute phase of the infection (Munoz et al., 2011). However, bradyzoite cysts and oocysts ingested orally both convert to tachyzoites in the host's gut. As a result, intraperitoneal infection of tachyzoites is another commonly used *in vivo* mouse model. Thus, wild-type and TRIM21-deficient

mice were infected intraperitoneally with $5x10^4$ avirulent type II *Toxoplasma* tachyzoites genetically engineered to express firefly luciferase. In contrast to the wild-type controls, TRIM21-deficient mice are highly susceptible to infection and succumb during the acute phase of the infection, at 7 to 10 days post-inoculation. At 10 days post-infection, 77% of the TRIM21-deficient mice had succumbed to infection while 83% of the control mice had survived (Figure 4.4a). Both wild-type and TRIM21-deficient mice show a similar pattern of weight loss (Figure 4.4b), but TRIM21-deficient mice exhibit a significantly higher clinical score (characterised by piloerection, hunching and reduced motility) from day 7 post-infection on (Figure 4.4c). These results suggest TRIM21 participates in the resistance against *Toxoplasma* infection *in vivo*.

4.2.2.2 TRIM21-deficient mice can mostly control parasite replication in the periphery

The different mouse knockout models infected with *Toxoplasma* so far generally succumb to infection due to an unchecked parasite replication, sometimes accompanied with a cytokine storm (Yarovinsky, 2014). In order to determine the cause of TRIM21-deficient mice death, I followed the progression of the parasite burden in infected mice using *in vivo* imaging. As the *Toxoplasma* strain is engineered to express firefly luciferase, mice were injected with the enzyme's substrate luciferin during the acute phase of infection at days 3, 5 and 7 post-inoculation. The higher the parasite load, the higher the luminescence signal measured is in infected animals. As can be seen in Figure 4.5, wild-type and TRIM21-deficient mice already present a high parasite load at day 3 of infection. At 5 days post-infection, TRIM21-deficient mice exhibit a significantly higher parasite burden compared to wild-type controls, but this difference disappears at 7 days post-infection when the knockout mice start dying.

These results indicate that TRIM21-deficient mice can mostly control *Toxoplasma* replication in the periphery, and is in accordance with the *in vitro* plaque assay data (see section 3.2.12).

4.2.2.3 TRIM21-deficient mice exhibit a decreased level of serum pro-inflammatory cytokines

TRIM21 mediates the upregulation of IL-12p40 expression, a cytokine important for innate immunity in macrophages and involved in the stimulation of IFNγ production via interaction and ubiquitination of IRF8 (Kong et al., 2007). TRIM21 has also been shown to downregulate NF-□B signalling in embryonic fibroblasts, leading to higher expression of pro-inflammatory cytokines (Yoshimi et al., 2009). Apart from unchecked parasite replication, infection with *Toxoplasma* can lead to a lethal hyper-immune response. Thus, I hypothesised that TRIM21 confers resistance to *Toxoplasma* infection by controlling cytokine levels to mediate immune responses rather than through direct labelling of the parasite for degradation. Therefore, I assessed the protein levels of cytokines and chemokines in the serum at 3 and 7 days post-infection. At the first time point corresponding to the early stage of infection, no difference was observed in the levels of serum pro-inflammatory cytokines (Figure 4.6). However at 7 days post-infection, corresponding to the time when mice start to succumb to the parasitic infection, TRIM21-deficient mice exhibit lower levels of IFNγ, IL-6, IL-10, IL-12p40, IFNγ-inducible protein 10 (IP-10) and MCP-1. Additionally, TRIM21-deficient mice show significantly decreased levels of regulated on activation, normal T cell expressed and secreted protein (RANTES) and of TNFα (Figure 4.6), cytokines and chemokines that are all induced by the NF-□B-mediated cytokine production signalling pathway.

Moreover, analysis by enzyme-linked immunosorbent assay (ELISA) of the protein levels of selected cytokines in the serum of mice infected for 7 days further confirmed the downregulation of IFNγ in TRIM21-deficient mice, while the levels of the type I interferons IFNα and IFNβ are not impacted by the absence of TRIM21 (Figure 4.7a). Interestingly, the level of IL-1β was significantly lower in the serum of TRIM21-deficient mice when measured by ELISA (Figure 4.7a). Finally, the protein levels of IFNγ, IL-12p40 and TNFα are not different in the peritoneum of TRIM21-deficient mice compared to wild-type controls, whereas the decreased level of IL-1β in the serum is also present in the peritoneum of TRIM21-deficient mice infected for 7 days (Figure 4.7b). These results suggest TRIM21 mediates resistance to *Toxoplasma* infection *in vivo* by inducing the production of pro-inflammatory cytokines, mainly in the serum.

4.2.2.4 TRIM21-deficient mice do not exhibit a differential recruitment of immune cells to the sites of infection

The components of the immune system can be divided in two categories. The primary lymphoid organs consist of the bone marrow and the thymus. The secondary lymphoid organs consist of the spleen, the lymph nodes and the Peyer's patches. In order to determine what cells could be involved in the dramatic survival phenotype as well as the differential level of cytokines in the serum, we performed a phenotyping of the immune cells in the peritoneum and the secondary lymphatic organs by flow cytometry. First, different populations of innate cells were analysed in a total of 4 independent experiments. The frequency and total cell number of neutrophils, dendritic cells, macrophages and inflammatory monocytes were determined each time, but no tendency or significant difference could be reproduced twice so that the analysis of the innate cells did not lead to any conclusive result. An example of the analysis can

be seen in Figure 4.8. Second, different populations of lymphocytes were analysed in a total of 2 to 4 independent experiments. The frequency and total cell number of B cells, T cells, NK cells, CD4 T cells, CD8 T cells, NK IFNγ^+ cells, CD4 IFNγ^+ cells and CD8 IFNγ^+ cells were determined in each experiment in the peritoneum (Figure 4.9), the spleen (Figure 4.10), the Peyer's patches (Figure 4.11), the mesenteric lymph nodes (Figure 4.12) and the draining lymph nodes (Figure 4.13). Similarly to the innate cells, no tendency or significant difference in the frequency of cell number could be reproduced twice, thus the phenotyping of the lymphocytes did not lead to any conclusive results. Examples of the analysis performed for each organ can be seen from Figure 4.9 to Figure 4.13. These results suggest it is likely that there is no clear and definite impact of TRIM21 deficiency on the proliferation, recruitment or activation of the immune cell populations during *Toxoplasma* infection.

4.2.2.5 TRIM21 deficiency does not lead to immunopathology

As TRIM21-deficient mice exhibit a high mortality characterised by an increased parasite burden at 5 days post-infection and a decrease in serum inflammatory cytokines at 7 days post-inoculation, I checked for tissue and organ damage or malfunction by measuring the level of specific biomarkers in the serum of mice infected for 7 days. The panel of biomarkers included detection of liver damage and abnormal function (albumin, alanine aminotransferase, aspartate aminotransferase and bilirubin), tissue damage (lactate and lactate dehydrogenase), kidney failure (urea), pancreas failure (lipase), lipid metabolism (cholesterol, low density lipoprotein cholesterol, and triglycerides). As can be seen in Figure 4.14, no abnormal level in any biomarker was detected in TRIM21-deficient mice compared to wild-type controls.

These observations were further confirmed by histopathology. Livers, spleens, lungs and brains from wild-type and TRIM21-deficient mice infected for 7 days with avirulent *Toxoplasma* were sent for pathology examination. Prof. Cheryl Scudamore (MRC Harwell) could not detect any abnormal levels of liver peritonitis, inflammation and necrosis (Figure 4.15a), and examination revealed equal levels of spleen peritonitis, extramedullary haematopoiesis and apoptosis (Figure 4.15b). Moreover, Prof. Gordon Stamp (Imperial College London) did not report any abnormal pathology in lungs and brains of TRIM21-deficient mice (data not shown). Altogether, these results imply TRIM21-deficient mice do not succumb to *Toxoplasma* infection from organ damage or failure.

4.2.2.6 TRIM21-deficient mice exhibit higher parasite load and decreased number of microglia in the brain

So far TRIM21 deficiency has been shown to lead to an increased parasite load at the periphery at 5 days post-infection, accompanied with a decreased level of inflammatory cytokines in the serum at 7 days post-infection. However, this does not lead to immunopathology in the periphery. As *Toxoplasma* tachyzoites ultimately migrate to the brain where they convert into the slow replicating bradyzoites, I assessed the number of parasites in this organ. Although the overall parasite burden has been investigated by *in vivo* imaging, it does not include what is happening in the brain due to the fact that the luminescence signal cannot be detected through the skull. Brains were isolated at 7 days post-infection and the GFP-expressing *Toxoplasma* were counted in wild-type and TRIM21-deficient samples in a blind fashion. In a consistent manner, TRIM21-deficient mice that presented rough physical conditions typical of infection with *Toxoplasma* exhibit higher parasite counts than healthy wild-

type animals (Figure 4.16a). Thus, TRIM21-deficient mice cannot control the parasite replication in or migration to the brain.

Furthermore, the immune cell populations in the brain of mice infected for 7 days with avirulent *Toxoplasma* were analysed by flow cytometry. In two independent experiments, the total number of microglial cells was consistently decreased in TRIM21-deficient mice, and this was associated with a frequency of microglia that was strongly decreased in one experiment (Figure 4.16b). As both naïve wild-type and TRIM21-deficient mice present the same number of microglial cells, it is likely that this population of resident myeloid cells of the central nervous system does not proliferate following *Toxoplasma* infection in the absence of TRIM21. Although a significant increase in the frequency of infiltrate cells can be observed in Figure 4.16b, the reverse phenomenon was seen in the previous experiment (data not shown). As far as the lymphocyte population is concerned, a significant increase in the frequency and total number of CD3+ T cells, as well as a significant decrease in the frequency of CD4+ T cells, were observed in TRIM21-deficient cells in one experiment (Figure 4.16c), while the reverse was spotted in the previous experiment. Thus, the phenotyping of infiltrate cells and lymphocytes remains inconclusive for now.

4.2.2.7 TRIM21-deficient mice present decreased transcripts involved in the immune inflammatory response

To understand what happens in the brain of a TRIM21-deficient mouse infected with avirulent *Toxoplasma* compared to a wild-type control, I performed a transcriptional analysis of the genes encoding for cytokines and chemokines or involved in neuroinflammation. A total of 164 targets were screened by quantitative PCR, out of which four show a significantly decreased expression level in infected TRIM21-

deficient animals (Figure 4.17). Indeed, type I interferon alpha (*Ifna2*), the pro-inflammatory cytokine IL-6 (*Il6*), the leukocyte adhesion regulator integrin alpha M (*Itgam*) and the immune modulatory peptide prokineticin 2 (*Prok2*) all exhibit lower mRNA levels in the brain of mice lacking TRIM21. This indicates that the higher parasite burden and the lower number of microglial cells in the brain of TRIM21-deficient mice is accompanied by a decreased transcriptional expression of genes involved in the immune inflammatory response. The expression profile of the remaining genes analysed can be found in the Appendix.

4.3 Discussion

So far, the role of TRIM21 has only been described during the course of viral infection in the mouse model. TRIM21 has been reported to bind to invading antibody-coated adenoviruses and target them to degradation by the proteasome due to its E3 ligase activity (Mallery et al., 2010), as well as to modulate the production of pro-inflammatory cytokines during viral infection (McEwan et al., 2013), thereby enabling to control viremia *in vivo* (Vaysburd et al., 2013). Our *in vitro* findings suggest TRIM21 participates in the response to *Toxoplasma* infection by mediating the ubiquitination status of the guanylate binding proteins around the parasitophorous vacuole. However, the consequences of these observations remain unclear. The aim of this work was to shed light on the consequences of TRIM21 deficiency during murine *Toxoplasma* infection at the organismal level.

In this thesis, I report for the first time the role of TRIM21 in *in vivo* resistance against a eukaryotic intracellular pathogen. Indeed, I show that TRIM21-deficient mice are highly susceptible to infection with *Toxoplasma*. Mice infected intraperitoneally with an avirulent strain of the parasite succumb during the acute phase of the infection,

between day 7 and 10. This kinetic strongly resembles the survival rate observed in IFNγ- and IL-12-deficient mice, the two known major mediators of the resistance against the apicomplexan parasite (Scharton-Kersten et al., 1996; Gazzinelli et al., 1994; Yap et al., 2000). Moreover, this survival pattern also mimics the one already reported in MyD88- and UNC93B-deficient mice, two proteins downstream of the TLR response and essential for activation of immune signalling (Scanga et al., 2002; Sukhumavasi et al., 2008; Melo et al., 2010). Thus, this places TRIM21 as another, new important player in the control of *Toxoplasma* infection.

Several parameters were investigated in this work in order to assess the cause of death in TRIM21-deficient mice infected with avirulent *Toxoplasma*. *In vivo* imaging allowed to follow the evolution of the parasite replication and showed TRIM21-deficient mice exhibit a higher parasite burden at 5 days post-infection, before the critical point when mice start succumbing to infection. At 7 days post-inoculation, the death of infected mice lacking TRIM21 correlates with a higher parasite load in the brain. This unchecked parasite replication is accompanied with a significant decrease in the total number of microglial cells and in the transcriptional expression levels of inflammatory cytokines in the brain. My results also show that TRIM21-deficient mice present a significantly lower secretion of inflammatory cytokines in the serum and do not exhibit any abnormal pathology. Taken together, these data suggest TRIM21 mediates the upregulation of inflammatory cytokines necessary to control avirulent *Toxoplasma* replication. Failing to do so leads to an increased parasite burden in the periphery and subsequently in the brain, where microglia appear not to activate and proliferate. The exact mechanisms by which TRIM21 regulates the production of inflammatory cytokines as well as what causes the defect in microglia activation remain to be elucidated. As TRIM21 has been reported to regulate the antiviral

response by the production of Lys63-ubiquitin chains (McEwan et al., 2013), I hypothesise that the E3 ubiquitin ligase activity of TRIM21 is essential also to mediate immune signalling during *Toxoplasma* infection. This could be investigated in the future by the generation of a mouse line expressing a mutant TRIM21 protein lacking the RING E3 ubiquitin ligase domain.

One controversial property of TRIM21 recently brought to the fore is its ability to bind to intracellular antibody-coated adenoviruses (Mallery et al., 2010). *Toxoplasma* has also been reported to retain antibodies once inside the host cell (Dubremetz et al., 1985). In the lab, preliminary work showed that avirulent *Toxoplasma* tachyzoites isolated from the peritoneum of a C57BL/6 mouse are mainly coated with IgG, while parasites isolated from the peritoneum of μMT mice lacking B cells and hence circulating antibodies, do not harbour any antibody (Figure 4.18a, c). Very interestingly, these preliminary data also show that avirulent *Toxoplasma* isolated from the immune privilege brain of a C57BL/6 mouse are mainly coated with IgM (Figure 4.18b, c). How this differential antibody decoration influences the immune response to the parasite at the site of infection remains unknown. As B cell-deficient mice die of a high parasite load in the brain (Kang et al., 2000), it is tempting to hypothesise that TRIM21 and antibodies act in concert during *Toxoplasma* infection, such that TRIM21 could sense antibody-coated parasites like it does detect adenoviruses. However, this hypothesis would prove to be difficult to test *in vivo*, as even backcrossing TRIM21-deficient mice on the μMT genetic background would not help determine the individual or combined role of TRIM21 and antibodies.

In summary, I have identified TRIM21 as an important mediator of *in vivo* resistance against a eukaryotic pathogen, *Toxoplasma*. TRIM21-deficient mice succumb to

avirulent *Toxoplasma* infection during the acute phase, and the death correlates with an enhanced parasite load in the brain accompanied with decreased inflammatory cytokines and microglial cells. The newly discovered implication of TRIM21 in *Toxoplasma* infection suggests that resistance mechanisms yet to be determined govern restriction of the parasite at the organismal level.

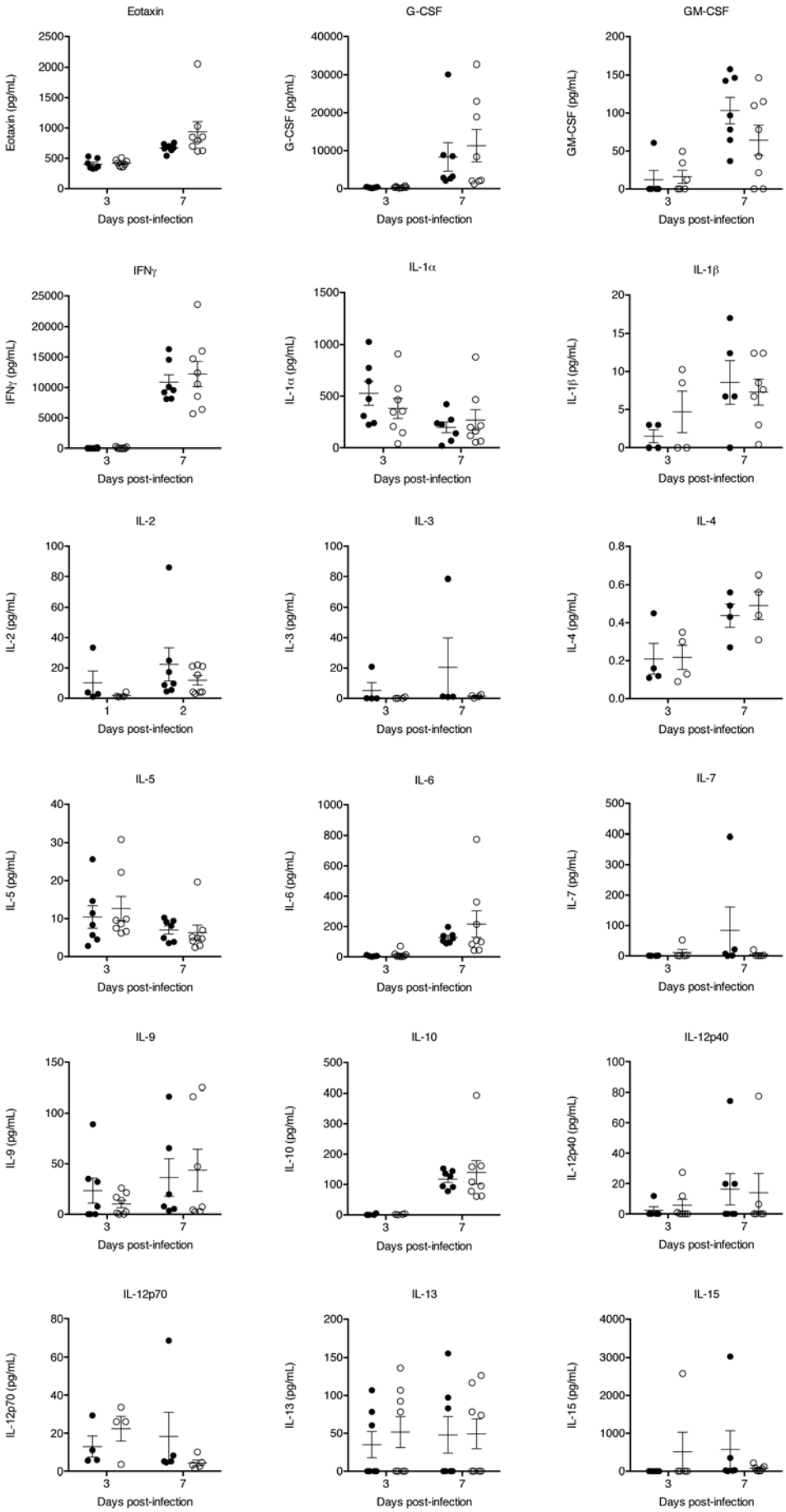
Eotaxin
Eotaxin (pg/mL)
Days post-infection
G-CSF
G-CSF (pg/mL)
Days post-infection
GM-CSF
GM-CSF (pg/mL)
Days post-infection
IFNγ
IFNγ (pg/mL)
Days post-infection
IL-1α
IL-1α (pg/mL)
Days post-infection
IL-1β
IL-1β (pg/mL)
Days post-infection
IL-2
IL-2 (pg/mL)
Days post-infection
IL-3
IL-3 (pg/mL)
Days post-infection
IL-4
IL-4 (pg/mL)
Days post-infection
IL-5
IL-5 (pg/mL)
Days post-infection
IL-6
IL-6 (pg/mL)
Days post-infection
IL-7
IL-7 (pg/mL)
Days post-infection
IL-9
IL-9 (pg/mL)
Days post-infection
IL-10
IL-10 (pg/mL)
Days post-infection
IL-12p40
IL-12p40 (pg/mL)
Days post-infection
IL-12p70
IL-12p70 (pg/mL)
Days post-infection
IL-13
IL-13 (pg/mL)
Days post-infection
IL-15
IL-15 (pg/mL)
Days post-infection

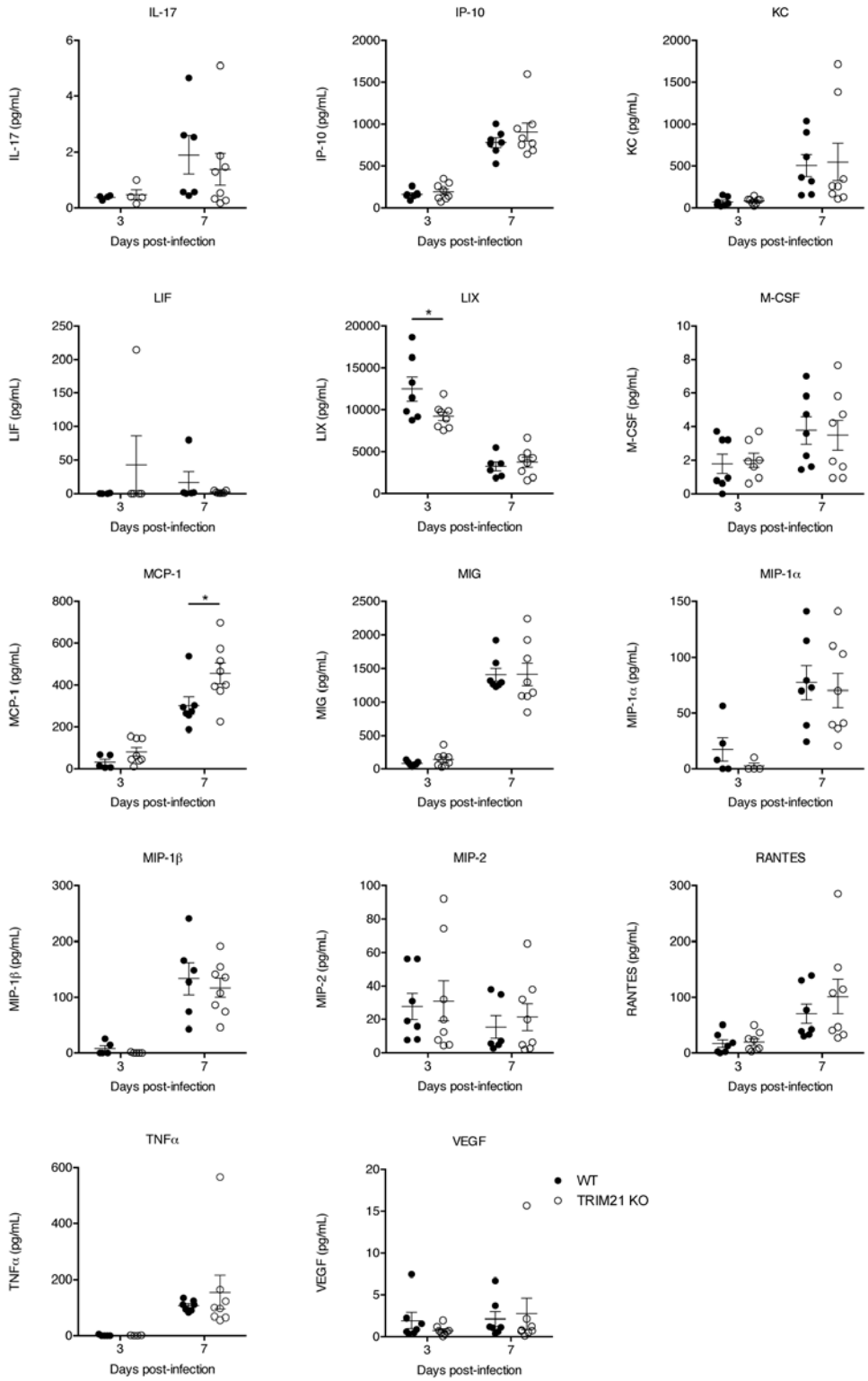

Figure 4.1: Production of serum cytokines in TRIM21-deficient mice following infection with 40 cysts of avirulent *Toxoplasma*.

The serum of wild-type and TRIM21-deficient mice infected *per os* with 40 cysts of avirulent *Toxoplasma* was collected at 3 and 7 days post-infection (dpi). Cytokine levels were measured using multiplex at Eve Technology as described in the Experimental Procedure. TRIM21-deficient mice show decreased levels of serum LIX at 3 dpi, and decreased levels of MCP-1 at 7 dpi. Mean + SEM, * $p<0.05$, unpaired t-test.

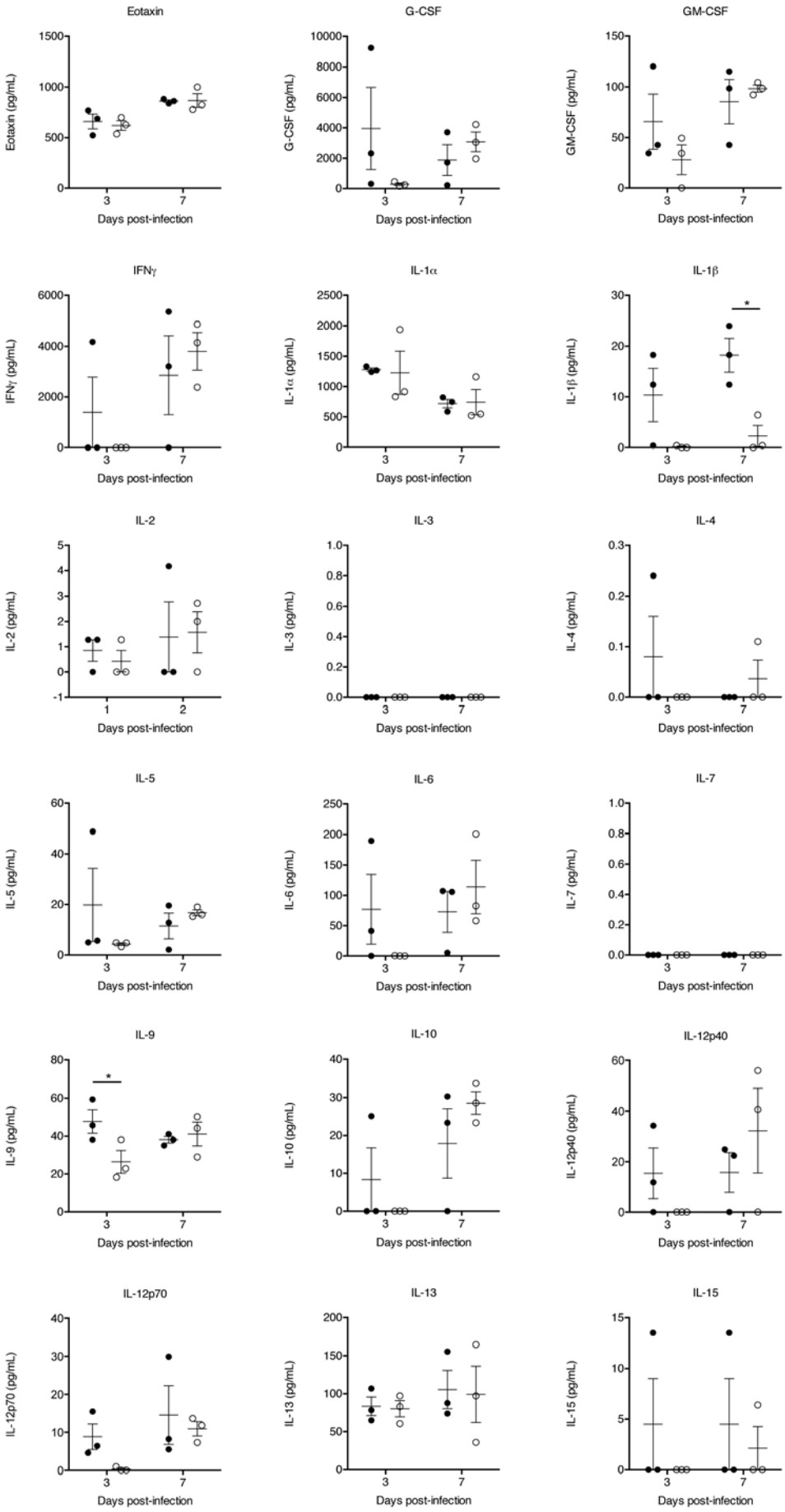
Eotaxin
Eotaxin (pg/mL)
1500
1000
500
0
3
7
Days post-infection
G-CSF
G-CSF (pg/mL)
10000
8000
6000
4000
2000
0
3
7
Days post-infection
GM-CSF
GM-CSF (pg/mL)
150
100
50
0
3
7
Days post-infection
IFNγ
IFNγ (pg/mL)
6000
4000
2000
0
3
7
Days post-infection
IL-1α
IL-1α (pg/mL)
2500
2000
1500
1000
500
0
3
7
Days post-infection
IL-1β
IL-1β (pg/mL)
30
20
10
0
*
3
7
Days post-infection
IL-2
IL-2 (pg/mL)
5
4
3
2
1
0
-1
1
2
Days post-infection
IL-3
IL-3 (pg/mL)
1.0
0.8
0.6
0.4
0.2
0.0
3
7
Days post-infection
IL-4
IL-4 (pg/mL)
0.3
0.2
0.1
0.0
3
7
Days post-infection
IL-5
IL-5 (pg/mL)
60
40
20
0
3
7
Days post-infection
IL-6
IL-6 (pg/mL)
250
200
150
100
50
0
3
7
Days post-infection
IL-7
IL-7 (pg/mL)
1.0
0.8
0.6
0.4
0.2
0.0
3
7
Days post-infection
IL-9
IL-9 (pg/mL)
80
60
40
20
0
*
3
7
Days post-infection
IL-10
IL-10 (pg/mL)
40
30
20
10
0
3
7
Days post-infection
IL-12p40
IL-12p40 (pg/mL)
60
40
20
0
3
7
Days post-infection
IL-12p70
IL-12p70 (pg/mL)
40
30
20
10
0
3
7
Days post-infection
IL-13
IL-13 (pg/mL)
200
150
100
50
0
3
7
Days post-infection
IL-15
IL-15 (pg/mL)
15
10
5
0
3
7
Days post-infection

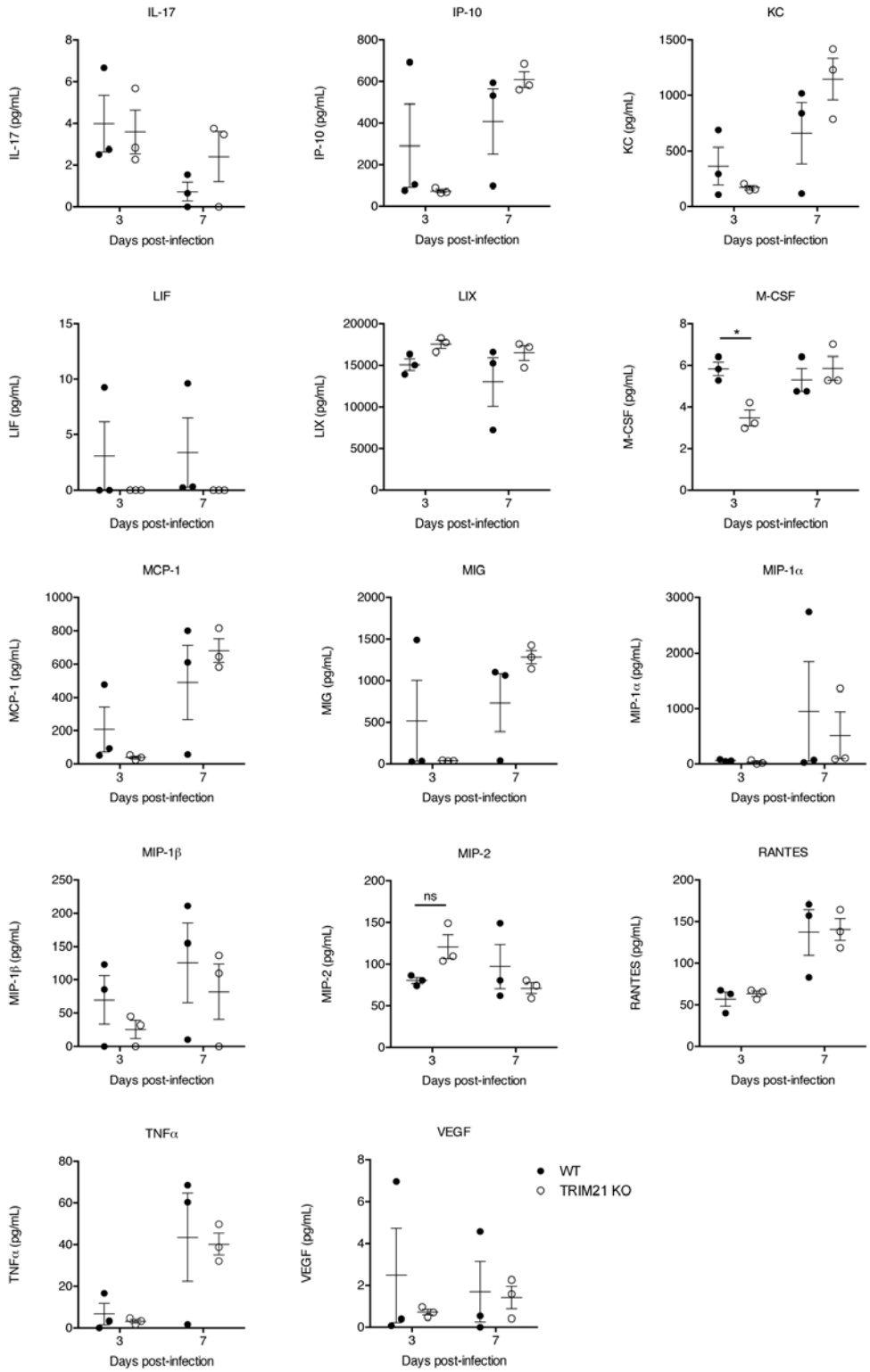

Figure 4.2: Production of serum cytokines in TRIM21-deficient mice following infection with 10 cysts of avirulent *Toxoplasma*.

The serum of wild-type and TRIM21-deficient mice infected *per os* with 10 cysts of avirulent *Toxoplasma* was collected at 3 and 7 days post-infection (dpi). Cytokine levels were measured using multiplex at Eve Technology as described in the Experimental Procedure. TRIM21-deficient mice show decreased levels of serum M-CSF at 3 dpi, and decreased levels of IL-1β at 7 dpi. Mean + SEM, * $p<0.05$, unpaired t-test.

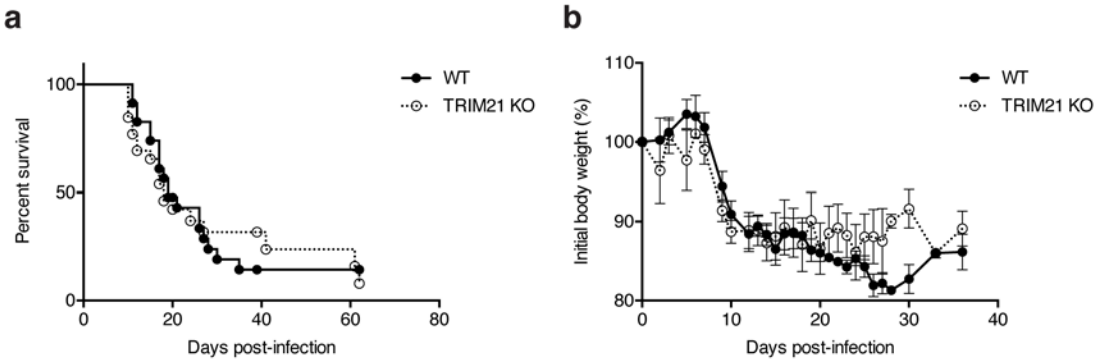

Figure 4.3: Survival of TRIM21-deficient mice infected with a low dose of avirulent *Toxoplasma* cysts.
Wild-type and TRIM21-deficient mice were infected *per os* with 5 cysts of avirulent *Toxoplasma.* The survival of infected mice was monitored (**a**) as well as the evolution of the body weight (**b**). Mice lacking TRIM21 infected orally with a low dose of avirulent *Toxoplasma* cysts do not exhibit a higher mortality.

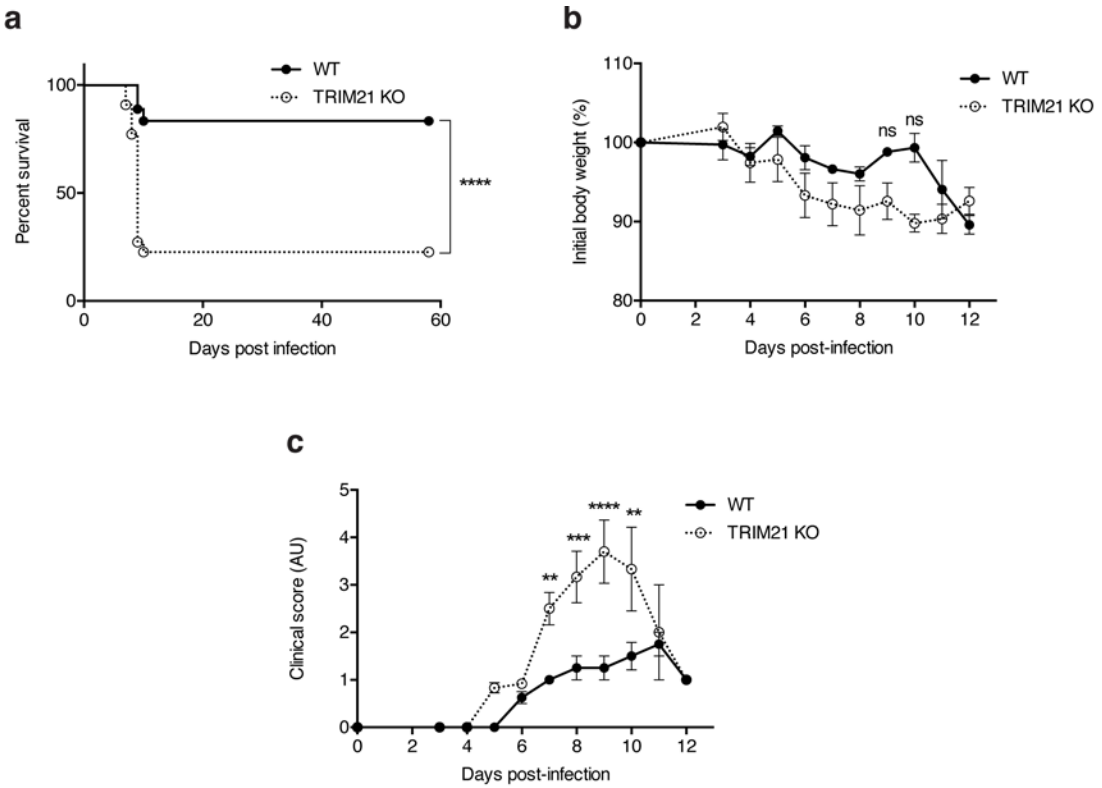

Figure 4.4: TRIM21-deficient mice are highly susceptible to intraperitoneal *Toxoplasma* infection. Wild-type and TRIM21-deficient mice were infected intraperitoneally with $5x10^4$ avirulent *Toxoplasma*. The survival of infected mice was monitored (**a**) as well as the evolution of the body weight (**b**). The clinical score, assessed by piloerection, a hunched position and immobility, was measured throughout the time of the experiment (**c**). Mice lacking TRIM21 infected peritoneally with avirulent *Toxoplasma* are very susceptible to *Toxoplasma* infection and present higher clinical score compared to wild-type controls. Survival curves were compared by log-rank survival analysis of Kaplan-Meier curves, **** $p<0.0001$. Weight curve and clinical score are represented by mean + SEM, ** $p<0.01$, *** $p<0.001$, **** $p<0.0001$, 2-way ANOVA.

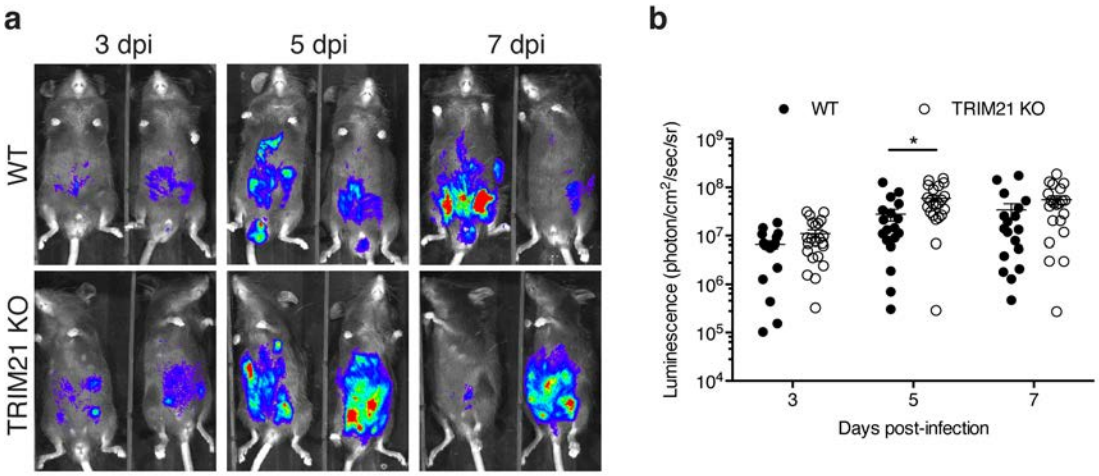

Figure 4.5: TRIM21-deficient mice exhibit higher parasite burden in the periphery.
Wild-type and TRIM21-deficient mice were infected intraperitoneally with $5x10^4$ avirulent *Toxoplasma.* (**a**) The evolution of the firefly luciferase-expressing parasite load was controlled by *in vivo* imaging after injection of luciferin at 3, 5 and 7 days post-infection (dpi) as described in the Experimental Procedure. (**b**) Mice lacking TRIM21 infected peritoneally with avirulent *Toxoplasma* exhibit a higher parasite burden at 5 dpi. Mean + SEM, * $p<0.05$, 2-way ANOVA.

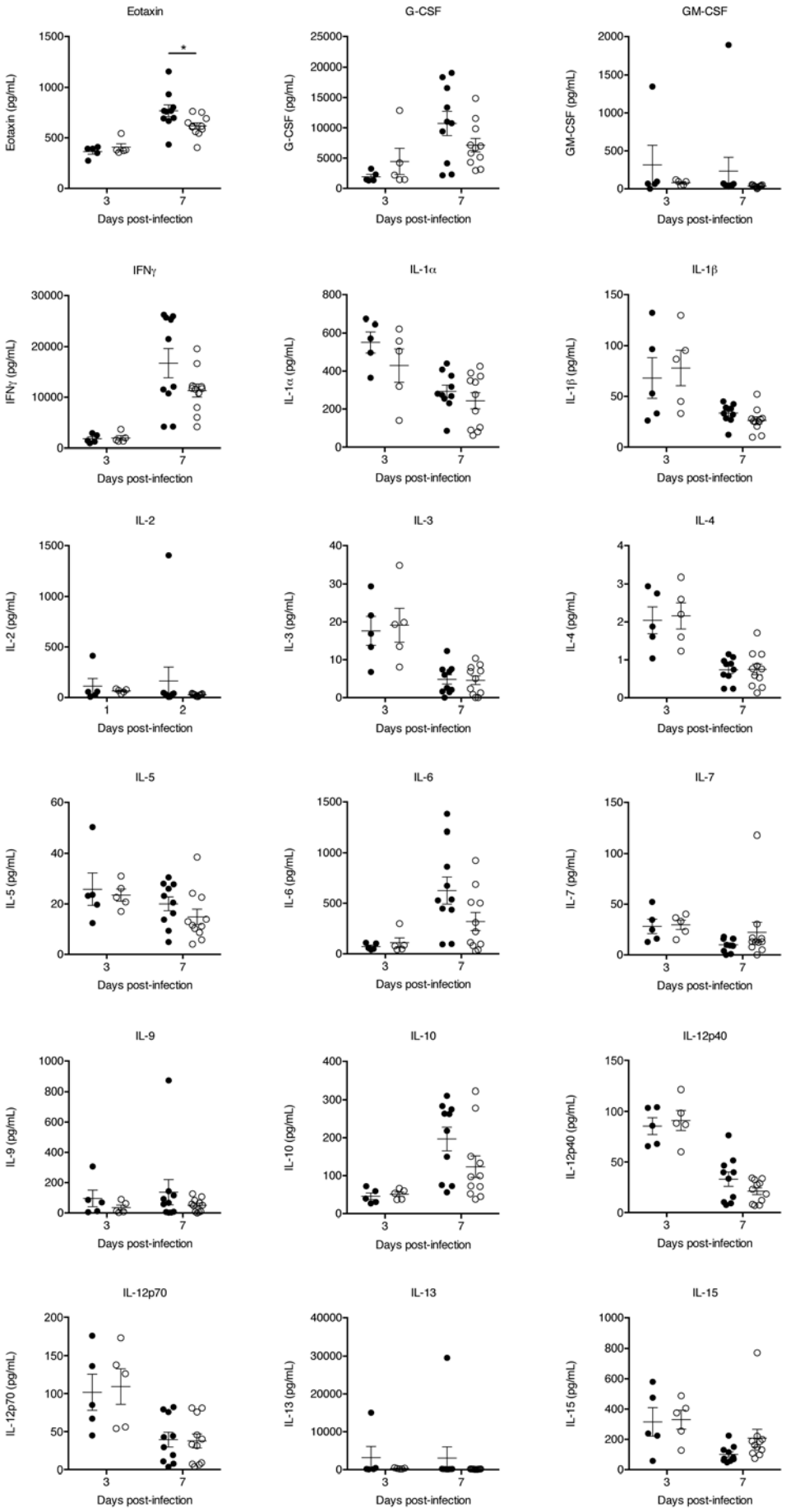
Eotaxin
Eotaxin (pg/mL)
1500
1000
500
0
*
3
7
Days post-infection
G-CSF
G-CSF (pg/mL)
25000
20000
15000
10000
5000
0
3
7
Days post-infection
GM-CSF
GM-CSF (pg/mL)
2000
1500
1000
500
0
3
7
Days post-infection
IFNγ
IFNγ (pg/mL)
30000
20000
10000
0
3
7
Days post-infection
IL-1α
IL-1α (pg/mL)
800
600
400
200
0
3
7
Days post-infection
IL-1β
IL-1β (pg/mL)
150
100
50
0
3
7
Days post-infection
IL-2
IL-2 (pg/mL)
1500
1000
500
0
1
2
Days post-infection
IL-3
IL-3 (pg/mL)
40
30
20
10
0
3
7
Days post-infection
IL-4
IL-4 (pg/mL)
4
3
2
1
0
3
7
Days post-infection
IL-5
IL-5 (pg/mL)
60
40
20
0
3
7
Days post-infection
IL-6
IL-6 (pg/mL)
1500
1000
500
0
3
7
Days post-infection
IL-7
IL-7 (pg/mL)
150
100
50
0
3
7
Days post-infection
IL-9
IL-9 (pg/mL)
1000
800
600
400
200
0
3
7
Days post-infection
IL-10
IL-10 (pg/mL)
400
300
200
100
0
3
7
Days post-infection
IL-12p40
IL-12p40 (pg/mL)
150
100
50
0
3
7
Days post-infection
IL-12p70
IL-12p70 (pg/mL)
200
150
100
50
0
3
7
Days post-infection
IL-13
IL-13 (pg/mL)
40000
30000
20000
10000
0
3
7
Days post-infection
IL-15
IL-15 (pg/mL)
1000
800
600
400
200
0
3
7
Days post-infection

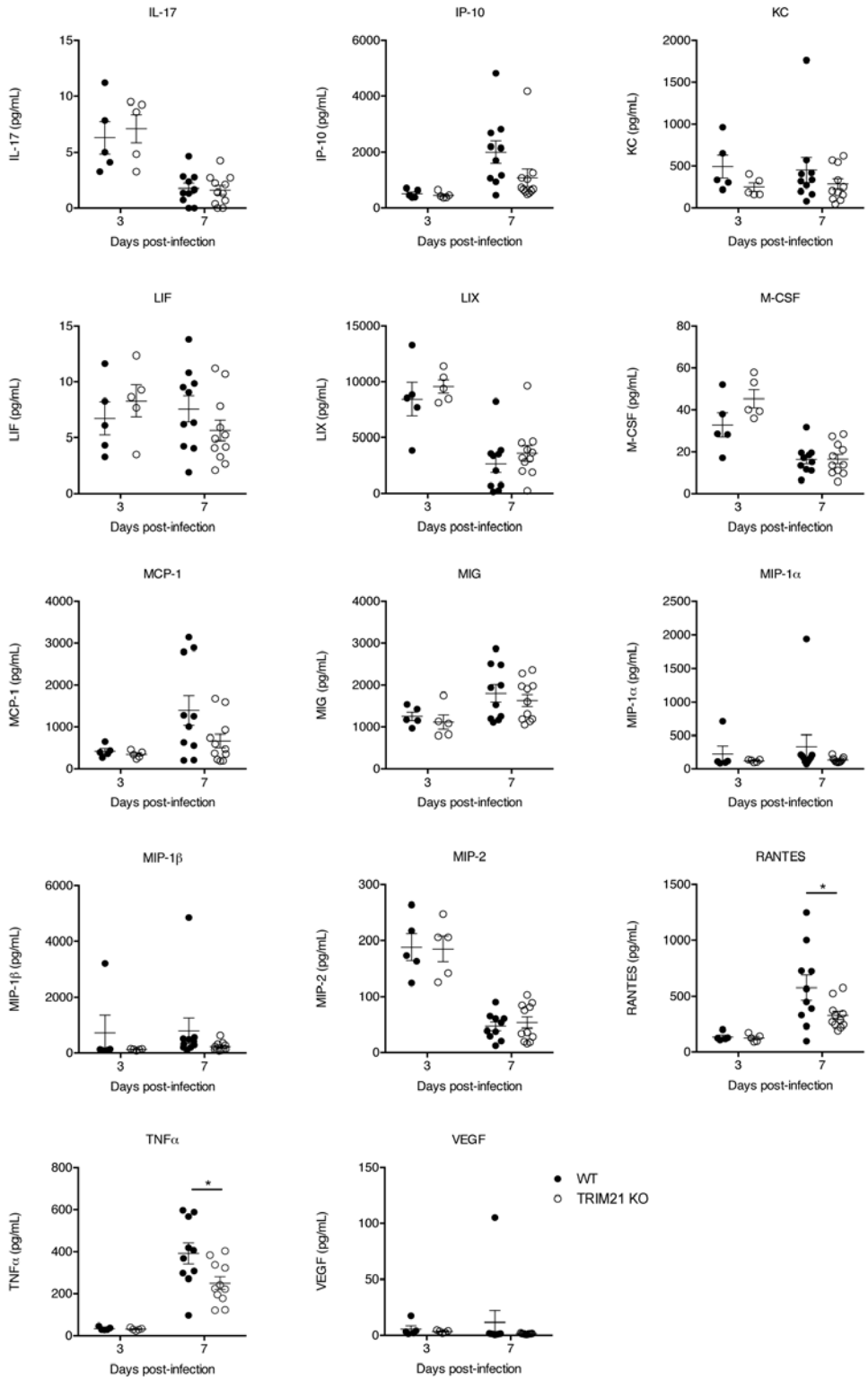

Figure 4.6: Production of serum cytokines in TRIM21-deficient mice following infection with $5x10^4$ avirulent *Toxoplasma*.

The serum of wild-type and TRIM21-deficient mice infected intraperitoneally with avirulent *Toxoplasma* was collected at 3 and 7 days post-infection (dpi). Cytokine levels were measured using multiplex at Eve Technology as described in the Experimental Procedure. TRIM21-deficient mice show decreased levels of serum eotaxin, RANTES and TNFα at 7 dpi. Data were pooled from three independent experiments. Mean + SEM, * $p<0.05$, unpaired t-test.

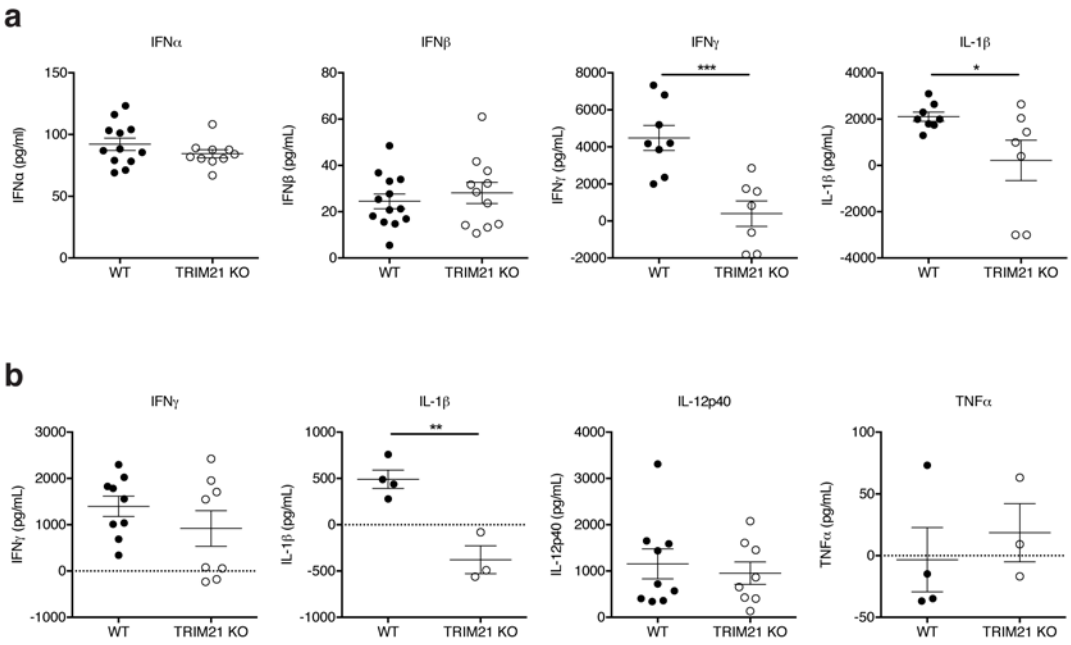

Figure 4.7: Production of selected serum and peritoneum cytokines in TRIM21-deficient mice following infection with $5x10^4$ avirulent *Toxoplasma*.
Wild-type and TRIM21-deficient mice infected intraperitoneally with avirulent *Toxoplasma* were sacrificed at 7 days post-infection (dpi) and serum (**a**) as well as peritoneal lavage (**b**) were collected. Cytokine levels were measured by enzyme-linked immunosorbent assay (ELISA) as described in the Experimental Procedure. TRIM21-deficient mice show decreased levels of serum IFNγ and IL-1β 7 dpi. Mice lacking TRIM21 also show decreased levels of IL-1β in the peritoneum at 7 dpi. Data were pooled from three independent experiments. Mean + SEM, * $p<0.05$, ** $p<0.01$, *** $p<0.001$, unpaired t-test.

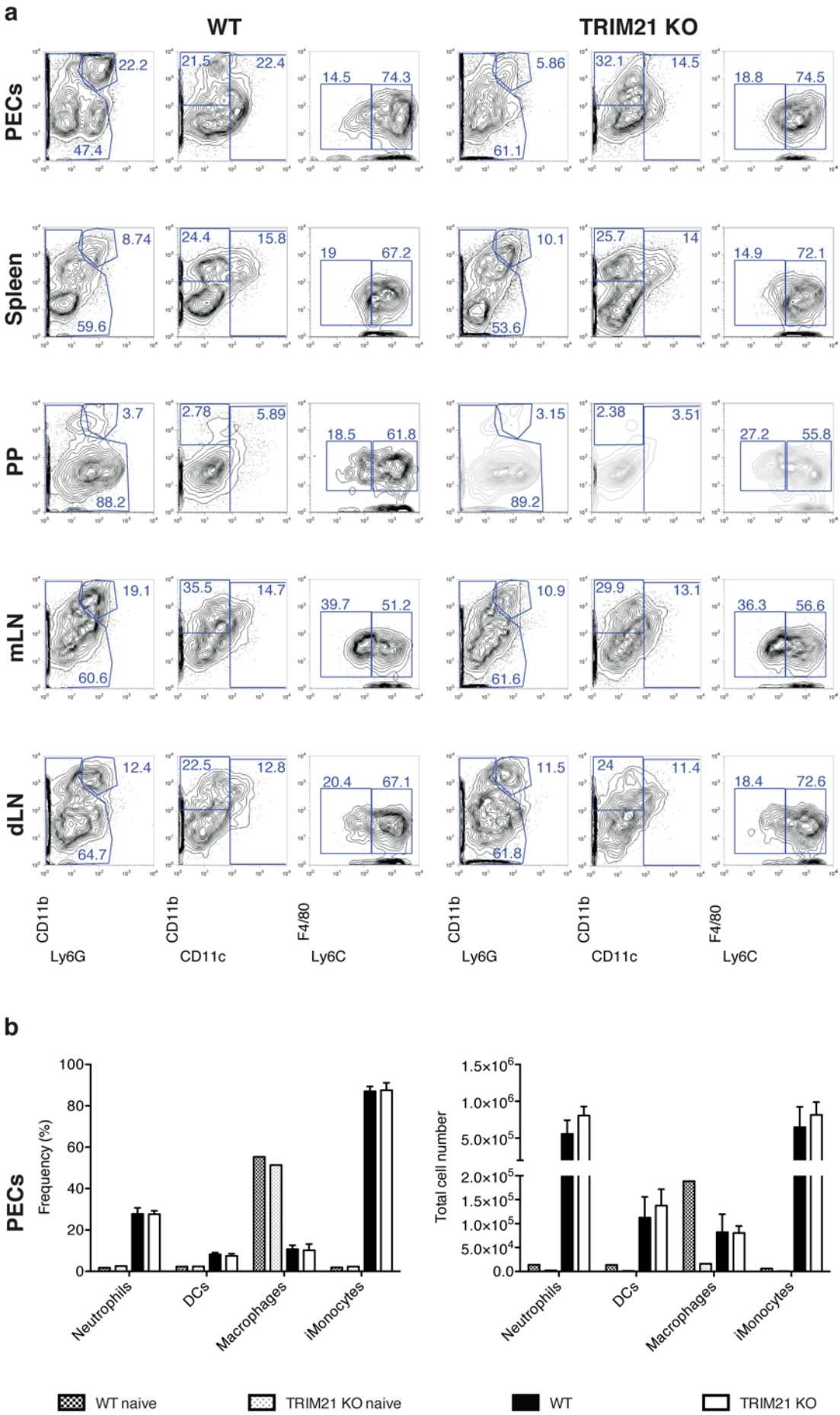
a
WT
TRIM21 KO
PECs
Spleen
PP
mLN
dLN
22.2
47.4
21.5
22.4
14.5
74.3
5.86
61.1
32.1
14.5
18.8
74.5
8.74
59.6
24.4
15.8
19
67.2
10.1
53.6
25.7
14
14.9
72.1
3.7
88.2
2.78
5.89
18.5
61.8
3.15
89.2
2.38
3.51
27.2
55.8
19.1
60.6
35.5
14.7
39.7
51.2
10.9
61.6
29.9
13.1
36.3
56.6
12.4
64.7
22.5
12.8
20.4
67.1
11.5
61.8
24
11.4
18.4
72.6
CD11b
Ly6G
CD11b
CD11c
F4/80
Ly6C
CD11b
Ly6G
CD11b
CD11c
F4/80
Ly6C
b
PECs
Frequency (%)
100
80
60
40
20
0
Neutrophils
DCs
Macrophages
iMonocytes
Total cell number
1.5x10^6
1.0x10^6
5.0x10^5
2.0x10^5
1.5x10^5
1.0x10^5
5.0x10^4
0.0
Neutrophils
DCs
Macrophages
iMonocytes
WT naive
TRIM21 KO naive
WT
TRIM21 KO

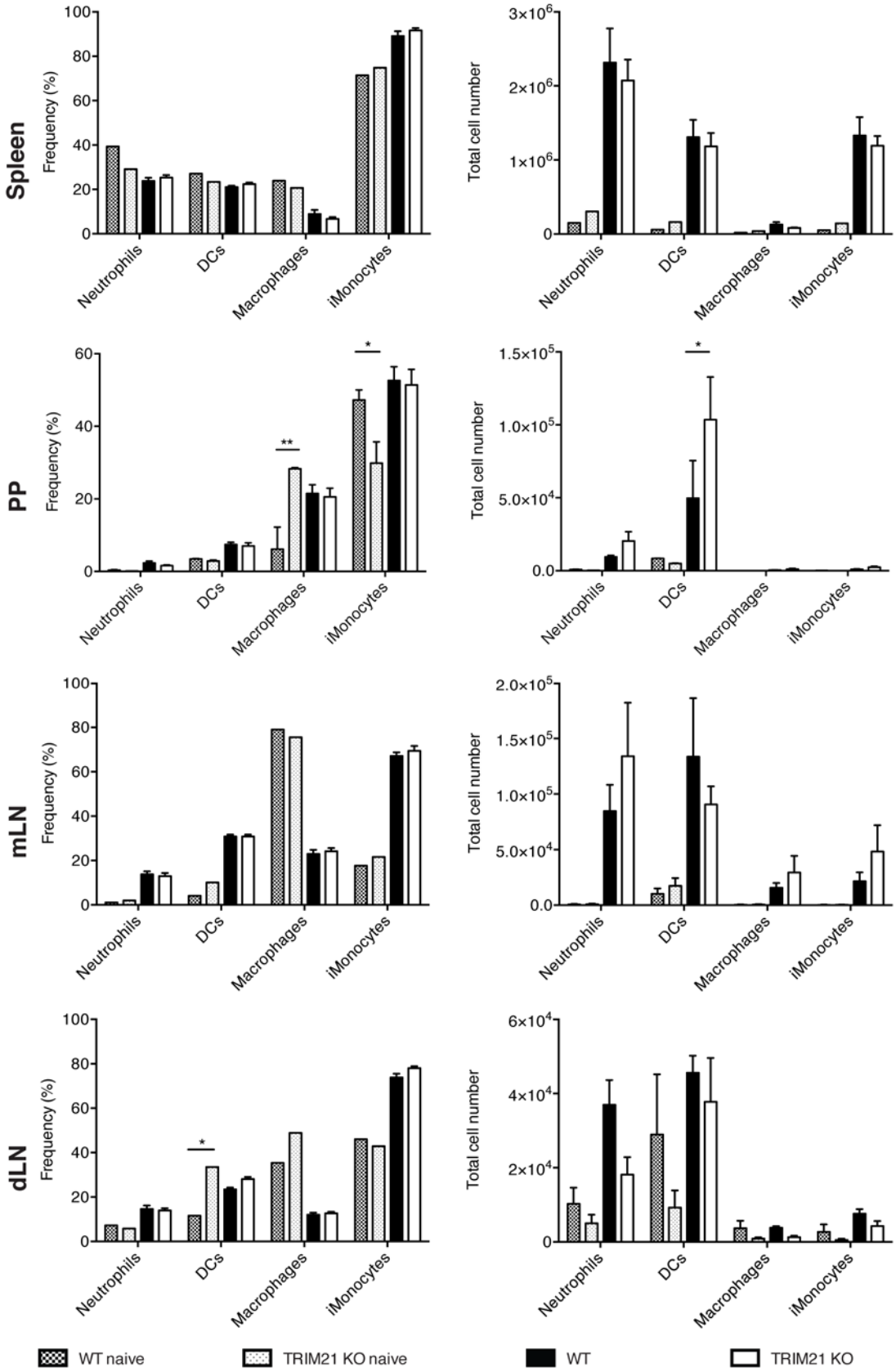

Figure 4.8: Analysis of innate cell populations in TRIM21-deficient mice infected with avirulent *Toxoplasma*.

Wild-type and TRIM21-deficient mice infected intraperitoneally with avirulent *Toxoplasma* were sacrificed at 7 days post-infection (dpi). Immune cells were isolated from the peritoneal exudate (PECs), spleen, Peyer's patches (PP), mesenteric lymph nodes (mLN) and draining lymph nodes dLN). Innate cell populations were analysed by flow cytometry as described in the Experimental Procedure. (**a**) Representative fluorescence-activated cell sorting (FACS) plots of the live, single innate cell populations in wild-type and TRIM21-deficient mice following avirulent *Toxoplasma* infection. (**b**) Example of quantitative analysis of the innate cell populations in wild-type and TRIM21-deficient mice following avirulent *Toxoplasma* infection by frequency (left panel) and total cell number (right panel). Data were chosen from 2 to 4 independent experiments. Mean + SEM, * $p<0.05$, ** $p<0.01$, 2-way ANOVA.

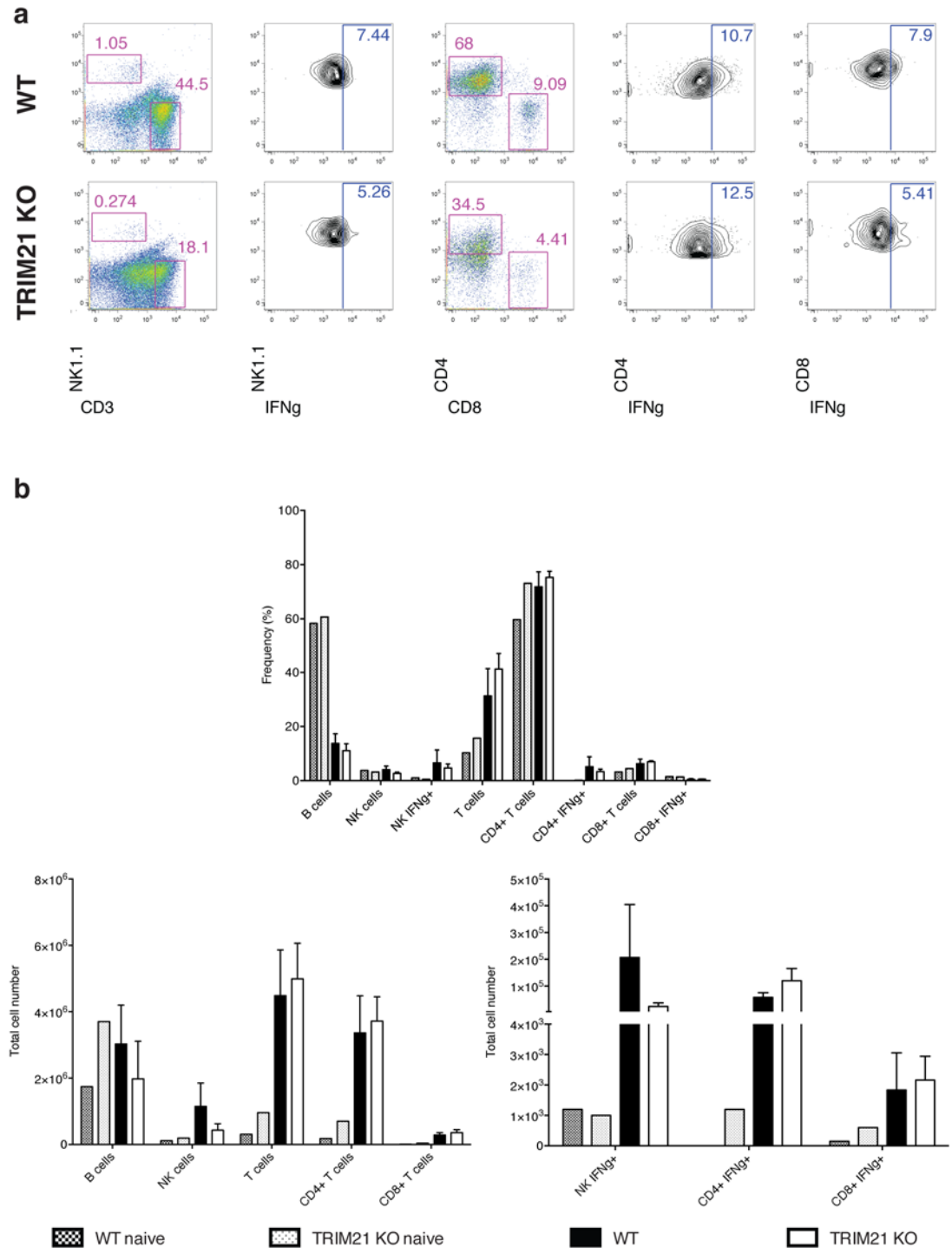

Figure 4.9: Analysis of lymphocyte populations in the peritoneal exudate of TRIM21-deficient mice infected with avirulent *Toxoplasma*.
Wild-type and TRIM21-deficient mice infected intraperitoneally with avirulent *Toxoplasma* were sacrificed at 7 days post-infection (dpi). Lymphocytes were isolated from the peritoneal exudate and lymphocyte populations were analysed by flow cytometry as described in the Experimental Procedure. (**a**) Representative fluorescence-activated cell sorting (FACS) plots of the live, single lymphocyte populations in the peritoneal exudate of wild-type and TRIM21-deficient mice following avirulent *Toxoplasma* infection. (**b**) Example of quantitative analysis of the lymphocyte populations in the peritoneal exudate of wild-type and TRIM21-deficient mice following avirulent *Toxoplasma* infection

by frequency (left panel) and total cell number (right panel). Data were chosen from 2 to 4 independent experiments. Mean + SEM, 2-way ANOVA.

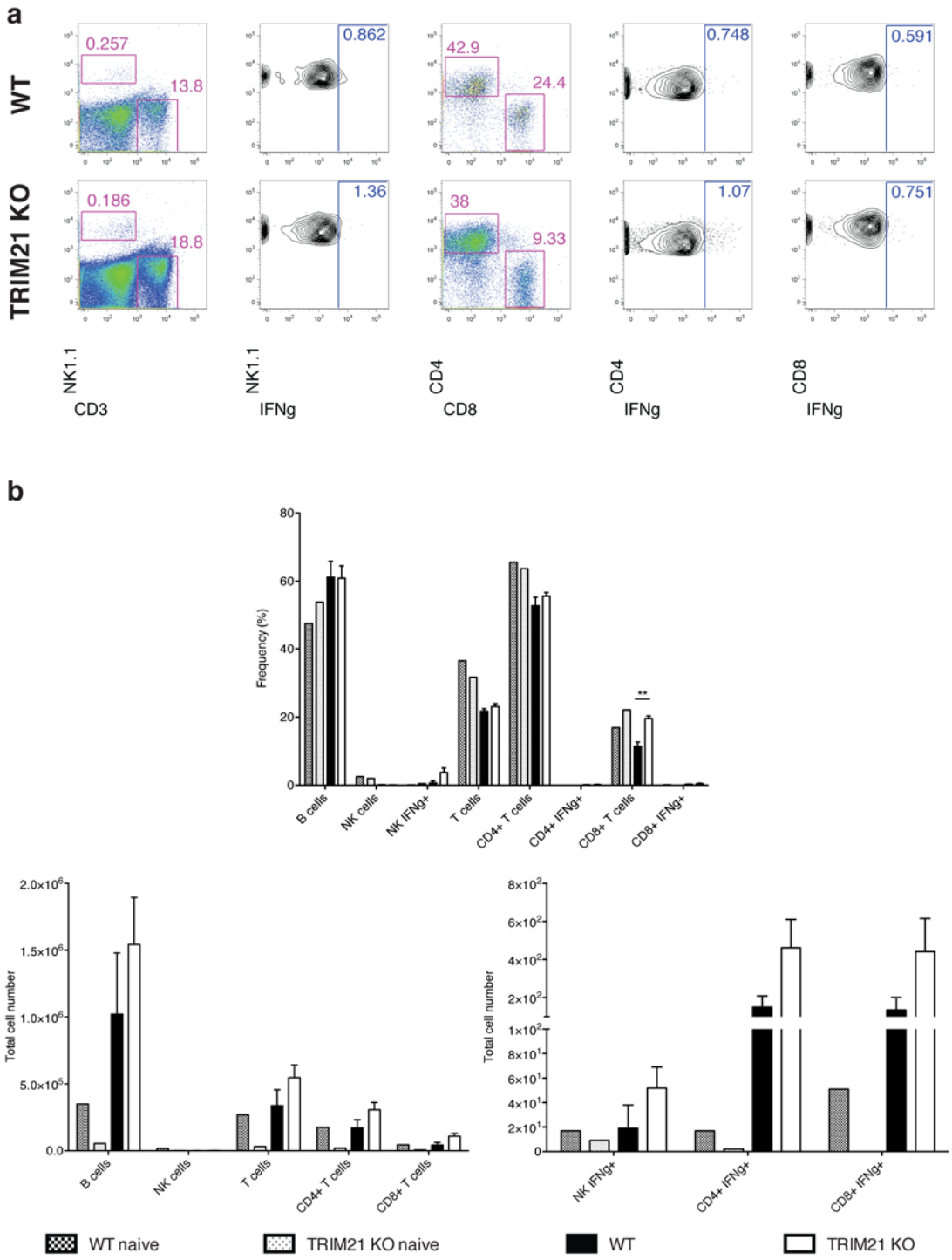

Figure 4.10: Analysis of lymphocyte populations in the spleen of TRIM21-deficient mice infected with avirulent *Toxoplasma*.
Wild-type and TRIM21-deficient mice infected intraperitoneally with avirulent *Toxoplasma* were sacrificed at 7 days post-infection (dpi). Lymphocytes were isolated from the spleen and lymphocyte populations were analysed by flow cytometry as described in the Experimental Procedure. (**a**) Representative fluorescence-activated cell sorting (FACS) plots of the live, single lymphocyte populations in the spleen of wild-type and TRIM21-deficient mice following avirulent *Toxoplasma* infection. (**b**) Example of quantitative analysis of the lymphocytes populations in the spleen of wild-type and TRIM21-deficient mice following avirulent *Toxoplasma* infection by frequency (left panel)

and total cell number (right panel). Data were chosen from 2 to 4 independent experiments. Mean + SEM, ** $p<0.01$, 2-way ANOVA.

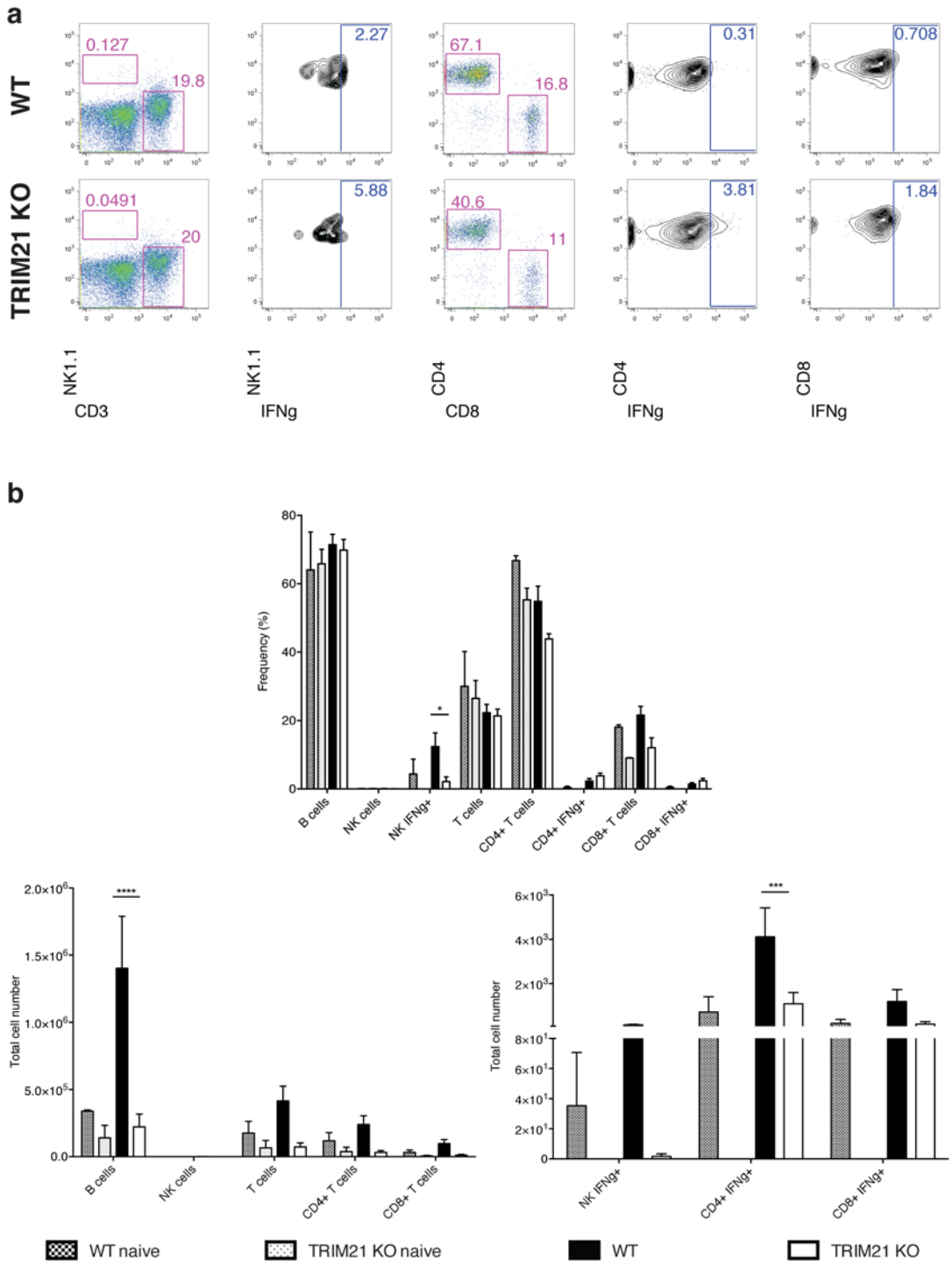

Figure 4.11: Analysis of lymphocyte populations in the Peyer's patches of TRIM21-deficient mice infected with avirulent *Toxoplasma*.
Wild-type and TRIM21-deficient mice infected intraperitoneally with avirulent *Toxoplasma* were sacrificed at 7 days post-infection (dpi). Lymphocytes were isolated from the Peyer's patches and lymphocytes populations were analysed by flow cytometry as described in the Experimental Procedure. (**a**) Representative fluorescence-activated cell sorting (FACS) plots of the live, single lymphocyte populations in the Peyer's patches of wild-type and TRIM21-deficient mice following avirulent *Toxoplasma* infection. (**b**) Example of quantitative analysis of the lymphocyte populations in the Peyer's patches of wild-type and TRIM21-deficient mice following avirulent *Toxoplasma* infection by

frequency (left panel) and total cell number (right panel). Data were chosen from 2 to 4 independent experiments. Mean + SEM, * $p<0.05$, *** $p<0.001$, **** $p<0.0001$, 2-way ANOVA.

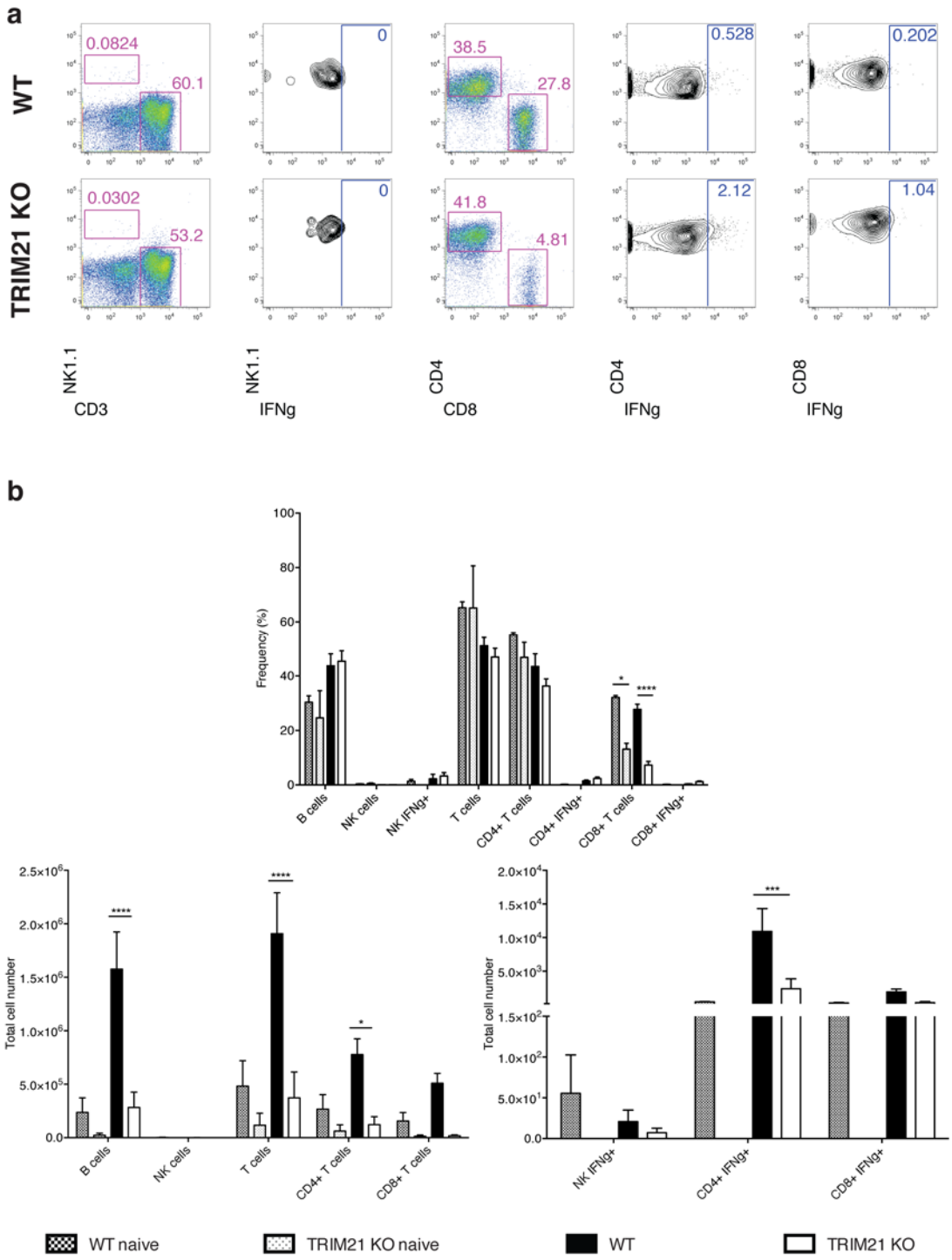

Figure 4.12: Analysis of lymphocytes population in the mesenteric lymph nodes of TRIM21-deficient mice infected with avirulent *Toxoplasma*.
Wild-type and TRIM21-deficient mice infected intraperitoneally with avirulent *Toxoplasma* were sacrificed at 7 days post-infection (dpi). Lymphocytes were isolated from the mesenteric lymph nodes and lymphocyte populations were analysed by flow cytometry as described in the Experimental Procedure. (**a**) Representative fluorescence-activated cell sorting (FACS) plots of the live, single lymphocyte populations in the mesenteric lymph nodes of wild-type and TRIM21-deficient mice following avirulent *Toxoplasma* infection. (**b**) Example of quantitative analysis of the lymphocyte populations in the mesenteric lymph nodes of wild-type and TRIM21-deficient mice following avirulent *Toxoplasma* infection by frequency (left panel) and total cell number (right panel). Data were chosen

from 2 to 4 independent experiments. Mean + SEM, * $p<0.05$, *** $p<0.001$, **** $p<0.0001$, 2-way ANOVA.

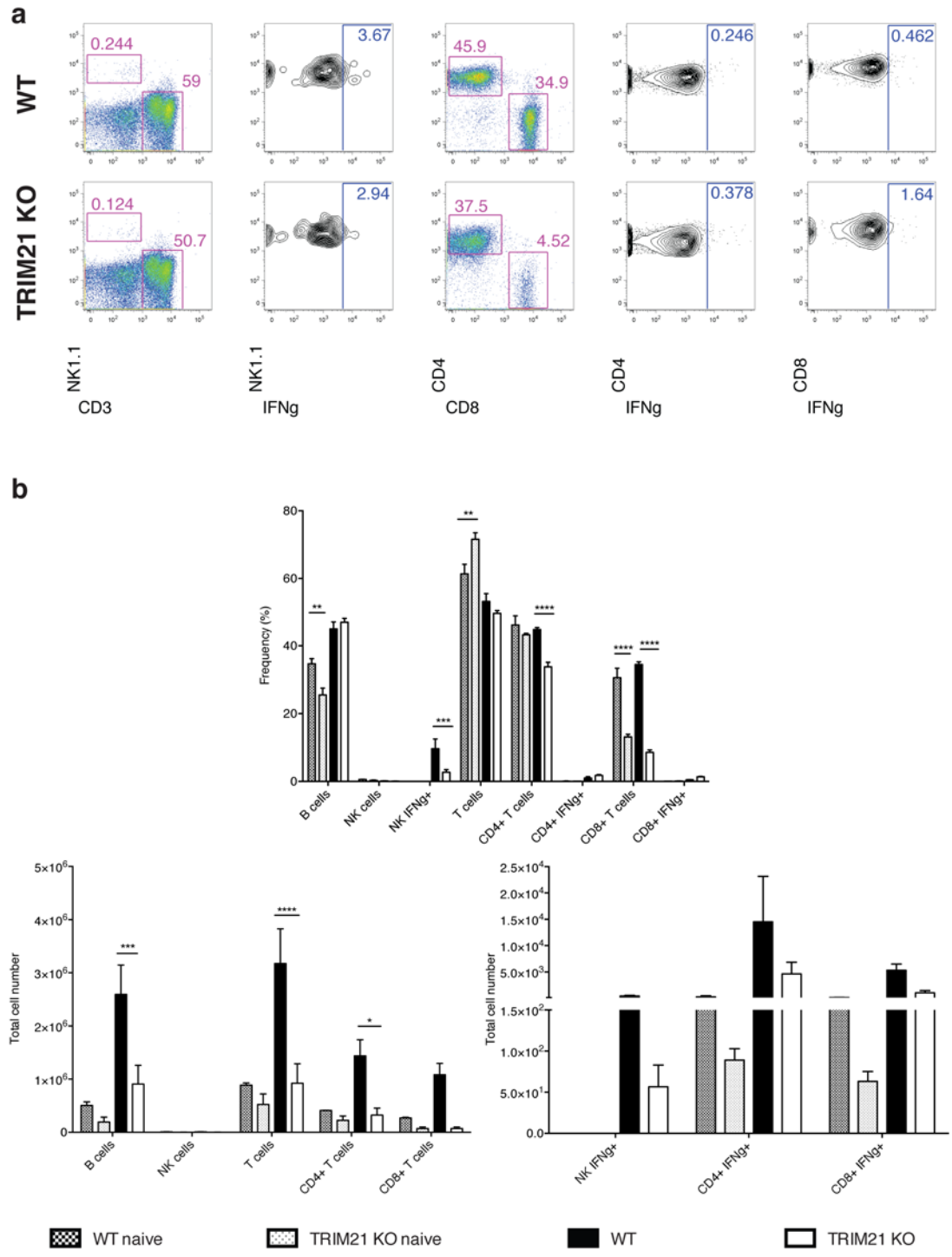

Figure 4.13: Analysis of the lymphocyte populations in the draining lymph nodes of TRIM21-deficient mice infected with avirulent *Toxoplasma*.
Wild-type and TRIM21-deficient mice infected intraperitoneally with avirulent *Toxoplasma* were sacrificed at 7 days post-infection (dpi). Lymphocytes were isolated from the draining lymph nodes and lymphocyte populations were analysed by flow cytometry as described in the Experimental Procedure. (**a**) Representative fluorescence-activated cell sorting (FACS) plots of the live, single lymphocyte populations in the draining lymph nodes of wild-type and TRIM21-deficient mice following avirulent *Toxoplasma* infection. (**b**) Example of quantitative analysis of the lymphocyte populations in the draining lymph nodes of wild-type and TRIM21-deficient mice following avirulent *Toxoplasma* infection by frequency (left panel) and total cell number (right panel). Data were chosen from 2 to 4

independent experiments. Mean + SEM, * $p<0.05$, ** $p<0.01$, *** $p<0.001$, **** $p<0.0001$, 2-way ANOVA.

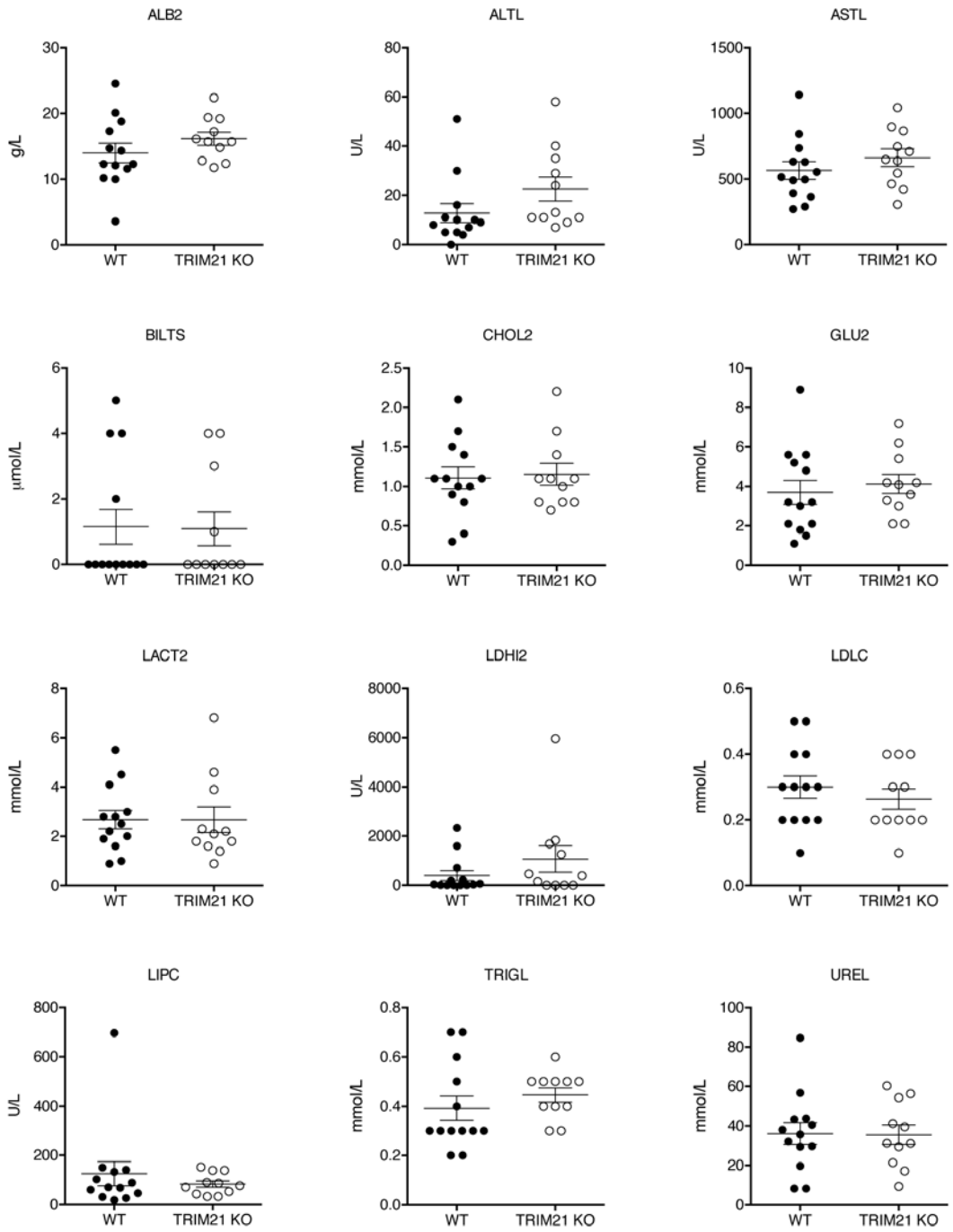

Figure 4.14: TRIM21-deficient mice infected with avirulent *Toxoplasma* do not develop organ dysfunction or damage.
Wild-type and TRIM21-deficient mice infected intraperitoneally with avirulent *Toxoplasma* were sacrificed at 7 days post-infection (dpi). Blood was collected and levels of selected serum biomarkers were measured on the Cobas C111 analyser as described in the Experimental procedure. TRIM21-deficient mice do not exhibit organ dysfunction or damage following infection with avirulent *Toxoplasma*. ALB2: albumin; ALTL: alanine aminotransferase; ASTL: aspartate aminotransferase; BILTS: bilirubin; CHOL2: cholesterol; GLU2: glucose; LACT2: lactate; LDHI2: lactate dehydrogenase; LDLC: low density lipoprotein cholesterol; LIPC: lipase; TRIGL: triglycerides; UREL: urea. Mean + SEM, unpaired t-test.

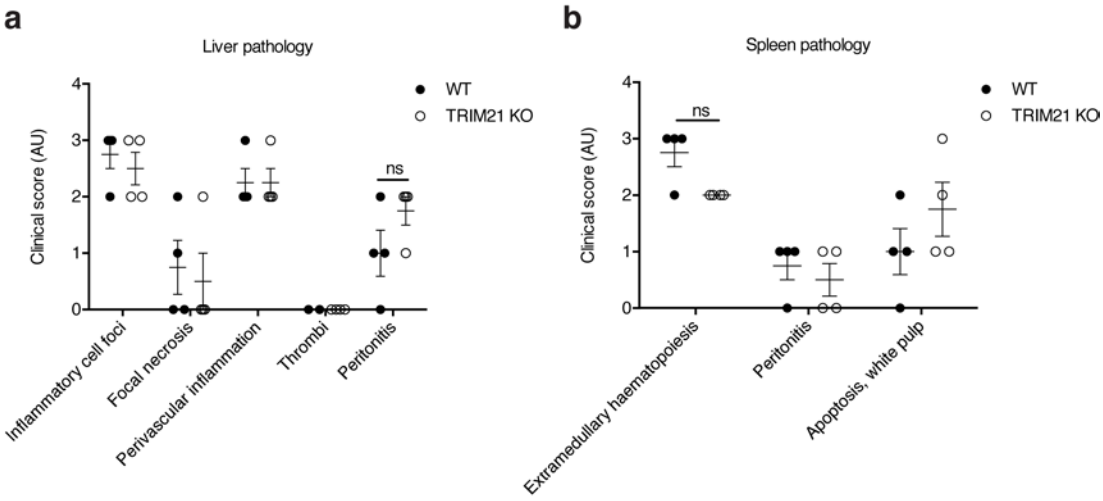

Figure 4.15: TRIM21-deficient mice infected with avirulent *Toxoplasma* do not develop abnormal pathology.
Wild-type and TRIM21-deficient mice infected intraperitoneally with avirulent *Toxoplasma* were sacrificed at 7 days post-infection (dpi). Liver and spleen were fixed in neutral buffered formalin and processed for histology as described in the Experimental Procedure. Analysis of pathology in the liver (**a**) and the spleen (**b**) was performed on hematoxylin and eosin slides by Prof. Cheryl Scudamore. TRIM21-deficient mice do not exhibit abnormal liver and spleen pathology following infection with avirulent *Toxoplasma*. Mean + SEM, 2-way ANOVA.

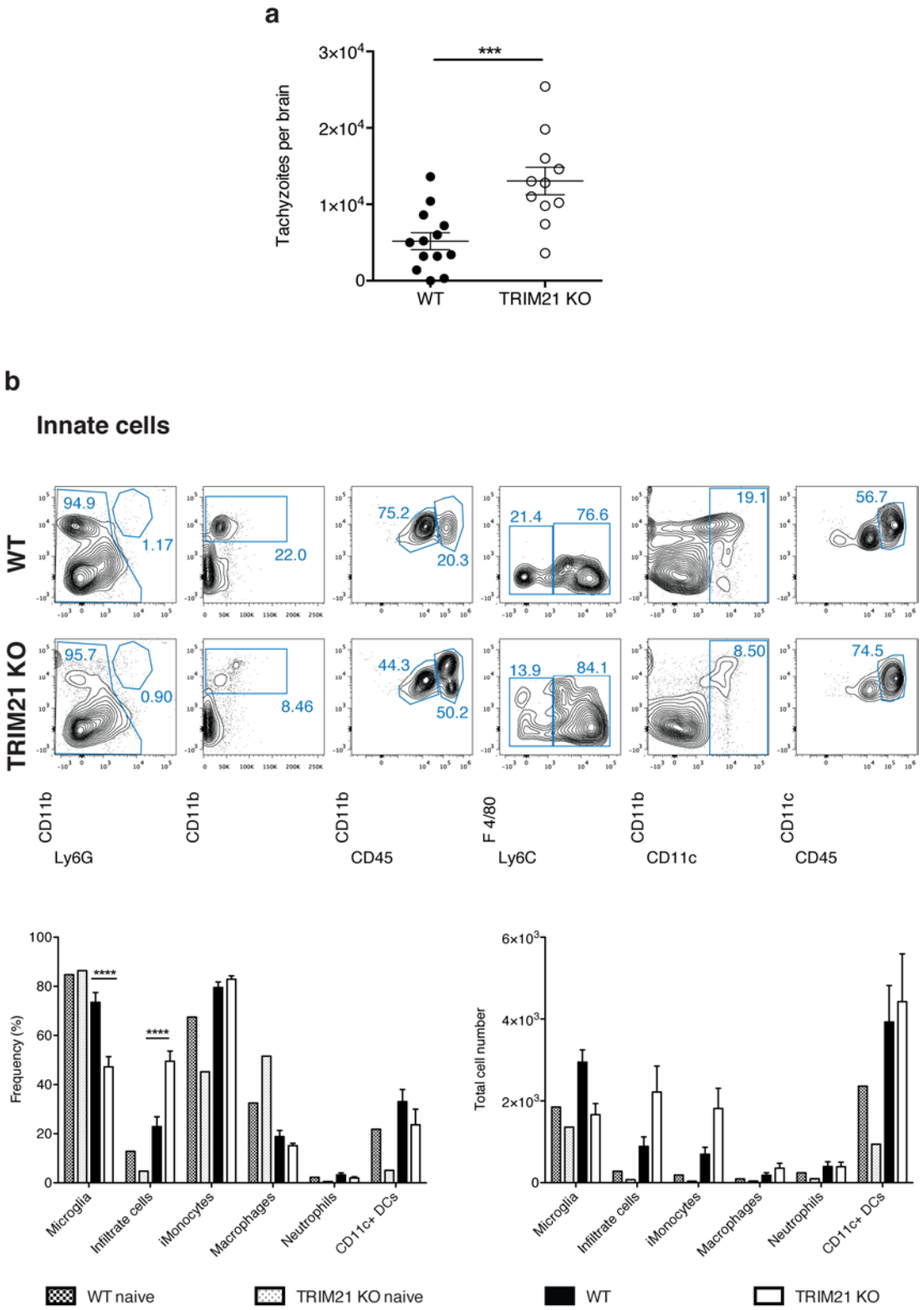
a
Tachyzoites per brain
3×10^4
2×10^4
1×10^4
0
***
WT
TRIM21 KO
b
Innate cells
WT
TRIM21 KO
94.9
1.17
22.0
75.2
20.3
21.4
76.6
19.1
56.7
95.7
0.90
8.46
44.3
50.2
13.9
84.1
8.50
74.5
CD11b
Ly6G
CD11b
CD11b
CD45
F 4/80
Ly6C
CD11b
CD11c
CD11c
CD45
Frequency (%)
100
80
60
40
20
0
****
****
Microglia
Infiltrate cells
iMonocytes
Macrophages
Neutrophils
CD11c+ DCs
Total cell number
6×10^3
4×10^3
2×10^3
0
Microglia
Infiltrate cells
iMonocytes
Macrophages
Neutrophils
CD11c+ DCs
WT naive
TRIM21 KO naive
WT
TRIM21 KO

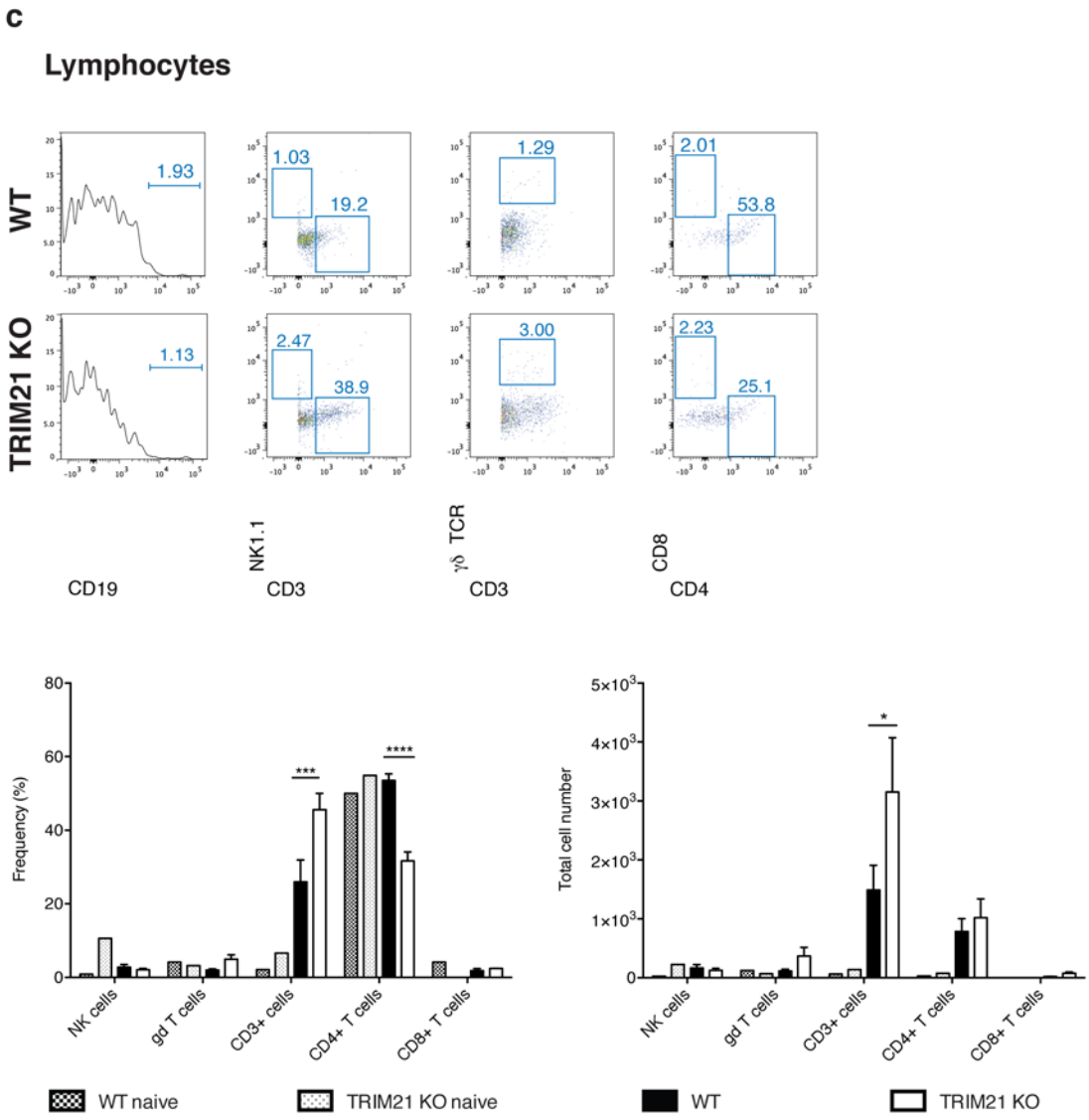

Figure 4.16: TRIM21-deficient mice exhibit a higher parasite burden and a decreased microglia population in the brain following avirulent *Toxoplasma* infection.
Wild-type and TRIM21-deficient mice infected intraperitoneally with avirulent *Toxoplasma* were sacrificed at 7 days post-infection (dpi). Brains were isolated and used for the determination of the parasite load or analysis of the immune cell populations. (**a**) Quantitative analysis of the number of GFP-expressing *Toxoplasma* tachyzoites in the brain of wild-type and TRIM21-deficient mice at 7 dpi. Data pooled from three independent experiments. Mean + SEM, *** $p<0.001$, unpaired t-test. (**b**) Innate cells were isolated from the brain and innate cell populations were analysed by flow cytometry as described in the Experimental Procedure. The plots are representative fluorescence-activated cell sorting (FACS) plots of the live, single innate cell populations in the brain of wild-type and TRIM21-deficient mice following avirulent *Toxoplasma* infection. The graphs are quantitative analyses of innate cell populations in the brain of wild-type and TRIM21-deficient mice following avirulent *Toxoplasma* infection by frequency (left panel) and total cell number (right panel). Data representative of two independent experiments. Mean + SEM, **** $p<0.0001$, 2-way ANOVA. (**c**) Lymphocytes were isolated from the brain and lymphocyte populations were analysed by flow cytometry as described in the Experimental Procedure. The plots are representative FACS plots of the live, single lymphocyte populations in the brain of wild-type and TRIM21-deficient mice following avirulent *Toxoplasma* infection. The graphs are quantitative analyses of lymphocyte populations in the brain of wild-type and TRIM21-deficient mice following avirulent *Toxoplasma* infection by frequency (left panel) and total cell number (right panel). Data representative of two independent experiments. Mean + SEM, * $p<0.05$, *** $p<0.001$, **** $p<0.0001$, 2-way ANOVA.

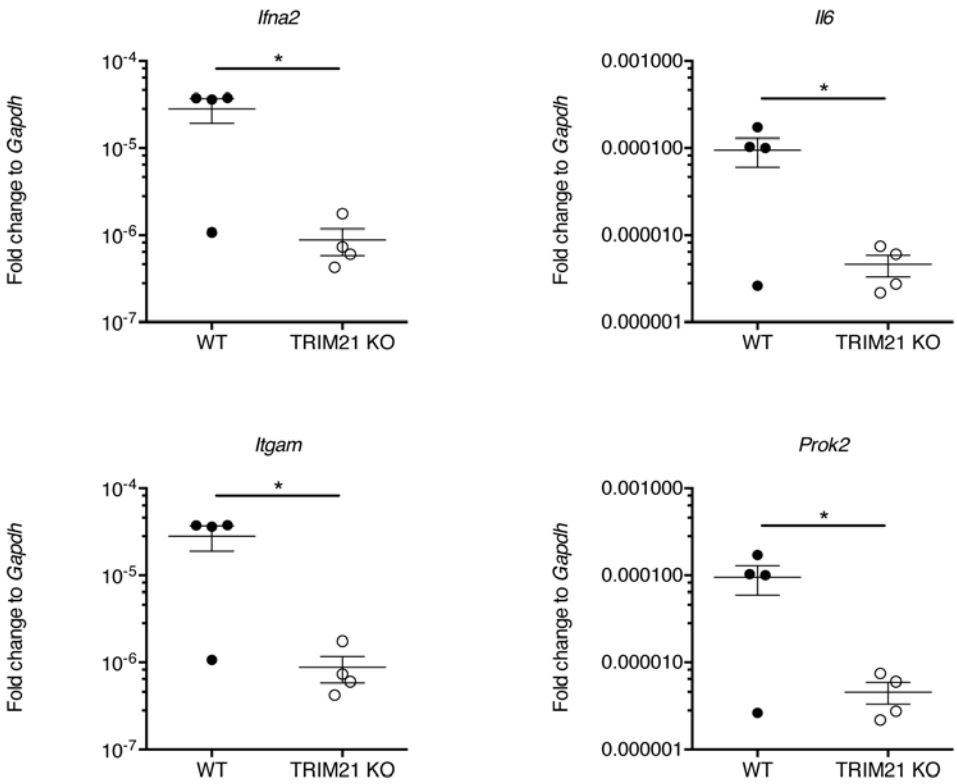

Figure 4.17: TRIM21-deficient mice exhibit decreased levels of transcripts involved in the brain immune inflammatory response to avirulent *Toxoplasma* infection.
Wild-type and TRIM21-deficient mice infected intraperitoneally with avirulent *Toxoplasma* were sacrificed at 7 days post-infection (dpi). Brains were isolated, RNA was isolated and gene expression was assessed by quantitative polymerase chain reaction as described in the Experimental Procedure. Mice lacking TRIM21 present significantly lower levels of transcripts involved in the inflammatory response. Mean + SEM, * $p<0.05$, unpaired t-test.

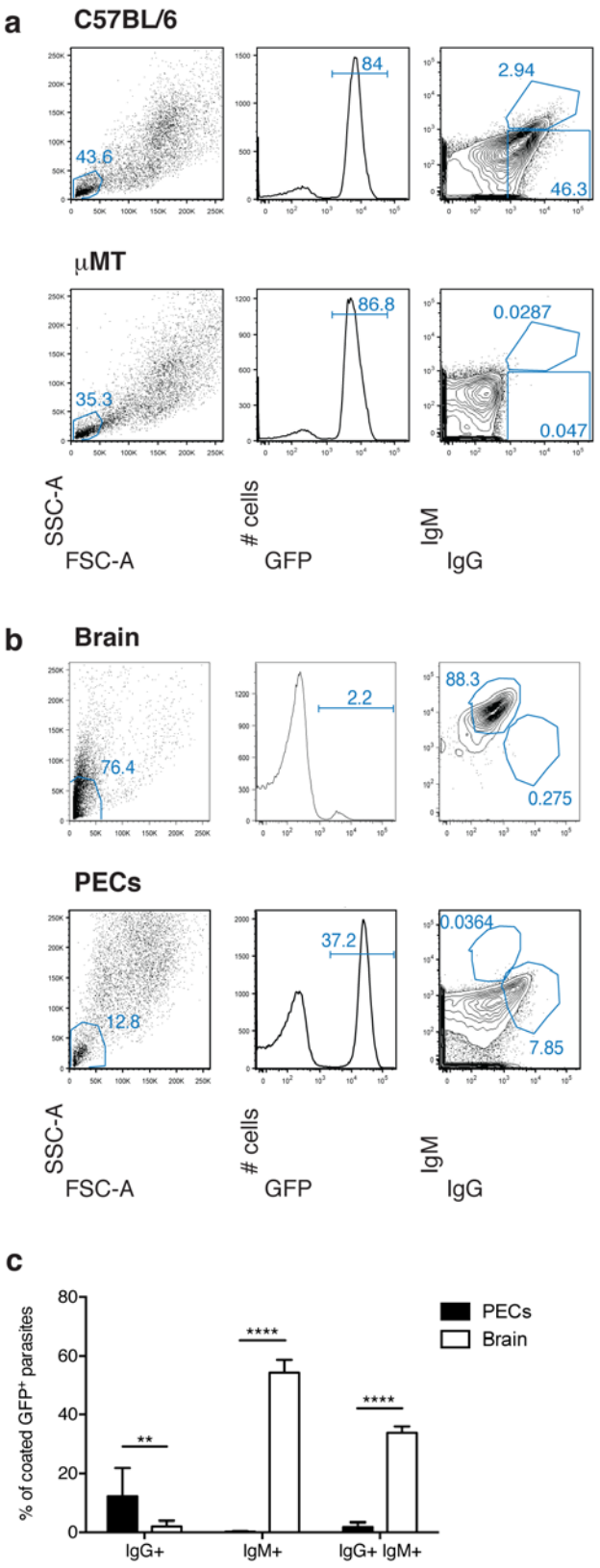

Figure 4.18: Analysis of the antibody coating of *in vivo Toxoplasma* tachyzoites.
Toxoplasma tachyzoites were isolated from the peritoneum and/or brain of infected mice and their potential antibody coating was analysed by flow cytometry as described in the Experimental Procedure. (**a**) Antibody coating profiles of *Toxoplasma* tachyzoites purified from the peritoneum of C57BL/6 mice (upper panel) or B cells-deficient mMT mice (lower panel) at 4 days post-infection. Fluorescence-

activated cell sorting (FACS) plots are representative of at least 4 independent experiments. In the presence of circulating antibodies, *Toxoplasma* parasites are mainly coated with IgG. (**b**) Antibody coating profiles of *Toxoplasma* tachyzoites purified from the brain (upper panel) or peritoneum (PECs, lower panel) of C57BL/6 mice at 7 days post-infection. FACS plots are representative of at least 3 independent experiments. *Toxoplasma* tachyzoites are coated with IgM in the brain and with IgG in the peritoneum. (**c**) Quantitative analysis of the antibody coating profile of *Toxoplasma* tachyzoites in the peritoneum (PECs) and brain of C57BL/6 mice at 7 days post-infection. Data representative of three independent experiments. *Toxoplasma* tachyzoites are coated with IgM in the brain and with IgG in the peritoneum. Mean + SEM, ** $p<0.01$, **** $p<0.0001$, 2-way ANOVA.

Chapter 5

Conclusion and Perspectives

During *Toxoplasma* infection, IFNγ is the main cytokine produced and it orchestrates the immune response that involves the recruitment of the two families of large GTPases, the p47 IRGs and p65 GBPs to the avirulent parasitophorous vacuole. This accumulation of large GTPases leads to the disruption of the avirulent *Toxoplasma* vacuole and its subsequent clearance by autophagy. The mechanisms by which the GBPs are recruited to the vacuole, as well as the downstream effectors triggered after the disruption of the parasitophorous vacuole remain unclear. The aim of this work was to identify new host factors that play a role at the parasitophorous vacuole and contribute to mediating the restriction of *Toxoplasma*.

In the first part of this study, I showed for the first time that ubiquitin decorates the parasitophorous vacuole of avirulent *Toxoplasma* in an IFNγ-dependent manner. The E3 ubiquitin ligase TRIM21 was identified as the first putative interaction partner of GBP1 during *Toxoplasma* infection. The IFNγ-mediated GBP1-TRIM21 cytoplasmic complex recruits to the avirulent *Toxoplasma* vacuole. TRIM21 has been shown bind to invading antibody-coated adenoviruses and targets them to degradation by the proteasome due to its E3 ligase activity (Mallery et al., 2010), thereby enabling to control viremia *in vivo* (Vaysburd et al., 2013). The *in vitro* experiments reported in this work have been performed in medium supplemented with FCS, where antibodies can hence be present. As a result, it remains to be assessed with antibody-free medium and parasites versus antibody-coated parasites whether the recruitment of TRIM21 and GBP1 to avirulent *Toxoplasma* vacuoles is dependent on antibodies. Additionally, TRIM21 regulates Lys63-linked ubiquitination in the vicinity of the vacuole, but the *in vitro* studies suggest TRIM21 does not participate in the restriction of *Toxoplasma* in mouse embryonic fibroblasts or in the regulation of immune signalling in

macrophages. Very interestingly, ubiquitinated proteins identified in this study include GBP1 and GBP2 proteins. Moreover, the TRIM21-mediated regulation of the GBPs appear to be both at the transcriptional and the protein level, with GBP1 being downregulated while GBP2 being upregulated. These results will be confirmed in the future by quantitative polymerase chain reaction, and point to TRIM21 having a role in regulating the differential biological function of GBP1 and GBP2 during *Toxoplasma* infection that still needs to be elucidated. As the SILAC results and the RNAseq data show that the protein abundance of both GBP1 and GBP2 is altered in cells lacking TRIM21, one cannot exclude that the differential ubiquitination profile of the GTPases is simply due to a difference in the protein level in TRIM21-deficient cells. To address this, a new SILAC experiment with a targeted quantification of the GBPs protein levels as well as with a targeted analysis of the GBPs diGLY sites would enable assessment of whether the ubiquitination patterns observed are real. Moreover, the difference in ubiquitination profiles will be confirmed by immunoprecipitating ubiquitinated proteins in wild-type and TRIM21 KO cells and immunoblotting for GBP1 or GBP2. As GBP1 recruitment is partly dependent on the presence of TRIM21, it is likely the E3 ubiquitin ligase mediates a ubiquitination cascade that GBP1 is dependent on. The IRGs- and GBPs-mediated disruption of the vacuole could possibly unmask abnormally localised intracellular antibodies coating *Toxoplasma*. Both the presence of intracellular antibodies in *Toxoplasma* infection and a binding to these by TRIM21 with the functional consequences this would trigger remain unclear. Finally, TRIM21 strikingly and mainly transcriptionally downregulates one specific biological pathway that is the biosynthesis of cholesterol. As *Toxoplasma* is auxotroph for cholesterol and hence relies on its host as a source for the molecule, this could be a mean by which TRIM21 fights against *Toxoplasma*.

In the second part of this work, I report that TRIM21-deficient mice are highly susceptible to *Toxoplasma* infection, hence highlighting the important role of the protein in resistance against the parasitic infection. Mice lacking TRIM21 succumb during the acute phase of the infection, between day 7 and 10 post-inoculation. The death of the animals is preceded by an increased parasite burden in the periphery at 5 days post-infection, and the death correlates with a higher parasite load in the brain at day 7 post-infection. Although TRIM21-deficient mice do not develop any abnormal pathology or differential immune cell populations in the periphery, they exhibit a decreased production of inflammatory cytokines in the serum. This lower immune response is also reflected in the brain, where the transcriptional levels of genes involved in the immune response and the number of microglial cells are both decreased. One property of TRIM21 recently brought to the fore is its ability to bind to intracellular antibody-coated adenoviruses (Mallery et al., 2010). As far as *Toxoplasma* is concerned, the presence of antibodies inside the vacuole at the surface of the parasite following invasion remains unclear. It is generally accepted that a fraction of the Toxoplasma-derived surface-exposed proteins are shed or not carried into the cell due to sieving at the Tight Junction during parasite invasion (Walzer and Genta, 1989). With regards to bound antibodies, electron microscopy of anti-P30 (the major *Toxoplasma* surface protein) coated parasites left to invade HeLa cells demonstrated that most of the parasite surface-attached antibody was shed, however, some escape was noted and a minor fraction of the parasites were faintly labelled with anti-P30 antibody intracellularly (Dubremetz et al., 1985). In terms of viral neutralisation, it has been calculated that 1.6 antibodies per virus particle suffice for TRIM21 activity in the presence of interferon (MacEwan et al., 2012). It is thus conceivable that very few residual antibodies bound to the parasite could trigger the

activity of TRIM21. I showed in preliminary work that avirulent *Toxoplasma* tachyzoites isolated from the peritoneum of a C57BL/6 mouse are mainly coated with IgG, while parasites isolated from the peritoneum of μMT mice lacking B cells and hence circulating antibodies, do not harbour any antibody. These preliminary data also show that avirulent *Toxoplasma* isolated from the immune privilege brain of a C57BL/6 mouse were mainly coated with IgM. How this differential antibody decoration influences the immune response to the parasite at the site of infection remains unknown. As B cell-deficient mice die of a high parasite load in the brain (Kang et al., 2000), it is tempting to hypothesise that TRIM21 and antibodies act in concert during *Toxoplasma* infection, such that TRIM21 could sense antibody-coated parasites like it does detect adenoviruses. However, this hypothesis would prove to be difficult to test *in vivo*, as even backcrossing TRIM21-deficient mice on the μMT genetic background would not help determine the individual or combined role of TRIM21 and antibodies.

Altogether, the data gathered during this study indicate TRIM21 is an important player in the resistance against *Toxoplasma* infection in the mouse model, acting on both the regulation of the immune response to the parasite and the restriction of the parasite replication. How this dual function is achieved remains to be further determined. First, TRIM21-mediated Lys63-linked ubiquitination at the vicinity of avirulent *Toxoplasma* could be responsible for the differential downstream immune signalling outcome. It is thus essential to determine the consequence of ubiquitination around the avirulent PV, whether it be by mediating the recruitment of other effectors to the vacuole or by regulating other E3 ligases or deubiquitinases. Second, it is tempting to speculate that the TRIM21-mediated ubiquitination of the GBPs as well as the downregulation of the cholesterol biosynthesis both impact on the ability of the parasite to successfully thrive

in the host. It is imperative to continue deciphering the precise role of the different GBPs at the *Toxoplasma* vacuole in order to understand how their TRIM21-mediated differential ubiquitination and expression level can affect the response to *Toxoplasma* infection. The importance of TRIM21 in the regulation of cholesterol metabolism during *Toxoplasma* infection could be further investigated by confirming the differential cholesterol levels *in vivo* by immunobloting, polymerase chain reaction and mass spectrometry, but also by treating the animals with statins, molecules that inhibit hydroxyl methyl glutaryl-CoA reductase, an enzyme crucial for the production of cholesterol in the liver (Endo et al., 1976). Should TRIM21-mediated downregulation of the cholesterol be important for the restriction of *Toxoplasma*, TRIM21-deficient mice treated with statins would present reduced levels of cholesterol and could be rescued. Moreover, the discrepancy between the *in vivo* imaging (where TRIM21-deficiency leads to a higher parasite load) and the *in vitro* plaque assay (where TRIM21-deficient cells can contain *Toxoplasma* replication) could be explained by the fact that the latter has been performed in the presence of serum-containing cholesterol, thereby allowing the parasite to grow and replicate happily in TRIM21-deficient cells. The plaque assay will be reproduced in the near future in the presence of a lipoprotein-free serum in order to determine whether the outcome of the experiment will be different.

To conclude, I have demonstrated in this work the importance of TRIM21 in the resistance against *Toxoplasma* infection, acting on both the restriction of the parasite itself as well as on the regulation of the inflammatory response. Further investigations will help understand the proper mechanisms underlying these two properties. However, I could hypothesise that by upregulating the production of inflammatory cytokines and downregulating the biosynthesis of cholesterol, TRIM21 participates in

the control of *Toxoplasma* replication, avoiding a high parasite burden in the periphery and subsequently in the brain that correlates with higher mortality in the mouse.

References

Abdullah, N., B. Srinivasan, N. Modiano, P. Cresswell, and A.K. Sau. 2009. Role of individual domains and identification of internal gap in human guanylate binding protein-1. *J. Mol. Biol.* 386:690–703. doi:10.1016/j.jmb.2008.12.060.

Abdullah, N., M. Balakumari, and A.K. Sau. 2010. Dimerization and its role in GMP formation by human guanylate binding proteins. *Biophys. J.* 99:2235–2244. doi:10.1016/j.bpj.2010.07.025.

Adams, L.B., J.B. Hibbs, R.R. Taintor, and J.L. Krahenbuhl. 1990. Microbiostatic effect of murine-activated macrophages for Toxoplasma gondii. Role for synthesis of inorganic nitrogen oxides from L-arginine. *J. Immunol.* 144:2725–2729.

Ajioka, J.W., J.M. Fitzpatrick, and C.P. Reitter. 2001. Toxoplasma gondii genomics: shedding light on pathogenesis and chemotherapy. *Expert Rev Mol Med*. 2001:1–19. doi:10.1017/S1462399401002204.

Al-Zeer, M.A., H.M. Al-Younes, D. Lauster, M. Abu Lubad, and T.F. Meyer. 2013. Autophagy restricts Chlamydia trachomatis growth in human macrophages via IFNG-inducible guanylate binding proteins. *Autophagy*. 9:50–62. doi:10.4161/auto.22482.

Al-Zeer, M.A., H.M. Al-Younes, P.R. Braun, J. Zerrahn, and T.F. Meyer. 2009. IFN-gamma-inducible Irga6 mediates host resistance against Chlamydia trachomatis via autophagy. *PLoS ONE*. 4:e4588. doi:10.1371/journal.pone.0004588.

Alaganan, A., S.J. Fentress, K. Tang, Q. Wang, and L.D. Sibley. 2014. Toxoplasma GRA7 effector increases turnover of immunity-related GTPases and contributes to acute virulence in the mouse. *Proc. Natl. Acad. Sci. U.S.A.* doi:10.1073/pnas.1313501111.

Alexander, D.L., J. Mital, G.E. Ward, P. Bradley, and J.C. Boothroyd. 2005. Identification of the moving junction complex of Toxoplasma gondii: a collaboration between distinct secretory organelles. *PLoS Pathog.* 1:e17. doi:10.1371/journal.ppat.0010017.

Alexopoulou, L., A.C. Holt, R. Medzhitov, and R.A. Flavell. 2001. Recognition of double-stranded RNA and activation of NF-kappaB by Toll-like receptor 3. *Nature*. 413:732–738. doi:10.1038/35099560.

Aliprantis, A.O., R.B. Yang, M.R. Mark, S. Suggett, B. Devaux, J.D. Radolf, G.R. Klimpel, P. Godowski, and A. Zychlinsky. 1999. Cell activation and apoptosis by bacterial lipoproteins through toll-like receptor-2. *Science*. 285:736–739.

Alix, E., S. Mukherjee, and C.R. Roy. 2011. Subversion of membrane transport pathways by vacuolar pathogens. *J. Cell Biol.* 195:943–952. doi:10.1083/jcb.201105019.

Alnemri, E.S., D.J. Livingston, D.W. Nicholson, G. Salvesen, N.A. Thornberry, W.W. Wong, and J. Yuan. 1996. Human ICE/CED-3 protease nomenclature. *Cell*. 87:171.

Alonso, S., K. Pethe, D.G. Russell, and G.E. Purdy. 2007. Lysosomal killing of

Mycobacterium mediated by ubiquitin-derived peptides is enhanced by autophagy. *Proc. Natl. Acad. Sci. U.S.A.* 104:6031–6036. doi:10.1073/pnas.0700036104.

Alvarado-Esquivel, C., Antonio Sifuentes-Alvarez, S.G. Narro-Duarte, S. Estrada-Martinez, Juan Humberto Diaz-Garcia, O. Liesenfeld, S.A. Martinez- Garcia, and A. Canales-Molina. 2006. Seroepidemiology of *Toxoplasma gondii* infection in pregnant women in a public hospital in northern Mexico. *BMC Infect. Dis.* 6:113–119.

Amer, A., L. Franchi, T.-D. Kanneganti, M. Body-Malapel, N. Ozören, G. Brady, S. Meshinchi, R. Jagirdar, A. Gewirtz, S. Akira, and G. Núñez. 2006. Regulation of Legionella phagosome maturation and infection through flagellin and host Ipaf. *J. Biol. Chem.* 281:35217–35223. doi:10.1074/jbc.M604933200.

Amer, A.O., and M.S. Swanson. 2005. Autophagy is an immediate macrophage response to Legionella pneumophila. *Cell. Microbiol.* 7:765–778. doi:10.1111/j.1462-5822.2005.00509.x.

Ancelle, T., V. Goulet, V. Tirard-Fleury, L. Baril, C. du Mazaubrun, P. Thulliez, M. Wcislo, and B. Carme. 1996. La toxoplasmose chez la femme enceinte en France en 1995. *Bull Epidemiol Hebdomadaire*. 51:227–229.

Anders, S., P.T. Pyl, and W. Huber. 2015. HTSeq--a Python framework to work with high-throughput sequencing data. *Bioinformatics*. 31:166–169. doi:10.1093/bioinformatics/btu638.

Anderson, C.L. 1982. Isolation of the receptor for IgG from a human monocyte cell line (U937) and from human peripheral blood monocytes. *J. Exp. Med.* 156:1794–1806.

Anderson, S.L., J.M. Carton, J. Lou, L. Xing, and B.Y. Rubin. 1999. Interferon-induced guanylate binding protein-1 (GBP-1) mediates an antiviral effect against vesicular stomatitis virus and encephalomyocarditis virus. *Virology*. 256:8–14. doi:10.1006/viro.1999.9614.

Antoniou, M., H. Tzouvali, S. Sifakis, E. Galanakis, E. Georgopoulou, V. Liakou, C. Giannakopoulou, E. Koumantakis, and Y. Tselentis. 2004. Incidence of toxoplasmosis in 5532 pregnant women in Crete, Greece: management of 185 cases at risk. *Eur. J. Obstet. Gynecol. Reprod. Biol.* 117:138–143. doi:10.1016/j.ejogrb.2004.03.001.

Arnheiter, H., S. Skuntz, M. Noteborn, S. Chang, and E. Meier. 1990. Transgenic mice with intracellular immunity to influenza virus. *Cell*. 62:51–61.

Asencio, M.A., O. Herraez, J.M. Tenias, E. Garduño, M. Huertas, R. Carranza, and J.M. Ramos. 2015. Seroprevalence survey of zoonoses in Extremadura, southwestern Spain, 2002-2003. *Jpn. J. Infect. Dis.* 68:106–112. doi:10.7883/yoken.JJID.2014.181.

Aubert, D., F. Foudrinier, I. Villena, J.M. Pinon, M.F. Biava, and E. Renoult. 1996. PCR for diagnosis and follow-up of two cases of disseminated toxoplasmosis after

kidney grafting. *J. Clin. Microbiol.* 34:1347.

Ayala, J.M., T.T. Yamin, L.A. Egger, J. Chin, M.J. Kostura, and D.K. Miller. 1994. IL-1 beta-converting enzyme is present in monocytic cells as an inactive 45-kDa precursor. *J. Immunol.* 153:2592–2599.

Ayi, I., S.A. Edu, K.A. Apea-Kubi, D. Boamah, K.M. Bosompem, and D. Edoh. 2009. Sero-epidemiology of toxoplasmosis amongst pregnant women in the greater accra region of ghana. *Ghana Med J*. 43:107–114.

Baboshina, O.V., and A.L. Haas. 1996. Novel multiubiquitin chain linkages catalyzed by the conjugating enzymes E2EPF and RAD6 are recognized by 26 S proteasome subunit 5. *J. Biol. Chem.* 271:2823–2831.

Bach, H., K.G. Papavinasasundaram, D. Wong, Z. Hmama, and Y. Av-Gay. 2008. Mycobacterium tuberculosis virulence is mediated by PtpA dephosphorylation of human vacuolar protein sorting 33B. *Cell Host and Microbe*. 3:316–322. doi:10.1016/j.chom.2008.03.008.

Baril, L., T. Ancelle, V. Goulet, P. Thulliez, V. Tirard-Fleury, and B. Carme. 1999. Risk factors for Toxoplasma infection in pregnancy: a case-control study in France. *Scand. J. Infect. Dis.* 31:305–309.

Barlow, P.N., B. Luisi, A. Milner, M. Elliott, and R. Everett. 1994. Structure of the C3HC4 domain by 1H-nuclear magnetic resonance spectroscopy. A new structural class of zinc-finger. *J. Mol. Biol.* 237:201–211. doi:10.1006/jmbi.1994.1222.

Baroja-Mazo, A., F. Martín-Sánchez, A.I. Gomez, C.M. Martínez, J. Amores-Iniesta, V. Compan, M. Barberà-Cremades, J. Yagüe, E. Ruiz-Ortiz, J. Antón, S. Buján, I. Couillin, D. Brough, J.I. Arostegui, and P. Pelegrín. 2014. The NLRP3 inflammasome is released as a particulate danger signal that amplifies the inflammatory response. *Nat. Immunol.* 15:738–748. doi:10.1038/ni.2919.

Barragan, A., and L.D. Sibley. 2002. Transepithelial migration of Toxoplasma gondii is linked to parasite motility and virulence. *J. Exp. Med.* 195:1625–1633.

Batz, M.B., S. Hoffmann, and J.G. Morris. 2012. Ranking the disease burden of 14 pathogens in food sources in the United States using attribution data from outbreak investigations and expert elicitation. *Journal of Food Protection*. 75:1278–1291. doi:10.4315/0362-028X.JFP-11-418.

Behring, von, E. 1890. Untersuchungen ueber das Zustandekommen der Diphteria-Immunitaet bei Thieren. *deutsche medizinische Wochenschrift (1946)*. 16:1145–1148.

Behring, von, E., and S. Kitasato. 1890. Ueber das Zustandekommen der Diphterie-Immunitaet und der Tetanus-Immunitaet bei Tieren. *deutsche medizinische Wochenschrift (1946)*. 13.

Bekpen, C., J.P. Hunn, C. Rohde, I. Parvanova, L. Guethlein, D.M. Dunn, E. Glowalla, M. Leptin, and J.C. Howard. 2005. The interferon-inducible p47 (IRG) GTPases in vertebrates: loss of the cell autonomous resistance mechanism in the human

lineage. *Genome Biol*. 6:R92. doi:10.1186/gb-2005-6-11-r92.

Ben-Chetrit, E., E.K. Chan, K.F. Sullivan, and E.M. Tan. 1988. A 52-kD protein is a novel component of the SS-A/Ro antigenic particle. *J. Exp. Med.* 167:1560–1571.

Berenreiterová, M., J. Flegr, A.A. Kuběna, and P. Němec. 2011. The distribution of Toxoplasma gondii cysts in the brain of a mouse with latent toxoplasmosis: implications for the behavioral manipulation hypothesis. *PLoS ONE*. 6:e28925. doi:10.1371/journal.pone.0028925.

Bernstein-Hanley, I., J. Coers, Z.R. Balsara, G.A. Taylor, M.N. Starnbach, and W.F. Dietrich. 2006. The p47 GTPases Igtp and Irgb10 map to the Chlamydia trachomatis susceptibility locus Ctrq-3 and mediate cellular resistance in mice. *Proc. Natl. Acad. Sci. U.S.A.* 103:14092–14097. doi:10.1073/pnas.0603338103.

Beuzón, C.R., S. Méresse, K.E. Unsworth, J. Ruíz-Albert, S. Garvis, S.R. Waterman, T.A. Ryder, E. Boucrot, and D.W. Holden. 2000. Salmonella maintains the integrity of its intracellular vacuole through the action of SifA. *EMBO J.* 19:3235–3249. doi:10.1093/emboj/19.13.3235.

Bidgood, S.R., J.C.H. Tam, W.A. McEwan, D.L. Mallery, and L.C. James. 2014. Translocalized IgA mediates neutralization and stimulates innate immunity inside infected cells. *Proc. Natl. Acad. Sci. U.S.A.* doi:10.1073/pnas.1410980111.

Bierly, A.L., W.J. Shufesky, W. Sukhumavasi, A.E. Morelli, and E.Y. Denkers. 2008. Dendritic cells expressing plasmacytoid marker PDCA-1 are Trojan horses during Toxoplasma gondii infection. *J. Immunol.* 181:8485–8491.

Birmingham, C.L., A.C. Smith, M.A. Bakowski, T. Yoshimori, and J.H. Brumell. 2006. Autophagy controls Salmonella infection in response to damage to the Salmonella-containing vacuole. *J. Biol. Chem.* 281:11374–11383. doi:10.1074/jbc.M509157200.

Black, R.A., S.R. Kronheim, and P.R. Sleath. 1989. Activation of interleukin-1 beta by a co-induced protease. *FEBS Lett.* 247:386–390.

Blommaart, E.F., U. Krause, J.P. Schellens, H. Vreeling-Sindelárová, and A.J. Meijer. 1997. The phosphatidylinositol 3-kinase inhibitors wortmannin and LY294002 inhibit autophagy in isolated rat hepatocytes. *Eur. J. Biochem.* 243:240–246.

Boehm, U., L. Guethlein, T. Klamp, K. Ozbek, A. Schaub, A. Fütterer, K. Pfeffer, and J.C. Howard. 1998. Two families of GTPases dominate the complex cellular response to IFN-gamma. *J. Immunol.* 161:6715–6723.

Borden, K.L., M.N. Boddy, J. Lally, N.J. O'Reilly, S. Martin, K. Howe, E. Solomon, and P.S. Freemont. 1995. The solution structure of the RING finger domain from the acute promyelocytic leukaemia proto-oncoprotein PML. *EMBO J.* 14:1532–1541.

Borkakoty, B.J., A.K. Borthakur, and M. Gohain. 2007. Prevalence of Toxoplasma gondii infection amongst pregnant women in Assam, India. *Indian J Med Microbiol*. 25:431–432.

Boyden, E.D., and W.F. Dietrich. 2006. Nalp1b controls mouse macrophage susceptibility to anthrax lethal toxin. *Nat. Genet.* 38:240–244. doi:10.1038/ng1724.

Breugelmans, M., A. Naessens, and W. Foulon. 2004. Prevention of toxoplasmosis during pregnancy--an epidemiologic survey over 22 consecutive years. *J Perinat Med*. 32:211–214. doi:10.1515/JPM.2004.039.

Broz, P., J. von Moltke, J.W. Jones, R.E. Vance, and D.M. Monack. 2010. Differential requirement for Caspase-1 autoproteolysis in pathogen-induced cell death and cytokine processing. *Cell Host and Microbe*. 8:471–483. doi:10.1016/j.chom.2010.11.007.

Bruckert, W.M., and Y. Abu Kwaik. 2015. Complete and Ubiquitinated Proteome of the Legionella-Containing Vacuole within Human Macrophages. *J. Proteome Res.* 14:236–248. doi:10.1021/pr500765x.

Brumell, J.H., P. Tang, M.L. Zaharik, and B.B. Finlay. 2002. Disruption of the Salmonella-containing vacuole leads to increased replication of Salmonella enterica serovar typhimurium in the cytosol of epithelial cells. *Infect. Immun.* 70:3264–3270.

Burg, J.L., C.M. Grover, P. Pouletty, and J.C. Boothroyd. 1989. Direct and sensitive detection of a pathogenic protozoan, Toxoplasma gondii, by polymerase chain reaction. *J. Clin. Microbiol.* 27:1787–1792.

Butcher, B.A., R.I. Greene, S.C. Henry, K.L. Annecharico, J.B. Weinberg, E.Y. Denkers, A. Sher, and G.A. Taylor. 2005. p47 GTPases Regulate Toxoplasma gondii Survival in Activated Macrophages. *Infect. Immun.* 73:3278–3286. doi:10.1128/iai.73.6.3278-3286.2005.

Buxton, D., and E.A. Innes. 1995. A commercial vaccine for ovine toxoplasmosis. *Parasitology*. 110 Suppl:S11–6.

Buxton, D., K.M. Thomson, S. Maley, S. Wright, and H.J. Bos. 1993. Experimental challenge of sheep 18 months after vaccination with a live (S48) Toxoplasma gondii vaccine. *Vet. Rec.* 133:310–312.

Buzby, J.C., and T. Roberts. 1996. ERS Updates US Foodborne Disease Costs for Seven Pathogens. *Food Safety*. 19:20–25.

Cai, X., J. Chen, H. Xu, S. Liu, Q.-X. Jiang, R. Halfmann, and Z.J. Chen. 2014. Prion-like polymerization underlies signal transduction in antiviral immune defense and inflammasome activation. *Cell*. 156:1207–1222. doi:10.1016/j.cell.2014.01.063.

Cainarca, S., S. Messali, A. Ballabio, and G. Meroni. 1999. Functional characterization of the Opitz syndrome gene product (midin): evidence for homodimerization and association with microtubules throughout the cell cycle. *Hum. Mol. Genet.* 8:1387–1396.

Campos, M.A., I.C. Almeida, O. Takeuchi, S. Akira, E.P. Valente, D.O. Procópio, L.R. Travassos, J.A. Smith, D.T. Golenbock, and R.T. Gazzinelli. 2001.

Activation of Toll-like receptor-2 by glycosylphosphatidylinositol anchors from a protozoan parasite. *J. Immunol.* 167:416–423.

Cao, T., K.L. Borden, P.S. Freemont, and L.D. Etkin. 1997. Involvement of the rfp tripartite motif in protein-protein interactions and subcellular distribution. *J. Cell. Sci.* 110 (Pt 14):1563–1571.

Carlow, D.A., J. Marth, I. Clark-Lewis, and H.S. Teh. 1995. Isolation of a gene encoding a developmentally regulated T cell-specific protein with a guanine nucleotide triphosphate-binding motif. *J. Immunol.* 154:1724–1734.

Carruthers, V.B. 1999. Armed and dangerous: Toxoplasma gondii uses an arsenal of secretory proteins to infect host cells. *Parasitol. Int.* 48:1–10.

Carruthers, V.B., and L.D. Sibley. 1997. Sequential protein secretion from three distinct organelles of Toxoplasma gondii accompanies invasion of human fibroblasts. *Eur. J. Cell Biol.* 73:114–123.

Carruthers, V.B., O.K. Giddings, and L.D. Sibley. 1999. Secretion of micronemal proteins is associated with toxoplasma invasion of host cells. *Cell. Microbiol.* 1:225–235.

Carter, C.C., V.Y. Gorbacheva, and D.J. Vestal. 2005. Inhibition of VSV and EMCV replication by the interferon-induced GTPase, mGBP-2: differential requirement for wild-type GTP binding domain. *Arch. Virol.* 150:1213–1220. doi:10.1007/s00705-004-0489-2.

Casson, C.N., A.M. Copenhaver, E.E. Zwack, H.T. Nguyen, T. Strowig, B. Javdan, W.P. Bradley, T.C. Fung, R.A. Flavell, I.E. Brodsky, and S. Shin. 2013. Caspase-11 activation in response to bacterial secretion systems that access the host cytosol. *PLoS Pathog.* 9:e1003400. doi:10.1371/journal.ppat.1003400.

Castro, A.T., A. Góngora, and M.E. González. 2008. *Toxoplasma gondii* antibody seroprevalence in pregnant women from Villavicencio, Colombia. *Orinoquia*. 12:91–100.

Celik, T., S. Kartalci, O. Aytas, G.A. Akarsu, H. Gozukara, and S. Unal. 2015. Association between latent toxoplasmosis and clinical course of schizophrenia - continuous course of the disease is characteristic for Toxoplasma gondii-infected patients. *Folia Parasitol.* 62. doi:10.14411/fp.2015.015.

Centers for Disease Control and Prevention. 2000. CDC recommendations regarding selected conditions effecting women's health. *Morbidity and Mortality Weekly Report*. 49:57–75.

Cérède, O., J.-F. Dubremetz, M. Soête, D. Deslée, H. Vial, D. Bout, and M. Lebrun. 2005. Synergistic role of micronemal proteins in Toxoplasma gondii virulence. *J. Exp. Med.* 201:453–463. doi:10.1084/jem.20041672.

Chamaillard, M., M. Hashimoto, Y. Horie, J. Masumoto, S. Qiu, L. Saab, Y. Ogura, A. Kawasaki, K. Fukase, S. Kusumoto, M.A. Valvano, S.J. Foster, T.W. Mak, G. Núñez, and N. Inohara. 2003. An essential role for NOD1 in host recognition of

bacterial peptidoglycan containing diaminopimelic acid. *Nat. Immunol.* 4:702–707. doi:10.1038/ni945.

Chan, E.K., J.C. Hamel, J.P. Buyon, and E.M. Tan. 1991. Molecular definition and sequence motifs of the 52-kD component of human SS-A/Ro autoantigen. *J. Clin. Invest.* 87:68–76. doi:10.1172/JCI115003.

Channon, J.Y., R.M. Seguin, and L.H. Kasper. 2000. Differential infectivity and division of Toxoplasma gondii in human peripheral blood leukocytes. *Infect. Immun.* 68:4822–4826.

Chastagner, P., A. Israel, and C. Brou. 2006. Itch/AIP4 mediates Deltex degradation through the formation of K29-linked polyubiquitin chains. *EMBO Rep.* 7:1147–1153. doi:10.1038/sj.embor.7400822.

Chau, V., J.W. Tobias, A. Bachmair, D. Marriott, D.J. Ecker, D.K. Gonda, and A. Varshavsky. 1989. A multiubiquitin chain is confined to specific lysine in a targeted short-lived protein. *Science*. 243:1576–1583.

Che, N., S. Li, T. Gao, Z. Zhang, Y. Han, X. Zhang, Y. Sun, Y. Liu, Z. Sun, J. Zhang, W. Ren, M. Tian, Y. Li, W. Li, J. Cheng, and C. Li. 2010. Identification of a novel IRGM promoter single nucleotide polymorphism associated with tuberculosis. *Clin. Chim. Acta*. 411:1645–1649. doi:10.1016/j.cca.2010.06.009.

Cheng, Y.S., R.J. Colonno, and F.H. Yin. 1983. Interferon induction of fibroblast proteins with guanylate binding activity. *J. Biol. Chem.* 258:7746–7750.

Choi, J., S. Park, S.B. Biering, E. Selleck, C.Y. Liu, X. Zhang, N. Fujita, T. Saitoh, S. Akira, T. Yoshimori, L.D. Sibley, S. Hwang, and H.W. Virgin. 2014. The parasitophorous vacuole membrane of Toxoplasma gondii is targeted for disruption by ubiquitin-like conjugation systems of autophagy. *Immunity*. 40:924–935. doi:10.1016/j.immuni.2014.05.006.

Ciechanover, A., D. Finley, and A. Varshavsky. 1984. Ubiquitin dependence of selective protein degradation demonstrated in the mammalian cell cycle mutant ts85. *Cell*. 37:57–66.

Ciechanover, A., H. Heller, S. Elias, A.L. Haas, and A. Hershko. 1980. ATP-dependent conjugation of reticulocyte proteins with the polypeptide required for protein degradation. *Proc. Natl. Acad. Sci. U.S.A.* 77:1365–1368.

Cohen, L., S. Sharp, and A. Kulczycki. 1983. Human monocytes, B lymphocytes, and non-B lymphocytes each have structurally unique Fc gamma receptors. *J. Immunol.* 131:378–383.

Collazo, C.M., G.S. Yap, G.D. Sempowski, K.C. Lusby, L. Tessarollo, G.F. Vande Woude, A. Sher, and G.A. Taylor. 2001. Inactivation of LRG-47 and IRG-47 Reveals a Family of Interferon Gamma–inducible Genes with Essential, Pathogen-specific Roles in Resistance to Infection. *J. Exp. Med.* 194:181–187.

Cook, A.J., R.E. Gilbert, W. Buffolano, J. Zufferey, E. Petersen, P.A. Jenum, W. Foulon, A.E. Semprini, and D.T. Dunn. 2000. Sources of toxoplasma infection in

pregnant women: European multicentre case-control study. European Research Network on Congenital Toxoplasmosis. *BMJ*. 321:142–147.

Coombes, J.L., B.A. Charsar, S.-J. Han, J. Halkias, S.W. Chan, A.A. Koshy, B. Striepen, and E.A. Robey. 2013. Motile invaded neutrophils in the small intestine of Toxoplasma gondii-infected mice reveal a potential mechanism for parasite spread. *Proc. Natl. Acad. Sci. U.S.A.* 110:E1913–22. doi:10.1073/pnas.1220272110.

Cooney, R., J. Baker, O. Brain, B. Danis, T. Pichulik, P. Allan, D.J.P. Ferguson, B.J. Campbell, D. Jewell, and A. Simmons. 2010. NOD2 stimulation induces autophagy in dendritic cells influencing bacterial handling and antigen presentation. *Nat. Med.* 16:90–97. doi:10.1038/nm.2069.

Coppens, I., A.P. Sinai, and K.A. Joiner. 2000. Toxoplasma gondii exploits host low-density lipoprotein receptor-mediated endocytosis for cholesterol acquisition. *J. Cell Biol.* 149:167–180.

Courret, N., S. Darche, P. Sonigo, G. Milon, D. Buzoni-Gâtel, and I. Tardieux. 2006. CD11c- and CD11b-expressing mouse leukocytes transport single Toxoplasma gondii tachyzoites to the brain. *Blood*. 107:309–316. doi:10.1182/blood-2005-02-0666.

Cox, J., I. Matic, M. Hilger, N. Nagaraj, M. Selbach, J.V. Olsen, and M. Mann. 2009. A practical guide to the MaxQuant computational platform for SILAC-based quantitative proteomics. *Nat Protoc.* 4:698–705. doi:10.1038/nprot.2009.36.

Cunningham, T. 1982. Pancarditis in acute toxoplasmosis. *Am. J. Clin. Pathol.* 78:403–405.

Da Gama, L.M., F.L. Ribeiro-Gomes, U. Guimarães, and A.C.V. Arnholdt. 2004. Reduction in adhesiveness to extracellular matrix components, modulation of adhesion molecules and in vivo migration of murine macrophages infected with Toxoplasma gondii. *Microbes Infect.* 6:1287–1296. doi:10.1016/j.micinf.2004.07.008.

Daffos, F., F. Forestier, M. Capella-Pavlovsky, P. Thulliez, C. Aufrant, D. Valenti, and W.L. Cox. 1988. Prenatal management of 746 pregnancies at risk for congenital toxoplasmosis. *N. Engl. J. Med.* 318:271–275. doi:10.1056/NEJM198802043180502.

De Paschale, M., C. Agrappi, P. Clerici, P. Mirri, M.T. Manco, S. Cavallari, and E.F. Viganò. 2008. Seroprevalence and incidence of Toxoplasma gondii infection in the Legnano area of Italy. *Clin. Microbiol. Infect.* 14:186–189. doi:10.1111/j.1469-0691.2007.01883.x.

de Veer, M.J., M. Holko, M. Frevel, E. Walker, S. Der, J.M. Paranjape, R.H. Silverman, and B.R.G. Williams. 2001. Functional classification of interferon-stimulated genes identified using microarrays. *J. Leukoc. Biol.* 69:912–920.

Debierre-Grockiego, F., M.A. Campos, N. Azzouz, J. Schmidt, U. Bieker, M.G. Resende, D.S. Mansur, R. Weingart, R.R. Schmidt, D.T. Golenbock, R.T.

Gazzinelli, and R.T. Schwarz. 2007. Activation of TLR2 and TLR4 by glycosylphosphatidylinositols derived from Toxoplasma gondii. *J. Immunol.* 179:1129–1137.

Degrandi, D., C. Konermann, C. Beuter-Gunia, A. Kresse, J. Wuerthner, S. Kurig, S. Beer, and K. Pfeffer. 2007. Extensive Characterization of IFN-Induced GTPases mGBP1 to mGBP10 Involved in Host Defense. *J. Immunol.* 179:7729–7740.

Degrandi, D., E. Kravets, C. Konermann, C. Beuter-Gunia, V. Klümpers, S. Lahme, E. Wischmann, A.K. Mausberg, S. Beer-Hammer, and K. Pfeffer. 2013. Murine Guanylate Binding Protein 2 (mGBP2) controls Toxoplasma gondii replication. *Proc. Natl. Acad. Sci. U.S.A.* 110:294–299. doi:10.1073/pnas.1205635110.

Delgado, M.A., R.A. Elmaoued, A.S. Davis, G. Kyei, and V. Deretic. 2008. Toll-like receptors control autophagy. *EMBO J.* 27:1110–1121. doi:10.1038/emboj.2008.31.

Dellacasa-Lindberg, I., J.M. Fuks, R.B.G. Arrighi, H. Lambert, R.P.A. Wallin, B.J. Chambers, and A. Barragan. 2011. Migratory activation of primary cortical microglia upon infection with Toxoplasma gondii. *Infect. Immun.* 79:3046–3052. doi:10.1128/IAI.01042-10.

Deng, L., C. Wang, E. Spencer, L. Yang, A. Braun, J. You, C. Slaughter, C. Pickart, and Z.J. Chen. 2000. Activation of the IkappaB kinase complex by TRAF6 requires a dimeric ubiquitin-conjugating enzyme complex and a unique polyubiquitin chain. *Cell*. 103:351–361.

Derouin, F., C. Sarfati, B. Beauvais, Y.J. Garin, and M. Larivière. 1990. Prevalence of pulmonary toxoplasmosis in HIV-infected patients. *AIDS*. 4:1036.

Desmonts, G., and J. Couvreur. 1974. Toxoplasmosis in pregnancy and its transmission to the fetus. *Bull N Y Acad Med*. 50:146–159.

Desmonts, G., F. Daffos, F. Forestier, M. Capella-Pavlovsky, P. Thulliez, and M. Chartier. 1985. Prenatal diagnosis of congenital toxoplasmosis. *Lancet*. 1:500–504.

Desmonts, G., Y. Naot, and J.S. Remington. 1981. Immunoglobulin M-immunosorbent agglutination assay for diagnosis of infectious diseases: diagnosis of acute congenital and acquired Toxoplasma infections. *J. Clin. Microbiol.* 14:486–491.

Diaz-Griffero, F., N. Vandegraaff, Y. Li, K. McGee-Estrada, M. Stremlau, S. Welikala, Z. Si, A. Engelman, and J. Sodroski. 2006. Requirements for capsid-binding and an effector function in TRIMCyp-mediated restriction of HIV-1. *Virology*. 351:404–419. doi:10.1016/j.virol.2006.03.023.

Diaz-Griffero, F., X.-R. Qin, F. Hayashi, T. Kigawa, A. Finzi, Z. Sarnak, M. Lienlaf, S. Yokoyama, and J. Sodroski. 2009. A B-box 2 surface patch important for TRIM5alpha self-association, capsid binding avidity, and retrovirus restriction. *J. Virol.* 83:10737–10751. doi:10.1128/JVI.01307-09.

Doudou, Y., P. Renaud, L. Coralie, F. Jacqueline, S. Hypolite, M. Hypolite, M. Patrick, I.D.L.R. Andreia, M. Van Sprundel, B. Marleen, J.-P. Van Geertruyden, and L. Pascal. 2014. Toxoplasmosis among pregnant women: high seroprevalence and risk factors in Kinshasa, Democratic Republic of Congo. *Asian Pac J Trop Biomed*. 4:69–74. doi:10.1016/S2221-1691(14)60211-2.

Dubey, J.P. 1998. Toxoplasma gondii oocyst survival under defined temperatures. *J. Parasitol.* 84:862–865.

Dubey, J.P., A.W. Kotula, A. Sharar, C.D. Andrews, and D.S. Lindsay. 1990. Effect of high temperature on infectivity of Toxoplasma gondii tissue cysts in pork. *J. Parasitol.* 76:201–204.

Dubey, J.P., and D.W. Thayer. 1994. Killing of different strains of Toxoplasma gondii tissue cysts by irradiation under defined conditions. *J. Parasitol.* 80:764–767.

Dubey, J.P., and J.K. Frenkel. 1972. Cyst-induced toxoplasmosis in cats. *J. Protozool.* 19:155–177.

Dubey, J.P., N.L. Miller, and J.K. Frenkel. 1970. The Toxoplasma gondii oocyst from cat feces. *J. Exp. Med.* 132:636–662.

Dubremetz, J.F., C. Rodriguez, and E. Ferreira. 1985. Toxoplasma gondii: redistribution of monoclonal antibodies on tachyzoites during host cell invasion. *Exp. Parasitol.* 59:24–32.

Duncan, L.M., S. Piper, R.B. Dodd, M.K. Saville, C.M. Sanderson, J.P. Luzio, and P.J. Lehner. 2006. Lysine-63-linked ubiquitination is required for endolysosomal degradation of class I molecules. *EMBO J.* 25:1635–1645. doi:10.1038/sj.emboj.7601056.

Dupont, C.D., D.A. Christian, E.M. Selleck, M. Pepper, M. Leney-Greene, G. Harms Pritchard, A.A. Koshy, S. Wagage, M.A. Reuter, L.D. Sibley, M.R. Betts, and C.A. Hunter. 2014. Parasite Fate and Involvement of Infected Cells in the Induction of CD4+ and CD8+ T Cell Responses to Toxoplasma gondii. *PLoS Pathog.* 10:e1004047. doi:10.1371/journal.ppat.1004047.

Dupont, N., S. Lacas-Gervais, J. Bertout, I. Paz, B. Freche, G.T. Van Nhieu, F.G. van der Goot, P.J. Sansonetti, and F. Lafont. 2009. Shigella phagocytic vacuolar membrane remnants participate in the cellular response to pathogen invasion and are regulated by autophagy. *Cell Host and Microbe*. 6:137–149. doi:10.1016/j.chom.2009.07.005.

Elmore, S.P., T. Qian, S.F. Grissom, and J.J. Lemasters. 2001. The mitochondrial permeability transition initiates autophagy in rat hepatocytes. *FASEB J.* 15:2286–2287. doi:10.1096/fj.01-0206fje.

Elnahas, A., A.S. Gerais, M.I. Elbashir, E.S. Eldien, and I. Adam. 2003. Toxoplasmosis in pregnant Sudanese women. *Saudi Med J*. 24:868–870.

Endo, A., M. Kuroda, and K. Tanzawa. 1976. Competitive inhibition of 3-hydroxy-3-methylglutaryl coenzyme A reductase by ML-236A and ML-236B fungal

metabolites, having hypocholesterolemic activity. *FEBS Lett.* 72:323–326.

Enzensberger, W., E.B. Helm, G. Hopp, W. Stille, and P.A. Fischer. 1985. [Toxoplasmosis encephalitis in patients with AIDS]. *deutsche medizinische Wochenschrift (1946)*. 110:83–87. doi:10.1055/s-2008-1068778.

Esch, K.J., and C.A. Petersen. 2013. Transmission and Epidemiology of Zoonotic Protozoal Diseases of Companion Animals. *Clinical Microbiology Reviews*. 26:58. doi:10.1128/CMR.00067-12.

Espinosa, A., V. Dardalhon, S. Brauner, A. Ambrosi, R. Higgs, F.J. Quintana, M. Sjöstrand, M.-L. Eloranta, J. Ní Gabhann, O. Winqvist, B. Sundelin, C.A. Jefferies, B. Rozell, V.K. Kuchroo, and M. Wahren-Herlenius. 2009. Loss of the lupus autoantigen Ro52/Trim21 induces tissue inflammation and systemic autoimmunity by disregulating the IL-23-Th17 pathway. *J. Exp. Med.* 206:1661–1671. doi:10.1084/jem.20090585.

Evengård, B., K. Petersson, M.L. Engman, S. Wiklund, S.A. Ivarsson, K. Teär-Fahnehjelm, M. Forsgren, R. Gilbert, and G. Malm. 2001. Low incidence of toxoplasma infection during pregnancy and in newborns in Sweden. *Epidemiol. Infect.* 127:121–127.

Ewald, S.E., J. Chavarria-Smith, and J.C. Boothroyd. 2013. NLRP1 is an inflammasome sensor for Toxoplasma gondii. *Infect. Immun.* doi:10.1128/IAI.01170-13.

Eyles, D.E., and N. Coleman. 1953. Synergistic effect of sulfadiazine and daraprim against experimental toxoplasmosis in the mouse. *Antibiot Chemother (Northfield)*. 3:483–490.

Fallah, M., S. Rabiee, M. Matini, and H. Taherkhani. 2008. Seroepidemiology of toxoplasmosis in primigravida women in Hamadan, Islamic Republic of Iran, 2004. *East. Mediterr. Health J.* 14:163–171.

Fentress, S.J., M.S. Behnke, I.R. Dunay, M. Mashayekhi, L.M. Rommereim, B.A. Fox, D.J. Bzik, G.A. Taylor, B.E. Turk, C.F. Lichti, R.R. Townsend, W. Qiu, R. Hui, W.L. Beatty, and L.D. Sibley. 2010. Phosphorylation of Immunity-Related GTPases by a Toxoplasma gondii-Secreted Kinase Promotes Macrophage Survival and Virulence. *Cell Host and Microbe*. 8:484–495. doi:10.1016/j.chom.2010.11.005.

Fentress, S.J., T. Steinfeldt, J.C. Howard, and L.D. Sibley. 2012. The arginine-rich N-terminal domain of ROP18 is necessary for vacuole targeting and virulence of Toxoplasma gondii. *Cell. Microbiol.* 14:1921–1933. doi:10.1111/cmi.12022.

Fernandes-Alnemri, T., J.-W. Yu, P. Datta, J. Wu, and E.S. Alnemri. 2009. AIM2 activates the inflammasome and cell death in response to cytoplasmic DNA. *Nature*. 458:509–513. doi:10.1038/nature07710.

Fernàndez-Sabé, N., C. Cervera, M.C. Fariñas, M. Bodro, P. Muñoz, M. Gurguí, J. Torre-Cisneros, P. Martín-Dávila, A. Noblejas, O. Len, A. García-Reyne, J.L. Del Pozo, and J. Carratalà. 2012. Risk factors, clinical features, and outcomes of

toxoplasmosis in solid-organ transplant recipients: a matched case-control study. *Clin. Infect. Dis.* 54:355–361. doi:10.1093/cid/cir806.

Fiedler, K., C. Hülsse, W. Straube, and V. Briese. 1999. Toxoplasmosis-antibody seroprevalence in Mecklenburg-Western Pomerania. *Zentralbl Gynakol*. 121:239–243.

Fink, S.L., T. Bergsbaken, and B.T. Cookson. 2008. Anthrax lethal toxin and Salmonella elicit the common cell death pathway of caspase-1-dependent pyroptosis via distinct mechanisms. *Proc. Natl. Acad. Sci. U.S.A.* 105:4312–4317. doi:10.1073/pnas.0707370105.

Finley, D., S. Sadis, B.P. Monia, P. Boucher, D.J. Ecker, S.T. Crooke, and V. Chau. 1994. Inhibition of proteolysis and cell cycle progression in a multiubiquitination-deficient yeast mutant. *Mol. Cell. Biol.* 14:5501–5509.

Fleckenstein, M.C., M.L. Reese, S. Könen-Waisman, J.C. Boothroyd, J.C. Howard, and T. Steinfeldt. 2012. A Toxoplasma gondii pseudokinase inhibits host IRG resistance proteins. *PLoS Biol.* 10:e1001358. doi:10.1371/journal.pbio.1001358.

Fleit, H.B., S.D. Wright, and J.C. Unkeless. 1982. Human neutrophil Fc gamma receptor distribution and structure. *Proc. Natl. Acad. Sci. U.S.A.* 79:3275–3279.

Fonseca, A.L., R.A. Silva, B. Fux, A.P. Madureira, F.F. de Sousa, and C. Margonari. 2012. Epidemiologic aspects of toxoplasmosis and evaluation of its seroprevalence in pregnant women. *Rev. Soc. Bras. Med. Trop.* 45:357–364.

Fortun, J., W.A. Dunn, S. Joy, J. Li, and L. Notterpek. 2003. Emerging role for autophagy in the removal of aggresomes in Schwann cells. *J. Neurosci.* 23:10672–10680.

Foureau, D.M., D.W. Mielcarz, L.C. Menard, J. Schulthess, C. Werts, V. Vasseur, B. Ryffel, L.H. Kasper, and D. Buzoni-Gâtel. 2010. TLR9-dependent induction of intestinal alpha-defensins by Toxoplasma gondii. *J. Immunol.* 184:7022–7029. doi:10.4049/jimmunol.0901642.

Franchi, L., A. Amer, M. Body-Malapel, T.-D. Kanneganti, N. Ozören, R. Jagirdar, N. Inohara, P. Vandenabeele, J. Bertin, A. Coyle, E.P. Grant, and G. Núñez. 2006. Cytosolic flagellin requires Ipaf for activation of caspase-1 and interleukin 1beta in salmonella-infected macrophages. *Nat. Immunol.* 7:576–582. doi:10.1038/ni1346.

Frank, M.B., K. Itoh, A. Fujisaku, P. Pontarotti, M.G. Mattei, and B.R. Neas. 1993. The mapping of the human 52-kD Ro/SSA autoantigen gene to human chromosome 11, and its polymorphisms. *Am. J. Hum. Genet.* 52:183–191.

Franklin, B.S., L. Bossaller, D. De Nardo, J.M. Ratter, A. Stutz, G. Engels, C. Brenker, M. Nordhoff, S.R. Mirandola, A. Al-Amoudi, M.S. Mangan, S. Zimmer, B.G. Monks, M. Fricke, R.E. Schmidt, T. Espevik, B. Jones, A.G. Jarnicki, P.M. Hansbro, P. Busto, A. Marshak-Rothstein, S. Hornemann, A. Aguzzi, W. Kastenmüller, and E. Latz. 2014. The adaptor ASC has extracellular and "prionoid" activities that propagate inflammation. *Nat. Immunol.* 15:727–737.

doi:10.1038/ni.2913.

Freemont, P.S., I.M. Hanson, and J. Trowsdale. 1991. A novel cysteine-rich sequence motif. *Cell*. 64:483–484.

Frenkel, J.K., J.P. Dubey, and N.L. Miller. 1970. Toxoplasma gondii in cats: fecal stages identified as coccidian oocysts. *Science*. 167:893–896.

Frese, M., G. Kochs, H. Feldmann, C. Hertkorn, and O. Haller. 1996. Inhibition of bunyaviruses, phleboviruses, and hantaviruses by human MxA protein. *J. Virol.* 70:915–923.

Frese, M., G. Kochs, U. Meier-Dieter, J. Siebler, and O. Haller. 1995. Human MxA protein inhibits tick-borne Thogoto virus but not Dhori virus. *J. Virol.* 69:3904–3909.

Frese, M., M. Weeber, F. Weber, V. Speth, and O. Haller. 1997. Mx1 sensitivity: Batken virus is an orthomyxovirus closely related to Dhori virus. *J. Gen. Virol.* 78 (Pt 10):2453–2458.

Friedman, S.L. 2008. Hepatic stellate cells: protean, multifunctional, and enigmatic cells of the liver. *Physiol. Rev.* 88:125–172. doi:10.1152/physrev.00013.2007.

Fujita, N., E. Morita, T. Itoh, A. Tanaka, M. Nakaoka, Y. Osada, T. Umemoto, T. Saitoh, H. Nakatogawa, S. Kobayashi, T. Haraguchi, J.-L. Guan, K. Iwai, F. Tokunaga, K. Saito, K. Ishibashi, S. Akira, M. Fukuda, T. Noda, and T. Yoshimori. 2013. Recruitment of the autophagic machinery to endosomes during infection is mediated by ubiquitin. *J. Cell Biol.* 203:115–128. doi:10.1083/jcb.201304188.

Fujita, N., T. Itoh, H. Omori, M. Fukuda, T. Noda, and T. Yoshimori. 2008. The Atg16L complex specifies the site of LC3 lipidation for membrane biogenesis in autophagy. *Mol. Biol. Cell*. 19:2092–2100. doi:10.1091/mbc.E07-12-1257.

Fuks, J.M., R.B.G. Arrighi, J.M. Weidner, S. Kumar Mendu, Z. Jin, R.P.A. Wallin, B. Rethi, B. Birnir, and A. Barragan. 2012. GABAergic signaling is linked to a hypermigratory phenotype in dendritic cells infected by Toxoplasma gondii. *PLoS Pathog.* 8:e1003051. doi:10.1371/journal.ppat.1003051.

Furtado, J.M., A.S. Bharadwaj, T.J. Chipps, Y. Pan, L.M. Ashander, and J.R. Smith. 2012. Toxoplasma gondii tachyzoites cross retinal endothelium assisted by intercellular adhesion molecule-1 in vitro. *Immunol. Cell Biol.* 90:912–915. doi:10.1038/icb.2012.21.

Furtado, J.M., L.M. Ashander, K. Mohs, T.J. Chipps, B. Appukuttan, and J.R. Smith. 2013. Toxoplasma gondii migration within and infection of human retina. *PLoS ONE*. 8:e54358. doi:10.1371/journal.pone.0054358.

Gack, M.U., Y.C. Shin, C.-H. Joo, T. Urano, C. Liang, L. Sun, O. Takeuchi, S. Akira, Z. Chen, S. Inoue, and J.U. Jung. 2007. TRIM25 RING-finger E3 ubiquitin ligase is essential for RIG-I-mediated antiviral activity. *Nature*. 446:916–920. doi:10.1038/nature05732.

Gale, S.D., B.L. Brown, A. Berrett, L.D. Erickson, and D.W. Hedges. 2014. Association between latent toxoplasmosis and major depression, generalised anxiety disorder and panic disorder in human adults. *Folia Parasitol.* 61:285–292.

Gallino, A., M. Maggiorini, W. Kiowski, X. Martin, W. Wunderli, J. Schneider, M. Turina, and F. Follath. 1996. Toxoplasmosis in heart transplant recipients. *Eur. J. Clin. Microbiol. Infect. Dis.* 15:389–393.

Ganser-Pornillos, B.K., V. Chandrasekaran, O. Pornillos, J.G. Sodroski, W.I. Sundquist, and M. Yeager. 2011. Hexagonal assembly of a restricting TRIM5alpha protein. *Proc. Natl. Acad. Sci. U.S.A.* 108:534–539. doi:10.1073/pnas.1013426108.

Gard, S., and J.H. Magnusson. 1951. A glandular form of toxoplasmosis in connection with pregnancy. *Acta Med Scand.* 141:59–64.

Garin, J.P., and D.E. Eyles. 1958. [Spiramycin therapy of experimental toxoplasmosis in mice]. *Presse Med.* 66:957–958.

Garnham, P.C., J.R. Baker, and R.G. Bird. 1962. Fine structure of cystic form of Toxoplasma gondii. *Br Med J.* 1:83–84.

Garnham, P.C., R.G. Bird, J.R. Baker, and R.S. Bray. 1961. Electron microsope studies of motile stages of malaria parasites. II. The fine structure of the sporozoite of Laverania (Plasmodium) falcipara. *Trans. R. Soc. Trop. Med. Hyg.* 55:98–102.

Gavin, M.A., T. Wanko, and L. Jacobs. 1962. Electron microscope studies of reproducing and interkinetic Toxoplasma. *J. Protozool.* 9:222–234.

Gazzinelli, R.T., M. Wysocka, S. Hayashi, E.Y. Denkers, S. Hieny, P. Caspar, G. Trinchieri, and A. Sher. 1994. Parasite-induced IL-12 stimulates early IFN-gamma synthesis and resistance during acute infection with Toxoplasma gondii. *J. Immunol.* 153:2533–2543.

Gazzinelli, R.T., S. Hieny, T.A. Wynn, S. Wolf, and A. Sher. 1993. Interleukin 12 is required for the T-lymphocyte-independent induction of interferon gamma by an intracellular parasite and induces resistance in T-cell-deficient hosts. *Proc. Natl. Acad. Sci. U.S.A.* 90:6115–6119.

Gebremedhin, E.Z., A.H. Abebe, T.S. Tessema, K.D. Tullu, G. Medhin, M. Vitale, V. Di Marco, E. Cox, and P. Dorny. 2013. Seroepidemiology of Toxoplasma gondii infection in women of child-bearing age in central Ethiopia. *BMC Infect. Dis.* 13:101. doi:10.1186/1471-2334-13-101.

Geetha, T., J. Jiang, and M.W. Wooten. 2005. Lysine 63 polyubiquitination of the nerve growth factor receptor TrkA directs internalization and signaling. *Mol. Cell.* 20:301–312. doi:10.1016/j.molcel.2005.09.014.

Ghosh, A., G.J.K. Praefcke, L. Renault, A. Wittinghofer, and C. Herrmann. 2006. How guanylate-binding proteins achieve assembly-stimulated processive cleavage of GTP to GMP. *Nature*. 440:101–104. doi:10.1038/nature04510.

Gilly, M., and R. Wall. 1992. The IRG-47 gene is IFN-gamma induced in B cells and encodes a protein with GTP-binding motifs. *J. Immunol.* 148:3275–3281.

Giordano, L.F.C., E.P. Lasmar, E.R.F. Tavora, and M.F. Lasmar. 2002. Toxoplasmosis transmitted via kidney allograft: case report and review. *Transplant. Proc.* 34:498–499.

Girardin, S.E., I.G. Boneca, J. Viala, M. Chamaillard, A. Labigne, G. Thomas, D.J. Philpott, and P.J. Sansonetti. 2003a. Nod2 is a general sensor of peptidoglycan through muramyl dipeptide (MDP) detection. *J. Biol. Chem.* 278:8869–8872. doi:10.1074/jbc.C200651200.

Girardin, S.E., I.G. Boneca, L.A.M. Carneiro, A. Antignac, M. Jéhanno, J. Viala, K. Tedin, M.-K. Taha, A. Labigne, U. Zähringer, A.J. Coyle, P.S. DiStefano, J. Bertin, P.J. Sansonetti, and D.J. Philpott. 2003b. Nod1 detects a unique muropeptide from gram-negative bacterial peptidoglycan. *Science*. 300:1584–1587. doi:10.1126/science.1084677.

Goldman, M., R.K. Carver, and A.J. Sulzer. 1958. Reproduction of Toxoplasma gondii by internal budding. *J. Parasitol.* 44:161–171.

Gordien, E., O. Rosmorduc, C. Peltekian, F. Garreau, C. Bréchot, and D. Kremsdorf. 2001. Inhibition of hepatitis B virus replication by the interferon-inducible MxA protein. *J. Virol.* 75:2684–2691. doi:10.1128/JVI.75.6.2684-2691.2001.

Gorfu, G., K.M. Cirelli, M.B. Melo, K. Mayer-Barber, D. Crown, B.H. Koller, S. Masters, A. Sher, S.H. Leppla, M. Moayeri, J.P.J. Saeij, and M.E. Grigg. 2013. Dual Role for Inflammasome Sensors NLRP1 and NLRP3 in Murine Resistance to Toxoplasma gondii. *MBio*. 5:e01117–13–e01117–13. doi:10.1128/mBio.01117-13.

Goujon, C., O. Moncorgé, H. Bauby, T. Doyle, C.C. Ward, T. Schaller, S. Hué, W.S. Barclay, R. Schulz, and M.H. Malim. 2013. Human MX2 is an interferon-induced post-entry inhibitor of HIV-1 infection. *Nature*. 502:559–562. doi:10.1038/nature12542.

Graham, R.W., D. Jones, and E.P. Candido. 1989. UbiA, the major polyubiquitin locus in Caenorhabditis elegans, has unusual structural features and is constitutively expressed. *Mol. Cell. Biol.* 9:268–277.

Greenlee, J.E., W.D. Johnson, J.F. campa, L.S. Adelman, and M.A. Sande. 1975. Adult toxoplasmosis presenting as polymyositis and cerebellar ataxia. *Ann. Intern. Med.* 82:367–371.

Gregg, B., B.C. Taylor, B. John, E.D. Tait-Wojno, N.M. Girgis, N. Miller, S. Wagage, D.S. Roos, and C.A. Hunter. 2013. Replication and distribution of Toxoplasma gondii in the small intestine after oral infection with tissue cysts. *Infect. Immun.* 81:1635–1643. doi:10.1128/IAI.01126-12.

Grütter, C., C. Briand, G. Capitani, P.R.E. Mittl, S. Papin, J. Tschopp, and M.G. Grütter. 2006. Structure of the PRYSPRY-domain: implications for autoinflammatory diseases. *FEBS Lett.* 580:99–106.

doi:10.1016/j.febslet.2005.11.076.

Gu, Y., K. Kuida, H. Tsutsui, G. Ku, K. Hsiao, M.A. Fleming, N. Hayashi, K. Higashino, H. Okamura, K. Nakanishi, M. Kurimoto, T. Tanimoto, R.A. Flavell, V. Sato, M.W. Harding, D.J. Livingston, and M.S. Su. 1997. Activation of interferon-gamma inducing factor mediated by interleukin-1beta converting enzyme. *Science*. 275:206–209.

Gupta, S.L., B.Y. Rubin, and S.L. Holmes. 1979. Interferon action: induction of specific proteins in mouse and human cells by homologous interferons. *Proc. Natl. Acad. Sci. U.S.A.* 76:4817–4821.

Gustafson, P.V., H.D. Agar, and D.I. Cramer. 1954. An electron microscope study of Toxoplasma. *Am. J. Trop. Med. Hyg.* 3:1008–1022.

Gutierrez, M.G., S.S. Master, S.B. Singh, G.A. Taylor, M.I. Colombo, and V. Deretic. 2004. Autophagy is a defense mechanism inhibiting BCG and Mycobacterium tuberculosis survival in infected macrophages. *Cell*. 119:753–766. doi:10.1016/j.cell.2004.11.038.

Gutiérrez-Zufiaurre, N., J. Sánchez-Hernández, S. Muñoz, R. Marín, N. Delgado, M.C. Sáenz, J.L. Muñoz-Bellido, and J.A. García-Rodríguez. 2004. Seroprevalence of antibodies against Treponema pallidum, Toxoplasma gondii, rubella virus, hepatitis B and C virus, and HIV in pregnant women. *Enferm. Infecc. Microbiol. Clin.* 22:512–516.

Hailey, D.W., A.S. Rambold, P. Satpute-Krishnan, K. Mitra, R. Sougrat, P.K. Kim, and J. Lippincott-Schwartz. 2010. Mitochondria supply membranes for autophagosome biogenesis during starvation. *Cell*. 141:656–667. doi:10.1016/j.cell.2010.04.009.

Haldar, A.K., A.S. Piro, D.M. Pilla, M. Yamamoto, and J. Coers. 2014. The E2-like conjugation enzyme Atg3 promotes binding of IRG and Gbp proteins to Chlamydia- and Toxoplasma-containing vacuoles and host resistance. *PLoS ONE*. 9:e86684. doi:10.1371/journal.pone.0086684.

Haldar, A.K., C. Foltz, R. Finethy, A.S. Piro, E.M. Feeley, D.M. Pilla-Moffett, M. Komatsu, E.-M. Frickel, and J. Coers. 2015. Ubiquitin systems mark pathogen-containing vacuoles as targets for host defense by guanylate binding proteins. *Proc. Natl. Acad. Sci. U.S.A.* doi:10.1073/pnas.1515966112.

Haldar, A.K., H.A. Saka, A.S. Piro, J.D. Dunn, S.C. Henry, G.A. Taylor, E.M. Frickel, R.H. Valdivia, and J. Coers. 2013. IRG and GBP host resistance factors target aberrant, "non-self" vacuoles characterized by the missing of “self” IRGM proteins. *PLoS Pathog.* 9:e1003414. doi:10.1371/journal.ppat.1003414.

Haller, O., M. Frese, D. Rost, P.A. Nuttall, and G. Kochs. 1995. Tick-borne thogoto virus infection in mice is inhibited by the orthomyxovirus resistance gene product Mx1. *J. Virol.* 69:2596–2601.

Haller, O., P. Staeheli, M. Schwemmle, and G. Kochs. 2015. Mx GTPases: dynamin-like antiviral machines of innate immunity. *Trends Microbiol.* 23:154–163.

doi:10.1016/j.tim.2014.12.003.

Halonen, S.K., G.A. Taylor, and L.M. Weiss. 2001. Gamma interferon-induced inhibition of Toxoplasma gondii in astrocytes is mediated by IGTP. *Infect. Immun.* 69:5573–5576.

Han, K., D.-W. Shin, T.-Y. Lee, and Y.-H. Lee. 2008. Seroprevalence of Toxoplasma gondii infection and risk factors associated with seropositivity of pregnant women in Korea. *J. Parasitol.* 94:963–965. doi:10.1645/GE-1435.1.

Han, K., D.I. Lou, and S.L. Sawyer. 2011. Identification of a genomic reservoir for new TRIM genes in primate genomes. *PLoS Genet.* 7:e1002388. doi:10.1371/journal.pgen.1002388.

Harma, M., M. Harma, N. Gungen, and N. Demir. 2004. Toxoplasmosis in pregnant women in Sanliurfa, Southeastern Anatolia City, Turkey. *J Egypt Soc Parasitol.* 34:519–525.

Hatakeyama, S. 2011. TRIM proteins and cancer. *Nat. Rev. Cancer*. 11:792–804. doi:10.1038/nrc3139.

Havelaar, A.H., J.M. Kemmeren, and L.M. Kortbeek. 2007. Disease burden of congenital toxoplasmosis. *Clin. Infect. Dis.* 44:1467–1474. doi:10.1086/517511.

Hayashi, F., K.D. Smith, A. Ozinsky, T.R. Hawn, E.C. Yi, D.R. Goodlett, J.K. Eng, S. Akira, D.M. Underhill, and A. Aderem. 2001. The innate immune response to bacterial flagellin is mediated by Toll-like receptor 5. *Nature*. 410:1099–1103. doi:10.1038/35074106.

Hayashi-Nishino, M., N. Fujita, T. Noda, A. Yamaguchi, T. Yoshimori, and A. Yamamoto. 2009. A subdomain of the endoplasmic reticulum forms a cradle for autophagosome formation. *Nat. Cell Biol.* 11:1433–1437. doi:10.1038/ncb1991.

Hefti, H.P., M. Frese, H. Landis, C. Di Paolo, A. Aguzzi, O. Haller, and J. Pavlovic. 1999. Human MxA protein protects mice lacking a functional alpha/beta interferon system against La crosse virus and other lethal viral infections. *J. Virol.* 73:6984–6991.

Hemmi, H., O. Takeuchi, T. Kawai, T. Kaisho, S. Sato, H. Sanjo, M. Matsumoto, K. Hoshino, H. Wagner, K. Takeda, and S. Akira. 2000. A Toll-like receptor recognizes bacterial DNA. *Nature*. 408:740–745. doi:10.1038/35047123.

Hemsath, F.A., and H. Pinkerton. 1956. Disseminated cytomegalic inclusion disease and disseminated toxoplasmosis in an adult with myeloid metaplasia; report of a case. *Am. J. Clin. Pathol.* 26:36–41.

Henry, S.C., X. Daniell, M. Indaram, J.F. Whitesides, G.D. Sempowski, D. Howell, T. Oliver, and G.A. Taylor. 2007. Impaired macrophage function underscores susceptibility to Salmonella in mice lacking Irgm1 (LRG-47). *J. Immunol.* 179:6963–6972.

Herberman, R.B., M.E. Nunn, and D.H. Lavrin. 1975a. Natural cytotoxic reactivity of

mouse lymphoid cells against syngeneic acid allogeneic tumors. I. Distribution of reactivity and specificity. *Int. J. Cancer*. 16:216–229.

Herberman, R.B., M.E. Nunn, H.T. Holden, and D.H. Lavrin. 1975b. Natural cytotoxic reactivity of mouse lymphoid cells against syngeneic and allogeneic tumors. II. Characterization of effector cells. *Int. J. Cancer*. 16:230–239.

Hermanns, T., U.B. Müller, S. Könen-Waisman, J.C. Howard, and T. Steinfeldt. 2015. The Toxoplasma gondii rhoptry protein ROP18 is an Irga6-specific kinase and regulated by the dense granule protein GRA7. *Cell. Microbiol.* doi:10.1111/cmi.12499.

Hershko, A., A. Ciechanover, H. Heller, A.L. Haas, and I.A. Rose. 1980. Proposed role of ATP in protein breakdown: conjugation of protein with multiple chains of the polypeptide of ATP-dependent proteolysis. *Proc. Natl. Acad. Sci. U.S.A.* 77:1783–1786.

Higgs, R., E. Lazzari, C. Wynne, J. Ní Gabhann, A. Espinosa, M. Wahren-Herlenius, and C.A. Jefferies. 2010. Self protection from anti-viral responses--Ro52 promotes degradation of the transcription factor IRF7 downstream of the viral Toll-Like receptors. *PLoS ONE*. 5:e11776. doi:10.1371/journal.pone.0011776.

Higgs, R., J. Ní Gabhann, N. Ben Larbi, E.P. Breen, K.A. Fitzgerald, and C.A. Jefferies. 2008. The E3 ubiquitin ligase Ro52 negatively regulates IFN-beta production post-pathogen recognition by polyubiquitin-mediated degradation of IRF3. *J. Immunol.* 181:1780–1786.

Hinze-Selch, D., W. Däubener, S. Erdag, and S. Wilms. 2010. The diagnosis of a personality disorder increases the likelihood for seropositivity to Toxoplasma gondii in psychiatric patients. *Folia Parasitol.* 57:129–135.

Hirschfeld, M., C.J. Kirschning, R. Schwandner, H. Wesche, J.H. Weis, R.M. Wooten, and J.J. Weis. 1999. Cutting edge: inflammatory signaling by Borrelia burgdorferi lipoproteins is mediated by toll-like receptor 2. *J. Immunol.* 163:2382–2386.

Hofmann, R.M., and C.M. Pickart. 1999. Noncanonical MMS2-encoded ubiquitin-conjugating enzyme functions in assembly of novel polyubiquitin chains for DNA repair. *Cell*. 96:645–653.

Hofmann, R.M., and C.M. Pickart. 2001. In vitro assembly and recognition of Lys-63 polyubiquitin chains. *J. Biol. Chem.* 276:27936–27943. doi:10.1074/jbc.M103378200.

Holland, G.N., C. Muccioli, C. Silveira, J.M. Weisz, R. Belfort, and G.R. O'Connor. 1999. Intraocular inflammatory reactions without focal necrotizing retinochoroiditis in patients with acquired systemic toxoplasmosis. *Am. J. Ophthalmol.* 128:413–420.

Holland, G.N., R.E. Engstrom, B.J. Glasgow, B.B. Berger, S.A. Daniels, Y. Sidikaro, J.A. Harmon, D.H. Fischer, D.S. Boyer, and N.A. Rao. 1988. Ocular toxoplasmosis in patients with the acquired immunodeficiency syndrome. *Am. J. Ophthalmol.* 106:653–667.

Horisberger, M.A., M. Wathelet, J. Szpirer, C. Szpirer, Q. Islam, G. Levan, G. Huez, and J. Content. 1988. cDNA cloning and assignment to chromosome 21 of IFI-78K gene, the human equivalent of murine Mx gene. *Somat. Cell Mol. Genet.* 14:123–131.

Horisberger, M.A., P. Staeheli, and O. Haller. 1983. Interferon induces a unique protein in mouse cells bearing a gene for resistance to influenza virus. *Proc. Natl. Acad. Sci. U.S.A.* 80:1910–1914.

Hornung, V., A. Ablasser, M. Charrel-Dennis, F. Bauernfeind, G. Horvath, D.R. Caffrey, E. Latz, and K.A. Fitzgerald. 2009. AIM2 recognizes cytosolic dsDNA and forms a caspase-1-activating inflammasome with ASC. *Nature*. 458:514–518. doi:10.1038/nature07725.

Horowitz, S.L., J.R. Bentson, F. Benson, I. Davos, B. Pressman, and M.S. Gottlieb. 1983. CNS toxoplasmosis in acquired immunodeficiency syndrome. *Arch. Neurol.* 40:649–652.

Hoshino, K., O. Takeuchi, T. Kawai, H. Sanjo, T. Ogawa, Y. Takeda, K. Takeda, and S. Akira. 1999. Cutting edge: Toll-like receptor 4 (TLR4)-deficient mice are hyporesponsive to lipopolysaccharide: evidence for TLR4 as the Lps gene product. *J. Immunol.* 162:3749–3752.

Howe, D.K., and L.D. Sibley. 1995. Toxoplasma gondii comprises three clonal lineages: correlation of parasite genotype with human disease. *J. Infect. Dis.* 172:1561–1566.

Hu, Y., J. Wang, B. Yang, N. Zheng, M. Qin, Y. Ji, G. Lin, L. Tian, X. Wu, L. Wu, and B. Sun. 2011. Guanylate Binding Protein 4 Negatively Regulates Virus-Induced Type I IFN and Antiviral Response by Targeting IFN Regulatory Factor 7. *J. Immunol.* doi:10.4049/jimmunol.1003691.

Huang, L., E. Kinnucan, G. Wang, S. Beaudenon, P.M. Howley, J.M. Huibregtse, and N.P. Pavletich. 1999. Structure of an E6AP-UbcH7 complex: insights into ubiquitination by the E2-E3 enzyme cascade. *Science*. 286:1321–1326.

Huett, A., R.J. Heath, J. Begun, S.O. Sassi, L.A. Baxt, J.M. Vyas, M.B. Goldberg, and R.J. Xavier. 2012. The LRR and RING Domain Protein LRSAM1Is an E3 Ligase Crucial for Ubiquitin-Dependent Autophagy of Intracellular Salmonella Typhimurium. *Cell Host and Microbe*. 12:778–790. doi:10.1016/j.chom.2012.10.019.

Huibregtse, J.M., M. Scheffner, S. Beaudenon, and P.M. Howley. 1995. A family of proteins structurally and functionally related to the E6-AP ubiquitin-protein ligase. *Proc. Natl. Acad. Sci. U.S.A.* 92:2563–2567.

Hunter, C.A., and L.D. Sibley. 2012. Modulation of innate immunity by Toxoplasma gondii virulence effectors. *Nature Reviews Microbiology*. 10:766–778. doi:10.1038/nrmicro2858.

Hunter, C.A., C.S. Subauste, V.H. Van Cleave, and J.S. Remington. 1994. Production of gamma interferon by natural killer cells from Toxoplasma gondii-infected

SCID mice: regulation by interleukin-10, interleukin-12, and tumor necrosis factor alpha. *Infect. Immun.* 62:2818–2824.

Huynh, K.K., E.-L. Eskelinen, C.C. Scott, A. Malevanets, P. Saftig, and S. Grinstein. 2007. LAMP proteins are required for fusion of lysosomes with phagosomes. *EMBO J.* 26:313–324. doi:10.1038/sj.emboj.7601511.

Huynh, M.-H., K.E. Rabenau, J.M. Harper, W.L. Beatty, L.D. Sibley, and V.B. Carruthers. 2003. Rapid invasion of host cells by Toxoplasma requires secretion of the MIC2-M2AP adhesive protein complex. *EMBO J.* 22:2082–2090. doi:10.1093/emboj/cdg217.

Inbar, D., J. Hochman, and D. Givol. 1972. Localization of antibody-combining sites within the variable portions of heavy and light chains. *Proc. Natl. Acad. Sci. U.S.A.* 69:2659–2662.

Intemann, C.D., T. Thye, S. Niemann, E.N.L. Browne, M. Amanua Chinbuah, A. Enimil, J. Gyapong, I. Osei, E. Owusu-Dabo, S. Helm, S. Rüsch-Gerdes, R.D. Horstmann, and C.G. Meyer. 2009. Autophagy gene variant IRGM -261T contributes to protection from tuberculosis caused by Mycobacterium tuberculosis but not by M. africanum strains. *PLoS Pathog.* 5:e1000577. doi:10.1371/journal.ppat.1000577.

Israelski, D.M., and J.S. Remington. 1988. Toxoplasmic encephalitis in patients with AIDS. *Infect. Dis. Clin. North Am.* 2:429–445.

Itakura, E., C. Kishi, K. Inoue, and N. Mizushima. 2008. Beclin 1 forms two distinct phosphatidylinositol 3-kinase complexes with mammalian Atg14 and UVRAG. *Mol. Biol. Cell*. 19:5360–5372. doi:10.1091/mbc.E08-01-0080.

Itoh, K., Y. Itoh, and M.B. Frank. 1991. Protein heterogeneity in the human Ro/SSA ribonucleoproteins. The 52- and 60-kD Ro/SSA autoantigens are encoded by separate genes. *J. Clin. Invest.* 87:177–186. doi:10.1172/JCI114968.

Itsui, Y., N. Sakamoto, M. Kurosaki, N. Kanazawa, Y. Tanabe, T. Koyama, Y. Takeda, M. Nakagawa, S. Kakinuma, Y. Sekine, S. Maekawa, N. Enomoto, and M. Watanabe. 2006. Expressional screening of interferon-stimulated genes for antiviral activity against hepatitis C virus replication. *J. Viral Hepat.* 13:690–700. doi:10.1111/j.1365-2893.2006.00732.x.

Itsui, Y., N. Sakamoto, S. Kakinuma, M. Nakagawa, Y. Sekine-Osajima, M. Tasaka-Fujita, Y. Nishimura-Sakurai, G. Suda, Y. Karakama, K. Mishima, M. Yamamoto, T. Watanabe, M. Ueyama, Y. Funaoka, S. Azuma, and M. Watanabe. 2009. Antiviral effects of the interferon-induced protein guanylate binding protein 1 and its interaction with the hepatitis C virus NS5B protein. *Hepatology*. 50:1727–1737. doi:10.1002/hep.23195.

Janeway, C.A. 2001. How the immune system protects the host from infection. *Microbes Infect.* 3:1167–1171.

Janku, J. 1923. Pathogenesa a patologocka anatomie tak nazvaneho vrozenehonalezem parasitu v sitnici. *Cas Lek Ces*. 62:1021–1027.

Jarvius, M., J. Paulsson, I. Weibrecht, K.-J. Leuchowius, A.-C. Andersson, C. Wählby, M. Gullberg, J. Botling, T. Sjöblom, B. Markova, A. Ostman, U. Landegren, and O. Söderberg. 2007. In situ detection of phosphorylated platelet-derived growth factor receptor beta using a generalized proximity ligation method. *Mol. Cell Proteomics*. 6:1500–1509. doi:10.1074/mcp.M700166-MCP200.

Jentsch, S., J.P. McGrath, and A. Varshavsky. 1987. The yeast DNA repair gene RAD6 encodes a ubiquitin-conjugating enzyme. *Nature*. 329:131–134. doi:10.1038/329131a0.

Jenum, P.A., B. Stray-Pedersen, K.K. Melby, G. Kapperud, A. Whitelaw, A. Eskild, and J. Eng. 1998. Incidence of Toxoplasma gondii infection in 35,940 pregnant women in Norway and pregnancy outcome for infected women. *J. Clin. Microbiol.* 36:2900–2906.

Jin, H.K., K. Yoshimatsu, A. Takada, M. Ogino, A. Asano, J. Arikawa, and T. Watanabe. 2001. Mouse Mx2 protein inhibits hantavirus but not influenza virus replication. *Arch. Virol.* 146:41–49.

Jin, L., A. Williamson, S. Banerjee, I. Philipp, and M. Rape. 2008. Mechanism of ubiquitin-chain formation by the human anaphase-promoting complex. *Cell*. 133:653–665. doi:10.1016/j.cell.2008.04.012.

Joazeiro, C.A., S.S. Wing, H. Huang, J.D. Leverson, T. Hunter, and Y.C. Liu. 1999. The tyrosine kinase negative regulator c-Cbl as a RING-type, E2-dependent ubiquitin-protein ligase. *Science*. 286:309–312.

Johnson, A.M. 1997. Speculation on possible life cycles for the clonal lineages in the genus toxoplasma. *Parasitol. Today (Regul. Ed.)*. 13:393–397.

Joiner, K.A., S.A. Fuhrman, H.M. Miettinen, L.H. Kasper, and I. Mellman. 1990. Toxoplasma gondii: fusion competence of parasitophorous vacuoles in Fc receptor-transfected fibroblasts. *Science*. 249:641–646.

Jondal, M., and H. Pross. 1975. Surface markers on human b and t lymphocytes. VI. Cytotoxicity against cell lines as a functional marker for lymphocyte subpopulations. *Int. J. Cancer*. 15:596–605.

Jones, J.L., and G.N. Holland. 2010. Annual burden of ocular toxoplasmosis in the US. *Am. J. Trop. Med. Hyg.* 82:464–465. doi:10.4269/ajtmh.2010.09-0664.

Jones, J.L., D. Kruszon-Moran, H. Rivera, C. Price, and P.P. Wilkins. 2014. Toxoplasma gondii Seroprevalence in the United States 2009-2010 and Comparison with the Past Two Decades. *Am. J. Trop. Med. Hyg.* doi:10.4269/ajtmh.14-0013.

Jones, J.W., N. Kayagaki, P. Broz, T. Henry, K. Newton, K. O'Rourke, S. Chan, J. Dong, Y. Qu, M. Roose-Girma, V.M. Dixit, and D.M. Monack. 2010. Absent in melanoma 2 is required for innate immune recognition of Francisella tularensis. *Proc. Natl. Acad. Sci. U.S.A.* 107:9771–9776. doi:10.1073/pnas.1003738107.

Jones, T.C., and J.G. Hirsch. 1972. The interaction between Toxoplasma gondii and

mammalian cells. II. The absence of lysosomal fusion with phagocytic vacuoles containing living parasites. *J. Exp. Med.* 136:1173–1194.

Jones, T.C., B.H. Kean, and A.C. Kimball. 1965. Pericarditis associated with toxoplasmosis: report of a case and review of the literature. *Ann. Intern. Med.* 62:786–790.

Jones, T.C., S. Yeh, and J.G. Hirsch. 1972. The interaction between Toxoplasma gondii and mammalian cells. I. Mechanism of entry and intracellular fate of the parasite. *J. Exp. Med.* 136:1157–1172.

Jumaian, N.F. 2005. Seroprevalence and risk factors for Toxoplasma infection in pregnant women in Jordan. *East. Mediterr. Health J.* 11:45–51.

Kabeya, Y., N. Mizushima, T. Ueno, A. Yamamoto, T. Kirisako, T. Noda, E. Kominami, Y. Ohsumi, and T. Yoshimori. 2000. LC3, a mammalian homologue of yeast Apg8p, is localized in autophagosome membranes after processing. *EMBO J.* 19:5720–5728. doi:10.1093/emboj/19.21.5720.

Kagan, J.C., and C.R. Roy. 2002. Legionella phagosomes intercept vesicular traffic from endoplasmic reticulum exit sites. *Nat. Cell Biol.* 4:945–954. doi:10.1038/ncb883.

Kagan, J.C., M.-P. Stein, M. Pypaert, and C.R. Roy. 2004. Legionella subvert the functions of Rab1 and Sec22b to create a replicative organelle. *J. Exp. Med.* 199:1201–1211. doi:10.1084/jem.20031706.

Kamadurai, H.B., J. Souphron, D.C. Scott, D.M. Duda, D.J. Miller, D. Stringer, R.C. Piper, and B.A. Schulman. 2009. Insights into ubiquitin transfer cascades from a structure of a UbcH5B approximately ubiquitin-HECT(NEDD4L) complex. *Mol. Cell.* 36:1095–1102. doi:10.1016/j.molcel.2009.11.010.

Kamadurai, H.B., Y. Qiu, A. Deng, J.S. Harrison, C. Macdonald, M. Actis, P. Rodrigues, D.J. Miller, J. Souphron, S.M. Lewis, I. Kurinov, N. Fujii, M. Hammel, R. Piper, B. Kuhlman, and B.A. Schulman. 2013. Mechanism of ubiquitin ligation and lysine prioritization by a HECT E3. *eLife*. 2:e00828. doi:10.7554/eLife.00828.

Kamsteeg, E.-J., G. Hendriks, M. Boone, I.B.M. Konings, V. Oorschot, P. van der Sluijs, J. Klumperman, and P.M.T. Deen. 2006. Short-chain ubiquitination mediates the regulated endocytosis of the aquaporin-2 water channel. *Proc. Natl. Acad. Sci. U.S.A.* 103:18344–18349. doi:10.1073/pnas.0604073103.

Kane, M., S.S. Yadav, J. Bitzegeio, S.B. Kutluay, T. Zang, S.J. Wilson, J.W. Schoggins, C.M. Rice, M. Yamashita, T. Hatziioannou, and P.D. Bieniasz. 2013. MX2 is an interferon-induced inhibitor of HIV-1 infection. *Nature*. 502:563–566. doi:10.1038/nature12653.

Kang, D.-C., R.V. Gopalkrishnan, Q. Wu, E. Jankowsky, A.M. Pyle, and P.B. Fisher. 2002. mda-5: An interferon-inducible putative RNA helicase with double-stranded RNA-dependent ATPase activity and melanoma growth-suppressive properties. *Proc. Natl. Acad. Sci. U.S.A.* 99:637–642.

doi:10.1073/pnas.022637199.

Kang, H., J.S. Remington, and Y. Suzuki. 2000. Decreased resistance of B cell-deficient mice to infection with Toxoplasma gondii despite unimpaired expression of IFN-gamma, TNF-alpha, and inducible nitric oxide synthase. *J. Immunol.* 164:2629–2634.

Kanková, S., and J. Flegr. 2007. Longer pregnancy and slower fetal development in women with latent "asymptomatic" toxoplasmosis. *BMC Infect. Dis.* 7:114. doi:10.1186/1471-2334-7-114.

Kanneganti, T.-D., N. Özören, M. Body-Malapel, A. Amer, J.-H. Park, L. Franchi, J. Whitfield, W. Barchet, M. Colonna, P. Vandenabeele, J. Bertin, A. Coyle, E.P. Grant, S. Akira, and G. Núñez. 2006. Bacterial RNA and small antiviral compounds activate caspase-1 through cryopyrin/Nalp3. *Nature*. 440:233–236. doi:10.1038/nature04517.

Kapperud, G., P.A. Jenum, B. Stray-Pedersen, K.K. Melby, A. Eskild, and J. Eng. 1996. Risk factors for Toxoplasma gondii infection in pregnancy. Results of a prospective case-control study in Norway. *Am. J. Epidemiol.* 144:405–412.

Karunajeewa, H., D. Siebert, R. Hammond, S. Garland, and H. Kelly. 2001. Seroprevalence of varicella zoster virus, parvovirus B19 and Toxoplasma gondii in a Melbourne obstetric population: implications for management. *Aust N Z J Obstet Gynaecol*. 41:23–28.

Kato, H., S. Sato, M. Yoneyama, M. Yamamoto, S. Uematsu, K. Matsui, T. Tsujimura, K. Takeda, T. Fujita, O. Takeuchi, and S. Akira. 2005. Cell type-specific involvement of RIG-I in antiviral response. *Immunity*. 23:19–28. doi:10.1016/j.immuni.2005.04.010.

Kayagaki, N., M.T. Wong, I.B. Stowe, S.R. Ramani, L.C. Gonzalez, S. Akashi-Takamura, K. Miyake, J. Zhang, W.P. Lee, A. Muszyński, L.S. Forsberg, R.W. Carlson, and V.M. Dixit. 2013. Noncanonical inflammasome activation by intracellular LPS independent of TLR4. *Science*. 341:1246–1249. doi:10.1126/science.1240248.

Kayagaki, N., S. Warming, M. Lamkanfi, L. Vande Walle, S. Louie, J. Dong, K. Newton, Y. Qu, J. Liu, S. Heldens, J. Zhang, W.P. Lee, M. Roose-Girma, and V.M. Dixit. 2011. Non-canonical inflammasome activation targets caspase-11. *Nature*. 479:117–121. doi:10.1038/nature10558.

Kean, B.H., and R.G. Grocott. 1945. Sarcosporidiosis or Toxoplasmosis in Man and Guinea-Pig. *Am. J. Pathol.* 21:467–483.

Kean, B.H., and R.G. Grocott. 1947. Asymptomatic toxoplasmosis. *Am. J. Trop. Med. Hyg.* 27:745–748.

Keeble, A.H., Z. Khan, A. Forster, and L.C. James. 2008. TRIM21 is an IgG receptor that is structurally, thermodynamically, and kinetically conserved. *Proc. Natl. Acad. Sci. U.S.A.* 105:6045–6050. doi:10.1073/pnas.0800159105.

Khaminets, A., J.P. Hunn, S. Könen-Waisman, Y.O. Zhao, D. Preukschat, J. Coers, J.P. Boyle, Y.-C. Ong, J.C. Boothroyd, G. Reichmann, and J.C. Howard. 2010. Coordinated loading of IRG resistance GTPases on to the Toxoplasma gondii parasitophorous vacuole. *Cell. Microbiol.* 12:939–961. doi:10.1111/j.1462-5822.2010.01443.x.

Khan, I.A., T. Matsuura, and L.H. Kasper. 1994. Interleukin-12 enhances murine survival against acute toxoplasmosis. *Infect. Immun.* 62:1639–1642.

Khweek, A.A., K. Caution, A. Akhter, B.A. Abdulrahman, M. Tazi, H. Hassan, N. Majumdar, A. Doran, E. Guirado, L.S. Schlesinger, H. Shuman, and A.O. Amer. 2013. A bacterial protein promotes the recognition of the Legionella pneumophila vacuole by autophagy. *Eur. J. Immunol.* 43:1333–1344. doi:10.1002/eji.201242835.

Kiessling, R., E. Klein, and H. Wigzell. 1975a. “Natural” killer cells in the mouse. I. Cytotoxic cells with specificity for mouse Moloney leukemia cells. Specificity and distribution according to genotype. *Eur. J. Immunol.* 5:112–117. doi:10.1002/eji.1830050208.

Kiessling, R., E. Klein, H. Pross, and H. Wigzell. 1975b. “Natural” killer cells in the mouse. II. Cytotoxic cells with specificity for mouse Moloney leukemia cells. Characteristics of the killer cell. *Eur. J. Immunol.* 5:117–121. doi:10.1002/eji.1830050209.

Kihara, A., T. Noda, N. Ishihara, and Y. Ohsumi. 2001a. Two distinct Vps34 phosphatidylinositol 3-kinase complexes function in autophagy and carboxypeptidase Y sorting in Saccharomyces cerevisiae. *J. Cell Biol.* 152:519–530.

Kihara, A., Y. Kabeya, Y. Ohsumi, and T. Yoshimori. 2001b. Beclin-phosphatidylinositol 3-kinase complex functions at the trans-Golgi network. *EMBO Rep.* 2:330–335. doi:10.1093/embo-reports/kve061.

Kim, B.-H., A.R. Shenoy, P. Kumar, R. Das, S. Tiwari, and J.D. MacMicking. 2011. A Family of IFN-g–Inducible 65-kD GTPases Protects Against Bacterial Infection. *Science*. 332:717–721.

Kim, D., G. Pertea, C. Trapnell, H. Pimentel, R. Kelley, and S.L. Salzberg. 2013. TopHat2: accurate alignment of transcriptomes in the presence of insertions, deletions and gene fusions. *Genome Biol*. 14:R36. doi:10.1186/gb-2013-14-4-r36.

Kim, S.-K., A. Karasov, and J.C. Boothroyd. 2007. Bradyzoite-specific surface antigen SRS9 plays a role in maintaining Toxoplasma gondii persistence in the brain and in host control of parasite replication in the intestine. *Infect. Immun.* 75:1626–1634. doi:10.1128/IAI.01862-06.

Kirschning, C.J., H. Wesche, T. Merrill Ayres, and M. Rothe. 1998. Human toll-like receptor 2 confers responsiveness to bacterial lipopolysaccharide. *J. Exp. Med.* 188:2091–2097.

Klamp, T., U. Boehm, D. Schenk, K. Pfeffer, and J.C. Howard. 2003. A giant GTPase,

very large inducible GTPase-1, is inducible by IFNs. *J. Immunol.* 171:1255–1265.

Kochs, G., and O. Haller. 1999. Interferon-induced human MxA GTPase blocks nuclear import of Thogoto virus nucleocapsids. *Proc. Natl. Acad. Sci. U.S.A.* 96:2082–2086.

Kochs, G., C. Janzen, H. Hohenberg, and O. Haller. 2002. Antivirally active MxA protein sequesters La Crosse virus nucleocapsid protein into perinuclear complexes. *Proc. Natl. Acad. Sci. U.S.A.* 99:3153–3158. doi:10.1073/pnas.052430399.

Komatsu, M., S. Waguri, M. Koike, Y.-S. Sou, T. Ueno, T. Hara, N. Mizushima, J.-I. Iwata, J. Ezaki, S. Murata, J. Hamazaki, Y. Nishito, S.-I. Iemura, T. Natsume, T. Yanagawa, J. Uwayama, E. Warabi, H. Yoshida, T. Ishii, A. Kobayashi, M. Yamamoto, Z. Yue, Y. Uchiyama, E. Kominami, and K. Tanaka. 2007. Homeostatic levels of p62 control cytoplasmic inclusion body formation in autophagy-deficient mice. *Cell*. 131:1149–1163. doi:10.1016/j.cell.2007.10.035.

Kong, H.J., D.E. Anderson, C.H. Lee, M.K. Jang, T. Tamura, P. Tailor, H.K. Cho, J. Cheong, H. Xiong, H.C. Morse III, and K. Ozato. 2007. Cutting Edge: Autoantigen Ro52 Is an Interferon Inducible E3 Ligase That Ubiquitinates IRF-8 and Enhances Cytokine Expression in Macrophages. *J. Immunol.* 179:26–30.

Kostura, M.J., M.J. Tocci, G. Limjuco, J. Chin, P. Cameron, A.G. Hillman, N.A. Chartrain, and J.A. Schmidt. 1989. Identification of a monocyte specific pre-interleukin 1 beta convertase activity. *Proc. Natl. Acad. Sci. U.S.A.* 86:5227–5231.

Kotula, A.W., J.P. Dubey, A.K. Sharar, C.D. Andrews, S.K. Shen, and D.S. Lindsay. 1991. Effect of Freezing on Infectivity of *Toxoplasma Gondii* Tissue Cysts in Pork. *Journal of Food Protection*. 687–690.

Kresse, A., C. Konermann, D. Degrandi, C. Beuter-Gunia, J. Wuerthner, K. Pfeffer, and S. Beer. 2008. Analyses of murine GBP homology clusters based on in silico, in vitro and in vivo studies. *BMC Genomics*. 9:158. doi:10.1186/1471-2164-9-158.

Krug, R.M., M. Shaw, B. Broni, G. Shapiro, and O. Haller. 1985. Inhibition of influenza viral mRNA synthesis in cells expressing the interferon-induced Mx gene product. *J. Virol.* 56:201–206.

Kudo, M., K. Sugasawa, T. Hori, T. Enomoto, F. Hanaoka, and M. Ui. 1991. Human ubiquitin-activating enzyme (E1): compensation for heat-labile mouse E1 and its gene localization on the X chromosome. *Exp. Cell Res.* 192:110–117.

Kuma, A., M. Hatano, M. Matsui, A. Yamamoto, H. Nakaya, T. Yoshimori, Y. Ohsumi, T. Tokuhisa, and N. Mizushima. 2004. The role of autophagy during the early neonatal starvation period. *Nature*. 432:1032–1036. doi:10.1038/nature03029.

Kumar, Y., and R.H. Valdivia. 2008. Actin and intermediate filaments stabilize the Chlamydia trachomatis vacuole by forming dynamic structural scaffolds. *Cell Host and Microbe*. 4:159–169. doi:10.1016/j.chom.2008.05.018.

Kunzelmann, S., G.J.K. Praefcke, and C. Herrmann. 2006. Transient kinetic investigation of GTP hydrolysis catalyzed by interferon-gamma-induced hGBP1 (human guanylate binding protein 1). *J. Biol. Chem.* 281:28627–28635. doi:10.1074/jbc.M604911200.

La Spada, A.R., and J.P. Taylor. 2010. Repeat expansion disease: progress and puzzles in disease pathogenesis. *Nat. Rev. Genet.* 11:247–258. doi:10.1038/nrg2748.

Lachenmaier, S.M., M.A. Deli, M. Meissner, and O. Liesenfeld. 2011. Intracellular transport of Toxoplasma gondii through the blood-brain barrier. *J. Neuroimmunol.* 232:119–130. doi:10.1016/j.jneuroim.2010.10.029.

Lafuse, W.P., D. Brown, L. Castle, and B.S. Zwilling. 1995. Cloning and characterization of a novel cDNA that is IFN-gamma-induced in mouse peritoneal macrophages and encodes a putative GTP-binding protein. *J. Leukoc. Biol.* 57:477–483.

Lambert, H., N. Hitziger, I. Dellacasa, M. Svensson, and A. Barragan. 2006. Induction of dendritic cell migration upon Toxoplasma gondii infection potentiates parasite dissemination. *Cell. Microbiol.* 8:1611–1623. doi:10.1111/j.1462-5822.2006.00735.x.

Lappalainen, M., P. Koskela, K. Hedman, K. Teramo, P. Ammälä, V. Hiilesmaa, and M. Koskiniemi. 1992. Incidence of primary toxoplasma infections during pregnancy in southern Finland: a prospective cohort study. *Scand. J. Infect. Dis.* 24:97–104.

Lebech, M., O. Andersen, N.C. Christensen, J. Hertel, H.E. Nielsen, B. Peitersen, C. Rechnitzer, S.O. Larsen, B. Nørgaard-Pedersen, and E. Petersen. 1999. Feasibility of neonatal screening for toxoplasma infection in the absence of prenatal treatment. Danish Congenital Toxoplasmosis Study Group . *Lancet.* 353:1834–1837.

Lebrun, M., A. Michelin, H. El Hajj, J. Poncet, P.J. Bradley, H. Vial, and J.-F. Dubremetz. 2005. The rhoptry neck protein RON4 re-localizes at the moving junction during Toxoplasma gondii invasion. *Cell. Microbiol.* 7:1823–1833. doi:10.1111/j.1462-5822.2005.00646.x.

Lees, M.P., S.J. Fuller, R. McLeod, N.R. Boulter, C.M. Miller, A.M. Zakrzewski, E.J. Mui, W.H. Witola, J.J. Coyne, A.C. Hargrave, S.E. Jamieson, J.M. Blackwell, J.S. Wiley, and N.C. Smith. 2010. P2X7 receptor-mediated killing of an intracellular parasite, Toxoplasma gondii, by human and murine macrophages. *J. Immunol.* 184:7040–7046. doi:10.4049/jimmunol.1000012.

Leroy, M., G. Pire, E. Baise, and D. Desmecht. 2006. Expression of the interferon-alpha/beta-inducible bovine Mx1 dynamin interferes with replication of rabies virus. *Neurobiol. Dis.* 21:515–521. doi:10.1016/j.nbd.2005.08.015.

Leslie, R.G. 1980. The binding of soluble immune complexes of guinea pig IgG2 to homologous peritoneal macrophages. Determination of the avidity constants at 4 degrees C. *Eur. J. Immunol.* 10:317–322. doi:10.1002/eji.1830100502.

Levine, B. 2005. Eating oneself and uninvited guests: autophagy-related pathways in cellular defense. *Cell*. 120:159–162. doi:10.1016/j.cell.2005.01.005.

Li, G., J. Zhang, Y. Sun, H. Wang, and Y. Wang. 2009a. The evolutionarily dynamic IFN-inducible GTPase proteins play conserved immune functions in vertebrates and cephalochordates. *Mol. Biol. Evol.* 26:1619–1630. doi:10.1093/molbev/msp074.

Li, H., B. Handsaker, A. Wysoker, T. Fennell, J. Ruan, N. Homer, G. Marth, G. Abecasis, R. Durbin, 1000 Genome Project Data Processing Subgroup. 2009b. The Sequence Alignment/Map format and SAMtools. *Bioinformatics*. 25:2078–2079. doi:10.1093/bioinformatics/btp352.

Li, P., H. Allen, S. Banerjee, S. Franklin, L. Herzog, C. Johnston, J. McDowell, M. Paskind, L. Rodman, and J. Salfeld. 1995. Mice deficient in IL-1 beta-converting enzyme are defective in production of mature IL-1 beta and resistant to endotoxic shock. *Cell*. 80:401–411.

Li, W., M.H. Bengtson, A. Ulbrich, A. Matsuda, V.A. Reddy, A. Orth, S.K. Chanda, S. Batalov, and C.A.P. Joazeiro. 2008. Genome-wide and functional annotation of human E3 ubiquitin ligases identifies MULAN, a mitochondrial E3 that regulates the organelle's dynamics and signaling. *PLoS ONE*. 3:e1487. doi:10.1371/journal.pone.0001487.

Li, X., and J. Sodroski. 2008. The TRIM5alpha B-box 2 domain promotes cooperative binding to the retroviral capsid by mediating higher-order self-association. *J. Virol.* 82:11495–11502. doi:10.1128/JVI.01548-08.

Liang, X.H., S. Jackson, M. Seaman, K. Brown, B. Kempkes, H. Hibshoosh, and B. Levine. 1999. Induction of autophagy and inhibition of tumorigenesis by beclin 1. *Nature*. 402:672–676. doi:10.1038/45257.

Lightfield, K.L., J. Persson, S.W. Brubaker, C.E. Witte, J. von Moltke, E.A. Dunipace, T. Henry, Y.-H. Sun, D. Cado, W.F. Dietrich, D.M. Monack, R.M. Tsolis, and R.E. Vance. 2008. Critical function for Naip5 in inflammasome activation by a conserved carboxy-terminal domain of flagellin. *Nat. Immunol.* 9:1171–1178. doi:10.1038/ni.1646.

Lin, Y.-L., Y.-S. Liao, L.-R. Liao, F.-N. Chen, H.-M. Kuo, and S. He. 2008. Seroprevalence and sources of Toxoplasma infection among indigenous and immigrant pregnant women in Taiwan. *Parasitol. Res.* 103:67–74. doi:10.1007/s00436-008-0928-1.

Lindenmann, J. 1964. Inheritance of resistance to influenza virus in mice. *Proc. Soc. Exp. Biol. Med.* 116:506–509.

Ling, Y.M., M.H. Shaw, C. Ayala, I. Coppens, G.A. Taylor, D.J. Ferguson, and G.S. Yap. 2006. Vacuolar and plasma membrane stripping and autophagic elimination of Toxoplasma gondii in primed effector macrophages. *J. Exp. Med.* 203:2063–2071. doi:10.1084/jem.20061318.

Liu, Z., Q. Pan, S. Ding, J. Qian, F. Xu, J. Zhou, S. Cen, F. Guo, and C. Liang. 2013.

The interferon-inducible MxB protein inhibits HIV-1 infection. *Cell Host and Microbe*. 14:398–410. doi:10.1016/j.chom.2013.08.015.

Logar, J., M. Petrovec, Z. Novak-Antolic, T. Premru-Srsen, M. Cizman, M. Arnez, and A. Kraut. 2002. Prevention of congenital toxoplasmosis in Slovenia by serological screening of pregnant women. *Scand. J. Infect. Dis.* 34:201–204.

Lorick, K.L., J.P. Jensen, S. Fang, A.M. Ong, S. Hatakeyama, and A.M. Weissman. 1999. RING fingers mediate ubiquitin-conjugating enzyme (E2)-dependent ubiquitination. *Proc. Natl. Acad. Sci. U.S.A.* 96:11364–11369.

Lu, A., V.G. Magupalli, J. Ruan, Q. Yin, M.K. Atianand, M.R. Vos, G.F. Schröder, K.A. Fitzgerald, H. Wu, and E.H. Egelman. 2014. Unified polymerization mechanism for the assembly of ASC-dependent inflammasomes. *Cell*. 156:1193–1206. doi:10.1016/j.cell.2014.02.008.

Lubeseder-Martellato, C., E. Guenzi, A. Jörg, K. Töpolt, E. Naschberger, E. Kremmer, C. Zietz, E. Tschachler, P. Hutzler, M. Schwemmle, K. Matzen, T. Grimm, B. Ensoli, and M. Stürzl. 2002. Guanylate-binding protein-1 expression is selectively induced by inflammatory cytokines and is an activation marker of endothelial cells during inflammatory diseases. *Am. J. Pathol.* 161:1749–1759. doi:10.1016/S0002-9440(10)64452-5.

Ludlam, G.B., and C.P. Beattie. 1963. Pulmonary toxoplasmosis? *Lancet*. 2:1136–1138.

Luft, B.J., and J.S. Remington. 1992. Toxoplasmic encephalitis in AIDS. *Clin. Infect. Dis.* 15:211–222.

Luft, B.J., F. Conley, J.S. Remington, M. Laverdiere, K.F. Wagner, J.F. Levine, P.C. Craven, D.A. Strandberg, T.M. File, N. Rice, and F. Meunier-Carpentier. 1983. Outbreak of central-nervous-system toxoplasmosis in western Europe and North America. *Lancet*. 1:781–784.

Luft, B.J., R. Hafner, A.H. Korzun, C. Leport, D. Antoniskis, E.M. Bosler, D.D. Bourland, R. Uttamchandani, J. Fuhrer, and J. Jacobson. 1993. Toxoplasmic encephalitis in patients with the acquired immunodeficiency syndrome. Members of the ACTG 077p/ANRS 009 Study Team. *N. Engl. J. Med.* 329:995–1000. doi:10.1056/NEJM199309303291403.

Luft, B.J., R.G. Brooks, F.K. Conley, R.E. McCabe, and J.S. Remington. 1984. Toxoplasmic encephalitis in patients with acquired immune deficiency syndrome. *JAMA*. 252:913–917.

Lukic, Z., S. Hausmann, S. Sebastian, J. Rucci, J. Sastri, S.L. Robia, J. Luban, and E.M. Campbell. 2011. TRIM5α associates with proteasomal subunits in cells while in complex with HIV-1 virions. *Retrovirology*. 8:93. doi:10.1529/biophysj.103.022087.

MacMicking, J.D., G.A. Taylor, and J.D. McKinney. 2003. Immune control of tuberculosis by IFN-gamma-inducible LRG-47. *Science*. 302:654–659. doi:10.1126/science.1088063.

Male, D., J. Brostoff, D.B. Roth, and I. Roitt. 2006. Immunology. Seventh. Elsevier Ltd.

Mallery, D.L., W.A. McEwan, S.R. Bidgood, G.J. Towers, C.M. Johnson, and L.C. James. 2010. Antibodies mediate intracellular immunity through tripartite motif-containing 21 (TRIM21). *Proc. Natl. Acad. Sci. U.S.A.* 107:19985–19990. doi:10.1073/pnas.1014074107/-/DCSupplemental.

Maltese, W.A. 1990. Posttranslational modification of proteins by isoprenoids in mammalian cells. *FASEB J.* 4:3319–3328.

Man, S.M., R. Karki, R.K.S. Malireddi, G. Neale, P. Vogel, M. Yamamoto, M. Lamkanfi, and T.-D. Kanneganti. 2015. The transcription factor IRF1 and guanylate-binding proteins target activation of the AIM2 inflammasome by Francisella infection. *Nat. Immunol.* 16:467–475. doi:10.1038/ni.3118.

Manocha, G.D., R. Mishra, N. Sharma, K.L. Kumawat, A. Basu, and S.K. Singh. 2014. Regulatory role of TRIM21 in the type-I interferon pathway in Japanese encephalitis virus-infected human microglial cells. *J Neuroinflammation*. 11:24. doi:10.1186/1742-2094-11-24.

Mansouri, El, B., M. Rhajaoui, F. Sebti, F. Amarir, M. Laboudi, R. Bchitou, M. Hamad, and M. Lyagoubi. 2007. Seroprevalence of toxoplasmosis in pregnant women in Rabat, Morocco. *Bull Soc Pathol Exot*. 100:289–290.

Markovitz, A.A., A.M. Simanek, R.H. Yolken, S. Galea, K.C. Koenen, S. Chen, and A.E. Aiello. 2015. Toxoplasma gondii and anxiety disorders in a community-based sample. *Brain Behav. Immun.* 43:192–197. doi:10.1016/j.bbi.2014.08.001.

Markson, G., C. Kiel, R. Hyde, S. Brown, P. Charalabous, A. Bremm, J. Semple, J. Woodsmith, S. Duley, K. Salehi-Ashtiani, M. Vidal, D. Komander, L. Serrano, P. Lehner, and C.M. Sanderson. 2009. Analysis of the human E2 ubiquitin conjugating enzyme protein interaction network. *Genome Res.* 19:1905–1911. doi:10.1101/gr.093963.109.

Martens, S., I. Parvanova, J. Zerrahn, G. Griffiths, G. Schell, G. Reichmann, and J.C. Howard. 2005. Disruption of Toxoplasma gondii Parasitophorous Vacuoles by the Mouse p47-Resistance GTPases. *PLoS Pathog.* 1:e24. doi:10.1371/journal.ppat.0010024.

Maspero, E., E. Valentini, S. Mari, V. Cecatiello, P. Soffientini, S. Pasqualato, and S. Polo. 2013. Structure of a ubiquitin-loaded HECT ligase reveals the molecular basis for catalytic priming. *Nat. Struct. Mol. Biol.* 20:696–701. doi:10.1038/nsmb.2566.

Massiah, M.A., B.N. Simmons, K.M. Short, and T.C. Cox. 2006. Solution structure of the RBCC/TRIM B-box1 domain of human MID1: B-box with a RING. *J. Mol. Biol.* 358:532–545. doi:10.1016/j.jmb.2006.02.009.

Massiah, M.A., J.A.B. Matts, K.M. Short, B.N. Simmons, S. Singireddy, Z. Yi, and T.C. Cox. 2007. Solution structure of the MID1 B-box2 CHC(D/C)C(2)H(2) zinc-binding domain: insights into an evolutionarily conserved RING fold. *J. Mol. Biol.*

369:1–10. doi:10.1016/j.jmb.2007.03.017.

McEwan, W.A., J.C.H. Tam, R.E. Watkinson, S.R. Bidgood, D.L. Mallery, and L.C. James. 2013. Intracellular antibody-bound pathogens stimulate immune signaling via the Fc receptor TRIM21. *Nat. Immunol.* 14:327–336. doi:10.1038/ni.2548.

Mead, P.S., L. Slutsker, V. Dietz, L.F. McCaig, J.S. Bresee, C. Shapiro, P.M. Griffin, and R.V. Tauxe. 1999. Food-related illness and death in the United States. *Emerging Infect. Dis.* 5:607–625. doi:10.3201/eid0505.990502.

Mellman, I.S. 1982. Endocytosis, membrane recycling and Fc receptor function. *Ciba Found. Symp.* 35–58.

Mellman, I.S., H. Plutner, R.M. Steinman, J.C. Unkeless, and Z.A. Cohn. 1983. Internalization and degradation of macrophage Fc receptors during receptor-mediated phagocytosis. *J. Cell Biol.* 96:887–895.

Melo, M.B., P. Kasperkovitz, A. Cerny, S. Könen-Waisman, E.A. Kurt-Jones, E. Lien, B. Beutler, J.C. Howard, D.T. Golenbock, and R.T. Gazzinelli. 2010. UNC93B1 Mediates Host Resistance to Infection with Toxoplasma gondii. *PLoS Pathog.* 6:e1001071. doi:10.1371/journal.ppat.1001071.

Mercier, C., D.K. Howe, D. Mordue, M. Lingnau, and L.D. Sibley. 1998a. Targeted disruption of the GRA2 locus in Toxoplasma gondii decreases acute virulence in mice. *Infect. Immun.* 66:4176–4182.

Mercier, C., M.F. Cesbron-Delauw, and L.D. Sibley. 1998b. The amphipathic alpha helices of the toxoplasma protein GRA2 mediate post-secretory membrane association. *J. Cell. Sci.* 111 (Pt 15):2171–2180.

Meroni, G., and G. Diez-Roux. 2005. TRIM/RBCC, a novel class of "single protein RING finger" E3 ubiquitin ligases. *Bioessays*. 27:1147–1157. doi:10.1002/bies.20304.

Meunier, E., M.S. Dick, R.F. Dreier, N. Schürmann, D.K. Broz, S. Warming, M. Roose-Girma, D. Bumann, N. Kayagaki, K. Takeda, M. Yamamoto, and P. Broz. 2014. Caspase-11 activation requires lysis of pathogen-containing vacuoles by IFN-induced GTPases. *Nature*. doi:10.1038/nature13157.

Meunier, E., P. Wallet, R.F. Dreier, S. Costanzo, L. Anton, S. Rühl, S. Dussurgey, M.S. Dick, A. Kistner, M. Rigard, D. Degrandi, K. Pfeffer, M. Yamamoto, T. Henry, and P. Broz. 2015. Guanylate-binding proteins promote activation of the AIM2 inflammasome during infection with Francisella novicida. *Nat. Immunol.* 16:476–484. doi:10.1038/ni.3119.

Meyer, H., and I.A. De Mendonça. 2007. Electron microscopic observations of toxoplasma Nicolle et Manceaux grown in tissue cultures. I. 45:449–451.

Meyer, H., and K.R. Porter. 2008. A study of Trypanosoma cruzi with the electron microscope. 44:16–23.

Miao, E.A., C.M. Alpuche-Aranda, M. Dors, A.E. Clark, M.W. Bader, S.I. Miller, and

A. Aderem. 2006. Cytoplasmic flagellin activates caspase-1 and secretion of interleukin 1beta via Ipaf. *Nat. Immunol.* 7:569–575. doi:10.1038/ni1344.

Miller, M.J., P.J. Sunshine, and J.S. Remington. 1969. Quantitation of cord serum IgM and IgA as a screening procedure to detect congenital infection: results in 5,006 infants. *J. Pediatr.* 75:1287–1291.

Mital, J., M. Meissner, D. Soldati, and G.E. Ward. 2005. Conditional expression of Toxoplasma gondii apical membrane antigen-1 (TgAMA1) demonstrates that TgAMA1 plays a critical role in host cell invasion. *Mol. Biol. Cell*. 16:4341–4349. doi:10.1091/mbc.E05-04-0281.

Mizushima, N., A. Kuma, Y. Kobayashi, A. Yamamoto, M. Matsubae, T. Takao, T. Natsume, Y. Ohsumi, and T. Yoshimori. 2003a. Mouse Apg16L, a novel WD-repeat protein, targets to the autophagic isolation membrane with the Apg12-Apg5 conjugate. *J. Cell. Sci.* 116:1679–1688.

Mizushima, N., A. Yamamoto, M. Hatano, Y. Kobayashi, Y. Kabeya, K. Suzuki, T. Tokuhisa, Y. Ohsumi, and T. Yoshimori. 2001. Dissection of autophagosome formation using Apg5-deficient mouse embryonic stem cells. *J. Cell Biol.* 152:657–668.

Mizushima, N., T. Yoshimori, and Y. Ohsumi. 2003b. Role of the Apg12 conjugation system in mammalian autophagy. *Int. J. Biochem. Cell Biol.* 35:553–561.

Molofsky, A.B., B.G. Byrne, N.N. Whitfield, C.A. Madigan, E.T. Fuse, K. Tateda, and M.S. Swanson. 2006. Cytosolic recognition of flagellin by mouse macrophages restricts Legionella pneumophila infection. *J. Exp. Med.* 203:1093–1104. doi:10.1084/jem.20051659.

Monroe, J.M., P.F. Buckley, and B.J. Miller. 2015. Meta-Analysis of Anti-Toxoplasma gondii IgM Antibodies in Acute Psychosis. *Schizophr Bull*. 41:989–998. doi:10.1093/schbul/sbu159.

Montoya, J.G., and J.S. Remington. 1996. Toxoplasmic chorioretinitis in the setting of acute acquired toxoplasmosis. *Clin. Infect. Dis.* 23:277–282.

Montoya, J.G., R. Jordan, S. Lingamneni, G.J. Berry, and J.S. Remington. 1997. Toxoplasmic myocarditis and polymyositis in patients with acute acquired toxoplasmosis diagnosed during life. *Clin. Infect. Dis.* 24:676–683.

Mordue, D.G., and L.D. Sibley. 1997. Intracellular fate of vacuoles containing Toxoplasma gondii is determined at the time of formation and depends on the mechanism of entry. *J. Immunol.* 159:4452–4459.

Morris, A., and M. Croxson. 2004. Serological evidence of Toxoplasma gondii infection among pregnant women in Auckland. *N. Z. Med. J.* 117:U770.

Mosti, M., B. Pinto, A. Giromella, S. Fabiani, R. Cristofani, M. Panichi, and F. Bruschi. 2013. A 4-year evaluation of toxoplasmosis seroprevalence in the general population and in women of reproductive age in central Italy. *Epidemiol. Infect.* 141:2192–2195. doi:10.1017/S0950268812002841.

Muniz-Feliciano, L., J. Van Grol, J.-A.C. Portillo, L. Liew, B. Liu, C.R. Carlin, V.B. Carruthers, S. Matthews, and C.S. Subauste. 2013. Toxoplasma gondii-Induced Activation of EGFR Prevents Autophagy Protein-Mediated Killing of the Parasite. *PLoS Pathog.* 9:e1003809. doi:10.1371/journal.ppat.1003809.

Munoz, M., O. Liesenfeld, and M.M. Heimesaat. 2011. Immunology of Toxoplasma gondii. *Immunological Review*. 240:269–285.

Murray, H.W., B.Y. Rubin, S.M. Carriero, A.M. Harris, and E.A. Jaffee. 1985. Human mononuclear phagocyte antiprotozoal mechanisms: oxygen-dependent vs oxygen-independent activity against intracellular Toxoplasma gondii. *J. Immunol.* 134:1982–1988.

Nakayama, E.E., H. Miyoshi, Y. Nagai, and T. Shioda. 2005. A specific region of 37 amino acid residues in the SPRY (B30.2) domain of African green monkey TRIM5alpha determines species-specific restriction of simian immunodeficiency virus SIVmac infection. *J. Virol.* 79:8870–8877. doi:10.1128/JVI.79.14.8870-8877.2005.

Nakayama, M., K. Nagata, A. Kato, and A. Ishihama. 1991. Interferon-inducible mouse Mx1 protein that confers resistance to influenza virus is GTPase. *J. Biol. Chem.* 266:21404–21408.

Naot, Y., and J.S. Remington. 1980. An enzyme-linked immunosorbent assay for detection of IgM antibodies to Toxoplasma gondii: use for diagnosis of acute acquired toxoplasmosis. *J. Infect. Dis.* 142:757–766.

Narendra, D., A. Tanaka, D.-F. Suen, and R.J. Youle. 2008. Parkin is recruited selectively to impaired mitochondria and promotes their autophagy. *J. Cell Biol.* 183:795–803. doi:10.1083/jcb.200809125.

Nash, J.Q., S. Chissel, J. Jones, F. Warburton, and N.Q. Verlander. 2005. Risk factors for toxoplasmosis in pregnant women in Kent, United Kingdom. *Epidemiol. Infect.* 133:475–483.

Nicolle, C., and L.H. Manceaux. 1908. Sur une infection a corps de Leishman (ou organismes voisins) du gondi. *C R Seances Acad Sci*. 147:763–766.

Nicolle, C., and L.H. Manceaux. 1909. Sur un protozoaire nouveau du gondi. *C R Seances Acad Sci*. 148:369–372.

Niedelman, W., J.K. Sprokholt, B. Clough, E.-M. Frickel, and J.P.J. Saeij. 2013. Cell death of gamma interferon-stimulated human fibroblasts upon Toxoplasma gondii infection induces early parasite egress and limits parasite replication. *Infect. Immun.* 81:4341–4349. doi:10.1128/IAI.00416-13.

Niemiec, K.T., P. Raczyński, K. Markiewicz, J. Leibschang, and A. Ceran. 2002. The prevalence of Toxoplasma gondii infection among 2016 pregnant women and their children in the Institute of Mother and Child in Warsaw. *Wiad Parazytol*. 48:293–299.

Nisole, S., J.P. Stoye, and A. Saïb. 2005. TRIM family proteins: retroviral restriction

and antiviral defence. *Nature Reviews Microbiology*. 3:799–808. doi:10.1038/nrmicro1248.

Nordmann, A., L. Wixler, Y. Boergeling, V. Wixler, and S. Ludwig. 2012. A new splice variant of the human guanylate-binding protein 3 mediates anti-influenza activity through inhibition of viral transcription and replication. *FASEB J.* 26:1290–1300. doi:10.1096/fj.11-189886.

Nowakowska, D., B. Stray-Pedersen, E. Spiewak, W. Sobala, E. Małafiej, and J. Wilczyński. 2006. Prevalence and estimated incidence of Toxoplasma infection among pregnant women in Poland: a decreasing trend in the younger population. *Clin. Microbiol. Infect.* 12:913–917. doi:10.1111/j.1469-0691.2006.01513.x.

O'Connell, E., M.F. Wilkins, and W.A. Te Punga. 1988. Toxoplasmosis in sheep. II. The ability of a live vaccine to prevent lamb losses after an intravenous challenge with Toxoplasma gondii. *N Z Vet J.* 36:1–4. doi:10.1080/00480169.1988.35461.

Ogino, N., and C. Yoneda. 1966. The fine structure and mode of division of Toxoplasma gondii. *Arch. Ophthalmol.* 75:218–227.

Ohshima, J., M. Sasai, J. Liu, K. Yamashita, J.S. Ma, Y. Lee, H. Bando, J.C. Howard, S. Ebisu, M. Hayashi, K. Takeda, D.M. Standley, E.-M. Frickel, and M. Yamamoto. 2015. RabGDIα is a negative regulator of interferon-γ-inducible GTPase-dependent cell-autonomous immunity to Toxoplasma gondii. *Proc. Natl. Acad. Sci. U.S.A.* doi:10.1073/pnas.1510031112.

Ohshima, J., Y. Lee, M. Sasai, T. Saitoh, J. Su Ma, N. Kamiyama, Y. Matsuura, S. Pann-Ghill, M. Hayashi, S. Ebisu, K. Takeda, S. Akira, and M. Yamamoto. 2014. Role of mouse and human autophagy proteins in IFN-γ-induced cell-autonomous responses against Toxoplasma gondii. *J. Immunol.* 192:3328–3335. doi:10.4049/jimmunol.1302822.

Oksenhendler, E., J. Cadranel, C. Sarfati, C. Katlama, A. Datry, C. Marche, M. Wolf, P. Roux, F. Derouin, and J.P. Clauvel. 1990. Toxoplasma gondii pneumonia in patients with the acquired immunodeficiency syndrome. *Am. J. Med.* 88:18N–21N.

Okusaga, O., P. Langenberg, A. Sleemi, D. Vaswani, I. Giegling, A.M. Hartmann, B. Konte, M. Friedl, M.W. Groer, R.H. Yolken, D. Rujescu, and T.T. Postolache. 2011. Toxoplasma gondii antibody titers and history of suicide attempts in patients with schizophrenia. *Schizophr. Res.* 133:150–155. doi:10.1016/j.schres.2011.08.006.

Oldham, R.K., and R.B. Herberman. 1973. Evaluation of cell-mediated cytotoxic reactivity against tumor associated antigens with 125I-iododeoxyuridine labeled target cells. *J. Immunol.* 111:862–871.

Olszewsky, M.A., J. Gray, and D.J. Vestal. 2006. In silico genomic analysis of the human and murine guanylate-binding protein (GBP) gene clusters. *J. Interferon Cytokine Res.* 26:328–352. doi:10.1089/jir.2006.26.328.

Opitz, B., N.W. Schröder, I. Spreitzer, K.S. Michelsen, C.J. Kirschning, W.

Hallatschek, U. Zähringer, T. Hartung, U.B. Göbel, and R.R. Schumann. 2001. Toll-like receptor-2 mediates Treponema glycolipid and lipoteichoic acid-induced NF-kappaB translocation. *J. Biol. Chem.* 276:22041–22047. doi:10.1074/jbc.M010481200.

Ordureau, A., C. Münch, and J.W. Harper. 2015. Quantifying ubiquitin signaling. *Mol. Cell*. 58:660–676. doi:10.1016/j.molcel.2015.02.020.

Orvedahl, A., S. MacPherson, R. Sumpter, Z. Tallóczy, Z. Zou, and B. Levine. 2010. Autophagy protects against Sindbis virus infection of the central nervous system. *Cell Host and Microbe*. 7:115–127. doi:10.1016/j.chom.2010.01.007.

Ossorio, P.N., J.F. Dubremetz, and K.A. Joiner. 1994. A soluble secretory protein of the intracellular parasite Toxoplasma gondii associates with the parasitophorous vacuole membrane through hydrophobic interactions. *J. Biol. Chem.* 269:15350–15357.

Ottosson, L., J. Hennig, A. Espinosa, S. Brauner, M. Wahren-Herlenius, and M. Sunnerhagen. 2006. Structural, functional and immunologic characterization of folded subdomains in the Ro52 protein targeted in Sjögren's syndrome. *Molecular Immunology*. 43:588–598. doi:10.1016/j.molimm.2005.04.013.

Ozato, K., D.-M. Shin, T.-H. Chang, and H.C. Morse. 2008. TRIM family proteins and their emerging roles in innate immunity. *Nat Rev Immunol*. 8:849–860. doi:10.1038/nri2413.

Pan, W., X. Zuo, T. Feng, X. Shi, and J. Dai. 2012. Guanylate-binding protein 1 participates in cellular antiviral response to dengue virus. *Virol. J.* 9:292. doi:10.1186/1743-422X-9-292.

Panaretou, C., J. Domin, S. Cockcroft, and M.D. Waterfield. 1997. Characterization of p150, an adaptor protein for the human phosphatidylinositol (PtdIns) 3-kinase. Substrate presentation by phosphatidylinositol transfer protein to the p150.Ptdins 3-kinase complex. *J. Biol. Chem.* 272:2477–2485.

Pankiv, S., T.H. Clausen, T. Lamark, A. Brech, J.-A. Bruun, H. Outzen, A. Øvervatn, G. Bjørkøy, and T. Johansen. 2007. p62/SQSTM1 binds directly to Atg8/LC3 to facilitate degradation of ubiquitinated protein aggregates by autophagy. *J. Biol. Chem.* 282:24131–24145. doi:10.1074/jbc.M702824200.

Pavlovic, J., H.A. Arzet, H.P. Hefti, M. Frese, D. Rost, B. Ernst, E. Kolb, P. Staeheli, and O. Haller. 1995. Enhanced virus resistance of transgenic mice expressing the human MxA protein. *J. Virol.* 69:4506–4510.

Pavlovic, J., T. Zürcher, O. Haller, and P. Staeheli. 1990. Resistance to influenza virus and vesicular stomatitis virus conferred by expression of human MxA protein. *J. Virol.* 64:3370–3375.

Paz, I., M. Sachse, N. Dupont, J. Mounier, C. Cederfur, J. Enninga, H. Leffler, F. Poirier, M.-C. Prevost, F. Lafont, and P. Sansonetti. 2010. Galectin-3, a marker for vacuole lysis by invasive pathogens. *Cell. Microbiol.* 12:530–544. doi:10.1111/j.1462-5822.2009.01415.x.

Perez-Caballero, D., T. Hatziioannou, A. Yang, S. Cowan, and P.D. Bieniasz. 2005. Human tripartite motif 5alpha domains responsible for retrovirus restriction activity and specificity. *J. Virol.* 79:8969–8978. doi:10.1128/JVI.79.14.8969-8978.2005.

Perrin, A.J., X. Jiang, C.L. Birmingham, N.S.Y. So, and J.H. Brumell. 2004. Recognition of bacteria in the cytosol of Mammalian cells by the ubiquitin system. *Curr. Biol.* 14:806–811. doi:10.1016/j.cub.2004.04.033.

Petersen, M.B., S.A. Slaugenhaupt, J.G. Lewis, A.C. Warren, A. Chakravarti, and S.E. Antonarakis. 1991. A genetic linkage map of 27 markers on human chromosome 21. *Genomics*. 9:407–419.

Petiot, A., E. Ogier-Denis, E.F. Blommaart, A.J. Meijer, and P. Codogno. 2000. Distinct classes of phosphatidylinositol 3'-kinases are involved in signaling pathways that control macroautophagy in HT-29 cells. *J. Biol. Chem.* 275:992–998.

Pickart, C.M. 2001. Mechanisms underlying ubiquitination. *Annu. Rev. Biochem.* 70:503–533. doi:10.1146/annurev.biochem.70.1.503.

Pilla, D.M., J.A. Hagar, A.K. Haldar, A.K. Mason, D. Degrandi, K. Pfeffer, R.K. Ernst, M. Yamamoto, E.A. Miao, and J. Coers. 2014. Guanylate binding proteins promote caspase-11-dependent pyroptosis in response to cytoplasmic LPS. *Proc. Natl. Acad. Sci. U.S.A.* doi:10.1073/pnas.1321700111.

Pinkerton, H., and R.G. Henderson. 1941. Adult toxoplasmosis. A previously unrecognized disease entity simulating the typhus spotted-fever group. *Journal of the American Medical Association*. 116:807–814. doi:10.1001/jama.1941.02820090007002.

Pino, P.A., and A.E. Cardona. 2011. Isolation of brain and spinal cord mononuclear cells using percoll gradients. *J Vis Exp*. doi:10.3791/2348.

Plaut, A. 1946. The Problem of Human Toxoplasma Carriers. *Am. J. Pathol.* 22:427–431.

Poh, J., C. Odendall, A. Spanos, C. Boyle, M. Liu, P. Freemont, and D.W. Holden. 2008. SteC is a Salmonella kinase required for SPI-2-dependent F-actin remodelling. *Cell. Microbiol.* 10:20–30. doi:10.1111/j.1462-5822.2007.01010.x.

Poltorak, A., X. He, I. Smirnova, M.Y. Liu, C. Van Huffel, X. Du, D. Birdwell, E. Alejos, M. Silva, C. Galanos, M. Freudenberg, P. Ricciardi-Castagnoli, B. Layton, and B. Beutler. 1998. Defective LPS signaling in C3H/HeJ and C57BL/10ScCr mice: mutations in Tlr4 gene. *Science*. 282:2085–2088.

Porter, R.R. 1959. The hydrolysis of Rabbit gamma-globulin and antibodies with crystalline papain. *Biochem. J.* 119–126. doi:10.1002/mgg3.17.

Porto, A.M.F., M.M.R. de Amorim, I.C.N. Coelho, and L.C. Santos. 2008. Serologic profile of toxoplasmosis in pregnant women attended at a teaching-hospital in Recife. *Rev Assoc Med Bras*. 54:242–248.

Praefcke, G.J., M. Geyer, M. Schwemmle, H. Robert Kalbitzer, and C. Herrmann. 1999. Nucleotide-binding characteristics of human guanylate-binding protein 1 (hGBP1) and identification of the third GTP-binding motif. *J. Mol. Biol.* 292:321–332. doi:10.1006/jmbi.1999.3062.

Prakash, B., G.J. Praefcke, L. Renault, A. Wittinghofer, and C. Herrmann. 2000a. Structure of human guanylate-binding protein 1 representing a unique class of GTP-binding proteins. *Nature*. 403:567–571. doi:10.1038/35000617.

Prakash, B., L. Renault, G.J.K. Praefcke, C. Herrmann, and A. Wittinghoffer. 2000b. Triphosphate structure of guanylate-binding protein 1 and implications for nucleotide binding and GTPase mechanism. *EMBO J.* 19:4555–4564.

Proikas-Cezanne, T., S. Waddell, A. Gaugel, T. Frickey, A. Lupas, and A. Nordheim. 2004. WIPI-1alpha (WIPI49), a member of the novel 7-bladed WIPI protein family, is aberrantly expressed in human cancer and is linked to starvation-induced autophagy. *Oncogene*. 23:9314–9325. doi:10.1038/sj.onc.1208331.

Qureshi, S.T., L. Larivière, G. Leveque, S. Clermont, K.J. Moore, P. Gros, and D. Malo. 1999. Endotoxin-tolerant mice have mutations in Toll-like receptor 4 (Tlr4). *J. Exp. Med.* 189:615–625.

Rabaud, C., T. May, J.C. Lucet, C. Leport, P. Ambroise-Thomas, and P. Canton. 1996. Pulmonary toxoplasmosis in patients infected with human immunodeficiency virus: a French National Survey. *Clin. Infect. Dis.* 23:1249–1254.

Raetz, M., A. Kibardin, C.R. Sturge, R. Pifer, H. Li, E. Burstein, K. Ozato, S. Larin, and F. Yarovinsky. 2013. Cooperation of TLR12 and TLR11 in the IRF8-dependent IL-12 response to Toxoplasma gondii profilin. *J. Immunol.* 191:4818–4827. doi:10.4049/jimmunol.1301301.

Rahighi, S., F. Ikeda, M. Kawasaki, M. Akutsu, N. Suzuki, R. Kato, T. Kensche, T. Uejima, S. Bloor, D. Komander, F. Randow, S. Wakatsuki, and I. Dikic. 2009. Specific recognition of linear ubiquitin chains by NEMO is important for NF-kappaB activation. *Cell*. 136:1098–1109. doi:10.1016/j.cell.2009.03.007.

Rajsbaum, R., J.P. Stoye, and A. O'Garra. 2008. Type I interferon-dependent and -independent expression of tripartite motif proteins in immune cells. *Eur. J. Immunol.* 38:619–630. doi:10.1002/eji.200737916.

Rakebrandt, N., S. Lentes, H. Neumann, L.C. James, and P. Neumann-Staubitz. 2014. Antibody- and TRIM21-dependent intracellular restriction of Salmonella enterica. *Pathogens Disease*. n/a–n/a. doi:10.1111/2049-632X.12192.

Randow, F., J.D. MacMicking, and L.C. James. 2013. Cellular self-defense: how cell-autonomous immunity protects against pathogens. *Science*. 340:701–706. doi:10.1126/science.1233028.

Ravikumar, B., K. Moreau, L. Jahreiss, C. Puri, and D.C. Rubinsztein. 2010. Plasma membrane contributes to the formation of pre-autophagosomal structures. *Nat. Cell Biol.* 12:747–757. doi:10.1038/ncb2078.

Ravikumar, B., R. Duden, and D.C. Rubinsztein. 2002. Aggregate-prone proteins with polyglutamine and polyalanine expansions are degraded by autophagy. *Hum. Mol. Genet.* 11:1107–1117.

Reeves, R.H., B.F. O'Hara, W.J. Pavan, J.D. Gearhart, and O. Haller. 1988. Genetic mapping of the Mx influenza virus resistance gene within the region of mouse chromosome 16 that is homologous to human chromosome 21. *J. Virol.* 62:4372–4375.

Reichelt, M., S. Stertz, J. Krijnse-Locker, O. Haller, and G. Kochs. 2004. Missorting of LaCrosse virus nucleocapsid protein by the interferon-induced MxA GTPase involves smooth ER membranes. *Traffic*. 5:772–784. doi:10.1111/j.1600-0854.2004.00219.x.

Remington, J.S. 1974. Toxoplasmosis in the adult. *Bull N Y Acad Med*. 50:211–227.

Remington, J.S., M.J. Miller, and I. Brownlee. 1968. IgM antibodies in acute toxoplasmosis. I. Diagnostic significance in congenital cases and a method for their rapid demonstration. *Pediatrics*. 41:1082–1091.

Remington, J.S., R. McLeod, C.B. Wilson, and G. Desmonts. 2011. Toxoplasmosis. J.S. Remington and J. Klein, editors. Infectious Diseases of the Foetus and Newborn Infant. 918–1041.

Renoult, E., E. Georges, M.F. Biava, C. Hulin, L. Frimat, D. Hestin, and M. Kessler. 1997. Toxoplasmosis in kidney transplant recipients: report of six cases and review. *Clin. Infect. Dis.* 24:625–634.

Reymond, A., G. Meroni, A. Fantozzi, G. Merla, S. Cairo, L. Luzi, D. Riganelli, E. Zanaria, S. Messali, S. Cainarca, A. Guffanti, S. Minucci, P.G. Pelicci, and A. Ballabio. 2001. The tripartite motif family identifies cell compartments. *EMBO J*. 20:2140–2151. doi:10.1093/emboj/20.9.2140.

Rhodes, D.A., and J. Trowsdale. 2007. TRIM21 is a trimeric protein that binds IgG Fc via the B30.2 domain. *Molecular Immunology*. 44:2406–2414. doi:10.1016/j.molimm.2006.10.013.

Rhodes, D.A., G. Ihrke, A.T. Reinicke, G. Malcherek, M. Towey, D.A. Isenberg, and J. Trowsdale. 2002. The 52 000 MW Ro/SS-A autoantigen in Sjögren's syndrome/systemic lupus erythematosus (Ro52) is an interferon-gamma inducible tripartite motif protein associated with membrane proximal structures. *Immunology*. 106:246–256.

Robert-Gangneux, F., and M.-L. Dardé. 2012. Epidemiology of and diagnostic strategies for toxoplasmosis. *Clinical Microbiology Reviews*. 25:264–296. doi:10.1128/CMR.05013-11.

Roberts, T., K.D. Murrell, and S. Marks. 1994. Economic losses caused by foodborne parasitic diseases. *Parasitol. Today (Regul. Ed.)*. 10:419–423.

Rold, C.J., and C. Aiken. 2008. Proteasomal degradation of TRIM5alpha during retrovirus restriction. *PLoS Pathog.* 4:e1000074.

doi:10.1371/journal.ppat.1000074.

Romand, S., M. Wallon, J. Franck, P. Thulliez, F. Peyron, and H. Dumon. 2001. Prenatal diagnosis using polymerase chain reaction on amniotic fluid for congenital toxoplasmosis. *Obstet Gynecol*. 97:296–300.

Roos, D.S., R.G. Donald, N.S. Morrissette, and A.L. Moulton. 1994. Molecular tools for genetic dissection of the protozoan parasite Toxoplasma gondii. *Methods Cell Biol.* 45:27–63.

Rosenberg, E.B., R.B. Herberman, P.H. Levine, R.H. Halterman, J.L. McCoy, and J.R. Wunderlich. 1972. Lymphocyte cytotoxicity reactions to leukemia-associated antigens in identical twins. *Int. J. Cancer*. 9:648–658.

Rosso, F., J.T. Les, A. Agudelo, C. Villalobos, J.A. Chaves, G.A. Tunubala, A. Messa, J.S. Remington, and J.G. Montoya. 2008. Prevalence of infection with Toxoplasma gondii among pregnant women in Cali, Colombia, South America. *Am. J. Trop. Med. Hyg.* 78:504–508.

Rothenfusser, S., N. Goutagny, G. DiPerna, M. Gong, B.G. Monks, A. Schoenemeyer, M. Yamamoto, S. Akira, and K.A. Fitzgerald. 2005. The RNA helicase Lgp2 inhibits TLR-independent sensing of viral replication by retinoic acid-inducible gene-I. *J. Immunol.* 175:5260–5268.

Roué, R., T. Debord, E. Denamur, M. Ferry, D. Dormont, F. Barre-Sinoussi, and C. Rouzioux. 1984. Diagnosis of Toxoplasma encephalitis in absence of neurological signs by early computerised tomographic scanning in patients with AIDS. *Lancet*. 2:1472.

Rupper, A.C., and J.A. Cardelli. 2008. Induction of guanylate binding protein 5 by gamma interferon increases susceptibility to Salmonella enterica serovar Typhimurium-induced pyroptosis in RAW 264.7 cells. *Infect. Immun.* 76:2304–2315. doi:10.1128/IAI.01437-07.

Sabbah, A., T.H. Chang, R. Harnack, V. Frohlich, K. Tominaga, P.H. Dube, Y. Xiang, and S. Bose. 2009. Activation of innate immune antiviral responses by Nod2. *Nat. Immunol.* 10:1073–1080. doi:10.1038/ni.1782.

Sabin, A.B. 1941. Toxoplasmic encephalitis in children. *Journal of American Medical Association*. 116:801. doi:10.1001/jama.1941.02820090001001.

Sabin, A.B., and A.L. Warren. 1942. Therapeutic Effectiveness of Certain Sulfonamides on Infection by an Intracellular Protozoon (Toxoplasma). *Experimental Biology and Medicine*. 51:19–23. doi:10.3181/00379727-51-13809.

Sabin, A.B., and H.A. Feldman. 1948. Dyes as Microchemical Indicators of a New Immunity Phenomenon Affecting a Protozoon Parasite (Toxoplasma). *Science*. 108:660–663. doi:10.1126/science.108.2815.660.

Sabin, A.B., and P.K. Olitsky. 1937. Toxoplasma and obligate intracellular paarsitism. *Science*. 85:336–338. doi:10.1126/science.85.2205.336.

Saeedi, M., G.R. Veghari, and A. Marjani. 2007. Seroepidemiologic evaluation of anti-Toxoplasma antibodies among women in North of Iran. *Pakistan journal of biological sciences*. 10:2359–2362.

Saeki, Y., T. Kudo, T. Sone, Y. Kikuchi, H. Yokosawa, A. Toh-e, and K. Tanaka. 2009. Lysine 63-linked polyubiquitin chain may serve as a targeting signal for the 26S proteasome. *EMBO J*. 28:359–371. doi:10.1038/emboj.2008.305.

Saffer, L.D., O. Mercereau-Puijalon, J.F. Dubremetz, and J.D. Schwartzman. 1992. Localization of a Toxoplasma gondii rhoptry protein by immunoelectron microscopy during and after host cell penetration. *J. Protozool.* 39:526–530.

Sagel, U., A. Krämer, and R.T. Mikolajczyk. 2011. Incidence of maternal Toxoplasma infections in pregnancy in Upper Austria, 2000-2007. *BMC Infect. Dis.* 11:348. doi:10.1186/1471-2334-11-348.

Saito, T., R. Hirai, Y.-M. Loo, D. Owen, C.L. Johnson, S.C. Sinha, S. Akira, T. Fujita, and M. Gale. 2007. Regulation of innate antiviral defenses through a shared repressor domain in RIG-I and LGP2. *Proc. Natl. Acad. Sci. U.S.A.* 104:582–587. doi:10.1073/pnas.0606699104.

Sakae, C., S. Natphopsuk, W. Settheetham-Ishida, and T. Ishida. 2013. Low prevalence of Toxoplasma gondii infection among women in northeastern Thailand. *J. Parasitol.* 99:172–173. doi:10.1645/GE-3222.1.

Sakikawa, M., S. Noda, M. Hanaoka, H. Nakayama, S. Hojo, S. Kakinoki, M. Nakata, T. Yasuda, T. Ikenoue, and T. Kojima. 2012. Anti-Toxoplasma antibody prevalence, primary infection rate, and risk factors in a study of toxoplasmosis in 4,466 pregnant women in Japan. *Clin. Vaccine Immunol.* 19:365–367. doi:10.1128/CVI.05486-11.

Sanchez, J.G., K. Okreglicka, V. Chandrasekaran, J.M. Welker, W.I. Sundquist, and O. Pornillos. 2014. The tripartite motif coiled-coil is an elongated antiparallel hairpin dimer. *Proc. Natl. Acad. Sci. U.S.A.* 111:2494–2499. doi:10.1073/pnas.1318962111.

Sanchez-Gutierrez, A., I. Martin-Hernandez, and S.M. Garcia-Izquierdo. 2003. Estudio de reactividad a Toxoplasma gondii en embarazadas de las provincias Ciudad de la Habana y Pinar del Rio, Cuba. *Bioquimia*. 28:3–8.

Sander, L.E., M.J. Davis, M.V. Boekschoten, D. Amsen, C.C. Dascher, B. Ryffel, J.A. Swanson, M. Müller, and J.M. Blander. 2011. Detection of prokaryotic mRNA signifies microbial viability and promotes immunity. *Nature*. 474:385–389. doi:10.1038/nature10072.

Sanjuan, M.A., C.P. Dillon, S.W.G. Tait, S. Moshiach, F. Dorsey, S. Connell, M. Komatsu, K. Tanaka, J.L. Cleveland, S. Withoff, and D.R. Green. 2007. Toll-like receptor signalling in macrophages links the autophagy pathway to phagocytosis. *Nature*. 450:1253–1257. doi:10.1038/nature06421.

Santiago, H.C., C.G. Feng, A. Bafica, E. Roffe, R.M. Arantes, A. Cheever, G. Taylor, L.Q. Vieira, L.Q. Vierira, J. Aliberti, R.T. Gazzinelli, and A. Sher. 2005. Mice

deficient in LRG-47 display enhanced susceptibility to Trypanosoma cruzi infection associated with defective hemopoiesis and intracellular control of parasite growth. *J. Immunol.* 175:8165–8172.

Sardiello, M., S. Cairo, B. Fontanella, A. Ballabio, and G. Meroni. 2008. Genomic analysis of the TRIM family reveals two groups of genes with distinct evolutionary properties. *BMC Evol. Biol.* 8:225. doi:10.1186/1471-2148-8-225.

Satoh, T., H. Kato, Y. Kumagai, M. Yoneyama, S. Sato, K. Matsushita, T. Tsujimura, T. Fujita, S. Akira, and O. Takeuchi. 2010. LGP2 is a positive regulator of RIG-I- and MDA5-mediated antiviral responses. *Proc. Natl. Acad. Sci. U.S.A.* 107:1512–1517. doi:10.1073/pnas.0912986107.

Scaffidi, P., T. Misteli, and M.E. Bianchi. 2002. Release of chromatin protein HMGB1 by necrotic cells triggers inflammation. *Nature*. 418:191–195. doi:10.1038/nature00858.

Scallan, E., R.M. Hoekstra, F.J. Angulo, R.V. Tauxe, M.-A. Widdowson, S.L. Roy, J.L. Jones, and P.M. Griffin. 2011. Foodborne illness acquired in the United States--major pathogens. *Emerging Infect. Dis.* 17:7–15. doi:10.3201/eid1701.091101p1.

Scanga, C.A., J. Aliberti, D. Jankovic, F. Tilloy, S. Bennouna, E.Y. Denkers, R. Medzhitov, and A. Sher. 2002. Cutting edge: MyD88 is required for resistance to Toxoplasma gondii infection and regulates parasite-induced IL-12 production by dendritic cells. *J. Immunol.* 168:5997–6001.

Schaefer, L.E., J.W. Dyke, F.D. Meglio, P.R. Murray, W. Crafts, and A.C. Niles. 1989. Evaluation of microparticle enzyme immunoassays for immunoglobulins G and M to rubella virus and Toxoplasma gondii on the Abbott IMx automated analyzer. *J. Clin. Microbiol.* 27:2410–2413.

Scharton-Kersten, T.M., G. Yap, J. Magram, and A. Sher. 1997. Inducible nitric oxide is essential for host control of persistent but not acute infection with the intracellular pathogen Toxoplasma gondii. *J. Exp. Med.* 185:1261–1273.

Scharton-Kersten, T.M., T.A. Wynn, E.Y. Denkers, S. Bala, E. Grunvald, S. Hieny, R.T. Gazzinelli, and A. Sher. 1996. In the absence of endogenous IFN-gamma, mice develop unimpaired IL-12 responses to Toxoplasma gondii while failing to control acute infection. *J. Immunol.* 157:4045–4054.

Scheibner, K.A., M.A. Lutz, S. Boodoo, M.J. Fenton, J.D. Powell, and M.R. Horton. 2006. Hyaluronan fragments act as an endogenous danger signal by engaging TLR2. *J. Immunol.* 177:1272–1281.

Schneider-Schaulies, S., J. Schneider-Schaulies, A. Schuster, M. Bayer, J. Pavlovic, and V. ter Meulen. 1994. Cell type-specific MxA-mediated inhibition of measles virus transcription in human brain cells. *J. Virol.* 68:6910–6917.

Schnorr, J.J., S. Schneider-Schaulies, A. Simon-Jödicke, J. Pavlovic, M.A. Horisberger, and V. ter Meulen. 1993. MxA-dependent inhibition of measles virus glycoprotein synthesis in a stably transfected human monocytic cell line. *J. Virol.*

67:4760–4768.

Schroeder, A., O. Mueller, S. Stocker, R. Salowsky, M. Leiber, M. Gassmann, S. Lightfoot, W. Menzel, M. Granzow, and T. Ragg. 2006. The RIN: an RNA integrity number for assigning integrity values to RNA measurements. *BMC Mol. Biol.* 7:3. doi:10.1186/1471-2199-7-3.

Schwandner, R., R. Dziarski, H. Wesche, M. Rothe, and C.J. Kirschning. 1999. Peptidoglycan- and lipoteichoic acid-induced cell activation is mediated by toll-like receptor 2. *J. Biol. Chem.* 274:17406–17409.

Schwemmle, M., and P. Staeheli. 1994. The interferon-induced 67-kDa guanylate-binding protein (hGBP1) is a GTPase that converts GTP to GMP. *J. Biol. Chem.* 269:11299–11305.

Selleck, E.M., S.J. Fentress, W.L. Beatty, D. Degrandi, K. Pfeffer, H.W. Virgin, J.D. MacMicking, and L.D. Sibley. 2013. Guanylate-binding protein 1 (Gbp1) contributes to cell-autonomous immunity against Toxoplasma gondii. *PLoS Pathog.* 9:e1003320. doi:10.1371/journal.ppat.1003320.

Seol, J.H., R.M. Feldman, W. Zachariae, A. Shevchenko, C.C. Correll, S. Lyapina, Y. Chi, M. Galova, J. Claypool, S. Sandmeyer, K. Nasmyth, R.J. Deshaies, A. Shevchenko, and R.J. Deshaies. 1999. Cdc53/cullin and the essential Hrt1 RING-H2 subunit of SCF define a ubiquitin ligase module that activates the E2 enzyme Cdc34. *Genes Dev.* 13:1614–1626.

Shahnazari, S., W.-L. Yen, C.L. Birmingham, J. Shiu, A. Namolovan, Y.T. Zheng, K. Nakayama, D.J. Klionsky, and J.H. Brumell. 2010. A diacylglycerol-dependent signaling pathway contributes to regulation of antibacterial autophagy. *Cell Host and Microbe*. 8:137–146. doi:10.1016/j.chom.2010.07.002.

Sheffield, H.G., and M.L. Melton. 1968. The fine structure and reproduction of Toxoplasma gondii. *J. Parasitol.* 54:209–226.

Shenoy, A.R., B.-H. Kim, H.-P. Choi, T. Matsuzawa, S. Tiwari, and J.D. MacMicking. 2008. Emerging themes in IFN-γ-induced macrophage immunity by the p47 and p65 GTPase families. *Immunobiology*. 212:771–784. doi:10.1016/j.imbio.2007.09.018.

Shenoy, A.R., D.A. Wellington, P. Kumar, H. Kassa, C.J. Booth, P. Cresswell, and J.D. MacMicking. 2012. GBP5 promotes NLRP3 inflammasome assembly and immunity in mammals. *Science*. 336:481–485. doi:10.1126/science.1217141.

Shi, Y., J.E. Evans, and K.L. Rock. 2003. Molecular identification of a danger signal that alerts the immune system to dying cells. *Nature*. 425:516–521. doi:10.1038/nature01991.

Short, K.M., and T.C. Cox. 2006. Subclassification of the RBCC/TRIM superfamily reveals a novel motif necessary for microtubule binding. *J. Biol. Chem.* 281:8970–8980. doi:10.1074/jbc.M512755200.

Sibley, L.D., A.J. LeBlanc, E.R. Pfefferkorn, and J.C. Boothroyd. 1992. Generation of

a restriction fragment length polymorphism linkage map for Toxoplasma gondii. *Genetics*. 132:1003–1015.

Sibley, L.D., and J.C. Boothroyd. 1992. Virulent strains of Toxoplasma gondii comprise a single clonal lineage. *Nature*. 359:82–85. doi:10.1038/359082a0.

Sibley, L.D., E. Weidner, and J.L. Krahenbuhl. 1985. Phagosome acidification blocked by intracellular Toxoplasma gondii. *Nature*. 315:416–419.

Signorell, L.M., D. Seitz, S. Merkel, R. Berger, and C. Rudin. 2006. Cord blood screening for congenital toxoplasmosis in northwestern Switzerland, 1982-1999. *Pediatr. Infect. Dis. J.* 25:123–128. doi:10.1097/01.inf.0000195542.43369.96.

Silveira, C., A.L. Vallochi, U. Rodrigues da Silva, C. Muccioli, G.N. Holland, R.B. Nussenblatt, R. Belfort, and L.V. Rizzo. 2011. Toxoplasma gondii in the peripheral blood of patients with acute and chronic toxoplasmosis. *Br J Ophthalmol*. 95:396–400. doi:10.1136/bjo.2008.148205.

Silveira, C., R. Belfort, M. Burnier, and R. Nussenblatt. 1988. Acquired toxoplasmic infection as the cause of toxoplasmic retinochoroiditis in families. *Am. J. Ophthalmol.* 106:362–364.

Simpore, J., A. Savadogo, D. Ilboudo, M.C. Nadambega, M. Esposito, J. Yara, S. Pignatelli, V. Pietra, and S. Musumeci. 2006. Toxoplasma gondii, HCV, and HBV seroprevalence and co-infection among HIV-positive and -negative pregnant women in Burkina Faso. *J. Med. Virol.* 78:730–733. doi:10.1002/jmv.20615.

Singh, S., and A.J. Pandit. 2004. Incidence and prevalence of toxoplasmosis in Indian pregnant women: a prospective study. *Am. J. Reprod. Immunol.* 52:276–283. doi:10.1111/j.1600-0897.2004.00222.x.

Singh, S.B., A.S. Davis, G.A. Taylor, and V. Deretic. 2006. Human IRGM induces autophagy to eliminate intracellular mycobacteria. *Science*. 313:1438–1441. doi:10.1126/science.1129577.

Sobhian, B., G. Shao, D.R. Lilli, A.C. Culhane, L.A. Moreau, B. Xia, D.M. Livingston, and R.A. Greenberg. 2007. RAP80 targets BRCA1 to specific ubiquitin structures at DNA damage sites. *Science*. 316:1198–1202. doi:10.1126/science.1139516.

Song, K.-J., J.-C. Shin, H.-J. Shin, and H.-W. Nam. 2005. Seroprevalence of toxoplasmosis in Korean pregnant women. *Korean J. Parasitol.* 43:69–71.

Sorace, J.M., R.J. Johnson, D.L. Howard, and B.E. Drysdale. 1995. Identification of an endotoxin and IFN-inducible cDNA: possible identification of a novel protein family. *J. Leukoc. Biol.* 58:477–484.

Söderberg, O., M. Gullberg, M. Jarvius, K. Ridderstråle, K.-J. Leuchowius, J. Jarvius, K. Wester, P. Hydbring, F. Bahram, L.-G. Larsson, and U. Landegren. 2006. Direct observation of individual endogenous protein complexes in situ by proximity ligation. *Nat. Methods*. 3:995–1000. doi:10.1038/nmeth947.

Splendore, A. 1908. Un nuovo protozoa parassita deconigli incontrato nelle lesioni

anatomiche d“une malattia che ricorda in molti punti il Kala-azar dell”uoma. *Rev Soc Sci Sao Paulo*. 109–112.

Staeheli, P., and J.G. Sutcliffe. 1988. Identification of a second interferon-regulated murine Mx gene. *Mol. Cell. Biol.* 8:4524–4528.

Staeheli, P., D. Pravtcheva, L.G. Lundin, M. Acklin, F. Ruddle, J. Lindenmann, and O. Haller. 1986a. Interferon-regulated influenza virus resistance gene Mx is localized on mouse chromosome 16. *J. Virol.* 58:967–969.

Staeheli, P., O. Haller, W. Boll, J. Lindenmann, and C. Weissmann. 1986b. Mx protein: constitutive expression in 3T3 cells transformed with cloned Mx cDNA confers selective resistance to influenza virus. *Cell*. 44:147–158.

Staeheli, P., P. Danielson, O. Haller, and J.G. Sutcliffe. 1986c. Transcriptional Activation of the Mouse Mx Gene by Type I Interferon. *Mol. Cell. Biol.* 6:4770–4774.

Staeheli, P., R. Grob, E. Meier, J.G. Sutcliffe, and O. Haller. 1988. Influenza virus-susceptible mice carry Mx genes with a large deletion or a nonsense mutation. *Mol. Cell. Biol.* 8:4518–4523.

Steinfeldt, T., S. Könen-Waisman, L. Tong, N. Pawlowski, T. Lamkemeyer, L.D. Sibley, J.P. Hunn, and J.C. Howard. 2010. Phosphorylation of Mouse Immunity-Related GTPase (IRG) Resistance Proteins Is an Evasion Strategy for Virulent Toxoplasma gondii. *PLoS Biol.* 8:e1000576. doi:10.1371/journal.pbio.1000576.

Stremlau, M., M. Perron, S. Welikala, and J. Sodroski. 2005. Species-specific variation in the B30.2(SPRY) domain of TRIM5alpha determines the potency of human immunodeficiency virus restriction. *J. Virol.* 79:3139–3145. doi:10.1128/JVI.79.5.3139-3145.2005.

Studenicová, C., F. Ondriska, and R. Holková. 2008. Seroprevalence of Toxoplasma gondii among pregnant women in Slovakia. *Epidemiologie, mikrobiologie, imunologie*. 57:8–13.

Sukhumavasi, W., C.E. Egan, A.L. Warren, G.A. Taylor, B.A. Fox, D.J. Bzik, and E.Y. Denkers. 2008. TLR adaptor MyD88 is essential for pathogen control during oral toxoplasma gondii infection but not adaptive immunity induced by a vaccine strain of the parasite. *J. Immunol.* 181:3464–3473.

Sun, L., J. Wu, F. Du, X. Chen, and Z.J. Chen. 2013a. Cyclic GMP-AMP synthase is a cytosolic DNA sensor that activates the type I interferon pathway. *Science*. 339:786–791. doi:10.1126/science.1232458.

Sun, X., H. Lu, B. Jia, Z. Chang, S. Peng, J. Yin, Q. Chen, and N. Jiang. 2013b. A comparative study of Toxoplasma gondii seroprevalence in three healthy Chinese populations detected using native and recombinant antigens. *Parasit Vectors*. 6:241. doi:10.1186/1756-3305-6-241.

Suss-Toby, E., J. Zimmerberg, and G.E. Ward. 1996. Toxoplasma invasion: the parasitophorous vacuole is formed from host cell plasma membrane and pinches

off via a fission pore. *Proc. Natl. Acad. Sci. U.S.A.* 93:8413–8418.

Suzuki, K., T. Kirisako, Y. Kamada, N. Mizushima, T. Noda, and Y. Ohsumi. 2001. The pre-autophagosomal structure organized by concerted functions of APG genes is essential for autophagosome formation. *EMBO J.* 20:5971–5981. doi:10.1093/emboj/20.21.5971.

Suzuki, Y., D.M. Israelski, B.R. Dannemann, P. Stepick-Biek, P. Thulliez, and J.S. Remington. 1988. Diagnosis of toxoplasmic encephalitis in patients with acquired immunodeficiency syndrome by using a new serologic method. *J. Clin. Microbiol.* 26:2541–2543.

Takeshige, K., M. Baba, S. Tsuboi, T. Noda, and Y. Ohsumi. 1992. Autophagy in yeast demonstrated with proteinase-deficient mutants and conditions for its induction. *J. Cell Biol.* 119:301–311.

Takeuchi, O., T. Kawai, P.F. Mühlradt, M. Morr, J.D. Radolf, A. Zychlinsky, K. Takeda, and S. Akira. 2001. Discrimination of bacterial lipoproteins by Toll-like receptor 6. *Int. Immunol.* 13:933–940.

Tantivanich, S., P. Amarapal, W. Suphadtanaphongs, C. Siripanth, and W. Sawatmongkonkun. 2001. Prevalence of congenital cytomegalovirus and Toxoplasma antibodies in Thailand. *Southeast Asian J. Trop. Med. Public Health*. 32:466–469.

Taylor, G.A. 2007. IRG proteins: key mediators of interferon-regulated host resistance to intracellular pathogens. *Cell. Microbiol.* 9:1099–1107. doi:10.1111/j.1462-5822.2007.00916.x.

Taylor, G.A., C.G. Feng, and A. Sher. 2004. p47 GTPases: regulators of immunity to intracellular pathogens. *Nat Rev Immunol*. 4:100–109. doi:10.1038/nri1270.

Taylor, G.A., C.M. Collazo, G.S. Yap, K. Nguyen, T.A. Gregorio, L.S. Taylor, B. Eagleson, L. Secrest, E.A. Southon, S.W. Reid, L. Tessarollo, M. Bray, D.W. McVicar, K.L. Komschlies, H.A. Young, C.A. Biron, A. Sher, and G.F. Vande Woude. 2000. Pathogen-specific loss of host resistance in mice lacking the IFN-gamma-inducible gene IGTP. *Proc. Natl. Acad. Sci. U.S.A.* 97:751–755.

Theologides, A., and B.J. Kennedy. 1969. Toxoplasmic myocarditis and pericarditis. *Am. J. Med.* 47:169–174.

Thimme, R., M. Frese, G. Kochs, and O. Haller. 1995. Mx1 but not MxA confers resistance against tick-borne Dhori virus in mice. *Virology*. 211:296–301. doi:10.1006/viro.1995.1404.

Thornberry, N.A., H.G. Bull, J.R. Calaycay, K.T. Chapman, A.D. Howard, M.J. Kostura, D.K. Miller, S.M. Molineaux, J.R. Weidner, and J. Aunins. 1992. A novel heterodimeric cysteine protease is required for interleukin-1 beta processing in monocytes. *Nature*. 356:768–774. doi:10.1038/356768a0.

Thurston, T.L.M., G. Ryzhakov, S. Bloor, N. von Muhlinen, and F. Randow. 2009. The TBK1 adaptor and autophagy receptor NDP52 restricts the proliferation of

ubiquitin-coated bacteria. *Nat. Immunol.* 10:1215–1221. doi:10.1038/ni.1800.

Thurston, T.L.M., M.P. Wandel, N. von Muhlinen, A. Foeglein, and F. Randow. 2012. Galectin 8 targets damaged vesicles for autophagy to defend cells against bacterial invasion. *Nature*. 482:414–418. doi:10.1038/nature10744.

Tietzel, I., C. El-Haibi, and R.A. Carabeo. 2009. Human guanylate binding proteins potentiate the anti-chlamydia effects of interferon-gamma. *PLoS ONE*. 4:e6499. doi:10.1371/journal.pone.0006499.

Tilahun, B., Y. Hailu, G. Tilahun, H. Ashenafi, M. Vitale, V. DI Marco, and E.Z. Gebremedhin. 2015. Seroprevalence and risk factors of Toxoplasma gondii infection in humans in East Hararghe Zone, Ethiopia. *Epidemiol. Infect.* 1–8. doi:10.1017/S0950268815001284.

Tokunaga, F., S.-I. Sakata, Y. Saeki, Y. Satomi, T. Kirisako, K. Kamei, T. Nakagawa, M. Kato, S. Murata, S. Yamaoka, M. Yamamoto, S. Akira, T. Takao, K. Tanaka, and K. Iwai. 2009. Involvement of linear polyubiquitylation of NEMO in NF-kappaB activation. *Nat. Cell Biol.* 11:123–132. doi:10.1038/ncb1821.

Travassos, L.H., L.A.M. Carneiro, M. Ramjeet, S. Hussey, Y.-G. Kim, J.G. Magalhães, L. Yuan, F. Soares, E. Chea, L. Le Bourhis, I.G. Boneca, A. Allaoui, N.L. Jones, G. Núñez, S.E. Girardin, and D.J. Philpott. 2010a. Nod1 and Nod2 direct autophagy by recruiting ATG16L1 to the plasma membrane at the site of bacterial entry. *Nat. Immunol.* 11:55–62. doi:10.1038/ni.1823.

Travassos, L.H., L.A.M. Carneiro, S. Girardin, and D.J. Philpott. 2010b. Nod proteins link bacterial sensing and autophagy. *Autophagy*. 6:409–411.

Triolo-Mieses, M., and L. Traviezo-Valles. 2006. Serological Prevalence of Toxoplasma gondii Antibodies in Pregnancy in Palavecino Municipality. Lara State, Venezuela. *Kasmera*. 34:7–13.

Tripal, P., M. Bauer, E. Naschberger, T. Mörtinger, C. Hohenadl, E. Cornali, M. Thurau, and M. Stürzl. 2007. Unique features of different members of the human guanylate-binding protein family. *J. Interferon Cytokine Res.* 27:44–52. doi:10.1089/jir.2007.0086.

Underhill, D.M., A. Ozinsky, K.D. Smith, and A. Aderem. 1999. Toll-like receptor-2 mediates mycobacteria-induced proinflammatory signaling in macrophages. *Proc. Natl. Acad. Sci. U.S.A.* 96:14459–14463.

Unno, A., K. Suzuki, X. Xuan, Y. Nishikawa, K. Kitoh, and Y. Takashima. 2008. Dissemination of extracellular and intracellular Toxoplasma gondii tachyzoites in the blood flow. *Parasitol. Int.* 57:515–518. doi:10.1016/j.parint.2008.06.004.

USPHS, IDSA. 1999. 1999 USPHS/IDSA guidelines for the prevention of opportunistic infections in persons infected with human immunodeficiency virus. *Morbidity and Mortality Weekly Report*. 48:10–12.

Vaillant, V., H. de Valk, E. Baron, T. Ancelle, P. Colin, M.-C. Delmas, B. Dufour, R. Pouillot, Y. Le Strat, P. Weinbreck, E. Jougla, and J.C. Desenclos. 2005.

Foodborne infections in France. *Foodborne Pathog. Dis.* 2:221–232. doi:10.1089/fpd.2005.2.221.

Vajjhala, P.R., R.E. Mirams, and J.M. Hill. 2012. Multiple binding sites on the pyrin domain of ASC protein allow self-association and interaction with NLRP3 protein. *J. Biol. Chem.* 287:41732–41743. doi:10.1074/jbc.M112.381228.

van den Broek, M.F., U. Müller, S. Huang, R.M. Zinkernagel, and M. Aguet. 1995. Immune defence in mice lacking type I and/or type II interferon receptors. *Immunol. Rev.* 148:5–18.

Van Opdenbosch, N., P. Gurung, L. Vande Walle, A. Fossoul, T.-D. Kanneganti, and M. Lamkanfi. 2014. Activation of the NLRP1b inflammasome independently of ASC-mediated caspase-1 autoproteolysis and speck formation. *Nat Commun*. 5:3209. doi:10.1038/ncomms4209.

Vaysburd, M., R.E. Watkinson, H. Cooper, M. Reed, K. O'Connell, J. Smith, J. Cruickshanks, and L.C. James. 2013. Intracellular antibody receptor TRIM21 prevents fatal viral infection. *Proc. Natl. Acad. Sci. U.S.A.* 110:12397–12401. doi:10.1073/pnas.1301918110.

Velimirovic, B. 1984. Toxoplasmosis in immunosuppression and AIDS. *Infection*. 12:315–317.

Verdecia, M.A., C.A.P. Joazeiro, N.J. Wells, J.-L. Ferrer, M.E. Bowman, T. Hunter, and J.P. Noel. 2003. Conformational flexibility underlies ubiquitin ligation mediated by the WWP1 HECT domain E3 ligase. *Mol. Cell*. 11:249–259.

Vergne, I., J. Chua, H.-H. Lee, M. Lucas, J. Belisle, and V. Deretic. 2005. Mechanism of phagolysosome biogenesis block by viable Mycobacterium tuberculosis. *Proc. Natl. Acad. Sci. U.S.A.* 102:4033–4038. doi:10.1073/pnas.0409716102.

Virreira Winter, S., W. Niedelman, K.D. Jensen, E.E. Rosowski, L. Julien, E. Spooner, K. Caradonna, B.A. Burleigh, J.P.J. Saeij, H.L. Ploegh, and E.-M. Frickel. 2011. Determinants of GBP Recruitment to Toxoplasma gondii Vacuoles and the Parasitic Factors That Control It. *PLoS ONE*. 6:e24434. doi:10.1371/journal.pone.0024434.

Vischer, T.L., C. Bernheim, and E. Engelbrecht. 1967. Two cases of hepatitis due to Toxoplasma gondii. *Lancet*. 2:919–921.

Voepel, T., C.S. Hengstenberg, T.-O. Peulen, Y. Ajaj, C.A.M. Seidel, C. Herrmann, and J.P. Klare. 2014. Triphosphate induced dimerization of human guanylate binding protein 1 involves association of the C-terminal helices - a joint DEER and FRET study. *Biochemistry*. doi:10.1021/bi500524u.

Volinia, S., R. Dhand, B. Vanhaesebroeck, L.K. MacDougall, R. Stein, M.J. Zvelebil, J. Domin, C. Panaretou, and M.D. Waterfield. 1995. A human phosphatidylinositol 3-kinase complex related to the yeast Vps34p-Vps15p protein sorting system. *EMBO J.* 14:3339–3348.

Walker, N.P., R.V. Talanian, K.D. Brady, L.C. Dang, N.J. Bump, C.R. Ferenz, S.

Franklin, T. Ghayur, M.C. Hackett, and L.D. Hammill. 1994. Crystal structure of the cysteine protease interleukin-1 beta-converting enzyme: a (p20/p10)2 homodimer. *Cell*. 78:343–352.

Walzer, P.D., and R.M. Genta. 1989. Parasitic Infections in the Compromised Host. Marcel Dekker Inc., New York.

Wang, G.G., K.R. Calvo, M.P. Pasillas, D.B. Sykes, H. Häcker, and M.P. Kamps. 2006. Quantitative production of macrophages or neutrophils ex vivo using conditional Hoxb8. *Nat. Methods*. 3:287–293. doi:10.1038/nmeth865.

Weidner, J.M., S. Kanatani, M.A. Hernández-Castañeda, J.M. Fuks, B. Rethi, R.P.A. Wallin, and A. Barragan. 2013. Rapid cytoskeleton remodelling in dendritic cells following invasion by Toxoplasma gondii coincides with the onset of a hypermigratory phenotype. *Cell. Microbiol.* 15:1735–1752. doi:10.1111/cmi.12145.

Weigel, R.M., J.P. Dubey, D. Dyer, and A.M. Siegel. 1999. Risk factors for infection with Toxoplasma gondii for residents and workers on swine farms in Illinois. *Am. J. Trop. Med. Hyg.* 60:793–798.

West, W.H., G.B. Cannon, H.D. Kay, G.D. Bonnard, and R.B. Herberman. 1977. Natural cytotoxic reactivity of human lymphocytes against a myeloid cell line: characterization of effector cells. *J. Immunol.* 118:355–361.

Wild, P., H. Farhan, D.G. McEwan, S. Wagner, V.V. Rogov, N.R. Brady, B. Richter, J. Korac, O. Waidmann, C. Choudhary, V. Dötsch, D. Bumann, and I. Dikic. 2011. Phosphorylation of the autophagy receptor optineurin restricts Salmonella growth. *Science*. 333:228–233. doi:10.1126/science.1205405.

Wileman, T. 2013. Autophagy as a defence against intracellular pathogens. *Essays Biochem.* 55:153–163. doi:10.1042/bse0550153.

Wilkins, M.F., E. O'Connell, and W.A. Te Punga. 1988. Toxoplasmosis in sheep III. Further evaluation of the ability of a live Toxoplasma gondii vaccine to prevent lamb losses and reduce congenital infection following experimental oral challenge. *N Z Vet J*. 36:86–89. doi:10.1080/00480169.1988.35489.

Wilson, R.J., and D.H. Williamson. 1997. Extrachromosomal DNA in the Apicomplexa. *Microbiol. Mol. Biol. Rev.* 61:1–16.

Witola, W.H., E. Mui, A. Hargrave, S. Liu, M. Hypolite, A. Montpetit, P. Cavailles, C. Bisanz, M.-F. Cesbron-Delauw, G.J. Fournié, and R. McLeod. 2011. NALP1 influences susceptibility to human congenital toxoplasmosis, proinflammatory cytokine response, and fate of Toxoplasma gondii-infected monocytic cells. *Infect. Immun.* 79:756–766. doi:10.1128/IAI.00898-10.

Wolf, A., D. Cowen, and B. Paige. 1939a. Human toxoplasmosis: occurence in infants as an encephalomyelitis verification by transmission to animals. *Science*. 89:226–227. doi:10.1126/science.89.2306.226.

Wolf, A., D. Cowen, and B.H. Paige. 1939b. Toxoplasmic encephalomyelitis: III. A

new case of granulomatous encephalomyelitis due to a protozoon. *Am. J. Pathol.* 15:657–694.11.

Wolf, A., D. Cowen, and B.H. Paige. 1940. Toxoplasmic encephalomyelitis : IV. Experimental transmission of the infection to animals from a human infant. *J. Exp. Med.* 71:187–214.

Wong, A., K.H. Tan, C.S. Tee, and G.S. Yeo. 2000. Seroprevalence of cytomegalovirus, toxoplasma and parvovirus in pregnancy. *Singapore Med J.* 41:151–155.

Woo, J.-S., H.-Y. Suh, S.-Y. Park, and B.-H. Oh. 2006. Structural basis for protein recognition by B30.2/SPRY domains. *Mol. Cell.* 24:967–976. doi:10.1016/j.molcel.2006.11.009.

Wu, J., L. Sun, X. Chen, F. Du, H. Shi, C. Chen, and Z.J. Chen. 2013. Cyclic GMP-AMP is an endogenous second messenger in innate immune signaling by cytosolic DNA. *Science*. 339:826–830. doi:10.1126/science.1229963.

Xu, P., D.M. Duong, N.T. Seyfried, D. Cheng, Y. Xie, J. Robert, J. Rush, M. Hochstrasser, D. Finley, and J. Peng. 2009. Quantitative proteomics reveals the function of unconventional ubiquitin chains in proteasomal degradation. *Cell*. 137:133–145. doi:10.1016/j.cell.2009.01.041.

Xu, Y., C. Jagannath, X.-D. Liu, A. Sharafkhaneh, K.E. Kolodziejska, and N.T. Eissa. 2007. Toll-like receptor 4 is a sensor for autophagy associated with innate immunity. *Immunity*. 27:135–144. doi:10.1016/j.immuni.2007.05.022.

Yamamoto, M., M. Okuyama, J.S. Ma, T. Kimura, N. Kamiyama, H. Saiga, J. Ohshima, M. Sasai, H. Kayama, T. Okamoto, D.C.S. Huang, D. Soldati-Favre, K. Horie, J. Takeda, and K. Takeda. 2012. A cluster of interferon γ-inducible p65 GTPases plays a critical role in host defense against Toxoplasma gondii. *Immunity*. 37:302–313. doi:10.1016/j.immuni.2012.06.009.

Yang, K., H.-X. Shi, X.-Y. Liu, Y.-F. Shan, B. Wei, S. Chen, and C. Wang. 2009. TRIM21 is essential to sustain IFN regulatory factor 3 activation during antiviral response. *J. Immunol.* 182:3782–3792. doi:10.4049/jimmunol.0803126.

Yang, R.B., M.R. Mark, A. Gray, A. Huang, M.H. Xie, M. Zhang, A. Goddard, W.I. Wood, A.L. Gurney, and P.J. Godowski. 1998. Toll-like receptor-2 mediates lipopolysaccharide-induced cellular signalling. *Nature*. 395:284–288. doi:10.1038/26239.

Yang, Z., J. Huang, J. Geng, U. Nair, and D.J. Klionsky. 2006. Atg22 recycles amino acids to link the degradative and recycling functions of autophagy. *Mol. Biol. Cell*. 17:5094–5104. doi:10.1091/mbc.E06-06-0479.

Yap, G., M. Pesin, and A. Sher. 2000. Cutting edge: IL-12 is required for the maintenance of IFN-gamma production in T cells mediating chronic resistance to the intracellular pathogen, Toxoplasma gondii. *J. Immunol.* 165:628–631.

Yap, M.W., S. Nisole, and J.P. Stoye. 2005. A single amino acid change in the SPRY

domain of human Trim5alpha leads to HIV-1 restriction. *Curr. Biol.* 15:73–78. doi:10.1016/j.cub.2004.12.042.

Yarovinsky, F. 2005. TLR11 Activation of Dendritic Cells by a Protozoan Profilin-Like Protein. *Science*. 308:1626–1629. doi:10.1126/science.1109893.

Yarovinsky, F. 2014. Innate immunity to *Toxoplasma gondii* infection. *Nat Rev Immunol*. 14:109–121. doi:10.1038/nri3598.

Yen, W.-L., T. Shintani, U. Nair, Y. Cao, B.C. Richardson, Z. Li, F.M. Hughson, M. Baba, and D.J. Klionsky. 2010. The conserved oligomeric Golgi complex is involved in double-membrane vesicle formation during autophagy. *J. Cell Biol.* 188:101–114. doi:10.1083/jcb.200904075.

Ylä-Anttila, P., H. Vihinen, E. Jokitalo, and E.-L. Eskelinen. 2009. 3D tomography reveals connections between the phagophore and endoplasmic reticulum. *Autophagy*. 5:1180–1185.

Yolken, R.H., S. Bachmann, I. Ruslanova, E. Lillehoj, G. Ford, E.F. Torrey, J. Schroeder, and I. Rouslanova. 2001. Antibodies to Toxoplasma gondii in individuals with first-episode schizophrenia. *Clin. Infect. Dis.* 32:842–844. doi:10.1086/319221.

Yoneyama, M., M. Kikuchi, T. Natsukawa, N. Shinobu, T. Imaizumi, M. Miyagishi, K. Taira, S. Akira, and T. Fujita. 2004. The RNA helicase RIG-I has an essential function in double-stranded RNA-induced innate antiviral responses. *Nat. Immunol.* 5:730–737. doi:10.1038/ni1087.

Yoshimi, R., T.H. Chang, H. Wang, T. Atsumi, H.C. Morse, and K. Ozato. 2009. Gene Disruption Study Reveals a Nonredundant Role for TRIM21/Ro52 in NF- B-Dependent Cytokine Expression in Fibroblasts. *J. Immunol.* 182:7527–7538. doi:10.4049/jimmunol.0804121.

Yoshimura, A., E. Lien, R.R. Ingalls, E. Tuomanen, R. Dziarski, and D. Golenbock. 1999. Cutting edge: recognition of Gram-positive bacterial cell wall components by the innate immune system occurs via Toll-like receptor 2. *J. Immunol.* 163:1–5.

Yu, Z., Z. Wang, J. Chen, H. Li, Z. Lin, F. Zhang, Y. Zhou, and J. Hou. 2008. GTPase activity is not essential for the interferon-inducible MxA protein to inhibit the replication of hepatitis B virus. *Arch. Virol.* 153:1677–1684. doi:10.1007/s00705-008-0168-9.

Zapata, M., L. Reyes, and I. Holst. 2005. Decreased prevalence of *Toxoplasma gondii* antibodies in adults from the central valley of Costa Rica. *Parasitol. latinoam.* 60. doi:10.4067/S0717-77122005000100004.

Zenner, L., F. Darcy, A. Capron, and M.F. Cesbron-Delauw. 1998. Toxoplasma gondii: kinetics of the dissemination in the host tissues during the acute phase of infection of mice and rats. *Exp. Parasitol.* 90:86–94. doi:10.1006/expr.1998.4301.

Zhang, Z., M. Bao, N. Lu, L. Weng, B. Yuan, and Y.-J. Liu. 2013. The E3 ubiquitin

ligase TRIM21 negatively regulates the innate immune response to intracellular double-stranded DNA. *Nat. Immunol.* 14:172–178. doi:10.1038/ni.2492.

Zhao, C., and K. Dahlman-Wright. 2010. Liver X receptor in cholesterol metabolism. *J. Endocrinol.* 204:233–240. doi:10.1677/JOE-09-0271.

Zhao, Y., D.J.P. Ferguson, D.C. Wilson, J.C. Howard, L.D. Sibley, and G.S. Yap. 2009a. Virulent Toxoplasma gondii Evade Immunity-Related GTPase-Mediated Parasite Vacuole Disruption within Primed Macrophages. *J. Immunol.* 182:3775–3781. doi:10.4049/jimmunol.0804190.

Zhao, Y.O., A. Khaminets, J.P. Hunn, and J.C. Howard. 2009b. Disruption of the Toxoplasma gondii Parasitophorous Vacuole by IFNγ-Inducible Immunity-Related GTPases (IRG Proteins) Triggers Necrotic Cell Death. *PLoS Pathog.* 5:e1000288. doi:10.1371/journal.ppat.1000288.

Zhao, Z., B. Fux, M. Goodwin, I.R. Dunay, D. Strong, B.C. Miller, K. Cadwell, M.A. Delgado, M. Ponpuak, K.G. Green, R.E. Schmidt, N. Mizushima, V. Deretic, L.D. Sibley, and H.W. Virgin. 2008. Autophagosome-Independent Essential Function for the Autophagy Protein Atg5 in Cellular Immunity to Intracellular Pathogens. *Cell Host and Microbe*. 4:458–469. doi:10.1016/j.chom.2008.10.003.

Zheng, N., P. Wang, P.D. Jeffrey, and N.P. Pavletich. 2000. Structure of a c-Cbl-UbcH7 complex: RING domain function in ubiquitin-protein ligases. *Cell*. 102:533–539.

Zheng, Y.T., S. Shahnazari, A. Brech, T. Lamark, T. Johansen, and J.H. Brumell. 2009. The adaptor protein p62/SQSTM1 targets invading bacteria to the autophagy pathway. *J. Immunol.* 183:5909–5916. doi:10.4049/jimmunol.0900441.

Zhu, H., Z.-M. Zhou, R. Huo, X.-Y. Huang, L. Lu, M. Lin, L.-R. Wang, Y.-D. Zhou, J.-M. Li, and J.-H. Sha. 2004. Identification and characteristics of a novel E1 like gene nUBE1L in human testis. *Acta Biochim. Biophys. Sin. (Shanghai).* 36:227–234.

Appendix

Transcripts in the brain of wild-type and TRIM21$^{-/-}$ mice infected with avirulent *Toxoplasma*

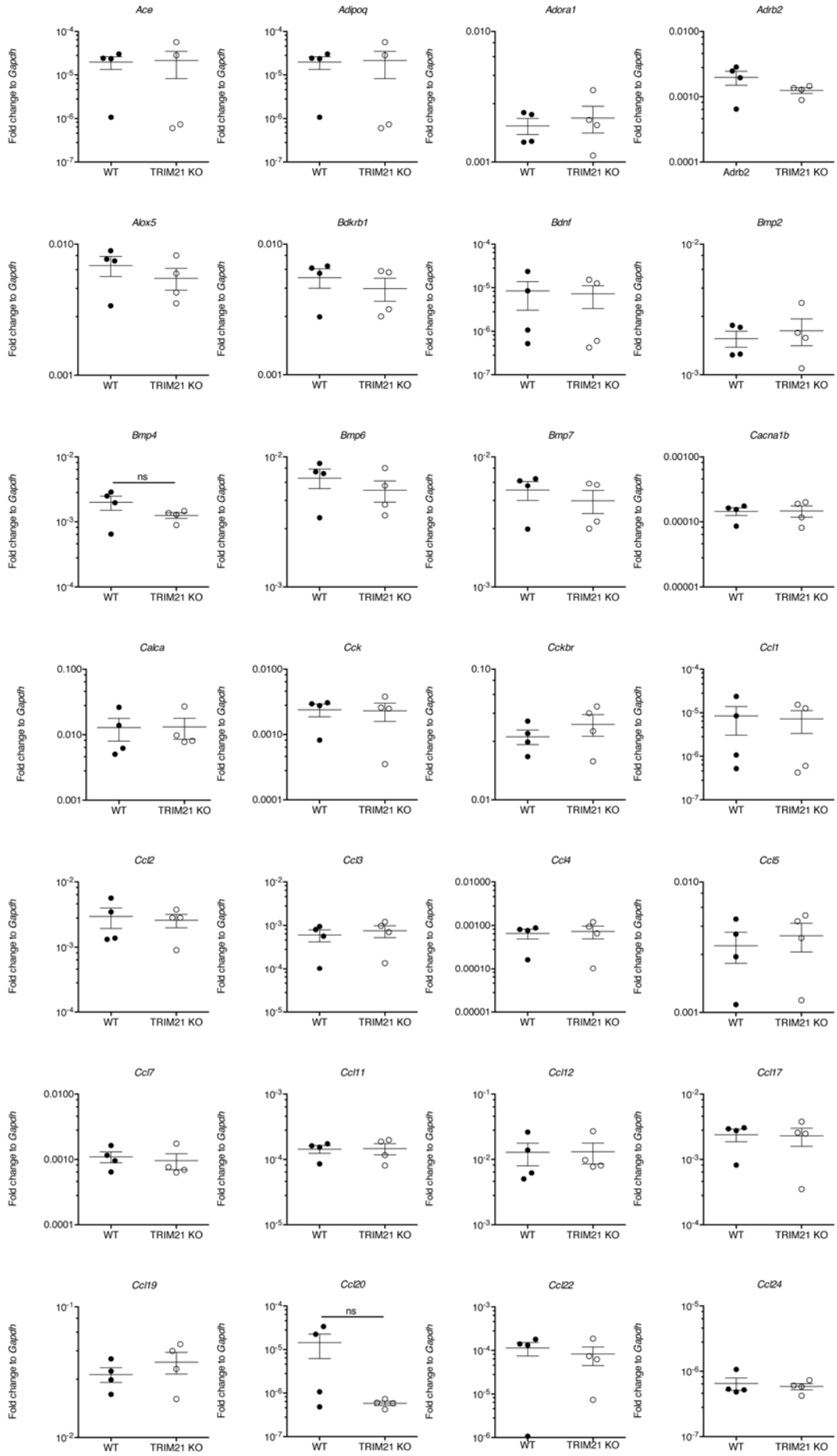
Ace
Adipoq
Adora1
Adrb2
Alox5
Bdkrb1
Bdnf
Bmp2
Bmp4
Bmp6
Bmp7
Cacna1b
Calca
Cck
Cckbr
Ccl1
Ccl2
Ccl3
Ccl4
Ccl5
Ccl7
Ccl11
Ccl12
Ccl17
Ccl19
Ccl20
Ccl22
Ccl24
Fold change to Gapdh
WT
TRIM21 KO
Adrb2
ns

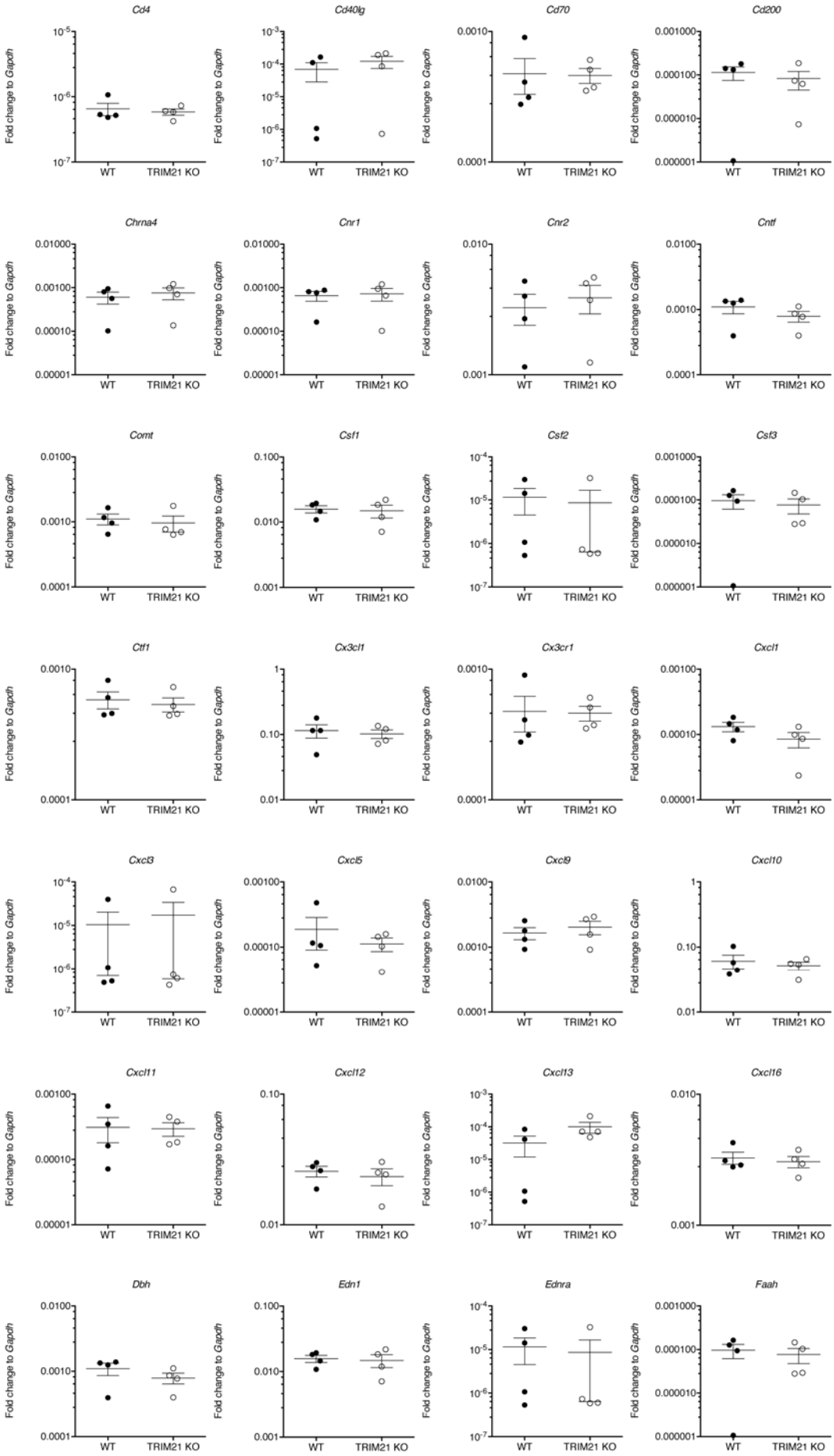
Cd4
Cd40lg
Cd70
Cd200
Chrna4
Cnr1
Cnr2
Cntf
Comt
Csf1
Csf2
Csf3
Ctf1
Cx3cl1
Cx3cr1
Cxcl1
Cxcl3
Cxcl5
Cxcl9
Cxcl10
Cxcl11
Cxcl12
Cxcl13
Cxcl16
Dbh
Edn1
Ednra
Faah
Fold change to Gapdh
WT
TRIM21 KO

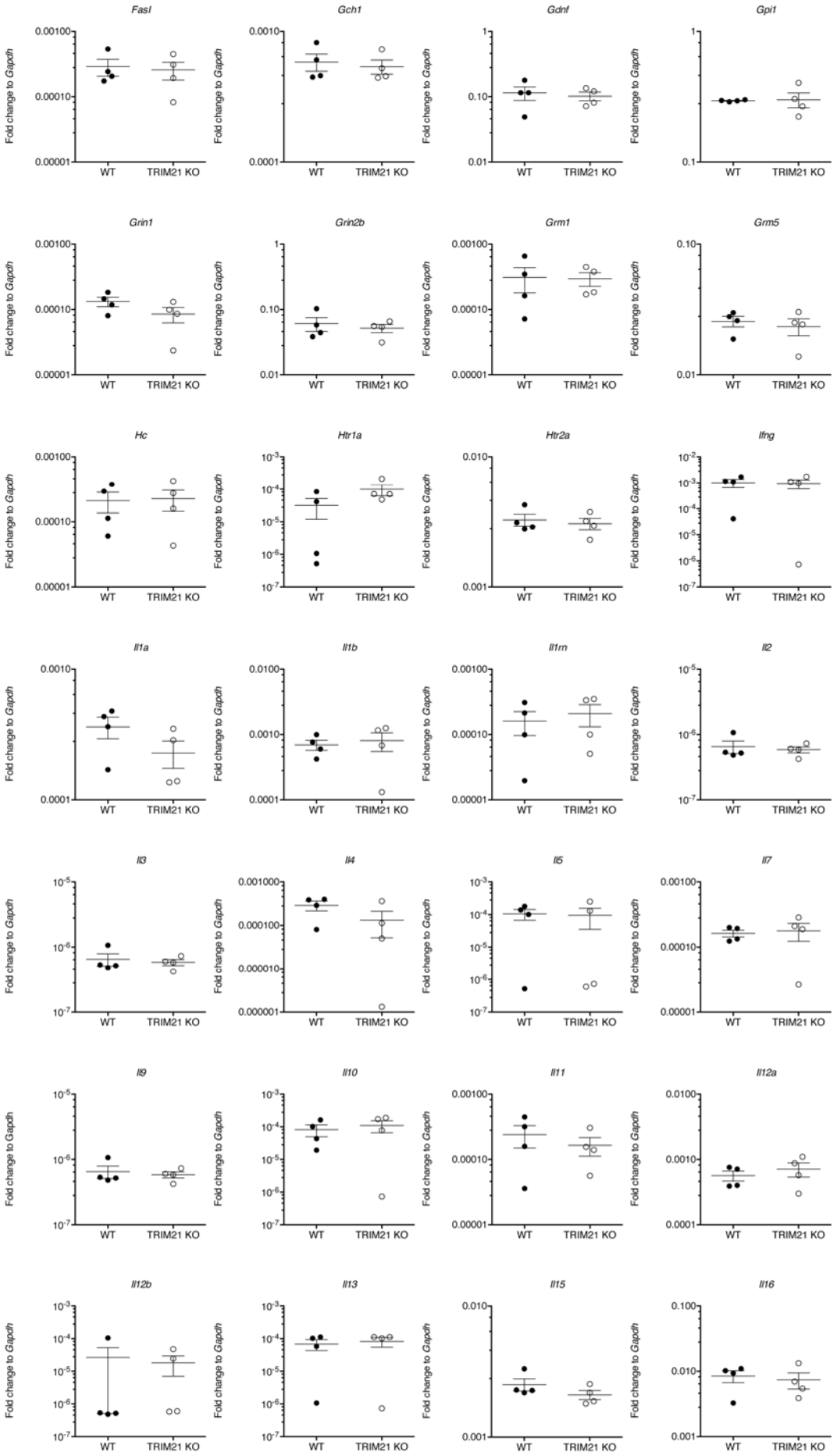
Fasl
Gch1
Gdnf
Gpi1
Grin1
Grin2b
Grm1
Grm5
Hc
Htr1a
Htr2a
Ifng
Il1a
Il1b
Il1rn
Il2
Il3
Il4
Il5
Il7
Il9
Il10
Il11
Il12a
Il12b
Il13
Il15
Il16
Fold change to Gapdh
WT
TRIM21 KO

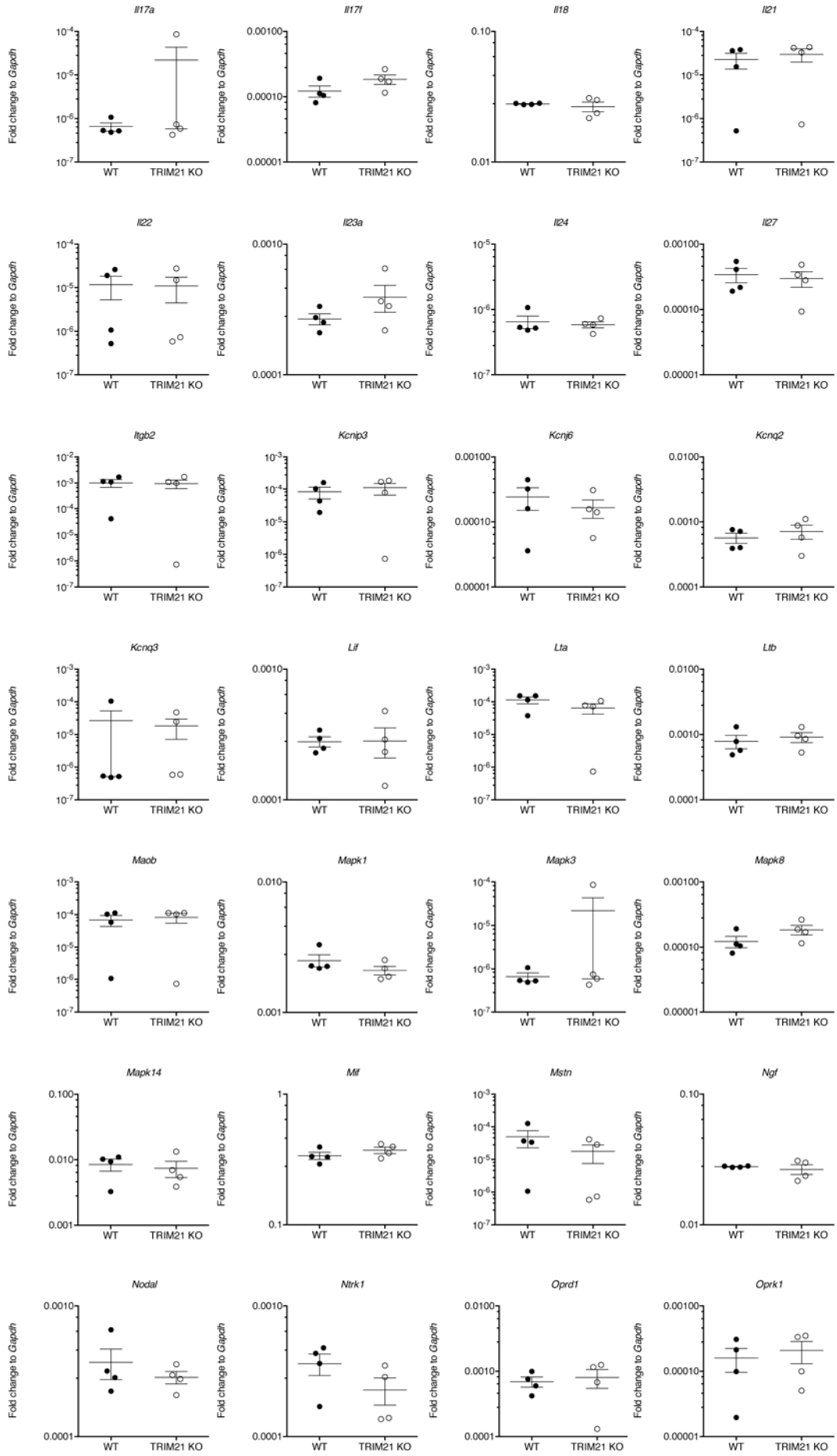
Il17a
Il17f
Il18
Il21
Il22
Il23a
Il24
Il27
Itgb2
Kcnip3
Kcnj6
Kcnq2
Kcnq3
Lif
Lta
Ltb
Maob
Mapk1
Mapk3
Mapk8
Mapk14
Mif
Mstn
Ngf
Nodal
Ntrk1
Oprd1
Oprk1
Fold change to Gapdh
WT
TRIM21 KO

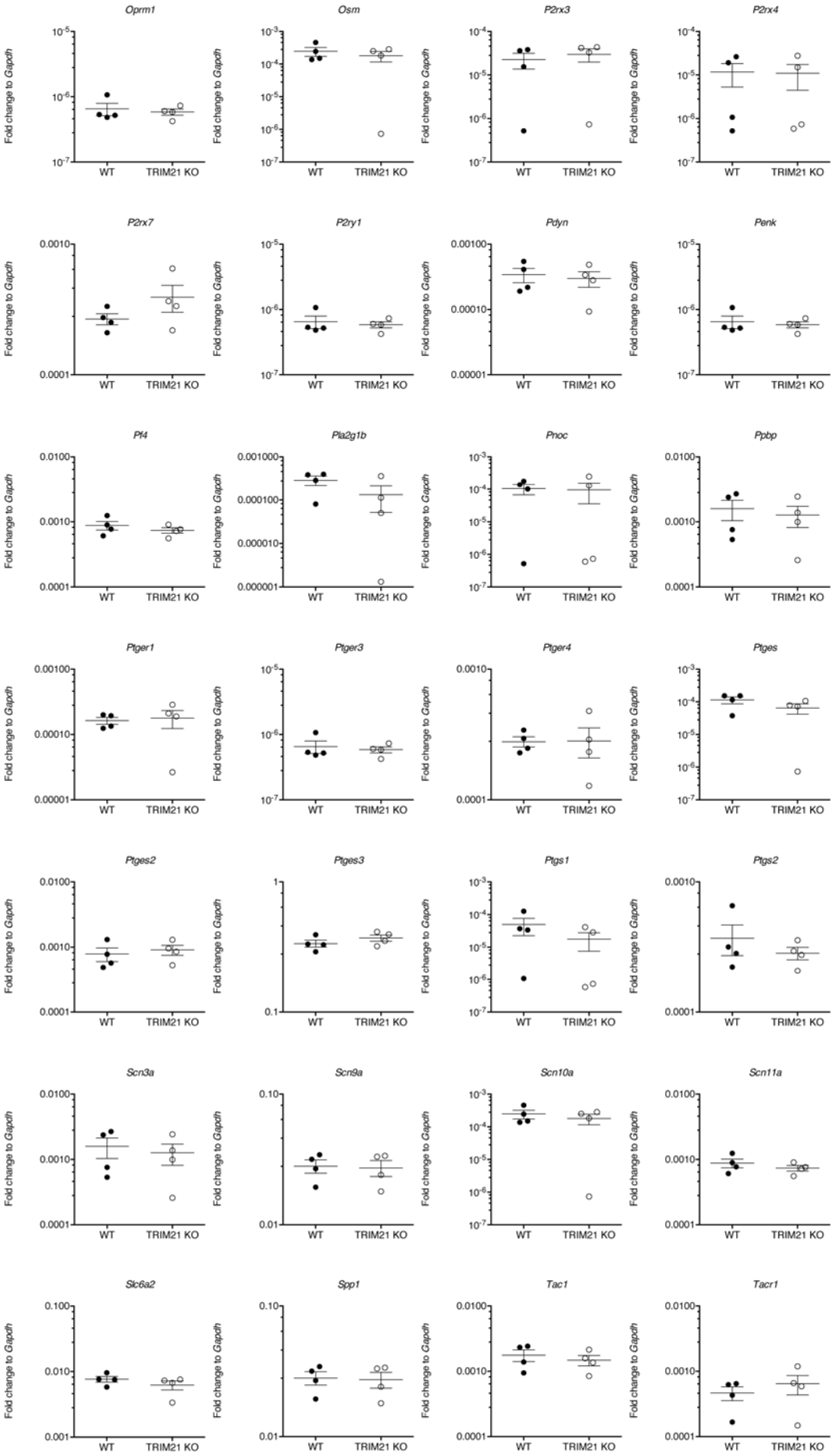
Oprm1
Osm
P2rx3
P2rx4
P2rx7
P2ry1
Pdyn
Penk
Pf4
Pla2g1b
Pnoc
Ppbp
Ptger1
Ptger3
Ptger4
Ptges
Ptges2
Ptges3
Ptgs1
Ptgs2
Scn3a
Scn9a
Scn10a
Scn11a
Slc6a2
Spp1
Tac1
Tacr1
Fold change to Gapdh
WT
TRIM21 KO

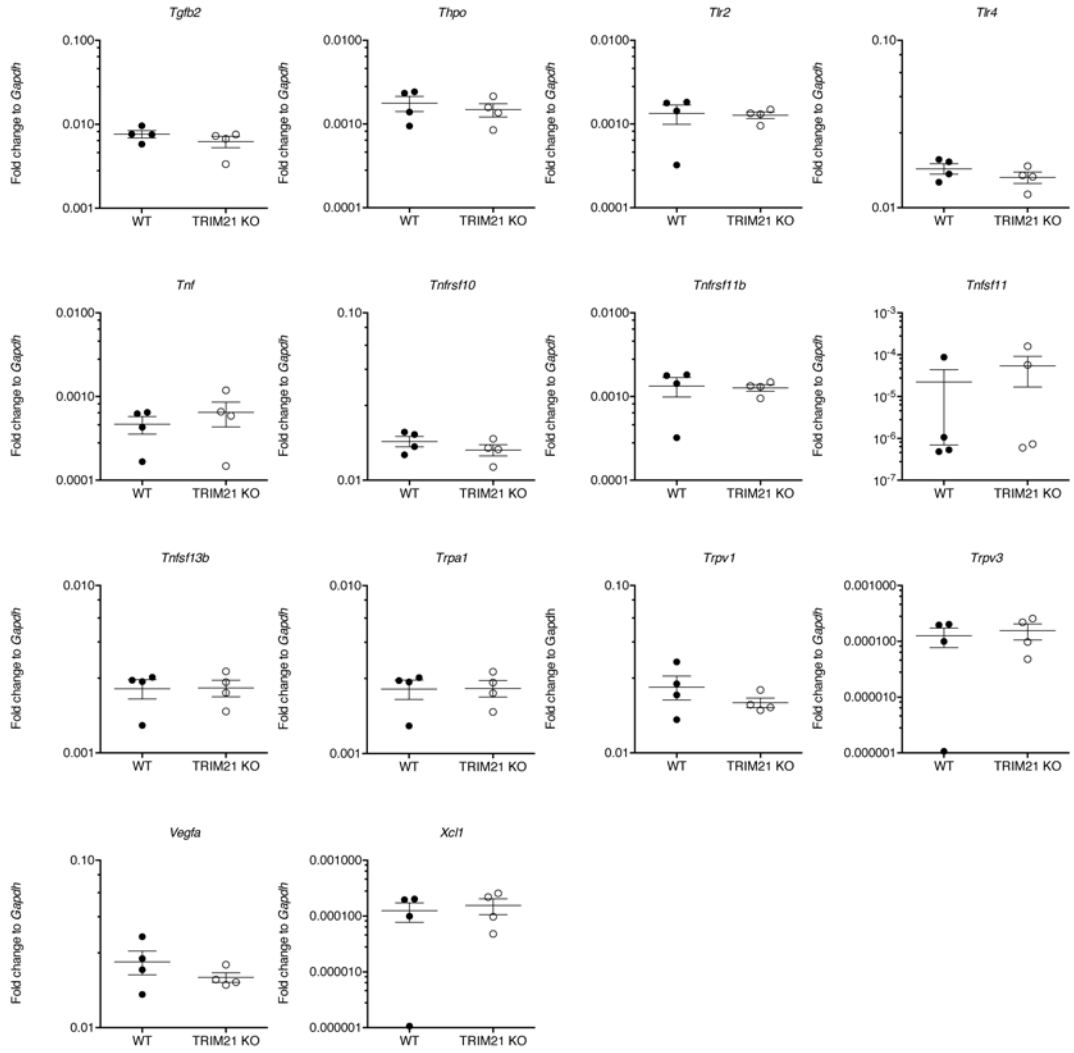

Figure A. 1: List of the transcripts in the brain of *Toxoplasma*-infected wild-type and TRIM21-deficient mice analysed by quantitative polymerase chain reactions.
Wild-type and TRIM21-deficient mice infected intraperitoneally with avirulent *Toxoplasma* were sacrificed at 7 days post-infection (dpi). Brains were isolated, RNA was extracted and gene expression was assessed by quantitative polymerase chain reaction as described in the Experimental Procedure. Mean + SEM, unpaired t-test.